# NUCLEOPHOSMIN AS A DIRECT INHIBITOR OF CASPASE-6 AND -8

**LEONG SAI MUN**
**(*B. Sc. (Hons.), NUS*)**

**A THESIS SUBMITTED**

**FOR THE DEGREE OF DOCTOR OF PHILOSOPHY**

**DEPARTMENT OF BIOLOGICAL SCIENCES**

**NATIONAL UNIVERSITY OF SINGAPORE**

**2005**

**Acknowledgments**

A journey is easier when you travel together. Interdependence is certainly more valuable than independence. This thesis is the result of four years of work whereby I have been accompanied and supported by many people. It is a pleasant aspect that I have now the opportunity to express my gratitude for all of them.

My most heartfelt gratitude goes to my thesis supervisor Associate Professor Lim Tit Meng for his invaluable guidance, encouragement and trust throughout my seven years stay in this laboratory. I have worked with A/P Lim since my first year as an undergraduate in NUS and stayed on with him for honours and postgraduate studies. I thank A/P Lim for bestowing me plenty of room for formulating my own research ideas for all these years, and for his unconditional support and relentless counselling during the turbulent times.

I wish to express my most sincere gratitude to Yan Tie, Rikki, Swee Tin, Bee Ling, Mdm Yap, Reena and Joan Choo for rendering such wonderful assistance to me in research, and most importantly, for bringing radiant sunshine into my somewhat miserable existence in the laboratory.

My most sincere thanks go to Associate Professor Sheu Fwu-shan, Associate Professor Leung Ka Yin, Associate Professor Gong Zhiyuan, Associate Professor Wang Shu, Assistant Professor Lim Kah Leong, Assistant Professor Low Boon Chuan, Assistant Professor Chew Fook Tim and members of their laboratories for rendering so much help to me in times of (experimental) troubles. My special thanks go to Yilian, Lili, Bee Leng, Wang Cheng, Haiyan, Teng Sia, Darryl, Hui Fang, Kavita, Li Mo and Hong Bin for being constantly pestered by me for protocols, reagents, juicy news or gossips. Thanks!

I also wish to express my gratitude to Mdm Say Tin, Xian Hui, Dr Bi, Dr John Foo, Shashi for their technical assistance in proteomics, and to Subha, Chye Fong and Alan for their professional assistance in daily research. I also thank members of my lab for their daily technical help.

Part of my postgraduate research live was, unfortunately, shrouded by severe depression blues. I am only glad that many friends came out in full force and provided me with the "invisible wings" to up-hoist my spirit and esteem. I thank Paul for his healing cycling trips through the most scenic parts of Singapore I never knew. I thank Jacqueline for her nonsensical and slapstick jokes to take away the blues. I thank Lance for being there for me when I turned into a depressive monster. I thank Wang Cheng, Kavita, Eunice and Debbie for their earnest listening ears and their thoughtful grip when I thought I was losing myself. I thank members of Plant Morphogenesis Lab for providing me a sanctuary to hide when whole world seemingly abandoned me. I thank members of the Sun-Moon Sect (SMS) – Layhua (aka Ren Wo Hua), Yan Ping (aka Ping Jie or the Holy Maiden), Weiqi (aka Royal Protoplast), Tuang Leng (aka Royal Tuanleng) for rallying behind me all these years without any complaints. The completion of this dissertation is beyond imagination without you guys.

My parents, my extended families (especially Ah Bo and family) and my close friends Yuru & the TJC LEP "loser gang", Joan Choo, Enzhi & the Chung Cheng gang, Tong King, Chong Yeow, Auntie Kim & family, William & Dennis Eap, Chelsea Park and Holly Ann Eap have been a great source of inspiration throughout my research. My most sincere thanks to all of them.

## Table of Contents

**Summary**

Parkinson's disease (PD) is a common, progressive neurodegenerative illness, associated with a selective loss of dopaminergic neuron in the nigrostriatal pathway of the brain, leading to impairment of voluntary motor control. While genetic studies have yielded several important pathogenetic factors such as alpha synuclein and parkin, the rapid development of novel and effective PD therapeutics requires the identification of a broader base of pathogenetic agents involved in dopaminergic cell death elicitation. To this aim, proteomics was performed on $MPP^+$-treated MN9D cells, which was used to recapitulate the biochemical and neuropathological changes reminiscent of those occurring in sporadic PD. Through this exercise, eight proteins with $MPP^+$-induced altered expression levels were identified. Among them, NPM stood out as the candidate for further studies due to its recently discovered interaction with the tumour suppressor p53, as well as its ability to inhibit apoptosis when overexpressed.

Up regulation in NPM protein level was observed on two-dimensional gel electrophoresis (2DGE) with four hours of exposure of the neurotoxin $MPP^+$ to the MN9D cells. The apparent increase in NPM amount was subsequently attributed to stress-induced release of the nucleoli-bound NPM into the nucleoplasm and cytoplasm, rather than due to *de novo* protein synthesis. Translocation of NPM into the cytoplasm was mediated by the nuclear export receptor Crm1, since Leptomycin B, an inhibitor of Crm1-mediated nuclear export, prevented cytoplasmic accumulation of NPM. Activation of the initiator caspase-8, but not executor caspase-3 or -6, promoted cytoplasmic accumulation of NPM. The results thus indicate cytoplasmic NPM build-up as part of the early cellular stress response. Subsequent *in vivo* and *in vitro* testings using a variety of cell lines implicate NPM as a caspase inhibitor. Overexpression of GFP-tagged NPM

ddition of recombinant NPM to the cytochrome-c induced HEK293 cytosolic extract inhibited the activation of caspase-3, -6, -7 and -8, but not that of caspase-9. Meanwhille., immunodepletion of endogenous NPM from apoptotic-induced cytosolic extracts resulted in significant increase in activation of the same four caspases. Our results hence indicate that NPM retards the caspase activation loop downstream of cytochrome *c*-induced caspase-9 activation. Measuring the activities of the various recombinant active caspases in the absence or presence of recombinant NPM revealed that NPM specifically inhibits the activities of caspase-6 and -8, in particular cleaving of their respective downstream procaspases and death substrates.

Further characterisation using co-immunprecipitation unravels specific physical associations between NPM and caspase-6/-8. NPM specifically interacts with only the cleaved form of both caspases in $MPP^+$-treated MN9D cells. This is reminiscent of X-linked Inhibitor of Apoptosis (XIAP)'s inhibition of and exclusive interactions with cleaved caspase-3 and -7, and appears to underlie the NPM's caspase inhibitory mechanism. In addition, NPM promoted the formation of an inhibitory complex involving active caspase-6/-8 and their procaspase substrates, and the complex was thought to sequester the active caspases away from other substrate molecules.

Taken together, the results suggest a role for nucleoli-released, cytoplasmic-accumulated NPM in the regulation of the caspase-8/-6-mediated death signalling network. The hypothesis is strongly supported by the discovery of the cytoplasmic NPM mutant (NPMc) mutant in approximately one third of patients suffering from acute myeloid leukaemia (AML). The disease is characterised by an accumulation in the bone marrow and peripheral blood of large numbers of

abnormal, immature myeloid cells. Cytoplasmic abundance of NPMc inhibited cytochrome *c*-induced caspase activation cascade in the HeLa cells and halted cleaving of downstream procaspase-3 by active caspase-8 in the AML-relevant OCI/AML3 cell line. The latter observation coincided with an attenuation of TRAIL-induced cell death and failure in caspase-8 and -3 activation in the same cell line, as compared to the OCI/AML2 cell line bearing wild type NPM only. The results hence implicate excessive inhibition of caspase-8 mediated death signalling by cytoplasmic NPMc as the primary cause underlying the pathogenesis of AML. They also support our hypothesis proposing stress-induced cytoplasmic NPM translocation as a cytoprotective strategy to delay caspase-8/-6-mediated death signalling until death commitment. The discovery made herein opens up therapeutic opportunities for AML and PD alike, both of which are likely to be characterised by deregulated cell death.

**List of Figures**

**List of Table**

# Chapter II. Translocation of nucleoli-released nucleophosmin (NPM) into the cytoplasm in response to diverse stress stimuli

# Chapter I. Proteomics analysis of MN9D cells with and without exposure to neurotoxin $MPP^+$

## 1.1 Introduction

Recent approaches to address complex biological systems include the use of cDNA microarrays and oligonucleotide chips to monitor changes in mRNA expression. Although gene-chip technology is certainly very powerful, it is clear that it has its limitations. Cells need to be able to dynamically modify protein function as well as to quickly regulate protein creation and degradation under both normal situations and in response to cellular perturbations (Pasinetti, 2001). However, mRNA-based assays are unable to detect covalent modification, regulated translation, or proteolysis, which are key regulatory events in signal transduction mechanisms. Furthermore, studies in human liver and *S. cerevisiae* have shown that mRNA levels correlate poorly with corresponding protein levels (Gygi *et al.*, 1999; Futcher *et al.*, 1999). As such, analysis of genomic information alone is incapable of providing a complete overview of protein activation. The emerging field of proteomics seeks to address the role of protein expression directly and offers a much richer source for the functional description of diseases and the discovery of diagnostic and therapeutic targets. An additional and unique advantage is that, in contrast with the genome, the inherently dynamic nature of the proteome allows us to monitor closely changes in the state of a cell, tissue or organism over time (Pandey & Mann, 2000).

Proteomics provides a complementary and potentially more comprehensive approach to the analysis of signalling mechanisms by resolving the expressed proteins of the cell ("proteome") followed by protein sequencing and identification (Pandey & Mann, 2000). Improved technologies that have emerged for comprehensive and high-throughput protein analysis yield novel insights into cell regulation. An established and widely accessible strategy for protein profiling is two-dimensional gel electrophoresis (2DGE), which displays changes in

protein expression and post-translational modifications based on protein staining intensities and electrophoretic mobility. By combining 2D gels and mass spectrometry with standard molecular pharmacological approaches, responses to specific signal transduction pathways can be monitored (Pandey & Mann, 2000). Several studies have successfully identified novel signal transduction targets by selectively activating or inhibiting pathways and screening molecular responses by 2DGE. Also, signature patterns containing diagnostic or functional information may be acquired from 2DGE profiles, aiding the quest for disease biomarkers and potential drug targets (Aebersold & Mann, 2003; Hanash, 2003).

### *1.1.1 Proteomic Methodologies*

Proteomics methodologies include a number of sample preparation steps that culminate in mass spectral analysis and automated identification. Harvested cells are lysed, and then proteins are reduced and alkylated. For quantitation and differential expression experiments, the alkylated proteins from specific cell states (e.g., normal versus diseased) can be labeled with stable isotope tags for quantitation. Proteins may be separated by 2DGE or chromatographic means. Differential image analysis of 2DGE-separated proteins can reveal pattern changes suggesting regulation of protein expression or post-translational modifications. Spots of interest are manually or robotically excised and digested, then analysed using matrix assisted laser desorption/ionisation-time-of-flight (MALDI-TOF) mass spectrometer (MS) (Pandey & Mann, 2000).

#### *1.1.1.1 Two dimensional Gel Electrophoresis (2DGE)*

For more than 30 years, the mainstay of protein expression profiling has been 2DGE, where proteins are separated according to their isoelectric points using isoelectric focussing in the first dimension, and by size using SDS/PAGE in the second dimension. Proteins may be stained by Coomassie brilliant blue, SYPRO Orange/Red or silver, in order of increasing sensitivity. Visualisation and analysis of 2D gels can be performed by imaging systems and software. The introduction of immobilised pH gradients and advanced bioinformatics have vastly improved the reproducibility and comparability between gels, although the high demand on labour is a serious obstacle to 2DGE becoming routine for a clinical laboratory (Hanash, 2000).

2DGE can resolve 1500–3000 protein spots per gel, which is still at the top end of any two-step separation procedure. By spreading the pH range across several gels, so called zoom gels (Gorg Electrophoresis 2000), between 5000–10000 protein spots can be resolved. Any additional purification step will display more proteins. In this aspect, subcellular fractionation offers the advantage of well-established protocols for many subcellular compartments and additional information derived from protein localisation (Huber *et al.*, 2003).

Although 2DGE is the most widely used tool for separating proteins in expression proteomics, it is not without its limitations. Challenges faced when utilizing this technology are co-migration of proteins, systematic exclusion of highly hydrophobic molecules and problems with detecting proteins with extremes of pH and size or low abundance proteins. To meet demands for greater detail and accuracy in protein separation techniques, companies are developing new products that are inexpensive and reliable, generate high-resolution protein separation and yield good visual detection of subtle differences. Also, fractionation methods that

reduce complexity or affinity purifications for selective enrichment are now commonly used to enhance proteomic analysis. Technologies such as microcapillary electrophoresis, capillary electrochromatography and ultra-HPLC are also emerging which promise excellent protein separations as well as detection of low abundance proteins (Lubec *et al.*, 2003).

#### *1.1.1.2 Mass Spectrometry (MS)*

MS is a highly sensitive and versatile technique for studying proteins. It can be used to derive sequences *de novo* and determine structural information (in particular post-translational modifications) as well as to quantify relative and absolute amounts of proteins. In proteomics, the most common approaches used are peptide mass fingerprinting and tandem mass MS sequencing (Aebersold & Mann, 2003). A mass spectrometer consists of three components: an ionization source, a mass analyser, and a detector. The ionization source adds a charge to the peptides in the sample, usually in the form of a proton to produce positively charged particles, and injects them into a vacuum chamber. The mass analyser uses an electromagnetic field to separate and sort the ionized peptides, while the detector registers the number of ions at each mass-to-charge value. True mass can only be determined if the charge state can be determined, which requires the resolution of naturally occurring isotopic variants (Kolch *et al.*, 2005)

On a mass spectrum, each peak represents an ionized peptide, originating from a protein in the sample, with the height of the peak proportional to the abundance of the peptide. Proteins may be identified by recording their peptide mass fingerprint (PMF) — the pattern of peaks in the mass spectrum after fragmentation by specific enzymes — or by amino-acid sequencing after

breaking down the protein fragments further into a series of peptides differing by one amino acid (Pandey & Mann, 2000).

### *1.1.2 Scope of Proteomics*

Two main areas of the proteomic field are profiling and functional proteomics. Profiling proteomics encompasses the description of the whole proteome of an organism (by analogy with the genome) and includes organelle mapping and differential measurement of expression levels between cells or conditions. The usefulness of profiling proteomics is well illustrated in the field of neuroscience. One detailed analysis of the mouse brain proteome established a protein index of over 8,500 proteins by 2DGE, with MS identification of about 500 (Klose *et al.*, 2002). Another profile of human fetal brain identified 1,700 proteins corresponding to 437 genes (Fountoulakis *et al.*, 2002). Differential protein expression analysis based on 2DGE separation and visualisation methods have been used to compare the anatomy of different brain regions and to profile molecular changes associated with physiological states and development. Comparative proteome analysis has also been used to study pathology associated with neurodegeneration, psychiatry, trauma, stroke and nervous system tumors. Also, expression proteomics of cerebrospinal fluids, astrocyte secretions and microdialysates of brain are under investigation to identify biomarkers for diagnostics and prognostics (Choudhary & Grant, 2004).

On the other hand. functional proteomics characterises protein activity, interactions and the presence of post-translational modifications (reviewed in Mirzabekov & Kolchinsky, 2001; MacBeath, 2002; Venkatasubbarao, 2004). It usually begins with a subset of proteins sharing a common trait (*e.g.* affinity for a particular small molecule), isolated from a starting material.

Coupled to the use of microarrays or protein chips, functional proteomics aids in the discovery of novel protein functions in complex biological processes, based on certain inherent properties of the proteins such as specific protein-ligand interactions, presence of distinct functional groups and post-translational modifications. Several large-scale functional proteomics technologies have been developed to generate comprehensive, cellular protein-protein interaction maps (Drewes & Bouwmeester, 2003), which will prove very useful for the drug discovery process.

### *1.1.3 Objective of current investigation: proteomics in the study of Parkinson's disease*

Parkinson's disease (PD) is a common, progressive neurodegenerative illness, associated with a selective loss of dopaminergic neuron in the nigrostriatal pathway of the brain (Olanow & Tatton, 1999). While the aetiology of PD is hitherto unclear, evidences are accumulating to suggest that, like other chronic neurodegenerative disorders such as Alzheimer's disease (AD), PD is caused by a combination of events that impaired neuronal functions, such as oxidative stress, mitochondrial dysfunction, environmental toxins, endogenous toxins, proteosome dysfunction, and genetic defects have been proposed to play a role (Bossy-Wetzel *et al.*, 2004). While genetic studies have yielded several important pathogenetic factors such as alpha synuclein (Polymeropoulos *et al.*, 1997) and parkin (Kitada *et al.*, 1998) which are mutated in some cases of PD, the rapid development of novel and effective PD therapeutics requires the identification of a broader base of pathogenetic agents involved in dopaminergic cell death elicitation. This is especially so since sporadic Parkinson's disease (PD) constitutes 99% of the disorder, while only a mere 1% of the cases is of genetic origin (Mandel *et al.*, 2005). The use of proteomics should thus shed light on the overall mechanisms underlying PD pathogenesis and reveal novel therapeutic targets. Nevertheless, up to now, proteomics has mainly studied the

identity and levels of the abundant human, rat, and mouse brain proteins as well as changes of their levels and their chemical modifications deriving from neurological disorders, such as AD and Down's syndrome and in animal model of those disease, collecting information about gene products involved in their respective aetiologies (Cheon *et al.*, 2003; Bajo *et al.*, 2002; Butterfield & Boyd-Kimball, 2004; Choi *et al.*, 2004; Butterfield, 2004). On the other hand, few proteomic investigations were employed in the study of Parkinson's disease (Lee *et al.*, 2003; Basso *et al.*, 2004).

With these in mind, proteomic study was performed here with the aim to unearth novel players involved in the pathogenesis of PD. In this study, we employed the dopaminergic cell model, MN9D (Choi *et al.*, 1991), to identify proteins with altered expression induced by the administration of 1-methyl-4-phenylpyridinium ($MPP^+$), the active ion of the Parkinson-inducing neurotoxin 1-methyl-4-phenyl-1,2,3,6-tetrahydropyride (MPTP) (Davis *et al.*, 1979). By applying proteomics to the cell model used to recapitulate the biochemical and neuropathological changes occurring in sporadic PD, we aim to uncover novel proteins of potential prognostic and therapeutic values.

## 1.2 Materials and Methods

### *1.2.1 Cell culture and induction of apoptosis*

MN9D (obtained with courtesy of Dr Jun Chen, University of Pittsburgh and with agreement from Dr Alfred Heller, University of Chicago), was cultured in DMEM medium supplemented with 10% fetal bovine serum and 1% penicillin/streptomycin in a humidified atmosphere of 5% $CO_2$ at 37°C. To induce apoptosis, MN9D cells were treated with 500 μM of 1-Methyl-4-phenil-pyridinium ($MPP^+$) for 0, 4, 8 or 16 hours, after which the cells were harvested, lysed using a cell lysis buffer containing 50 mM HEPES pH 7.4 and 1% Triton X-100, and subjected to centrifugation at 12, 000 x *g* for 10 min at 4°C. The supernatant was then collected and concentrated using the Ultrafree-CL centrifugal units Biomax-5 with molecular weight cut-off of 5 kDa (Millipore, USA).

### *1.2.2 Two-dimensional gel electrophoresis*

The protein content of the cell lysates was determined by the Bradford protein assay. 2DGE was performed according to the manufacturer's protocol for the PROTEAN® II xi 2-D Cell Systems (Biorad, USA) based on the publications of O'Farrell & Goodman (1975) and Garrels (1979). 200 μg aliquots of the total cellular lysates proteins were loaded onto the immobilised pH gradient (IPG) strips (Biorad, USA) for IEF. Each IPG strip was rehydrated for 16 hours in 300 μL of rehydration buffer containing 8 M urea (Biorad, USA), 2% CHAPS (w/v, Sigma, USA), 2.8% DTT (w/v, Sigma, USA), 0.5% (v/v) ampholytes (Biorad, USA) and 200 μg

of cell lysates. Isoelectric focusing was performed at 20°C with the following setting: 300 V, 1 h; 1000 V, 1 h; 3000 V, 1 h; rapid ramp 6000 V, for 60 000VH; 500 V, 12 h.

Prior to the second dimensional separation by SDS-PAGE, the IPG-strips were first equilibrated for 15 min in 10 mL of equilibration buffer containing 50 mM Tris-HCl (pH 8.8), 6 M Urea, 30% glycerol (Merck, USA), 2% SDS (Merck, USA) and 1% DTT (w/v, Sigma, USA), after which the strips were equilibrated for a further 15 min in the same buffer in which DTT was replaced with 2.5% Iodoacetamide (IAA, w/v, Sigma, USA) to alkylate the free thiol groups of the reduced cysteine residues. SDS-PAGE was carried out on a PROTEAN® II xi 2-D apparatus (Biorad, USA) using a 12% resolving gel. SDS-PAGE was performed at a constant current of 5 mA for half an hour and subsequently, 25 mA per gel.

### *1.2.3 Silver stain visualisation of protein spots*

The gels were fixed overnight in 50% methanol (v/v, Fisher Chemicals, USA) and 5% acetic acid (v/v Merck, USA). Prior to silver staining, the gels were washed with 3 changes of deionised water for 1 h, after which the gels were sensitised with 0.2 g/L sodium thiosulphate (Sigma, USA) for 2 min. Subsequently, the gels were rinsed twice in deionised water for 1 min before staining in 0.1% silver nitrate (w/v, Sigma, USA) for 20 min at 4°C. The gels were rinsed twice in water for 1 min to remove the excess silver ions. The gels were then rinsed briefly with a small amount of developing solution containing 2% sodium carbonate (w/v, Sigma, USA) and 1.48% formaldehyde (v/v, Sigma, USA). Subsequently, the protein spots were developed to the desired intensity in fresh developing. The developing step was arrested by the addition of 5%

acetic acid, and then the gels were stored in 1% acetic acid until the spots of interest were excised for analysis.

### *1.2.4 Gel imaging and Identification of spots with up- or down-regulation*

Silver-stained 2-D gels were scanned using a GS-710 imaging densitometer (Biorad, USA), and the raw scans were processed by PDQuest software (Biorad, USA). Two-dimensional gels were evaluated visually pairwise, and changes of spots were considered with respect to variation in the presence or absence, quantity, and spot position.

### *1.2.5 In-gel tryptic digestion and mass spectrometry*

The protein spots of interest were excised by manual means and rinsed twice in deionised water. The spots were then washed in fresh deionised water for 10 min with agitation to completely remove traces of acetic acid. Freshly prepared potassium ferricyanide (10 mg/mL) and sodium thiosulphate (16 mg/mL) were mixed in equal volumes and 50 μL aliquots were immediately added to the gel fragments. The gel pieces were destained on a shaker for 30 min, after which the mixtures were spun briefly and the destaining solution was discarded. The gel fragments were washed in copious amount of deionised water before addition of 100 mM ammonium bicarbonate. The mixtures were vortexed for 20 min until the gel pieces were cleaned of silver stain. The mixtures were spun briefly and the solution was discarded. The gel pieces were then washed for 15 min in 50 mM ammonium bicarbonate/50% acetonitrile (J.T. Baker, USA) prior to shrinkage by addition of acetonitrile. The gels were dried to completion in a vacuum centrifuge.

Reswelling was carried out by the addition of 30μL of digestion solution containing 12.5 ng/μL trypsin (Promega, USA) in 50 mM ammonium bicarbonate for 30 min at 4°C. Excess trypsin was removed and tryptic digestion was carried out for 15 h at 37°C. The mixtures were cooled to room temperature before centrifugation at 3300 x *g* for 10 min. The supernatant fractions were saved whilst the gel pieces were treated with 20 mM ammonium bicarbonate for 10 min and centrifuged at 3300 x *g*. The resulting supernatants were combined were combined with the first supernatants. Final extraction was done by treatment with 5% formic acid (Fluka, USA) in 50% acetonitrile. The mixture was allowed to stand for 10 min and subsequently centrifuged at 3300 x *g* to collect the third supernatant, which was combined with the previous two supernatants. This combined supernatant was dried in a vacuum centrifuge.

The dried samples were then submitted to the Protein and Proteomic Centre, NUS, for MALDI-TOF. Briefly, each peptide obtained was dissolved in 1.5 μL of 50% acetonitrile and 0.5% trifluoroacetic acid (TFA, v/v), from which 1-μL aliquot was mixed with 0.5 μL of matrix solution on the stainless steel matrix assisted laser desorption ionisation (MALDI) target plate. The mixture was allowed to dry at room temperature and pressure. α-Cyano-4-hydroxycinnamic acid was used as the matrix. A Voyager-DE PRO MALDI-TOF mass spectrometer (Applied Biosystems, USA) equipped with delayed extraction and a nitrogen laser (337 nm, with a focal diameter of 25 nm) was used for all analyses. The flight tube length in the reflector mode is 2 m. The MALDI mass spectra were internally calibrated with angiotensin II and ACTH-clip 18-39 (Sigma, USA) and were optimised for the range 800-2000. The spectra were acquired in the positive-ion reflector mode using an accelerating voltage of 20 kV. Spectral data were obtained by averaging 10 spectra, each of which was the composite of 10 laser firings.

### *1.2.6 Protein identification through peptide mass fingerprinting*

Peptide masses obtained by MALDI-MS analysis were used to search the National Centre for Biotechnology Information database (NCBI, www.matrixscience.com) to identify the intact proteins. Often, a series of spots that differ slightly in pI represent the same proteins. Accordingly, some of the proteins that have a relatively low score but are positioned within such a series that match the predicted molecular mass and pI are also listed.

## 1.3 Results

### *1.3.1 Treatment with $MPP^+$ resulted in differential proteome profiles*

$MPP^+$, which is the active metabolite of the neurotoxin MPTP, is widely used as a neurotoxin in various models to study Parkinson's disease, as it was found to induce many of the biochemical and neuropathological changes that are observed in postmortem brains of PD patients (Davis *et al*., 1979). $MPP^+$ exerts its effect by inhibiting the complex I of the oxidative phosphorylation chain (Nicklas *et al*., 1985). The mitochondrial inhibition leads to a decrease in ATP production, as well as the formation of superoxide anion (Hasegawa *et al*., 1990). By-products generated with the reaction of the superoxide anion with other reactive oxygen species (ROS) e.g. nitric oxide (NO) could produce more damaging effects within the cell (Beckman, 1994). In our laboratory, we have previously demonstrated time- and dosage-dependent cell death of our model cell line, the mouse dopaminergic MN9D cells, in response to $MPP^+$ (Chee *et al.*, 2005). The optimum concentration of $MPP^+$ required for inducing about 50% cell death (LD50) was found to be 500 μM and was therefore chosen as a standard dosage for current investigations, since higher concentrations of $MPP^+$ did not further increase cell death.

For proteomic analysis, we used 2DGE to resolve several hundreds MN9D cell proteins. Differential gel analysis yielded quite a number of proteins showing altered level of expression with $MPP^+$ treatment of the MN9D cells. In the current investigation, the narrow range or zoom gels were utilised to better resolve closely spaced protein spots, so as to facilitate in their excision and eventual identification through MALDI. A representative of well-resolved gels of pH range 3-6 and 5-8 is shown in Figure 1.1 and 1.2, respectively. Comparison of the 2DGE protein profiles of unchallenged and $MPP^+$-challenged MN9D cells treated for various durations

(0, 2, 4, 8, 16 hours) revealed some differences in the protein patterns, even though the general profiles were similar between various treatments. Selected proteins that showed marked differences in expression across treatments were identified by peptide mass fingerprinting using MALDI-TOF. Figures 1.3-1.10 show the up- and down-regulation of proteins with $MPP^+$ treatments. It was noted that proteins that were up-regulated in one treatment, say 8 hours of $MPP^+$ exposure, might not be up-regulated in another treatment, say 16 hours of $MPP^+$ exposure (results not shown). Such dynamic kinetics of protein expression levels attests to the complexities of the molecular mechanisms involved in stress response.

### *1.3.2 Proposed roles of proteins identified by MALDI-TOF*

The identities of the proteins, as recognised through the use of MALDI-TOF, are listed in Table 1.1 and their proposed roles in $MPP^+$-exposed MN9D cells are presented below:

*(a)* *Nucleophosmin (NPM)* – Expression is up-regulated four hours after $MPP^+$ treatment (Figure 1.3). NPM is proposed to function in ribosomal assembly and transport. It is associated with pre-ribosomal particles and is localised in the granular region of the nucleolus (Prestayko *et al*., 1974; Spector *et al*., 1984; Yung *et al*., 1985). It also function as a molecular chaperone that prevents protein from aggregating in the crowded environment of the nucleolus (Szebeni & Oslon, 1999). NPM is recently shown to interact directly with the tumour suppressor protein, p53 and regulates its stability and transcriptional activation after different types of stress. It also induces p53-dependent premature senescence upon overexpression in diploid fibroblast (Colombo *et al*., 2002). NPM probably has a role in regulating p53 stability in MPP+-treated MN9D cells, but

given NPM's diverse cellular duties, its involvement may be much more complex than that.

*(b)* *Proteosome subunit, beta type 6* – Expression was up-regulated after eight hours of $MPP^+$ exposure (Figure 1.4). The proteosome is the major cellular proteolytic machinery responsible for the degradation of both the normal and damaged proteins, and hence play a pivotal role in retaining cellular homeostasis. It was shown that in human embryonic fibroblast cultures undergoing replicative senescence, the reduced levels of proteosomal activities during the process are accompanied by lower proteosome content and protein expression levels of some, but not all, proteosome subunits. Specifically, it was discovered that the loss of proteosome function is a result of reduced levels of beta type subunits, whereas the alpha-type subunits are in excess as "free" subunits in senescent cells (Chondrogianni *et al.*, 2003). Meanwhile, over-expression of the beta-type 5 subunit was shown to enhance proteosome activities, increased protein expression levels of the other proteosome subunits, and efficiently assembled proteosome. The increased amount of assembled proteosome resulted in more functional proteosome being produced, which in turn conferred enhanced survival following treatment with oxidants (Chondrogianni *et al.*, 2005). Its up-regulation with $MPP^+$ treatment may hence be indicative of elevated amount of ROS-damaged proteins in the cell and is probably required for assembly of more proteosomal complex to cope with cellular stress.

*(c)* *Ribosomal protein Large P2 subunit* – Up-regulated after eight hours of $MPP^+$ treatment (Figure 1.5). This eukaryotic acidic protein, together with P1 protein, modulate the

activity of the ribosomal stalk. These are the only ribosomal components for which there is a cytoplasmic pool (Mitsui *et al.*, 1988). Phosphorylation and N-terminal region of yeast ribosomal P1 mediate its degradation. However, association of P2 protects the P1 proteins from the proteosomal-independent degradation (Nusspaumer *et al.*, 2000). Elevated P2 level may lead to increased stability of P1, and the ribosomal structure, hence avoiding a halt in protein synthesis during cellular stress. Conversely, the increase in the amount of P2 detected with $MPP^+$ treatment may be a consequence of their release from oxidant-damaged ribosomal complex. An excess of proteins could be damaging to the cell, probably due to the tendency of these proteins to bind RNA, interfering with the translational machinery (Nusspaumer *et al.*, 2000). Other components of the ribosomal complex have been implicated in the regulation cellular response to stress and apoptosis. For example, over-expresison of ribosomal protein S13 and L23 can promote multi-drug resistance in gastric cancer cells by suppressing apoptosis (Shi *et al.*, 2004). Meanwhile, ribosomal protein L11 was shown to bind to and suppress the E3 ligase function of HDM2, thus activating p53 which can lead to cell cycle arrest and/or apoptosis (Bhat *et al.*, 2004). Research into alternative physiological function(s) of ribosomal protein P2 subunit may thus shed light on the significance of its heightened expression in the MN9D cells after $MPP^+$ treatment.

*(d)* *Glycinamide ribonucleotide synthetase* - Up-regulated after eight hours of $MPP^+$ treatment (Figure 1.6). Purines are critical for energy metabolism, cell signalling and cell reproduction. Purine nucleotides function as precursors for RNA and DNA synthesis, coenzymes, energy transfer molecules and regulatory factors in higher organisms

(Brodsky *et al.*, 1997). Nevertheless, little is known about the regulation of this essential biochemical pathway during mammalian development. In humans, the second step of *de novo* purine biosynthesis are catalysed by a trifunctional protein with glycinamide ribonucleotide synthetase (GARS). The expression of GARS is highly regulated during development of the human cerebellum. It is expressed at high levels during normal prenatal cerebellum development and become undetectable in this tissue shortly after birth. In contrast, it continues to be expressed during the postnatal development of the cerebellum in individuals with Down syndrome (Brodsky *et al.*, 1997). Individuals with Down syndrome have elevated serum purine levels (Pant *et al.*, 1968), and elevated purine levels have been associated with mental retardation (Lesch & Nyhan, 1964; Jaeken & Van den Berghe, 1984). Down syndrome patients have a very high incidence of early onset of clinical, as well as neuropathological symptoms associated with Alzheimer disease like white matter lesions (de la Monte *et al.*, 1990). Though the level of GRAS expression in Parkinson's disease patients brain has yet to be determined, its marked up-regulation in the cell model here still renders it a potential candidate as a biomarker for diseases involving neuronal degeneration, such as Down syndrome, Parkinson's and Alzheimer disease.

*(e)* *Phosphoglycerate Mutase* – Expression is down-regulated after eight hours of $MPP^+$ treatment (Figure 1.7). The enzyme catalyzes the interconversion of 3-phosphoglycerate and 2-phosphoglycerate in the glycolysis and gluconeogenesis pathway. Expression of this protein was also shown to be down-regulated in methamphetamine-induced dopaminergic neurotoxicity in the ventral midbrain (Xie *et al.*, 2002). Growing evidence

suggests that brain injury after methamphetamine administration is due to an increase in free radical formation and mitochondria damage, resulting in a failure of cellular energy metabolism and secondary excitoxicity (Virmani *et al*., 2002). Down regululation of phosphoglycerate mutase 1 was also discovered through proteomic analysis of corticobasal degeration, which is an adult-onset progressive neurodegenerative disorder (Chen *et al*., 2005). Interestingly, when proteome techniques was used to examine the regional *in vivo* protein oxidation induced by amyloid beta-peptide (1-42) injected into nucleus basalis magnocellularis of rat brain compared with saline-injected control, phosphoglycerate mutase 1 was found to be one of the few proteins to be extensively oxidised (Boyd-Kimball *et al*., 2005). Down-regulation of phosphoglycerate mutase in $MPP^+$-treated MN9D cells, as well as in other neurodegenerative disease cell models, may thus be a consequence of proteosome-mediated degradation of the oxidised protein, and may represent an important biomarker for neurodegenerative diseases in general.

*(f)* *PKCq- interacting protein (PICOT)* – Expression is up-regulated four hours after $MPP^+$ treatment (Figure 1.8). PICOT interacts with protein kinase C-θ, mediated by an N-terminal thioredoxin homology domain, and is thought to play a role in regulating the function of thioredoxin system (Witte *et al*., 2000). The latter is thought to be involved in free-radical scavenging, as well as redox modification of the DNA-binding domain of *fos* and *jun*, hence controlling the DNA binding of AP-1. Transient over-expression of full-length PICOT in T-cells inhibited the activation of c-jun N-terminal kinase, and the transcriptional factors AP-1 and NF-κB (Witte *et al*., 2000). Heightened expression of PICOT may hence be indicative of elevated oxidative stress within the cells with $MPP^+$

treatment, and may regulate diverse cellular processes in response to cell stress via inhibition of transcriptional factors activation.

*(g)* *Spermidine synthase* – Expression is up-regulated four hours of $MPP^+$ exposure (Figure 1.9). This enzyme adds an aminopropyl group to a polyamine spermidine, forming spermine. Together with putrescine, the three are essential for cell survival and proliferation. Depletion of intracellular polyamines using inhibitors of polyamine biosynthesis triggers the mitochondria-mediated pathway for apoptosis, resulting in caspase activation and apoptotic cell death in both the murine and human B cell line and Jurkat cells (Nitta *et al*., 2002). Also, spermine has been shown to be capable of scavenging free radicals generated by amyloid beta-peptide in solution as measured by electron paramagnetic resonance spectroscopy. By extrapolation then, its up-regulation may serve as a defense mechanism against oxidative damage and apoptosis activation in the current cell model, and is useful as an indicator of free radical damage upon $MPP^+$ treatment.

*(h)* *Peptidylprolyl isomerase A* - Also called cyclophilin-A. Down-regulated after eight hours of $MPP^+$ treatment (Figure 1.10). Cyclophilin-A is the cytosolic isoform of a cyclosporin-A binding family of peptidylproline cis-trans-isomerases that catalyze rotation of Xaa–Pro peptide bonds. It binds to the heat shock protein hsp90 (Nadeau *et al*., 1993) and stiumlate the activity of the thiol-specific antioxidant protein Aop1 (Jaschke *et al*., 1998). Rat neonatal cardiomyocyte depleted of cyclophilin-A using siRNA were shown to be more sensitive to treatment by t-butylhydroperoxide, which

mimics the oxidative stress associated with reperfusion-induced cell death (Doyle *et al.*, 1999). Knockdown of cyclophilin-A resulted in slower growth, decreased proliferation, and a greater degree of apoptosis in the tumors overexpressing the protein. On the other hand, overexpression of cyclophilin-A protected cells from death after overexpression of SODV148G, a familial amyotrophic lateral sclerosis (FALS)-associated mutant Cu/Zn superoxide dismutase-1 (SOD) gene (Lee *et al*., 1999). Though these indicate a protective function of cyclophilin-A against cell death, other evidences seem to show otherwise. For example, over-expression of a yeast apoptosis-inducing factor (AIF) was shown to strongly stimulate apoptotic cell death induced by hydrogen peroxide and this effect was attenuated by disruption of cyclophilin A (Wissing *et al*., 2004). AIF was further demonstrated to interact with cyclophilin-A, and that recombinant AIF and CypA proteins synergised *in vitro* in the degradation of plasmid DNA, as well as in the capacity to induce DNA loss in purified nuclei. The apoptogenic cooperation between AIF and cyclophilin-A did not rely on the cyclophilin-A's peptidyl-prolyl *cis-trans* isomerase activity (Cande *et al*., 2004). As such, the role that cyclophilin-A plays during apoptosis and oxidative stress seems to be contradictory, and manifestation of a specific role instead of the other may well depend on the cell-/tissue-type, as well as the death stimuli involved. Whether down-regulation of cyclophilin-A with $MPP^+$ treatment in the MN9D cells is a sign of the cells' waning defence against oxidative stress, or that it represents an anti-apoptotic mechanism remains to be further verified.

As many more spots with altered expression were observed with $MPP^+$ treatment, it was clearly an attractive proposal to identify all of them. The identification of these proteins, which may either mediate anti-oxidative or anti-apoptotic effect or participate in the cell death signalling,

would aid in intervention of dopaminergic neuronal degeneration in the Parkinson's disease. Though these spots are discernable on the 2DE gel, identifying them through MALDI-TOF proved to be a challenge due to insufficiency of the protein quantity contained within the silver-stained excised spots. The possibility that two or more protein might be present within a single spot could not be dispelled, as revealed by the inclusion of proteins of widely different nature and functions within the same peptide mass fingerprinting search results for several spots. More cell lysates could be loaded onto the 2-DE gels to ensure sufficient protein quantity within a single spot for MALDI-TOF analysis. However, this strategy calls for more stringent desalting protocol to be implemented to prevent 'burning' of the IEF strips during the first-dimensional separation. This could be achieved with multiple washes with low salt buffer using desalting column from Millipore. Meanwhile, the use of micro-Range IEF strips (e.g. pH 3.9-5.1 or pH 5.5-6.7) could aid in separating overlapping spots for their precise excision for MALDI-TOF.

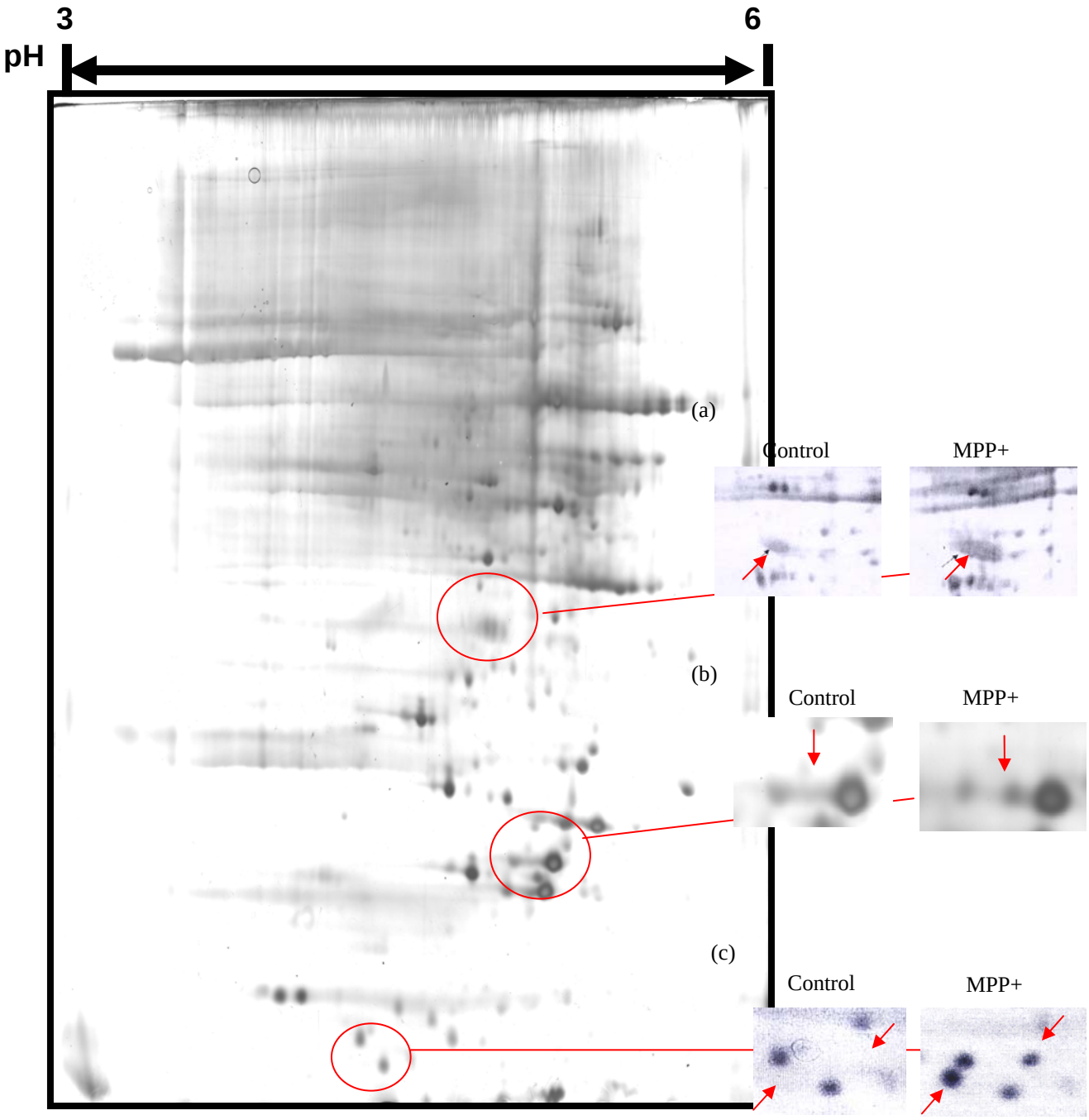


**Figure 1.1. 2-D gel electrophoresis of control or MPP$^+$-treated MN9D cells.** Extracted proteins were separated by 2-D gel electrophoresis as detailed in Materials and Methods using pH range 3-6 IEF strips (Biorad, USA). The gels were silver-stained and analysed visually for altered protein expressions. Protein spot outlined (a-c) showed consistent altered expression in two or more gels and were selected for MALDI-TOF analysis.

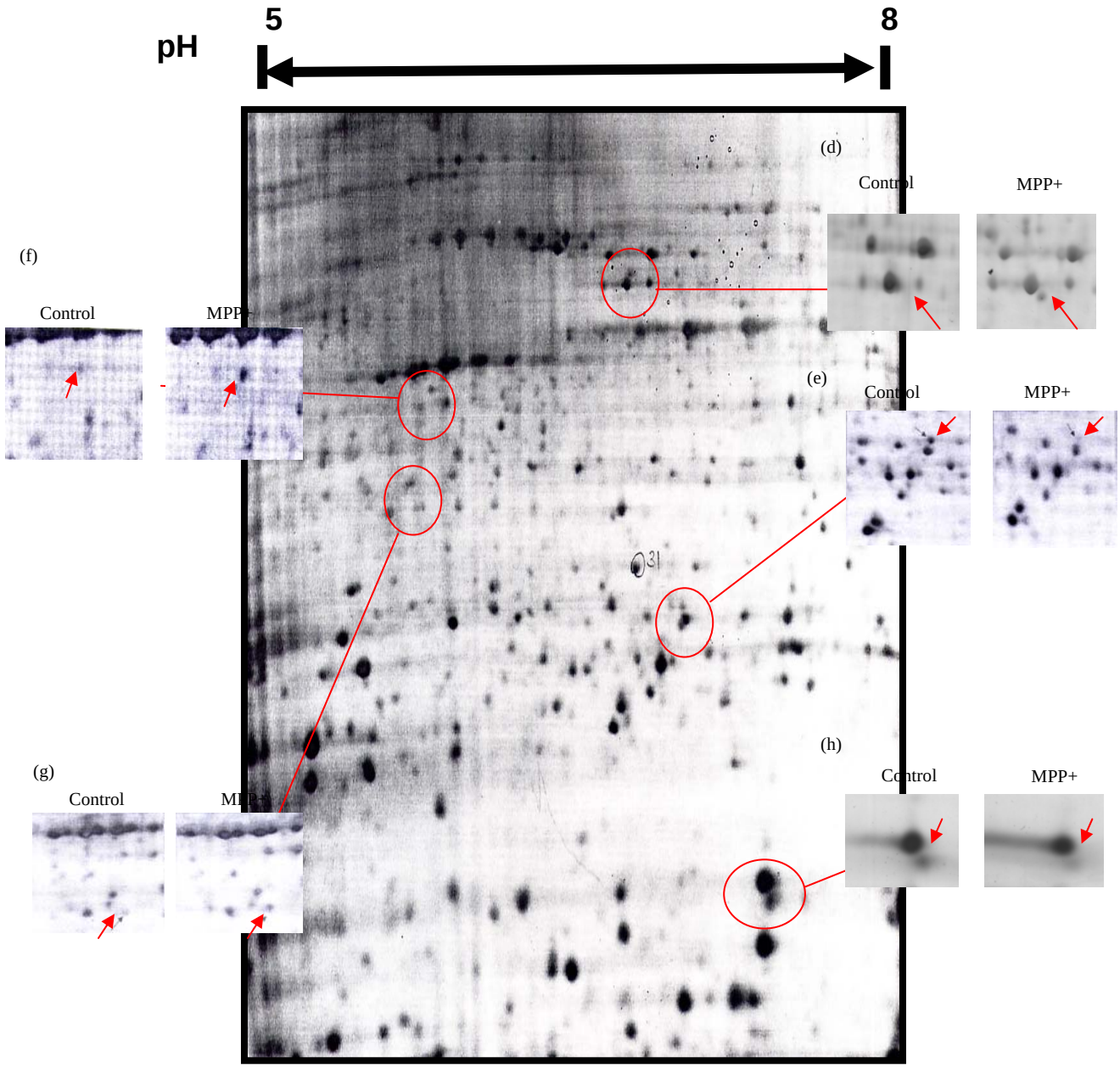


**Figure 1.2. 2-D gel electrophoresis of control or MPP$^+$-treated MN9D cells.** Extracted proteins were separated by 2-D gel electrophoresis as detailed in Materials and Methods using pH range 5-8 IEF strips (Biorad, USA). The gels were silver-stained and analysed visually for altered protein expressions. Protein spot outlined (d-h) showed consistent altered expression in two or more gels and were selected for MALDI-TOF analysis.

| No. | Identity | pI | Mr (kDa) | MOWSE Score | Functions | Level Up/Down regulated after MPP+ Treatment? |
|---|---|---|---|---|---|---|
| **a** | **Nucleophosmin** | 4.62 | 32.0 | 9.22e + 0.05 | •Ribosome biogenesis<br>•Shuttle protein in the nuclear import<br>•Molecular chaperoning activities<br>•Regulates p53 stability | ↑ |
| **b** | **Proteosome subunit, beta type 6** | 4.99 | 21.7 | 2.36e + 0.05 | •Essential component of complexes involved in extralysosomal energy and ubiquitin-dependent proteolytic pathway. | ↑ |
| **c** | **Ribosomal Protein, Large P2** | 4.42 | 12.0 | 4.47e + 0.04 | •Along with P0 and P1 ribosomal units constitute part of the elongation factor-binding site connected to GTPase centre in the 60S ribosomal unit | ↑ |
| **d** | **Glycinamide ribonucleotide synthetase** | 6.15 | 45.6 | 2.27e + 0.05 | •catalyzes the second step of the de novo purine biosynthetic pathway; the conversion of phosphoribosylamine, glycine, and ATP to glycinamide ribonucleotide (GAR). | ↑ |
| **e** | **Phosphoglycerate Mutase** | 6.68 | 28.0 | 3.003 + 0.09 | •Catalyzes the interconversion of 3-phosphoglycerate (3PG) and 2-phosphoglycerate (2PG) in the glycolysis and gluconeogenesis pathway.<br>•Expression of this protein was also shown to be down regulated in methamphetamine-induced dopaminergic neurotoxicity in the ventral midbrain | ↓ |
| **f** | **PKCq-Interacting Cousin of Thioredoxin (PICOT)** | 5.43 | 37.0 | 1.68e + 0.03 | •Interacts with protein kinase C-θ, mediated by an N-terminal thioredoxin homology domain<br>•Play a role in regulating the function of thioredoxin system<br>•Redox modification of DNA-binding domain of *fos* and *jun*, hence controlling the DNA binding of AP-1. | ↑ |
| **g** | **Spermidine synthase** | 5.31 | 34.0 | 2.50e + 0.07 | •May function directly as a free radical scavenger; its up-regulation may indicate free radical damage upon MPP+ treatment | ↑ |
| **h** | **Peptidylprolyl isomerase A** | 7.73 | 18.0 | 2.27e + 0.05 | •accelerate folding of some proteins both in vivo and in vitro by catalyzing slow steps in the initial folding and rearrangement of proline-containing proteins | ↓ |

**Table 1.** Table listing the identities of some up/down regulated spots identified through differential gel comparison (MPP+-treated gels vs non-treated control gels, as shown in Figure 1.1 and 1.2), expected pI and molecular weight, MOWSE scores, their physiological functions known to date, as well as their direction of alteration of expression with $MPP^+$ treatment.

**Figure 1.3. MALTI-TOF identification of protein marked (a) in Figure 1.1 with $MPP^+$ -induced altered expression**. (i) The spot marked in Figure 1.1 (a) showed consistent up-regulation of protein expression with four hours of $MPP^+$ treatment. (ii) MALDI-TOF peptide mass mapping of spot (a). Peptides were produced by in-gel tryptic digestion. The peptide masses were used for NCBI database search to identify intact protein. Tryptic peptides that map to the protein sequence with the right molecular mass and pI within a mass accuracy of 100 parts per million (ppm) were indicated by an arrow in (ii) and a solid black underline in (iii). (iv) indicates the identity of the protein sequence as revealed through NCBI database search using the peptide mass fingerprint obtained in (ii).

(a)

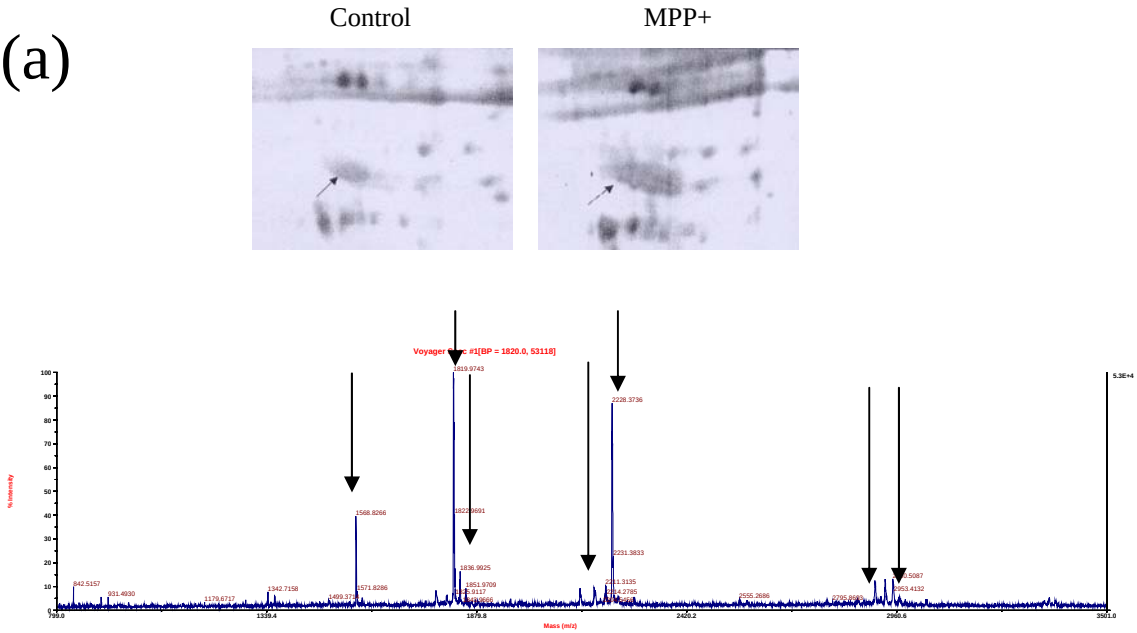


1 medsmdmdms plrpqnylfg celkadkdyh fkvdndeneh qlslrtvslg agakdelhiv

61 eaeamnyegs pikvtlatlk msvqptvslg gfeitppvvl rlkcgsgpvh isgqhlvave

121 edaesedede edvkllgmsg krsapgggnk vpqkkvklde ddedddedde ddeddddddf

181 deeeteekvp vkksvrdtpa knaqksnqng kdlkpstprs kgqesfkkqe ktpktpkgps

241 svedikakmq asiekggslp kveakfinyv kncfrmtdqe aiqdlwqwrk sl

| Identity | pI | Mr (kDa) | MOWSE Score | % Coverage | Functions | Level Up/Down regulated after MPP+ Treatment? |
|---|---|---|---|---|---|---|
| **Nucleo-phosmin** | 4.62 | 32 | 9.22e + 0.05 | 28% | •Ribosome biogenesis<br>•Shuttle protein in the nuclear import<br>•Molecular chaperoning activities<br>•Regulates p53 stability | ↑ |

**Figure 1.4. MALTI-TOF identification of protein marked (b) in Figure 1.1 with $MPP^+$ -induced altered expression**. (i) The spot marked in Figure 1.1 (b) showed consistent up-regulation of protein expression with eight hours of $MPP^+$ treatment. (ii) MALDI-TOF peptide mass mapping of spot (b). Peptides were produced by in-gel tryptic digestion. The peptide masses were used for NCBI database search to identify intact protein. Tryptic peptides that map to the protein sequence with the right molecular mass and pI within a mass accuracy of 100 parts per million (ppm) were indicated by an arrow in (ii) and a solid black underline in (iii). (iv) indicates the identity of the protein sequence as revealed through NCBI database search using the peptide mass fingerprint obtained in (ii).

(b)

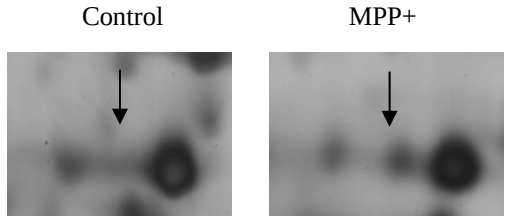


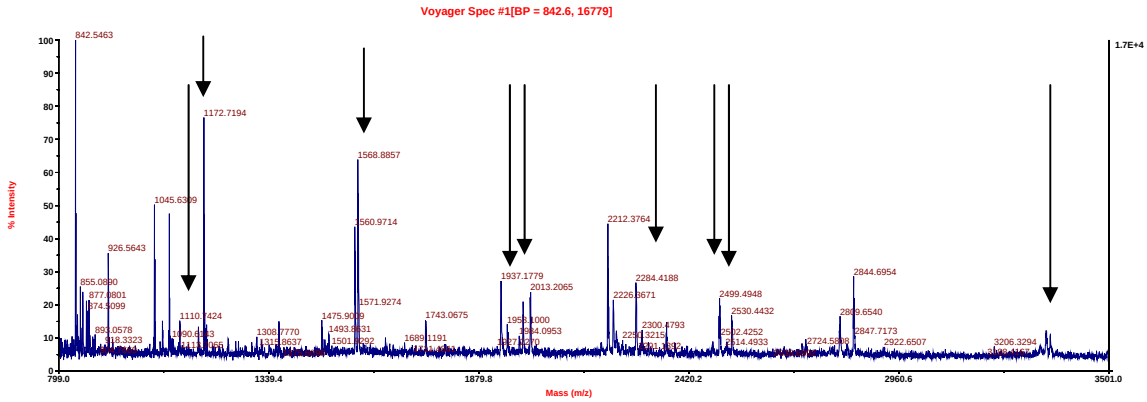


1 mavqfnggvv lgadsrtttg syianrvtdk ltpihdhifc crsgsaadtq avadavtyql

61 gfhsielnep plvhtaaslf kemcyryred lmagiiiagw dpqeggqvys vpmggmmvrq

121 sfaiggsgss yiygyvdaty regmtkdecl qftanalala merdgssggv irlaaiqesg

181 verqvllgdq ipkftiatlp pp

| Identity | pI | Mr (kDa) | MOWSE Score | % Coverage | Functions | Level Up/Down regulated after MPP+ Treatment? |
|---|---|---|---|---|---|---|
| **Proteosome subunit, beta type 6** | 4.99 | 21.7 | 2.36e + 0.05 | 60% | •essential components of complexes involved in an extralysosomal energy- and ubiquitin-dependent proteolytic pathway | ↑ |

**Figure 1.5. MALTI-TOF identification of protein marked (c) in Figure 1.1 with $MPP^+$ -induced altered expression**. (i) The spot marked in Figure 1.1 (c) showed consistent up-regulation of protein expression with eight hours of $MPP^+$ treatment. (ii) MALDI-TOF peptide mass mapping of spot (c). Peptides were produced by in-gel tryptic digestion. The peptide masses were used for NCBI database search to identify intact protein. Tryptic peptides that map to the protein sequence with the right molecular mass and pI within a mass accuracy of 100 parts per million (ppm) were indicated by an arrow in (ii) and a solid black underline in (iii). (iv) indicates the identity of the protein sequence as revealed through NCBI database search using the peptide mass fingerprint obtained in (ii).

(c)

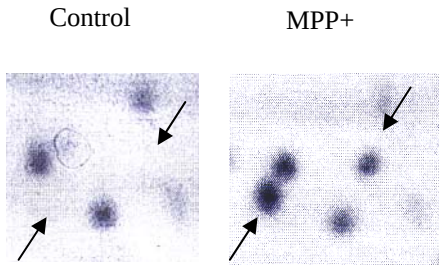


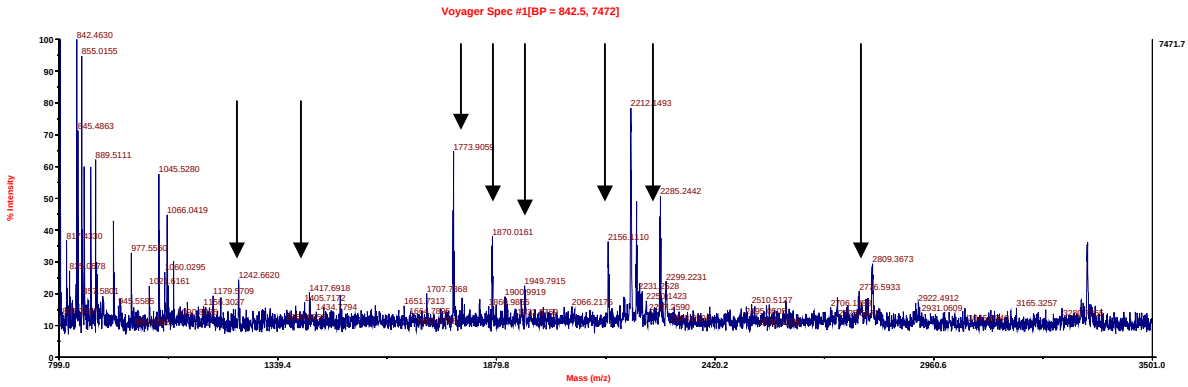


1 mryvasylla alggnsspsa kdikkildsv gieadddrln kviselngkn iedviaqgvg

61 klasvpagga vavsaapgsa apaagsapaa aeekkdekke eseesdddmg fglfd

| Identity | pI | Mr (kDa) | MOWSE Score | % Coverage | Functions | Level Up/Down regulated after MPP+ Treatment? |
|---|---|---|---|---|---|---|
| **Ribosomal Protein, Large P2** | 4.42 | 12 | 4.47e + 0.04 | 87% | •Along with P0 and P1 ribosomal units constitute part of the elongation factor-binding site connected to GTPase centre in the 60S ribosomal unit | ↑ |

**Figure 1.6. MALTI-TOF identification of protein marked (d) in Figure 1.2 with $MPP^+$ -induced altered expression**. (i) The spot marked in Figure 1.2 (d) showed consistent up-regulation of protein expression with eight hours of $MPP^+$ treatment. (ii) MALDI-TOF peptide mass mapping of spot (d). Peptides were produced by in-gel tryptic digestion. The peptide masses were used for NCBI database search to identify intact protein. Tryptic peptides that map to the protein sequence with the right molecular mass and pI within a mass accuracy of 100 parts per million (ppm) were indicated by an arrow in (ii) and a solid black underline in (iii). (iv) indicates the identity of the protein sequence as revealed through NCBI database search using the peptide mass fingerprint obtained in (ii).

(d)

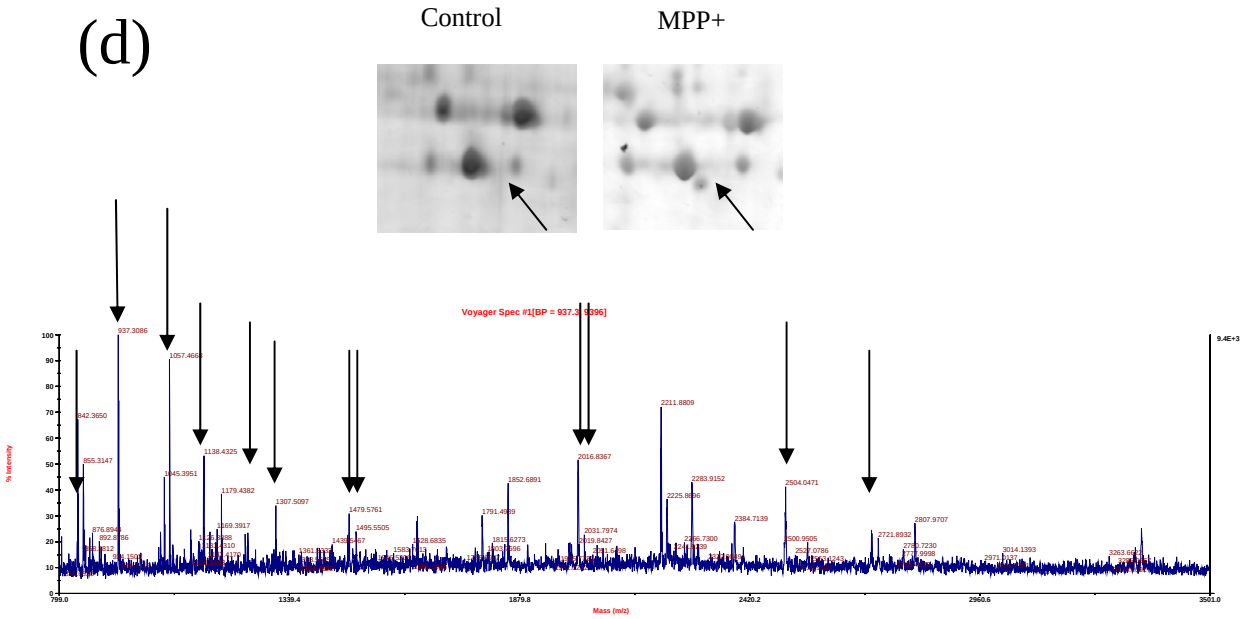


1 maarvlvigs ggrehtlawk laqspqvkqv lvapgnagta gagkisnaav svndhsalaq

61 fckdekielv vvgpeaplaa givgdltsag vrcfgptaqa aqlesskkfa kefmdrheip

121 taqwraftnp edacsfitsa nfpalvvkas glaagkgviv aksqaeacra vqeimqeksf

181 gaagetvvve eflegeevsc lcftdgktva emppaqdhkr lldgdegpnt ggmgaycpap

241 qvskdllvki kntilqravd gmqqegapyt gilyagimlt kdgpkvlefn crfgdpecqv

301 ilpllksdly evmqstlggl lsaslpvwle nhsavtvvma skgypgaytk gveitgfpea

361 qalglqvfha gtalkdgkvv tsggrvltvt avqenlmsal aearkglaal kfegaiyrkd

421 igfravaflq rpr

| Identity | pI | Mr (kDa) | MOWSE Score | % Coverage | Functions | Level Up/Down regulated after MPP+ Treatment? |
|---|---|---|---|---|---|---|
| **Glycinamide ribonucleotide synthetase** | 6.15 | 45.6 | 2.27e + 0.05 | 33% | •catalyzes the second step of the de novo purine biosynthetic pathway; the conversion of phosphoribosylamine, glycine, and ATP to glycinamide ribonucleotide (GAR) | ↑ |

**Figure 1.7. MALTI-TOF identification of protein marked (e) in Figure 1.2 with $MPP^+$ -induced altered expression**. (i) The spot marked in Figure 1.2 (e) showed consistent down-regulation of protein expression with eight hours of $MPP^+$ treatment. (ii) MALDI-TOF peptide mass mapping of spot (e). Peptides were produced by in-gel tryptic digestion. The peptide masses were used for NCBI database search to identify intact protein. Tryptic peptides that map to the protein sequence with the right molecular mass and pI within a mass accuracy of 100 parts per million (ppm) were indicated by an arrow in (ii) and a solid black underline in (iii). (iv) indicates the identity of the protein sequence as revealed through NCBI database search using the peptide mass fingerprint obtained in (ii).

(e)

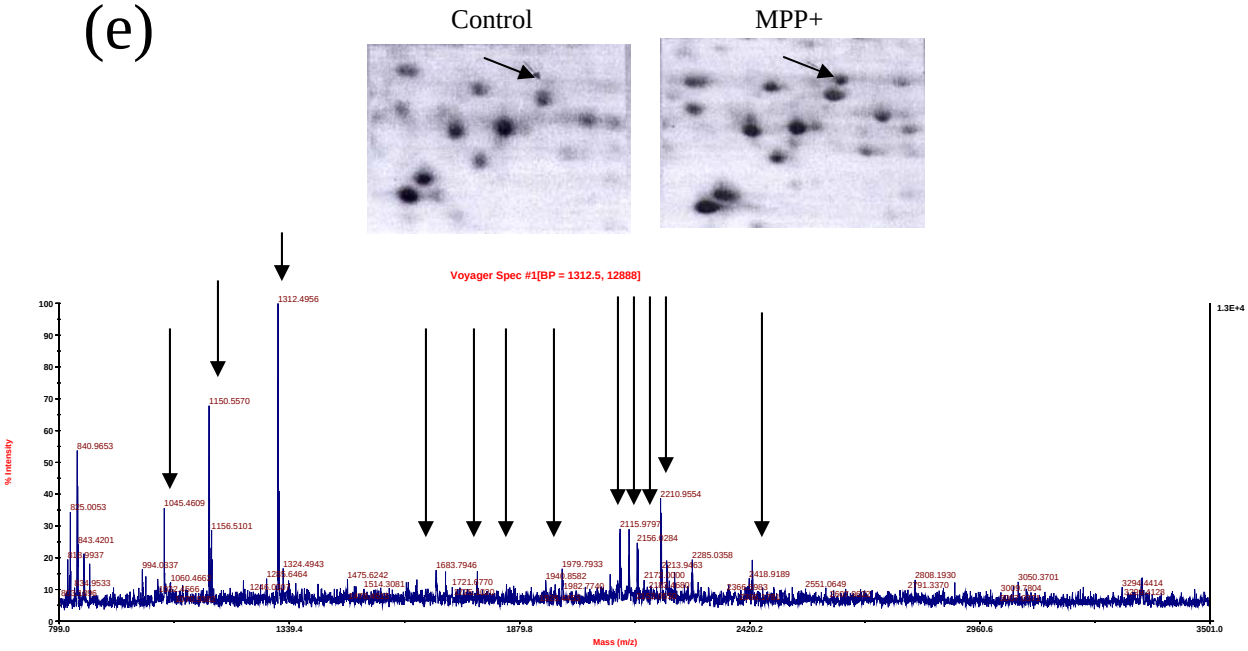


1 maayklvlir hgesawnlen rfsgwydadl spagheeakr ggqalrdagy efdicftsvq

61 krairtlwtv ldaidqmwlp vvrtgrlner hyggltglnk aetaakhgea qvkiwrrsyd

121 vppppmepdh pfysniskdr ryadltedql psceslkdti aralpfwnee ivpqikegkr

181 vliaahgnsl rgivkhlegl seeaimelnl ptgipivyel dknlkpikpm qflgdeetvr

241 kameavaaqg kvkk

| Identity | pI | Mr (kDa) | MOWSE Score | % Coverage | Functions | Level Up/Down regulated after MPP+ Treatment? |
|---|---|---|---|---|---|---|
| **Phosphoglycerate Mutase** | 6.68 | 28 | 3.003 + 0.09 | 54% | •Catalyzes the interconversion of 3-phosphoglycerate (3PG) and 2-phosphoglycerate (2PG) in the glycolysis and gluconeogenesis pathway.<br><br>•Expression of this protein was also shown to be down regulated in methamphetamine-induced dopaminergic neurotoxicity in the ventral midbrain | ↓ |

**Figure 1.8. MALTI-TOF identification of protein marked (f) in Figure 1.2 with $MPP^+$ -induced altered expression**. (i) The spot marked in Figure 1.2 (f) showed consistent up-regulation of protein expression with four hours of $MPP^+$ treatment. (ii) MALDI-TOF peptide mass mapping of spot (f). Peptides were produced by in-gel tryptic digestion. The peptide masses were used for NCBI database search to identify intact protein. Tryptic peptides that map to the protein sequence with the right molecular mass and pI within a mass accuracy of 100 parts per million (ppm) were indicated by an arrow in (ii) and a solid black underline in (iii). (iv) indicates the identity of the protein sequence as revealed through NCBI database search using the peptide mass fingerprint obtained in (ii).

(f)

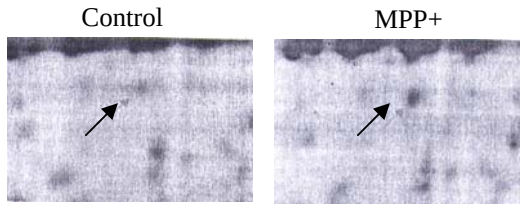


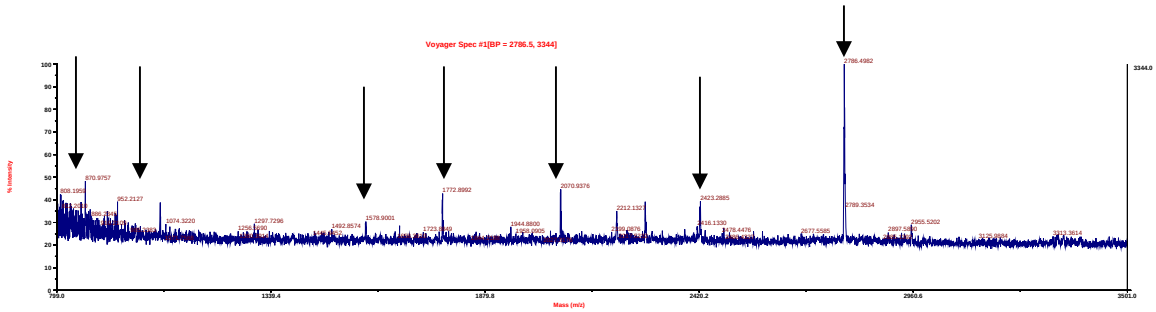


1 maagaaeage aavavvevgs aqqfeellrl ktksllvvhf wapwapqcvq mndvmaelak

61 ehphvsfvkl eaeavtevse kyeissvptf lffknsqkvd rldgahapel tkkvqrhvss

121 gafppstneh lkedlslrlk klthaapcml fmkgtpqepr cgfskqmvei lhkhniqfss

181 fdifsdeevr qglktysnwp typqlyvsge liggldiike leaseeldti cpkapkleer

241 lkvltnkasv mlfmkgnkqe akcgfskqil eilnstgvey etfdiledee vrqglktfsn

301 wptypqlyvr gdlvggldiv kelkdngell pilkgen

| Identity | pI | Mr (kDa) | MOWSE Score | % Coverage | Functions | Level Up/Down regulated after MPP+ Treatment? |
|---|---|---|---|---|---|---|
| **PKCq-Interacting Cousin of Thioredoxin (PICOT)** | 5.43 | 37 | 1.68e + 0.03 | 32% | •Interacts with protein kinase C-θ, mediated by an N-terminal thioredoxin homology domain<br><br>•Play a role in regulating the function of thioredoxin system<br><br>•Redox modification of DNA-binding domain of *fos* and *jun*, hence controlling the DNA binding of AP-1 | ↑ |

**Figure 1.9. MALTI-TOF identification of protein marked (g) in Figure 1.2 with $MPP^+$ -induced altered expression**. (i) The spot marked in Figure 1.2 (g) showed consistent up-regulation of protein expression with four hours of $MPP^+$ treatment. (ii) MALDI-TOF peptide mass mapping of spot (g). Peptides were produced by in-gel tryptic digestion. The peptide masses were used for NCBI database search to identify intact protein. Tryptic peptides that map to the protein sequence with the right molecular mass and pI within a mass accuracy of 100 parts per million (ppm) were indicated by an arrow in (ii) and a solid black underline in (iii). (iv) indicates the identity of the protein sequence as revealed through NCBI database search using the peptide mass fingerprint obtained in (ii).

(g)

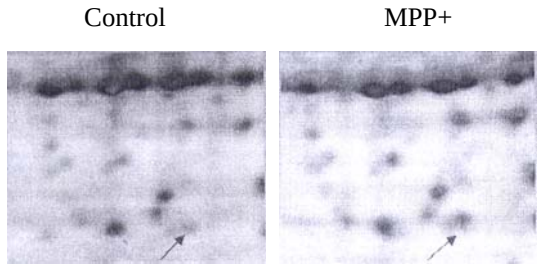


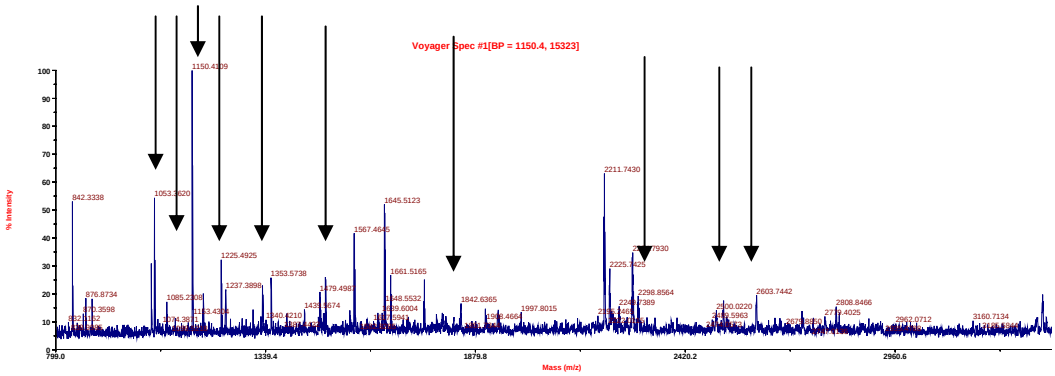


1 mepgpdgpaa pgpaairegw fretcslwpg qalslqveql lhhrrsryqd ilvfrsktyg

61 nvlvldgviq cterdefsyq emianlplcs hpnprkvlii gggdggvlre vvkhpsvesv

121 vqceidedvi evskkflpgm avgfssskIt lhvgdgfefm kqnqdafdvi itdssdpmgp

181 aeslfkesyy qlmktalked gilccqgecq wlhldlikem rhfckslfpv vdyaycsipt

241 ypsgqigfml csknpstnfr epvqqltqaq veqmqlkyyn sdmhraafvl peftrkalnd

301 is

| Identity | pI | Mr (kDa) | MOWSE Score | % Coverage | Functions | Level Up/Down regulated after MPP+ Treatment? |
|---|---|---|---|---|---|---|
| **Spermidine synthase** | 5.31 | 34 | 2.50e + 0.07 | 54% | •May function directly as a free radical scavenger; its up-regulation may indicate free radical damage upon MPP+ treatment | ↑ |

**Figure 1.10. MALTI-TOF identification of protein marked (h) in Figure 1.2 with $MPP^+$ -induced altered expression**. (i) The spot marked in Figure 1.2 (h) showed consistent down-regulation of protein expression with eight hours of $MPP^+$ treatment. (ii) MALDI-TOF peptide mass mapping of spot (h). Peptides were produced by in-gel tryptic digestion. The peptide masses were used for NCBI database search to identify intact protein. Tryptic peptides that map to the protein sequence with the right molecular mass and pI within a mass accuracy of 100 parts per million (ppm) were indicated by an arrow in (ii) and a solid black underline in (iii). (iv) indicates the identity of the protein sequence as revealed through NCBI database search using the peptide mass fingerprint obtained in (ii).

(h)

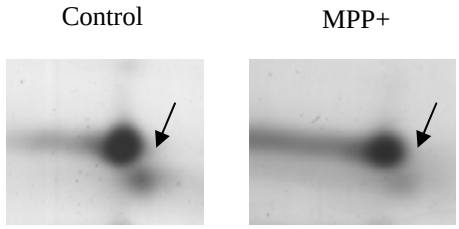


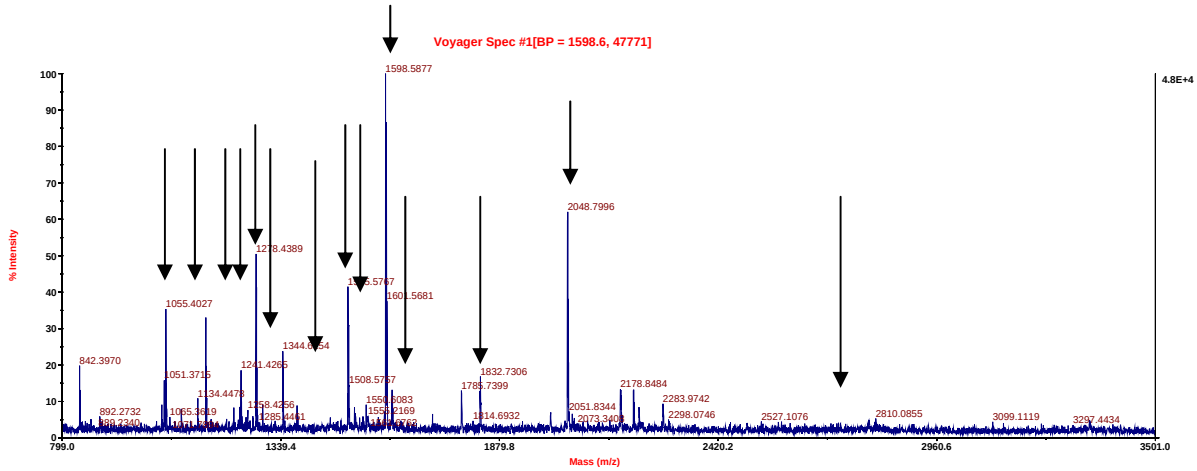


1 mvnptvffdi taddeplgrv sfelfadkvp ktaenfrals tgekgfgykg ssfhriipgf

61 mcqggdftrh ngtggrsiyg ekfedenfil khtgpgilsm anagpntngs qffictakte

121 wldgkhvvfg kvkegmnive amerfgsrng ktskkitisd cgql

| Identity | pI | Mr (kDa) | MOWSE Score | % Coverage | Functions | Level Up/Down regulated after MPP+ Treatment? |
|---|---|---|---|---|---|---|
| **peptidylprolyl isomerase A** | 7.73 | 18.0 | 2.27e + 0.05 | 73% | •accelerate folding of some proteins both in vivo and in vitro by catalyzing slow steps in the initial folding and rearrangement of proline-containing proteins | ↓ |

## 1.4 Discussion

Two-dimensional electrophoresis comparisons of the protein expression patterns between the normal and diseased tissues or before and after therapeutic treatment allow for the identification of proteins involved in pathogenesis (Pandey & Mann, 2000). Through MALDI-TOF analysis, eight proteins were identified which are associated with several distinct functional categories: cell cycle arrest and p53 binding/protein chaperoning (nucleophosmin), energy metabolism (glycinamide ribonucleotide synthetase), protein synthesis (ribosomal large P2 subunit) or degradation (proteosome subunit beta 6), stress response (PICOT), antioxidant enzyme (peptidylprolyl isomerase A and spermidine synthase), and anaerobic glycolysis (phosphoglycerate mutase). With the exception of phosphoglycerate mutase and peptidylprolyl isomerase A, which were down-regulated after treatment, the other six proteins showed heightened expression level with $MPP^+$ treatment. These data suggest that the $MPP^+$-induced cell stress and apoptosis involves the systematic activation of multiple pathways that are glycolysis-relevant, oxidative stress-mediated, and possibly mediated through inter-organelle crosstalks.

### *1.4.1 Deployment of cellular defence mechanisms in response to $MPP^+$ insults*

It is apparent that some of the proteins identified with altered expression are connected to processes known to be associated with cellular defence against oxidative stress and cell death. This is not unexpected, since the fate of the cell is ultimately dependent on the coordinated balance between pro-survival and apoptotic signals. In the face of acute oxidative damages elicited by $MPP^+$, a plethora of defence mechanisms are invoked as a last ditch effort to rescue

the cells from death commitment. More often than not, such protective strategies entail heightened expression of proteins involved in the synthesis of antioxidants, such as PICOT (which regulates the redox-regulating thioredoxin system, Figure 1.8) and spermine synthase (in the production of the free radical scavenger spermine, Figure 1.9), as identified in our current investigation. Proteome analysis of the human substantia nigra in the Parkinson's disease had also unravelled the involvement of other ROS-scavenging proteins. For example, an increased expression of peroxiredoxin II was observed in the substantia nigra of postmortem Parkinson's disease victims and this was in agreement with the oxidative stress hypothesis in Parkinson's disease (Basso *et al*., 2004) The latter suggests the substantia nigra (SN) to be a preferential candidate to oxidative damage, since it contains oxidizable dopamine, neuromelanin, polyunsaturated fatty acids, iron, and relatively low antioxidant complement (Jenner, 2003). In this context, mitochondria are involved in a number of cellular reactions that potentially lead to the formation of ROS. Peroxiredoxin II is a sacrificial antioxidant that catalyzes ROS oxidation/reduction by direct reaction with the ROS, and hence its heightened expression is probably required to combat ROS-induced stress. Also, proteomic approach to study the protein levels of three subtypes of human peroxiredoxin in brain regions from patients with Alzheimer's disease (AD) and Down Syndrome (DS) showed that the protein levels of peroxiredoxin I and peroxiredoxin II were significantly increased in AD and DS. It was thus concluded that increased protein levels of peroxiredoxin I and peroxiredoxin II could provide protection against neuronal cell death induced by ROS implicated in the pathogenesis of these neurodegenerative diseases (Kim *et al*., 2001).

Up-regulation of the antioxidants is, however, not noted in some transgenic mice models of neurodegenerative diseases. For example, in transgenic mice overexpressing the P301L

mutant human tau protein created to model tauopathies *in vivo*, down-regulation of antioxidant enzymes perioredoxin III, peroxiredoxin VI, GST P2 and Mu1, and phospholipid hydroperoxide glutathione peroxidase were observed with mutant tau overexpression **(**David *et al*., 2005). Also, comparative proteome analysis of wild-type and *parkin-/-* mice brain samples revealed down-regulation of peroxiredoxin I, II, VI and Lactoylglutathione lyase, hence suggesting that the *parkin-/-* mouse might have a reduced ability to respond to the generation of ROS **(**Palacino *et al*., 2004). The disparity observed in the direction of alteration in antioxidant expression level may be attributed to the different model systems chosen for proteomic analysis, as well as the various treatments/manipulations involved. For example, 8.5–10-month-old P301L tau mice were used for the proteomics analysis to study the consequences of tau pathology, though these mice showed tau-containing intracellular neurofibrillary tangles formation as early as six-month-old (David *et al*., 2005). The accumulation of mutant tau for several months prior to the killing of the mice might lead to chronic ROS-induced stress, which could compromise the cellular antioxidant mechanisms significantly way before the commencement of proteomic analysis. In contrast, the dopaminergic MN9D cells were subjected to an acute neurotoxic insult for relatively short durations (2-16 hours) before the protein lysates were harvested for 2DGE. The experiment was designed to chart the cell's early response to neurotoxin-induced stress, in an effort to unearth novel therapeutic candidates for the Parkinson's disease. As such, we speculate that in the face of a sudden ROS outburst, an initial up-regulation of the various antioxidants may represent a 'reflexive' response to cope with the stressful situation. On the other hand, chronic exposure of the cells to ROS, such as in the above-mentioned mouse models, may seriously undermine the cellular defence system, especially so since the ROS can react with the antioxidants directly. In any case, the results clearly implicate oxidative stress in the aetiology of

various neurodegenerative diseases, including the Parkinson's disease, and emphasize the potential of the various antioxidants for therapeutic considerations.

### *1.4.2 Enhanced housekeeping operations to cope with acute oxidative stress*

Sustained expressions of the plethora of housekeeping genes are important in maintaining the operations of the numerous basal cellular activities. Some of the most important housekeeping genes are involved in protein synthesis and degradation. Inactivation of the housekeeping proteins involved in these processes can thus lead to severe deregulation in protein turnover and cause cell death. For example, caspase-mediated cleavage of three specific subunits of the 19S regulatory complex of the proteosome leads to inhibition of proteasomal activities and ultimately, apoptosis (Sun *et al*., 2004). Meanwhile, caspase-mediated proteolysis of eukaryotic translation initiation factor eIF4G, which serves as a docking site for initiation factors and proteins involved in RNA translation, is often detected during the onset of apoptosis (Marissen *et al*., 2000).

While targeted degradation of certain housekeeping genes can lead to cell death, the converse is shown to be true as well, i.e., their overexpression can rescue cells from stress-induced apoptosis and promote survival. For example, overexpression of the eukaryotic translation initiation factor eIF4E stimulates cell proliferation and suppress apoptosis in growth factor restricted cells (Tan *et al*., 2000). Also, overexpression of proteasome beta5 assembled subunit increases the amount of proteasome and confers ameliorated response to oxidative stress and higher survival rates (Chondrogianni *et al*., 2005). In the present investigation, heightened levels of ribosomal protein large P2 subunit (Figure 1.5) and proteasomal subunit beta 6 (Figure

1.4), which form part of the translational and protein degradation machineries respectively, were noted with $MPP^+$ exposure to the MN9D cells. With the above-mentioned examples in mind, we speculate that the up-regulations may represent pro-survival strategies to enable the cell to cope with acute oxidative stress elicited by $MPP^+$. While an improved translational rate may be directly responsible for increasing output of proteins involved in defence against free radicals and cellular repair, an enhanced proteasomal capability may allow the cell to dispose off aberrantly oxidised proteins efficiently to prevent their undesirable accumulation in the cellular milieu. Enhancing housekeeping operations through overexpression of selected genes involved may thus represent viable therapeutic options to enable the dopaminergic neurons to combat against free radicals-mediated damages in PD.

### *1.4.3 Decreased anaerobic glycolysis indicative of mitochondrial dysfunction*

Phosphoglycerate mutase, an enzyme that catalyses the interconversion of 3-phosphoglycerate and 2-phosphoglycerate in the glycolysis and glyconeogenesis pathway, was found to be down-regulated eight hours after $MPP^+$ treatment (Figure 1.7). Being one of the key enzymes that control the glucose flux through the glycolytic pathway, reduced amount of the enzyme is indicative of impairment in energy metabolism and mitochondrial dysfunction with $MPP^+$ treatment. This finding is reminiscent of that yielded by applying Affymetrix oligonucleotide microarray technique in the substantia nigra pars compacta of sporadic parkinsonian patients for studying global gene expression analysis. In this study, reduced expression of phosphofructokinase, another regulatory enzyme controlling glycolysis, was observed (Mandel *et al*., 2005). These two findings support previous reports in human PD patients using positron emission tomography (PET) analysis, demonstrating a decrease in glucose

uptake into the SN (Berding *et al*., 2001), and give a wider view of major survival pathways affected by the disease. Taken together, our finding is consistent with the hypothesis that mitochondrial dysfunction contributes to the pathogenesis of PD (Mandel *et al*., 2005).

### *1.4.4 Involvement of Nucleophosmin in $MPP^+$-induced cell death*

Nucleophosmin (NPM), which is predominantly nucleoli-localised, is a multifunctional protein that is involved in regulating numerous cellular processes, such as processing and transport of ribosomal RNA (Borer *et al.*, 1989), molecular chaperoning (Szebeni & Oslon, 1999) and regulating nucleo-cytoplasmic shuttling (Borer *et al*., 1989), to name a few. Given its numerous and diverse functions, it will be difficult to pin-point the exact function of heightened level of NPM in $MPP^+$-treated MN9D cells (Figure 1.1). A clue to the possible role(s) of NPM in this case comes from insights derived from investigating the association between NPM and cancer. NPM has been proposed as a tumour marker for colon (Nozawa *et al*., 1996) and gastric (Tanaka *et al*., 1992) cancers because NPM expression is markedly higher in these tumour cells than in the corresponding normal cells. In fact, over-expression of NPM made NIH 3T3 cells more resistant to UV-induced cell growth inhibition and death as compared with control vector-transfected cells (Wu *et al*., 2002), while depletion of NPM with small inferring RNA has increased apoptosis induced by different agents in various cell type (Li *et al*., 2004; Li *et al*., 2005; Maiguel *et al*., 2004). Taken together, these observations indicate that NPM may possess pro-survival and/or anti-apoptotic capabilities, which may in turn, underlie oncogenesis in several cancer types.

One way via which NPM may promote survival is through p53 regulation. NPM inhibits hypoxia-induced p53 phosphorylation at Ser-15 and interacts with p53 in hypoxic cells (Li *et al*.,

2004). Phosphorylation at Ser-15 stimulates p53-dependent transactivation, and thus NPM-mediated inhibition of p53 phosphorylation prevents the activation of p53 responsive genes such as p21, bax and PUMA (Dumaz & Meek, 1999). Overexpression of the mutant NPMDeltaC, which lacks the p53-interacting domain, fails to confer cellular resistance to stress-induced apoptosis, thus further supporting the notion that NPM protects cells from apoptotic cell death through a mechanism involving p53 inhibition (Li *et al*., 2005). In addition, NPM interacts with the nuclear PI(3,4,5)P3 to form a complex that mediates anti-apoptotic effects of Nerve Growth Factor by inhibiting DNA fragmentation activity of caspase-activated DNase (CAD) (Ahn *et al*., 2005). Notably, the discovery of the cytoplasmic NPM mutant, which is implicated in the pathogenesis of Acute Myeloid Leukaemia (AML) (Falini *et al*., 2005), strongly suggests a hitherto unknown cytoplasmic function for NPM that underlies leukaemogenesis.

As such, up-regulation in NPM level with $MPP^+$ exposure may confer temporary resistance to apoptosis for cellular defence and repair to commence. Given that NPM possible involvement in the pathogenesis of several cancer types, the scope for research into the pro-survival mechanisms of NPM appears to be wide and promising.

### *1.4.5 Concluding remarks*

Current study of the proteomes of $MPP^+$-exposed *versus* normal MN9D cells has identified several players that are involved in multiple pathways thought to underlie the aetiology of PD. The regulated proteins we identified are associated with several distinct functional categories: cell cycle arrest and p53 binding, energy metabolism, protein synthesis and degradation, stress response, antioxidant enzymes, and anaerobic glycolysis. Further exploitation

of these proteins' therapeutic values calls for more thorough and rigorous investigations into the precise mechanisms underlying their involvement in $MPP^+$-elicited stress response and toxicity, as we shall see for NPM in the subsequent chapters.

## 2.1 Introduction

The nucleolus is the site for ribosome assembly, a multi-step process involving numerous proteins (Maxwell & Fournier, 1995). Nucleophosmin/B23 (NPM/B23, NO38 or numatrin), a ubiquitously expressed abundant nucleolar phosphoprotein, is one such candidate thought to be involved in the ribosome assembly process (Maxwell & Fournier, 1995; Olson *et al.,* 2002). It has the ability to bind RNA and DNA that are abundant in the nucleolus (Wang *et al.,* 1994), and to associate with maturing preribosomal ribonucleoprotein particles (Prestayko *et al.,* 1974; Schmidt-Zachmann *et al.,* 1987). NPM also possesses intrinsic endoribonuclease activity (Herrera *et al.,* 1995), and its ability to preferentially cleave the internal transcribed spacer region 2 (ITS2) region of pre-RNA further suggests that it could participate in the late stages of ribosome biogenesis (Savkur & Olson 1998). Other nucleolar-localised proteins are thought to function in the different stages of ribosome biogenesis. For example, nucleolin/C23 facilitates the early stages of pre-rRNA processing, possibly by first interacting with the 5′ region of pre-rRNA and then recruiting processing components (Pluk *et al.,* 1998). The tumour suppressor ARF regulates pre-rRNA processing through interacting with NPM and promoting the polyubiquitination and degradation of NPM (Itahana *et al.*, 2003).

The discovery of nucleolus-localised proteins with no apparent relation to the ribosome biogenesis process in recent years has led to the notion that the nucleolus may also perform non-traditional cellular duties, such as in signal recognition particle assembly, cell cycle regulation, control of aging, modification of small nuclear RNAs, and modulation of telomerase function. (Olson, 2004). For example, recent results indicate that biosyntheses of signal recognition

particle RNA and telomerase RNA involve a nucleolar stage and that nucleolus is a site critical to cellular aging (Pederson *et al.,* 1998). The involvement of the nucleolus in numerous diverse tasks reflects its pivotal role in maintaining cross talks between various cellular processes and compartments, which in turn ensures proper regulation of both cell proliferation and survival. On the other hand, nucleolar disruption can result in cessation of ribosome and protein synthesis, leading to activation of the cytoprotective mechanisms. Inhibitors of RNA synthesis (for example, actinomycin D or camptothecin), DNA-damaging agents (for example, ultraviolet (UV) irradiation and anticancer agents), and cellular stressors (for example, heat shock and hypoxia) have all been documented to disrupt the nucleolar structure, leading to the impairment of nucleolar function, and thereby inducing the stabilisation of the tumour suppressor p53 (Rubbi & Milner, 2003). The latter is capable of protecting against cancer via its ability to induce cell cycle arrest or ultimately, apoptosis against a variety of cellular stresses (Jin & Levine, 2001). In this way, the nucleolus may function as a stress sensor converging the wide array of stress signals into the appropriate cellular response(s).

A common phenomenon accompanying stress-induced nucleolar disruption is the release of nucleolar components out of the organelle. Nucleolin is observed to translocate into the nucleoplasm to interact directly with p53 under stress conditions (Daniely & Borowiec, 2000). It is thought that such relocalisation allows nucleolin to transiently repress genomic replication by binding and inhibiting an essential DNA replication factor RPA. This sequesters RPA in nuclear foci away from sites of ongoing DNA synthesis, while mobilizing DNA repair factors. Meanwhile, ribosomal protein L11 is also released from the nucleolus to bind and inhibit the p53-antagonist Mdm2 in the nucleoplasm during serum starvation. This in turn leads to cell cycle

arrest through p53 activation. In a cell undergoing a transient arrest, p53 transcriptional targets such as $p21^{WAF1/CIP1}$ and Gadd45 are prominently induced, representing the arrest and ongoing DNA repair, followed by a subsequent induction of Mdm2 terminating the response (Reinke & Lozano, 1997; Zhang *et al.,* 2003). ARF released from the nucleolus following the latter's perturbation is also thought to stabilise p53 in the same way as L11, since ARF can also directly bind Mdm2 (Llanos *et al.,* 2001). Nucleophosmin has also been observed to translocate into the nucleoplasm in response to serum deprivation (Chan *et al.,* 1985) and drug treatments such as exposure to actinomycin D (Chan *et al.,* 1985) and deferoxamine (Yung *et al.,* 1991). NPM was shown to bind to Mdm2 after its translocation to the nucleoplasm. This interaction prevents Mdm2 binding to p53 and stabilizes p53, hence potentiating the p53 response to UV radiation (Kurki *et al.,* 2004). Short exposure to the transcriptional inhibitor actinomycin D was reported to induce reversible translocation of NPM into the nucleoplasm, as well as reversible inhibition of cell growth and RNA synthesis in HeLa cells (Yung *et al.,* 1990). In fact, NPM translocation, as observed by immunofluorescence, have been used as a simple and rapid method for assessing inhibition of cell growth in response to anti-proliferative drugs in cancer chemotherapy (Yung *et al.,* 1991).

Other than ribosome biogenesis, a number of cellular activities associated with NPM indicate that NPM has multiple cellular functions, especially in the regulation of cell proliferation. Its ability to shuttle between the nucleus and the cytoplasm, and to bind to proteins via their nuclear localisation signals suggest a role in nucleo-cytoplasmic transport (Borer *et al.,* 1989; Szebeni and Olson, 1999). It has also been proposed that NPM acts as a molecular chaperone that prevents protein from aggregating in the crowded environment of the nucleolus,

protects enzymes from thermal denaturation, and facilitates renaturation of chemically denatured proteins (Szebeni *et al.,* 2003). Recently, NPM was shown to bind to different cellular and viral proteins and play a critical role in the regulation of subcellular localisation and activities of these proteins. NPM physically interacts with p53 (Colombo *et al.,* 2002; Kurki *et al.,* 2004), Arf tumor suppressor protein (Bertwistle *et al.,*2004), Polo-like kinase (Zhang *et al.,* 2004), NF-κB (Dhar *et al.,* 2004), p120 (Valdez *et al.,* 1994), nucleolin (Li *et al.,* 1996)), and several viral proteins such as Rex of human T-cell leukemia virus (Adachi *et al.,* 1993) and hepatitis δ-virus antigen (Huang *et al.,* 2001a).

NPM was also found to be associated with a number of cancers, indicating NPM's possible role in cell proliferation. It was shown to be more abundant in cancer cells than in normal resting cells (Chan *et al.,* 1989). In fact, NPM has been proposed as a tumour marker for colon, ovarian, prostate and gastric cancers because NPM expression is markedly higher in these tumour cells than in the corresponding normal cells. Cancers of later stages have relatively higher nucleophosmin/B23 mRNA levels than the matched adjacent "normal" tissues. Notably, overexpression of the nucleolar protein in NIH 3T3 cells resulted in malignant transformation, pointing to a possible oncogenic role for NPM (Kondo *et al.,* 1997). NPM is also frequently found in the chromosomal translocation associated with several haematopoietic malignancies, such as acute promyelocytic leukaemia, anaplastic large cell lymphomas, and myelodysplasia/acute myeloid leukaemia. Finally, a frame-shift mutation occurring at the extreme C-terminal of the *NPM* gene cause aberrant cytoplasmic localisation of the mutated NPM, which has been proposed as a biomarker for certain acute myelogenous leukaemia (AML) (Falini *et al.,* 2005).

Given NPM's versatile nature and wide range of cellular duties, it is possible that some functions of the cytoplasmic NPM remain undiscovered. In this chapter, the subcellular localisation of NPM after its release from the nucleoli, as well as factors promoting its release are investigated. Here, we show that apart from the nucleoplasm, NPM was translocated into the cytoplasm as well in response to diverse stress signals. In the subsequent chapters (III-V), we further investigate a possible role of the cytoplasmic-translocated NPM in the regulation of apoptotic signalling via caspase inhibition.

## 2.2 Materials and methods

### *2.2.1 Cell culture and induction of apoptosis*

MN9D (obtained with courtesy of Dr Jun Chen, University of Pittsburgh and with agreement from Dr Alfred Heller,University of Chicago), HeLa (a gift from Dr Ge Rou Wen, NUS), SHSY5Y (a gift from Dr Lim Kah Leong, National Neuroscience Institute, Singapore), 293T and NIH 3T3 (both gifts from Dr Low Boon Chuan, NUS) cell lines were cultured in DMEM medium (RPMI 1640 medium for 293T cells) supplemented with 10% fetal bovine serum and 1% penicillin/streptomycin in a humidified atmosphere of 5% $CO_2$ at 37°C. To induce apoptosis, MN9D cells were treated with varying dosage of 1-Methyl-4-phenil-pyridinium ($MPP^+$), NIH 3T3 with cyclohexamide, SHSY5Y and 293T cells with rotenone and HeLa cells with UV-C irradiation, Camptothecin or Actinomycin.

### *2.2.2 Plasmids and Transfection*

Total RNA was prepared using TRIZOL (Invitrogen, USA) from human HeLa cells according to the protocol by TRIZOL's manufacturer. Amplification of the human caspase cDNA was performed using the Access RT-PCR kit (Promega, USA) from the extracted RNA, using the following primers:

For caspase-3: Forward primer 5' – ATG GAG AAC ACT GAA AAC TC –3'

Reverse primer 5' – TTT AGT GAT AAA AAT AGA GT –3'

For caspase-6: Forward primer 5' – CAT GAC AGA AAC CGA TGG –3'

Reverse primer 5' – CAG ATG GCC CTA CTT GCT –3'

For caspase-8: Forward primer 5' – ATG GAC TTC AGC AGA AAT CT –3'

Reverse primer 5' – CTT GCG GTG AGC CGA GAT CA –3'

The PCR cycles were (i) 95 C for 5 min; (ii) 95°C for 1 min, 50°C for 2 min, 72 C for 1 min (30 cycles); and (iii) 72 C for 10 min. The full-length PCR product was purified by low melting-agarose gel electrophoresis and cloned into pGem-T Easy vector (Promega, USA) for sequencing. The caspase cDNAs were then subcloned into the pXJ40-HA plasmid (a generous gift from Dr Low Boon Chuan, NUS) using the EcoRI restriction site for non-directional cloning. For plasmid transfection, HeLa cells were seeded at a density of 1.5 x $10^5$ per well in six well plates in DMEM supplemented with 10% fetal bovine serum. 24 h later, the cells were transfected with varying amount of plasmid DNA using Lipofectamine (Invitrogen, USA) according to the manufacturer's instructions. After 24-48 hours, the cells were harvested and protein extracted for further analysis.

### *2.2.3 Caspase inhibition*

MN9D cells transfected with caspases or exposed to $MPP^+$ were washed with PBS exposed for 12-24 h to caspase-3 inhibitor (Calbiochem, USA) at 16μM; caspase-8 inhibitor

(Calbiochem, USA) at concentrations of 0.5μM; and caspase-6 inhibitor at 20μM. All chemicals used were dissolved in DMSO and filtered through a 0.22μm pore-size filter before use

### *2.2.4 Rapid preparation of total cell lysate (total cytosolic - nucleoplasmic extract)*

Treated MN9D cells were washed with PBS to remove the medium. A volume of 200μl of cell lysis buffer (100mM HEPES pH 7.5, 5mM MgCl2, 150mM NaCl, 1mM EDTA, 1% Triton X-100 + 1% protease inhibitor cocktail [AEBSF-Hydrochloride, Aprotinin, E-64-Protease Inhibitor, EDTA-Disodium, Leupeptin-Hemisulfate] ) was added to lyse the cells. The cell lysate was further pipetted through a 271/2G needle to break up the genomic DNA. The cell lysate was finally centrifuged at 13,000rpm for 1 minute to pellet the DNA and the supernatant was stored at $-20^{o}$C.

### *2.2.5 Preparation of subcellular fractions*

Nuclear and cytosolic fractions were prepared using the Nuclear/Cytosol fractionation kit (BioVision, USA), according to the manufacturer's protocol. Briefly, cells were washed with PBS two times to remove the medium. A volume of 200μl of Cytoplasm Extraction Buffer A (CEB-A) was added and the cells scraped down using a rubber policeman. The cell suspension was then vortexed for 15 sec and incubated on ice for 10 min. 11μl of the Cytoplasm Extraction Buffer B (CEB-B) was next added to the suspension and vortexed for 5 sec. The suspension was then incubated on ice for 1 min, vortexed for another 5 sec, before being centrifuged at 16, 000 g for 5 min at 4°C. The supernantant, which is the cytoplasmic fraction, was then collected. Next,

100µl of the Nuclear Extraction Buffer (NEB) added to the pellet and vortexed vigorously for 15 sec and incubated on ice for 10 min before being subjected to another round of vortexing. This was repeated over a duration of 40 min, after which the suspension was centrifuged at 16, 000 g for 10 min at 4°C. The supernatant, which is the nuclear fraction, was finally collected. The fractions were immunoblotted against the nuclear marker oct-1 to ensure clean separation of the two fractions.

### *2.2.6 Electrophoresis and Western Blot analysis*

Equal amount of proteins were resuspended in SDS-PAGE buffer (62.5 mM Tris-HCl, pH 6.8, 2% SDS, 10% glycerol, 5% dithiothreitol) and boiled in a water bath for 5 min. Lysates were stored at -20°C until further analysis. Proteins were separated under reducing conditions for 2 h at 120 V in 12 or 15% SDS-polyacrylamide gels. Gels were transblotted onto the nitrocellulose membranes at 100V for 1.5 h. Membranes were blocked for 1h in TBS Tween with 5% milk powder, and then incubated overnight with anti-NPM (1:10000, Zymed, USA), -caspase-3 (1:1000, Santa Cruz, USA), -caspase-6 (1:2000, Cell Signalling, USA), -caspase-7 (1:600, Neomarkers, USA), -caspase-8 (1:1000, Santa Cruz, USA), oct-1 (1:1000, Chemicon, USA) and actin (1:1000, Santa Cruz, USA), followed by incubation with HRP-conjugated secondary antibodies (Santa Cruz), goat-anti-mouse or anti-rabbit (1:1000). Protein bands were visualised by applying chemiluminescent substrate (Pierce, USA)

### *2.2.7 Immunofluorescence microscopy*

The various cell lines were cultured under normal conditions. After exposure of the cells to apoptotic stimuli for various durations, the cells were then rinsed once with PBS and fixed in 3% paraformaldehyde for 30 min at room temperature. Cells were then incubated in blocking buffer (10% horse serum/0.4% Triton X-100 in PBS) for 10 min, followed by a wash with 0.4% Triton X-100 in PBS. The cells were then incubated with primary antibody (anti-NPM at 1:200, anti-active caspase-6 at 1:50) overnight at 4°C in a humidified chamber. Excess antibody was removed by washing with PBS (five times, 5 min each), followed by incubation with anti-mouse FITC-conjugated secondary antibody for 45 min at room temperature, with protection against light. Hoechst 33342 was added to a final concentration of 4 μM and incubated for an additional 5 min at room temperature, before washing with 0.4% Triton X-100 in PBS (5 times, 5 min each). Images were collected using an inverted fluorescence microscope (model Axiovert 25; Carl Zeiss Meditech, Germany).

### *2.2.8 Quantitative Reverse Transcription Polymerase Chain Reaction (RT-PCR)*

Total RNA was prepared using TRIZOL (Invitrogen, USA) from human HeLa and mouse MN9D cells after varying duration of exposure to 0.50 μg/mL of actinomycin D and 500 μM $MPP^+$, respectively. Concentration of the extracted RNA was then measured at OD 260. RT-PCR was performed using the Access RT-PCR system (Promega, USA) in 25 μl reactions containing a 200 μM concentration of each dNTP, 1 mM $MgSO_4$, 5 units of avian myeloblastosis virus reverse transcriptase, 5 units of *Tfl* DNA polymerase, 10 μl of 5x avian myeloblastosis

virus/*Tfl* buffer, 50 pmol each of primers (see below), and 20 μg of various extracted RNA. The primers used were as follow:

For human NPM: Forward primer 5' – CGATG GACAT GGACA TGAGC –3'

Reverse primer 5' – TTCGTAATTC ATTGCCTCTG –3'

For mouse NPM: Forward primer 5' – CGATG GATAT GAACA TGAGT –3'

Reverse primer 5' – ACTGCCTTCA TAGTTCATTG –3'

For human beta actin: Forward primer 5' – CGCGCTCGTC GTCGACAACG –3'

Reverse primer 5' – CCATGTCGTC CCAGTTGGTG –3'

For mouse beta actin: Forward primer 5' – GCTGGTCGTC GACAACGGCT –3'

Reverse primer 5' – TGCCAGATCT TCTCCATGTC –3'

All four sets of primers amplified a single band each of about 0.2 kb. Thermocycling conditions were as follows: 48°C for 45 min, 94°C for 2 min; then 40 cycles of 94°C for 30 sec, 50 °C for 1 min, and 68°C for 2 min; and ending with 68°C for 7 min. Amplified products were then run on a 1% agarose gel and visualised under the UV. Bands intensities for NPM and β-actin were determined by densitometric scanning. The values of NPM were normalised with respect to the intensities of β-actin. Data were analysed by Gel pro Imager (Image Porcessing Solutions, USA).

### *2.2.9 Isolation of naked nuclei*

Naked nuclei were isolated from HeLa or MN9D cells using the Nuclei EZ Prep Kit (Sigma, USA) according to the manufacturer's protocol. Briefly, cells were cultured in a 10 cm diameter culture dish and grown to about 90% confluence. During harvesting, the cells were washed with two washes of ice cold PBS. 4 mL of ice cold Nuclei EZ lysis buffer was next added and the cells scraped down, vortexed and set on ice for 5 min. The released nuclei were then collected by centrifugation at 500 x *g* for 5 min at 4°C, before subjected to another wash of ice cold Nuclei EZ lysis buffer and centrifugation. The collected nuclei were finally resuspended in ice cold Nuclei EZ storage buffer. Equal volume of 2x reaction buffer (10 mM Tris pH 8.0, 5 mM magnesium chloride, 0.3M potassium chloride) was added to the nuclei suspension before treatment with actinomycin D, α-amanitin or $MPP^+$.

## 2.3 Results

### *2.3.1 NPM translocates into the cytoplasm upon stress induction*

Intrigued by how proteins released out of the nucleolus can play various cytoprotective functions, we sought to determine if NPM, a nucleolar component known to be translocated out into the nucleoplasm in response to drug treatments (Chan *et al.,* 1985; Yung *et al.,* 1985a & b; Yung *et al.,* 1990; Yung *et al.,* 1991; Wu & Yung, 2002), also play a similar function once out of the nucleoli. We first used immunofluorescence to determine the subcellular distribution of NPM when different cell lines were subjected to four hours of various drug treatments (MN9D cells with 500 μM $MPP^+$, HeLa with 0.40 μM transcriptional inhibitor Actinomycin D and 10μg/mL topoisomerase inhibitor Camptothecine, NIH 3T3 with 50 μM translational inhibitor Cycloheximide). Apart from the nucleoplasmic localisation of NPM as previously reported (Chan *et al.,* 1985; Yung *et al.,* 1985a & b; Yung *et al.,* 1990; Yung *et al.,* 1991; Wu and Yung 2002), we also observed prominent localisation of NPM outside the nucleus in the treated HeLa and NIH-3T3 cells (stained blue with nuclear stain Hoechst 33342) (Figure 2.1 A-C). Translocation of NPM into the cytoplasm and nucleoplasm correlated well with the dissolution of the nucleolar structure. Expectedly, western blot analysis demonstrated an increase in cytoplasmic accumulation of NPM and concomitant decrease in nuclear NPM, with increasing drug dosage used (Figure 2.2 A-C). In comparison, cytoplasmic and nucleoplasmic localisation of NPM was not so uniformly observed across all MN9D cells with $MPP^+$ treatment. Many treated cells were observed to retain distinct nucleolar structure, even though the nucleolar edge appeared to be fuzzy and less defined (Figure 2.1D). This may indicate limited dissociation of

NPM from the edge of the nucleoli for translocation into the nucleoplasm and cytoplasm. This is supported by western blot analysis which showed early cytoplasmic NPM build-up with $MPP^+$ treatment. Meanwhile, HEK293 cells also showed cytoplasmic accumulation of NPM eight hours after a 42°C heat shock treatment, coinciding with the cytoplasmic accumulation of the anti-apoptotic Hsp70 (Figure 2.2 D). The cytoplasmic fractions are free from nuclear contamination, as no nuclear protein oct-1 was detected. These data indicate that in addition to the well-documented nucleoplasmic accumulation of NPM, its cytoplasmic build-up is also a general phenomenon in response to cell stress as observed in the various cell lines used.

### *2.3.2 Early cytoplasmic build-up of NPM precedes the onset of apoptosis*

Though visually we detected little cytoplasmic NPM and no massive nucleolar disruption in $MPP^+$ treated MN9D cells, we went on to perform a time-course analysis of both the cyto-nucleoplasmic and cytoplasmic NPM level using immunoblotting. Here, we demonstrated early cytosolic-nucleoplasmic build-up of NPM, which decreased at the onset of apoptosis. NPM's protein level was elevated by the second hour after $MPP^+$ exposure, and peaked at the fourth hour, before declining steadily till the $16^{th}$ hour. This is reminiscent to the findings of Wu and Yung (2002), who, using UV to induce acute DNA damage response, showed that NPM's protein level peaked by the $12^{th}$ hour, before returning to near baseline by the $24^{th}$. NPM's possible role in genotoxic stress response was speculated, but the exact purpose and molecular mechanism of its involvement remained unknown. We further demonstrated that the peak in NPM protein level coincided with early initiator caspase-8 activation, but preceded the cleaving of key apoptogenic factors such as the executioner caspase-7 and Poly-(ADP-ribose) Polymerase

(PARP), both of which indicated the onset of cellular apoptotic destruction (Figure 2.3). Earlier results from our laboratory have demonstrated early activation of caspase-8 in MPP+-treated MN9D cells (Chee *et al.*, 2005). In addition, caspase-8 is the apical caspase activated in diverse apoptotic signalling pathways (Kruidering & Evan, 2000). As such, coordinated transitions in the level of early-activated marker of cell death such as caspase-8, and NPM with $MPP^+$ treatment, which preceded the appearance of two downstream apoptotic markers, suggest a role for NPM in the regulation of caspase-mediated apoptotic signalling.

### *2.3.3 Stress-induced cytoplasmic build-up of NPM can occur in the absence of de novo NPM protein synthesis*

We demonstrated early cytoplasmic accumulation of NPM under stressful conditions, but the source of NPM remains hitherto unclear. Wu and Yung (2002) demonstrated rapid and transient stimulation of NPM mRNA expression by UV irradiation in HeLa cells and NIH 3T3 cells. They further showed that stimulation of NPM mRNA expression by UV was inhibited by the transcription inhibitor actinomycin D. These strongly suggest the appearance of the cytoplasmic NPM as a direct consequence of stress-induced *de novo* protein synthesis. However, as discussed above in Section 2.3.1, cytoplasmic (and nucleoplasmic) accumulation of NPM commenced even in the presence of increasing dosage of transcriptional or translational inhibitors that could block *de novo* protein synthesis. This led to our speculation that the nucleoli could be the source of both the nucleoplasmic and cytoplasmic NPM. Here, using reverse transcription PCR, we sought to determine changes in transcript level of NPM with respect to that of β-actin after exposure of HeLa cells to actinomycin D or MN9D cells to $MPP^+$. We were

able to determine that the increase in cytoplasmic NPM is not regulated by transcription during stress conditions, as the level of NPM transcripts remained almost the same or lower for up to 16 hours of drug exposure (Figure. 2.4 a & b). Since no *de novo* NPM synthesis is involved during stress conditions, the results point to the disrupted nucleoli as the source of the cytoplasmic NPM.

### *2.3.4 Translocation of NPM into the cytoplasm is dependent on the Crm1*

Nucleo-cytoplasmic transport is accomplished by specific receptors of the β-importin family, such as the importin receptors that bind to nuclear localisation signals (NLS) (Imamoto *et al.*, 1995) and the export receptor Crm1 that binds to nuclear export signals (NES) (Ossareh-Nazari *et al*., 1997). These processes require a small GTPase, Ran, which controls the interaction of these receptors with their substrates (Fornerod *et al.*, 1997). The guanine nucleotide-exchange factor RCC1 facilitates Ran binding to Crm1, whereas RanBP1, a major regulator of Ran, promotes Crm1 dissociation from Ran (Kehlenbach *et al.*, 1999). Nucleocytoplasmic transport can be disrupted with Leptomycin B, an unsaturated, branched chain fatty acid that blocks the binding of Crm1 to the NES by direct binding to Crm1 (Fornerod *et al.*, 1997). It was discovered previously that NPM may be a Ran−Crm1 substrate that controls centrosome duplication. NPM contains a functional nuclear export signal (NES) that is responsible for both its nucleocytoplasmic shuttling and its association with centrosomes, which are Ran−Crm1-dependent as they are sensitive to Crm1-specific nuclear export inhibition, such as leptomycin B (Wang *et al.*, 2005). Here, we investigated whether stress-induced cytoplasmic accumulation of NPM is dependent on Crm1. We first demonstrated an increase in cytoplasmic NPM content

with concomitant decrease in nuclear NPM amount, when the Jurkat cells were exposed to increasing dosage of the topoisomerase inhibitor etoposide (Figure 2.5 A). We next showed that leptomycin B inhibited the etoposide-induced cytoplasmic accumulation of NPM (Figure 2.5 B). Our finding here thus indicates that stress-induced translocation of NPM from the nucleus to the cytoplasm is mediated by Crm1, and inhibition of the latter with Leptomycin B prevents the stress-induced cytoplasmic NPM build-up.

### *2.3.5 NPM is released from isolated nuclei as a result of drug-induced nucleoli disruption in in vitro nuclei assay*

Various stress-inducing agents are known to disrupt the nucleolar structure and translocation of nucleolar components were often observed to occur as a consequence of such disruption (Olson, 2004). It is, however, unknown whether the nucleolar components are passively released due to dissolution of the nucleolar structure, or if there are other factors actively regulating their release. Here, we investigated factors mediating the release of NPM from the nucleoli. In the presence of actinomycin D and α-amanitin, drugs which are known to disrupt the nucleoli structure (Rubbi & Milner, 2003), GFP-tagged NPM was released out from isolated nuclei (Figure 2.6 A). Figure 2.6 (B) shows the disruption of the nucleoli structure and dispersal of NPM into the nucleplasm of the intact isolated nuclei treated with 1.25 μg/mL of actinomycin D. In contrast, intact nuclei showed distinct nuclei structure, with little or no GFP-NPM localisation detected visually in the nucleoplasm. On the other hand, nuclei treated with various concentration of the mitochondrial complex I inhibitor $MPP^+$ did not show marked increase in GFP-NPM release from the nuclei. As such, any nucleoli-disrupting agents or cellular

signal leading to the dissolution of the nucleoli structure can promote the massive release of NPM into the nucleoplasm. This *in vitro* experiment was designed to test the availability of NPM in the nucleoplasm for translocation into cytoplasm in the *in vitro* system, and it is not meant to be used to measure the effectiveness of the Ran-Crm1 system which should have been disabled during the nuclei isolation process. Coupled with the Ran-Crm 1 network regulating nucleocytoplasmic shuttling, the agents/signals can also indirectly lead to elevation in cytoplasmic NPM level, which is usually much lower since much of the nucleoli-bound NPM is not available for nucleo-cytoplasmic shuttling.

### ***2.3.6*** *Activation of the initiator caspase-8 leads to cytoplasmic accumulation of NPM*

We have shown earlier in Section 2.3.1 and 2.3.2 that cytoplasmic accumulation of NPM occurs in response to $MPP^+$ treatment. However, it was demonstrated in Section 2.3.4 that $MPP^+$, which targets the mitochondria, did not result in the release of GFP-NPM out of the isolated nuclei in the *in vitro* nuclei assay, unlike nucleoli-disrupting drugs such as actinomycin D and α-amanitin. A question thus arises as to how $MPP^+$ can promote the cytoplasmic build-up of NPM, especially since it does not directly cause nucleoli disruption. We have observed in Section 2.3.2 that cytoplasmic accumulation of NPM occurred alongside with cleaving of caspase-8 and preceded the activation of executor caspase-7 by at least six hours. Based on this observation, we sought to determine the relationship between cytoplasmic accumulation of NPM and the activation status of the initiator and executor caspases. It was previously shown in our lab that with $MPP^+$ treatment, the initiator caspase-8 and effector caspase-7 were activated, using a combination of caspase-inhibition and western blot studies (Chee *et al.,* 2005). We further

demonstrated here that with caspase-8 inhibition, levels of both total cytosolic-nucleoplasmic NPM and cleaved PARP were reduced significantly by the 12$^{th}$ hour of $MPP^+$ exposure (Figure 2.7). Meanwhile, level of total cytoplasmic and nucleoplasmic NPM remained unchanged with an inhibitor targeting either caspase-6 or effector caspase in general, even though the level of cleaved PARP declined in both cases. It should be noted here that since there is no known inhibitor for caspase-7, a high concentration of caspase-3 inhibitor (100μM) was used to achieve general effector caspase inhibition. The results demonstrated that the cytosolic-nucleoplasmic accumulation of NPM in MN9D cells requires the activation of caspase-8 but not that of the effector caspases. We went on to further examine specifically the cytoplasmic build-up of NPM with overexpression of the initiator or executor caspases. Expectedly, overexpression of caspase-8, but not that of caspase-3 and -6, in HeLa cells resulted in cytoplasmic NPM build-up, with concomitant decrease in the nuclear NPM content (Figure 2.8). It is noteworthy that transfection of the cells with a lower amount (1 μg) of caspase-8 overexpressing plasmid resulted in greater cytoplasmic build-up of NPM, as compared to when higher amounts were used (10 and 50 μg). Marked decrease in the nuclear NPM content was also noted with greater caspase-8 overexpression. It is hence possible that alteration in the cytoplasmic and nuclear NPM content is dependent on the level of apoptotic signalling through caspase-8, which in turn dictates the cell's commitment to either survival or death. We hypothesise that low level of active caspase-8 activates the cytoplasm translocation of NPM, which may act against cell death commitment. On the other hand, high amount of active caspase-8 promotes depletion of nuclear NPM, leading to a decline in ribosome and protein synthesis, and hence resulting in committed cell death. The

scenario depicted here is of course based on the assumption that NPM plays a protective role in the cytoplasm, and at this juncture, we have yet to ascribe an anti-apoptotic role for NPM.

### ***2.3.7*** *Stress-induced cytoplasmic build-up of NPM is not dependent on the presence of p53*

Nucleolin was shown to translocate from the nucleus into the nucleoplasm following exposure to ionizing radiation (IR) and treatment with camptothecin. It was further demonstrated that the formation of the p53-nucleolin complex is required for nucleolin mobilisation in response to stress, as such mobilisation was not observed in p53-null Sao2 cells (Daniely *et al.*, 2002). Since NPM was shown previously to interact with p53 (Colombo *et al.*, 2002; Maiguel *et al.*, 2004), we sought to determine if the presence of p53 is essential for stress-induced cytoplasmic translocation of NPM. Using the $p53^{+/+}$ and $p53^{-/-}$ mouse embryonic fibroblast (MEF), it was determined that NPM accumulates in the cytoplasm in both cell lines after exposure to UV, even though the apoptotic response was attenuated in the p53-null MEF as shown by a decrease in the amount of cleaved PARP detected by immunoblotting (Figure 2.9). Cytoplasmic build-up of NPM is hence not affected by the absence of p53. Unlike nucleolin, interaction and formation of complex between p53 and NPM is not a pre-requisite for NPM's translocation into the cytoplasm.

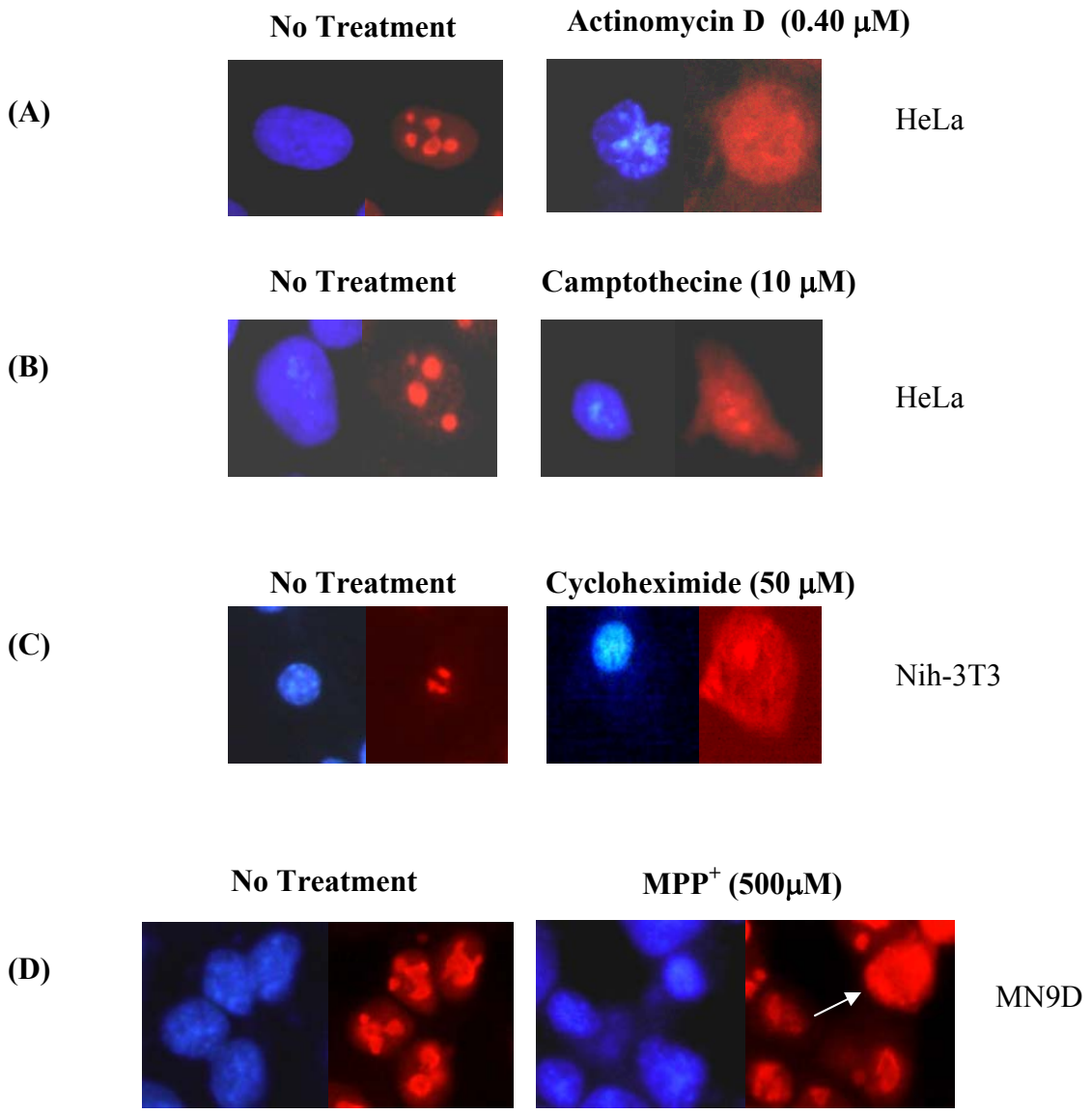


**Figure 2.1. Selective nucleoplasmic and cytoplasmic mobilisation of NPM induced by various treatments.** HeLa, Nih-3T3 or MN9D cells were either left untreated (A-D, left panels) or subjected to various drug treatments for four hours using concentration as indicated (A-D, right panels). In all cases, cells were fixed by treatment with 3% (wt/vol) paraformaldehyde for 30 min at RT and stained for NPM as described in Materials and Methods, Section 2.2.7. NPM localisation was observed by fluorescence microscopy using a Zeiss Axiophot (Germany). White arrow indicates an MN9D cell with promionent nucleoplasmic and cytoplasmic NPM localisation with $MPP^+$ treatment.

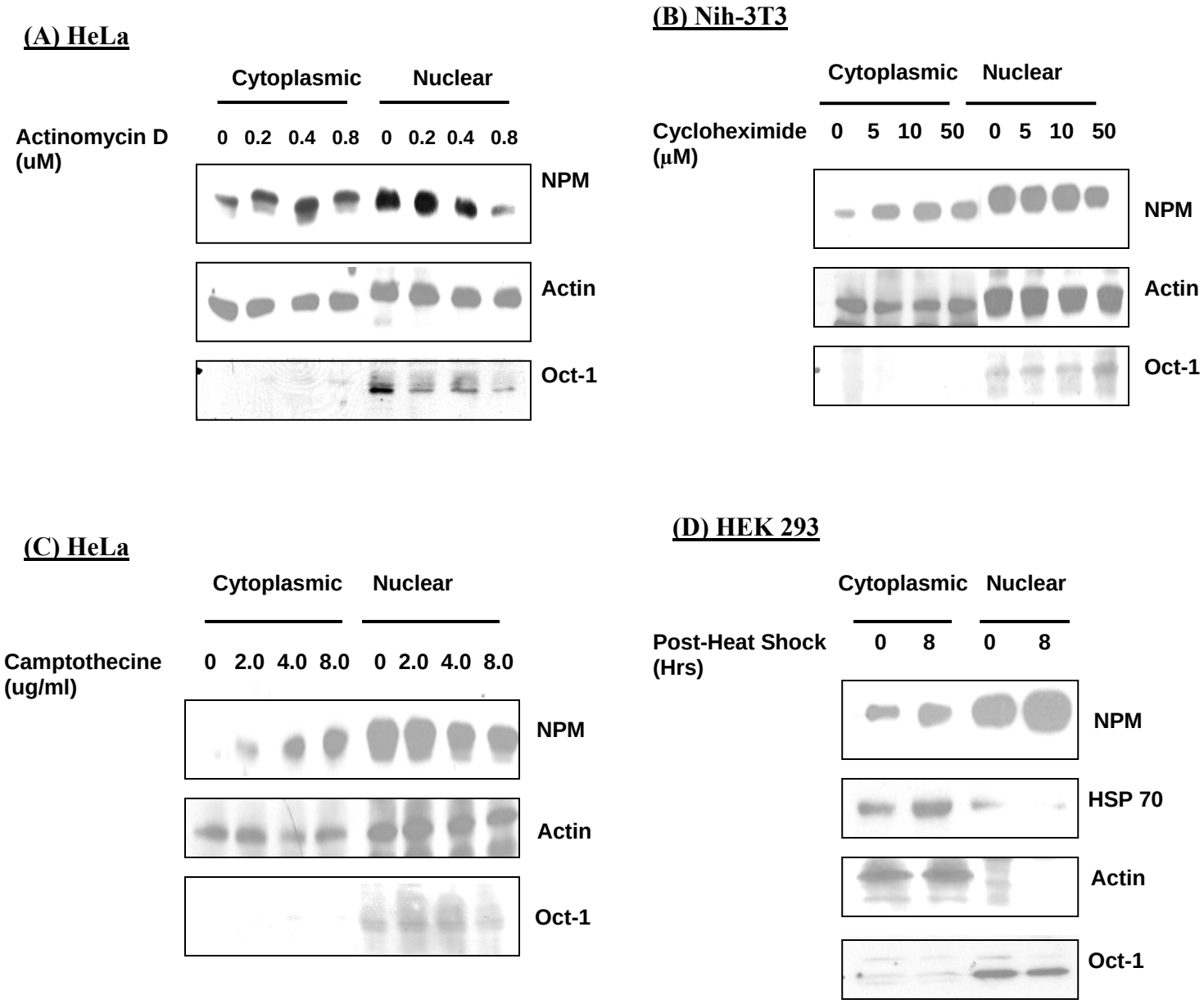


**Figure 2.2. Cytoplasmic NPM translocation is selective induced in response to stress.** Cytoplasmic and nuclear fractions were prepared from various cell lines either after a four-hour exposure to the various drugs of increasing dosage, as indicated (A, B, and C) or after a one-hour 42°C heat shock followed by zero or eight hours of recovery at 37°C (D). Harvested cells were subjected to subcellular fraction as described in Materials and Methods, Section 2.2.5. Collected fractions were next subjected to SDS-PAGE and immunoblot analysis using anti-NPM, anti-oct-1, anti-ß-actin (A-D) or anti-Hsp70 (D) antibody, as indicated to the right of each panel. 20 μg of the cytoplasmic extract and 10 μg of the nuclear extract were electrophoresed to monitor the relative cytoplasmic and nuclear amount of NPM following stress.

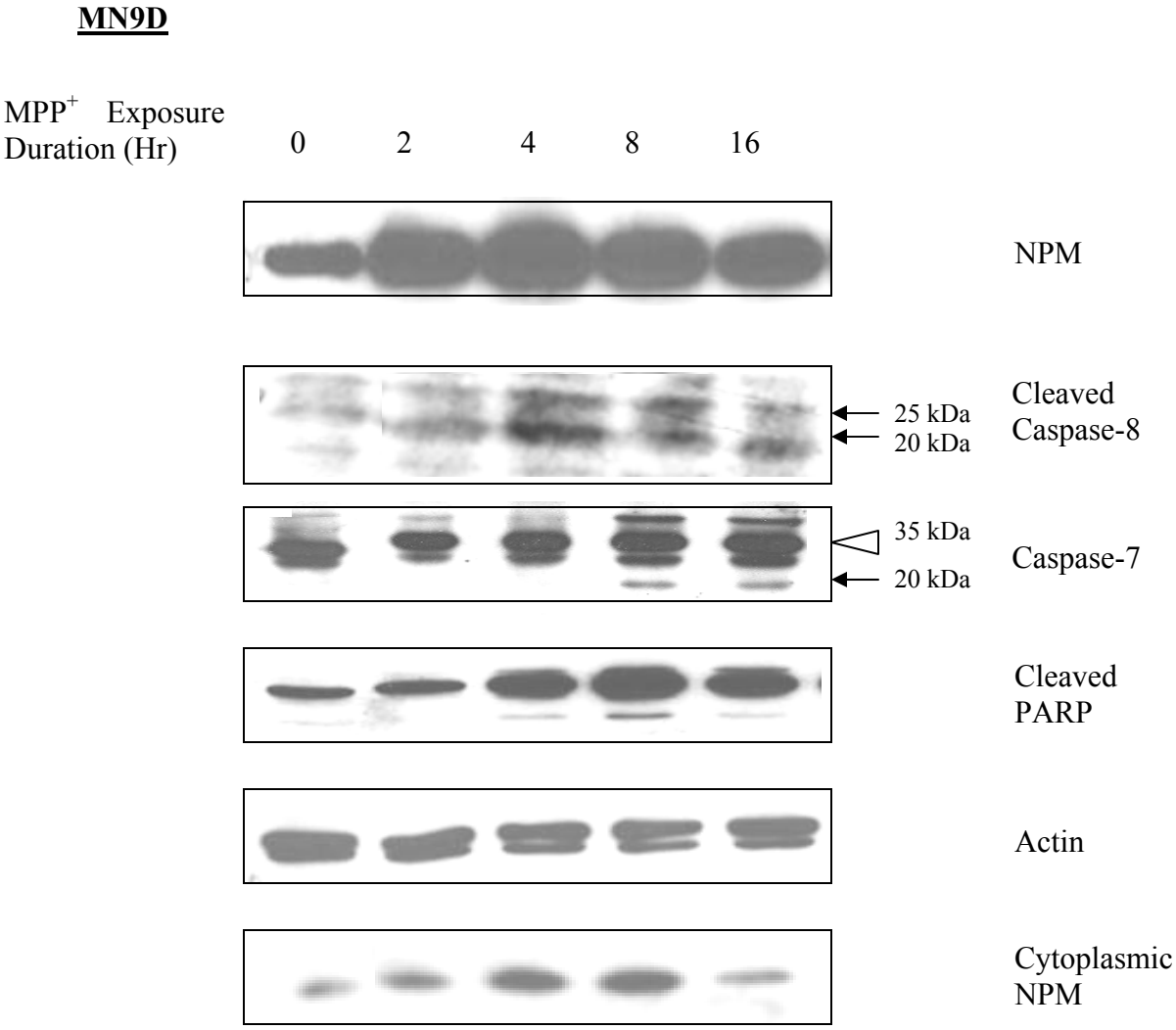


**Figure 2.3. Early cytoplasmic and nucleoplasmic NPM build-up coincides with caspase-8 activation but precedes cleavage of caspase-7 and PARP.** MN9D cells were exposed to 500 μM $MPP^+$ for varying duration as indicated. Cells harvested at various time points were lysed and the total cell extracted collected as described in Material & Methods, Section 2.2.4. Portion of the harvested cells were subjected to subcellular fractionation to obtain the cytoplasmic fraction. The total cytosolic-nucleoplasmic lysates and cytoplasmic protein extract were next subjected to SDS-PAGE and immunoblot analysis using anti-NPM, anti-ß-actin, anti-caspase-8, anti-caspase-7 or anti-cleaved PARP antibody, as indicated to the right of each panel. 20 μg of the total cellular extract and cytoplasmic extract extract (80 μg for caspase-8 immunoblotting) were electrophoresed to monitor the cyto-nucleoplasmic and cytoplasmic NPM level following various length of exposure to $MPP^+$. White triangle indicates procaspase, while black arrows indicate cleaved caspase form.

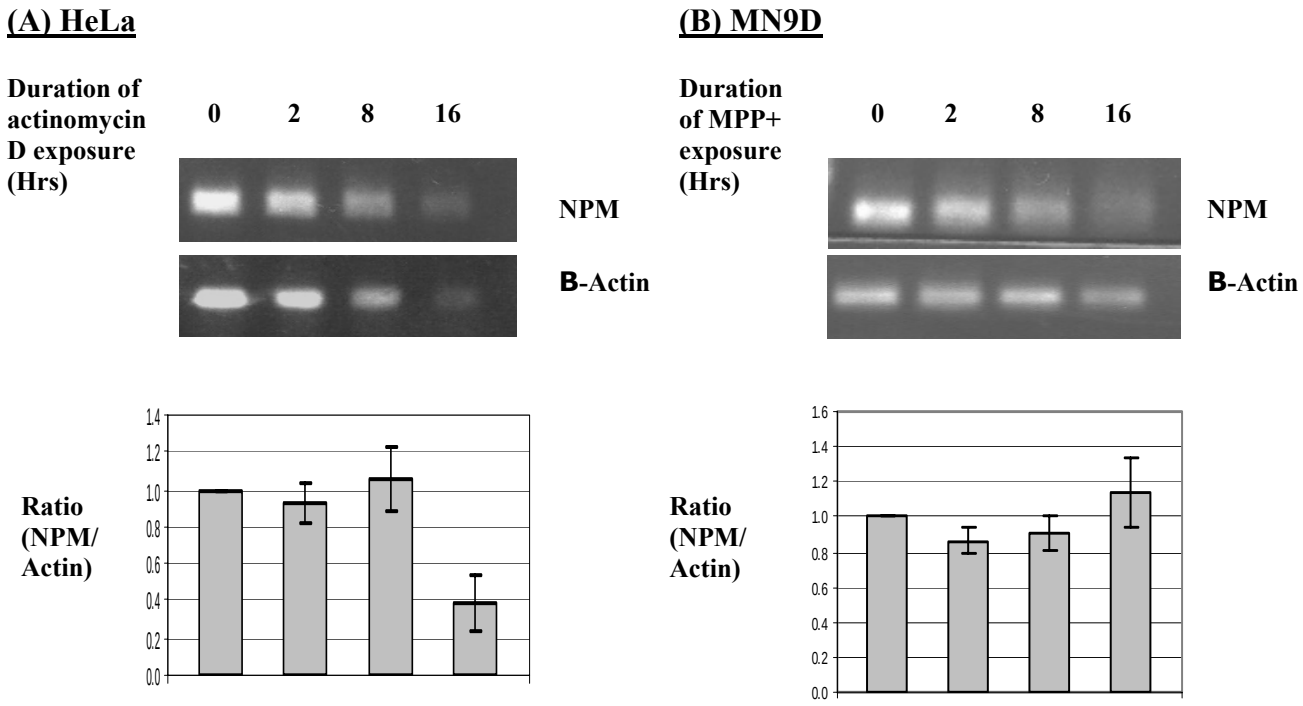


**Figure 2.4. Significant elevation in NPM gene expression is not observed with actinomycin D or $MPP^+$ treatment in HeLa and MN9D cells respectively.** HeLa (A) or MN9D cells (B) were treated with 0.40 μM of actinomycin D or 500 μM of $MPP^+$ respectively. The cells were harvested at indicated times, and total RNA was prepared. RT-PCR was performed as described in Materials and Methods, Section 2.2.8, with 20 μg of RNA for each sample. The primers used were designed to specifically amplify short fragments of about 200 bp corresponding to portion of the NPM or β-actin cDNA. Amplified products were then run on a 1% agarose gel and visualised under the UV. Bands intensities for NPM and β-actin were determined by densitometric scanning. The values of NPM were normalised with respect to the intensities of β-actin. Data were analysed by Gel pro Imager (Image Processing Solutions, USA).

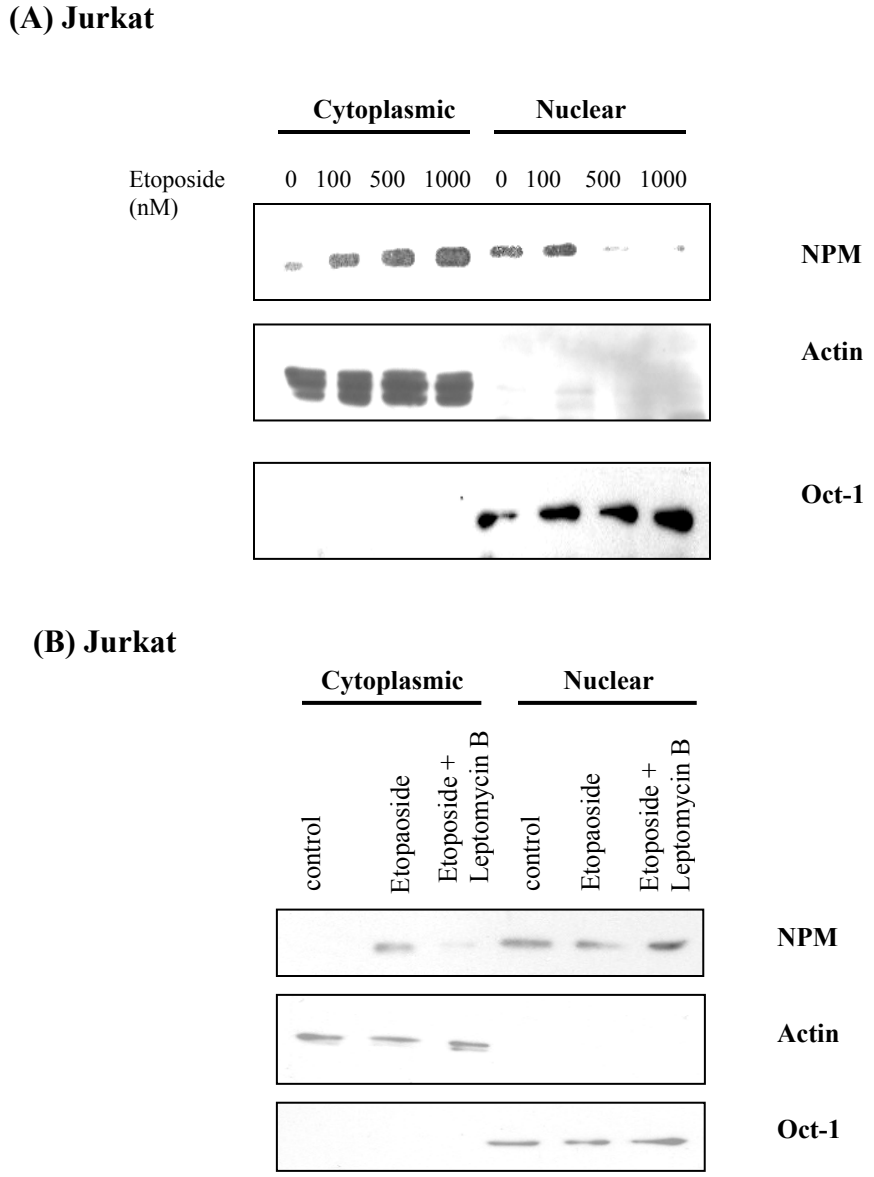


**Figure 2.5. Cytoplasmic translocation of NPM is dependent on Crm1-mediated nucleo-cytoplasmic shuttling.** Cytoplasmic and nuclear fractions were prepared from Jurkat cells after a four-hour exposure to (A) etoposide of increasing dosage or (B) 500 nM etoposide alone or etoposide with 2.5 ng/mLof Leptomycin B. Harvested cells were subjected to subcellular fraction as described in Materials and Methods, Section 2.2.5. Collected fractions were next subjected to SDS-PAGE and immunoblot analysis using anti-NPM, anti-oct-1 or anti-actin antibody, as indicated to the right of each panel.

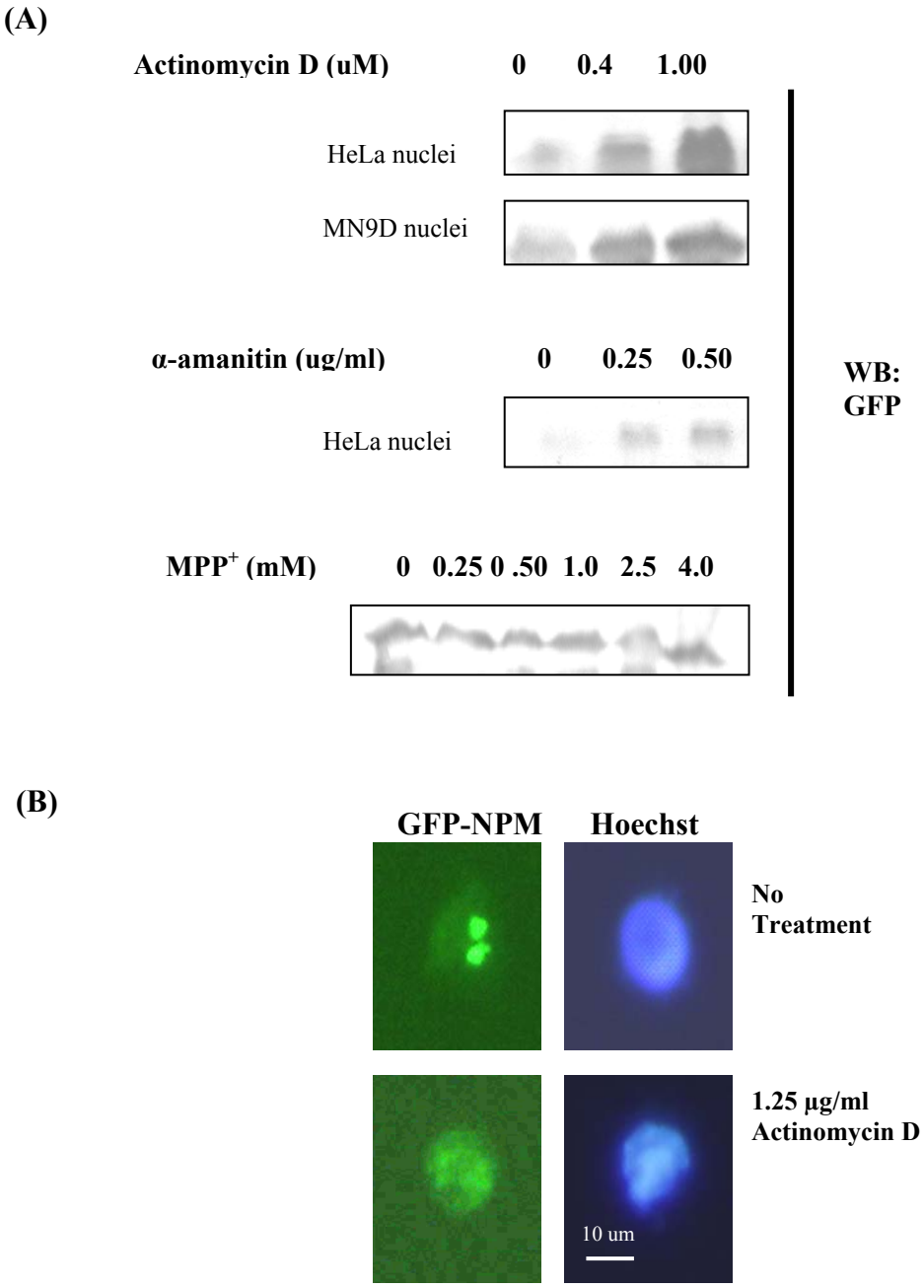


**Figure 2.6. NPM is released from isolated nuclei as a result of drug-induced nucleoli disruption in in vitro nuclei assay.** HeLa or MN9D cells were transfected with GFP-tagged NPM and their nuclei extracted as described in Material and Methods, Section 2.2.9. The resuspended nuclei were then exposed to various concentrations of actinomycin D, α-amanitin and $MPP^+$ as indicated for one hour. The nuclei were next spun down and the supernatant collected were subjected to SDS-PAGE and immunoblot analysis using an anti-GFP antibody (A). The pelleted actinomycin D-exposed nuclei were then resuspended in Nuclei EZ Prep suspension buffer, stained with Hoechst-33342 and observed by fluorescence microscopy using a Zeiss Axiophot (Germany) (B).

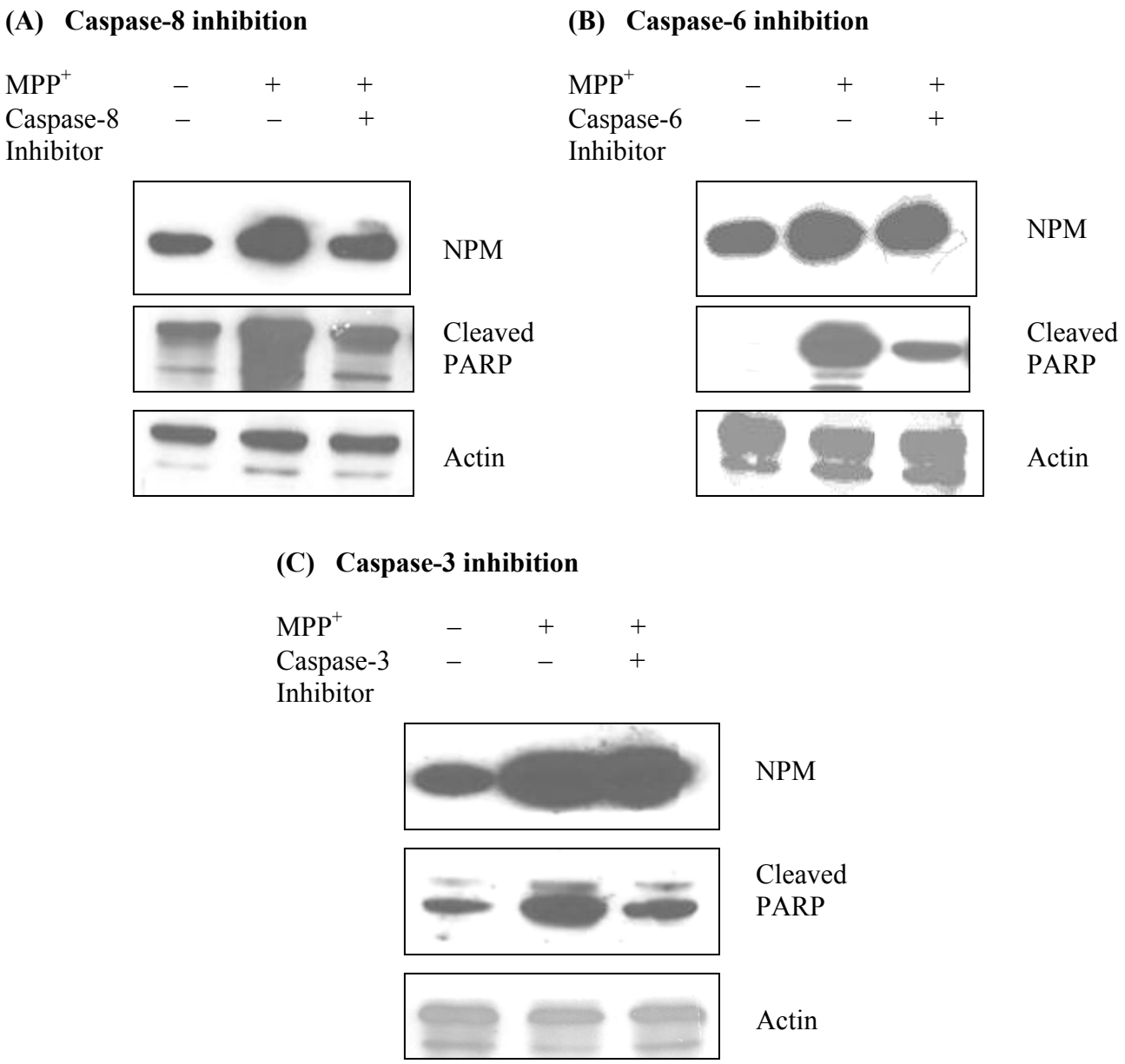


**Figure 2.7. Inhibition of caspase-8, but not caspase-3 or 6, suppressed total cytosolic-nucleoplasmic accumulation of NPM in MN9D cells exposed to $MPP^+$.** MN9D cells were pre-incubated with 0.5 μM of caspase-8 inhibitor (A), 20 μM of caspase-6 inhibitor (B) or 100 μM of caspase-3 inhibitor (C) for 30 min, and then treated with 500 μM $MPP^+$ for 12 h. The cells were then harvested, and total cell lysates extracted as described in Materials and Methods, Section 2.2.4. The extracts were next subjected to SDS-PAGE and immunoblot analysis using anti-NPM, anti-cleaved PARP and anti-actin antibody, as indicated to the right of each panel.

**(A) C3 Overexpression**

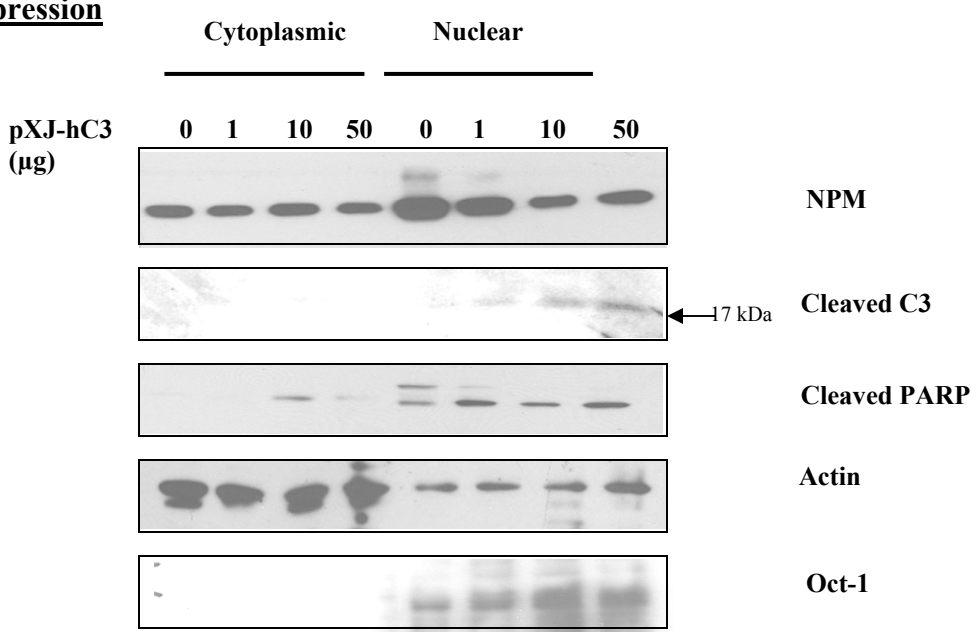


**(B) C6 Overexpression**

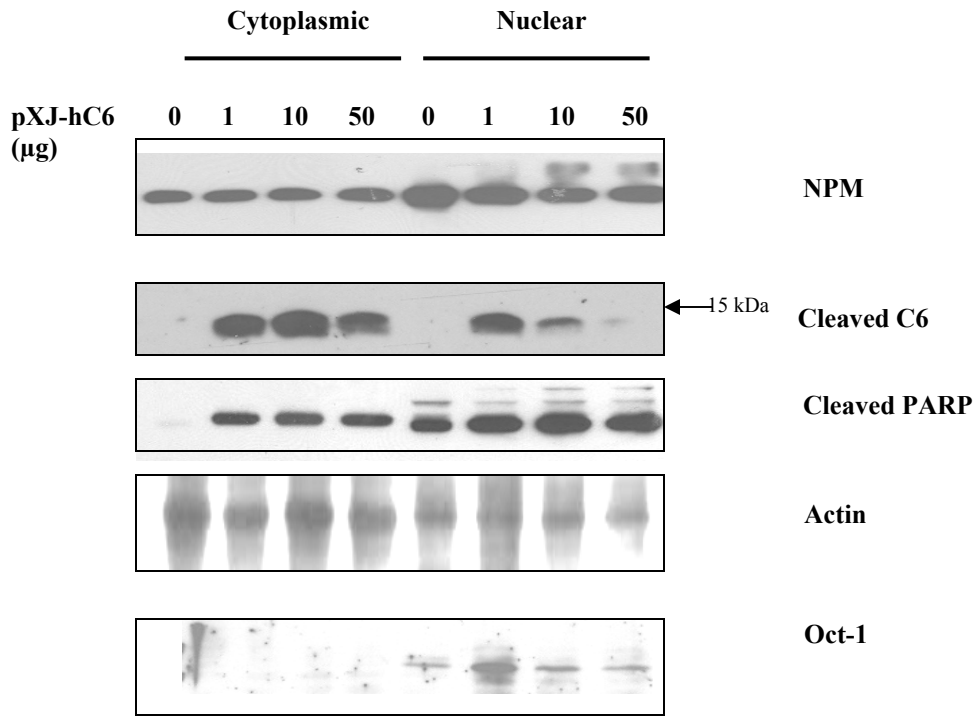


**Figure 2.8. Overexpression of caspase-8, but not caspase-3 and -6, in the HeLa cells induced cytoplasmic accumulation of NPM.** HeLa cells were transfected with various amount of caspase3 (A), caspase-6 (B) or caspase-8 (C) overexpressing plasmid for 24 hours. The cells were then harvested and subjected to subcellular fractionation as described in Materials and Methods,

**(C) C8 Overexpression**

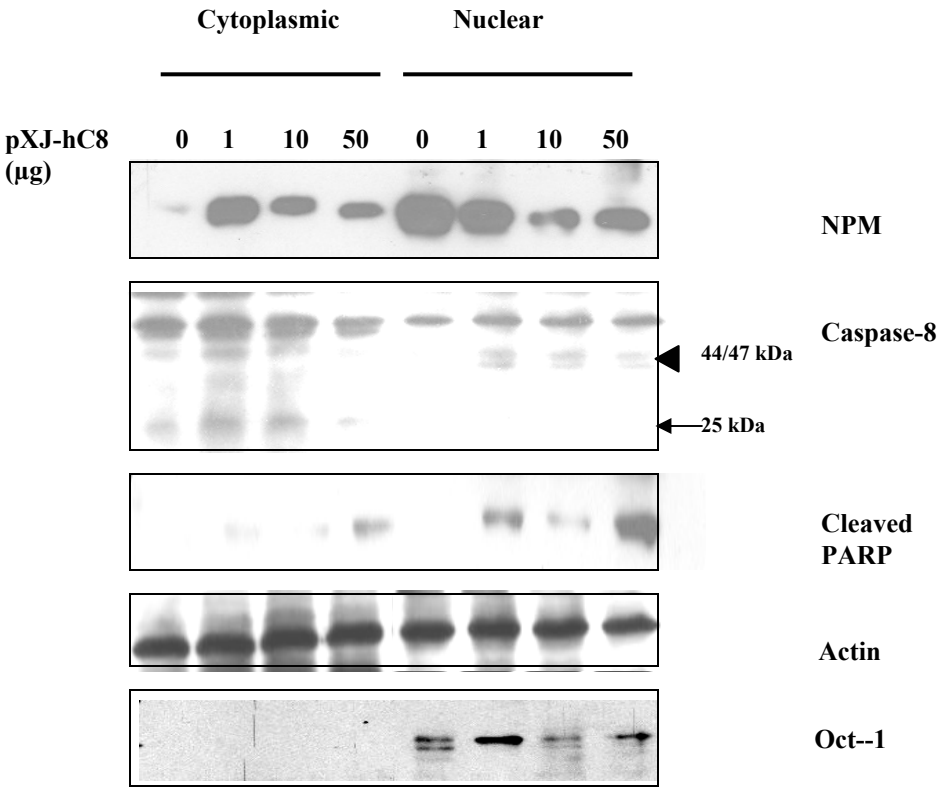


(*Continued from previous page*) Section 2.2.5. Collected fractions were next subjected to SDS-PAGE and immunoblot analysis using anti-NPM, anti-oct-1, anti-cleaved PARP, anti-ß-actin (A-C) , anti-caspase-3 (A), anti-caspase-6 (B) or anti-caspase-8 (C) antibody, as indicated to the right of each panel. 20 µg of the cytoplasmic extract and 10 µg of the nuclear extract were electrophoresed to monitor the relative cytoplasmic and nuclear amount of NPM following caspase overexpression. Black triangle indicates intermediate cleaved caspase fragment, and black arrow indicates cleaved caspase.

**MEF**

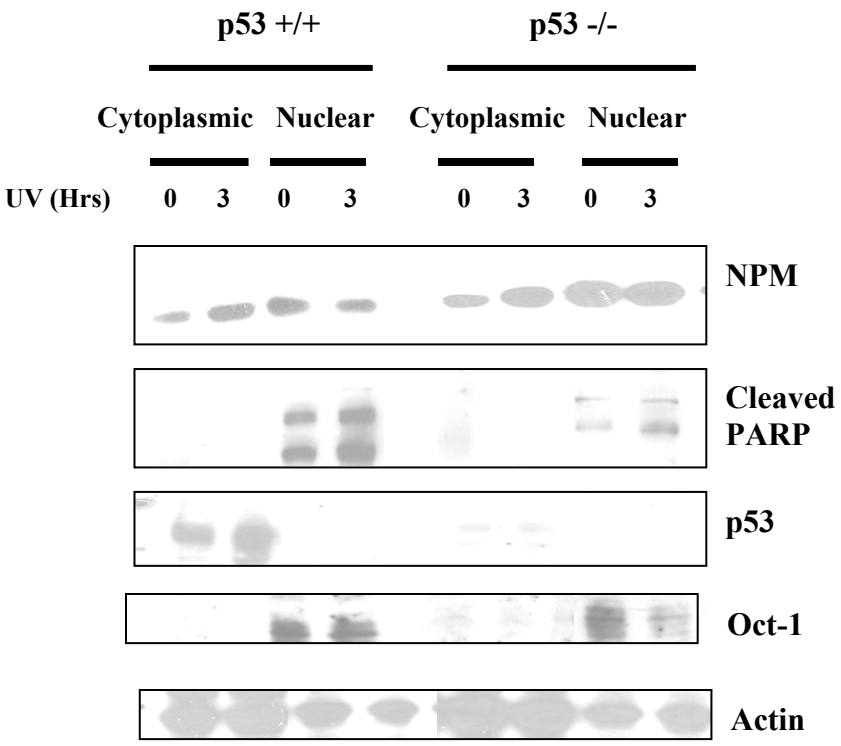


**Figure 2.9. Cytoplasmic NPM accumulation in UV-irradiated p53+/+ and p53 null cells.** p53 +/+ and -/- MEF cells were irradiated with UV (X J/$m^2$) for one hour. These cells, as well as non-irradiated control cells, were harvested and subjected to subcellular fractionation as described in Materials and Methods, Section 2.2.5. Collected fractions were next subjected to SDS-PAGE and immunoblot analysis using anti-NPM, anti-oct-1, anti-actin, anti-cleaved PARP or anti-p53 antibody, as indicated to the right of each panel.

## 2.4 Discussion

In Chapter I, we have observed NPM's up-regulation on the 2DGE. We subsequently noted that the protein extraction used, a low salt HEPES buffer with 1% Triton X-100, was unable to solubilise NPM tightly bound to the nucleoli. As reported previously, nucleoli-bound NPM is resistant to extraction by a 0.5% Triton X-100 containing PBS buffer, but the addition of RNase A is sufficient to release it from the nucleoli (Zatsepina *et al.*, 1997). Since RNase A was not included during the concoction of our protein extraction buffer, the NPM spot observed on our 2D gels most probably represented the combined cytosolic and nucleoplasmic NPM protein amount, rather than the total cellular NPM amount (which takes into account the nucleoli-bound NPM as well). It thus follows that the apparent up-regulation of NPM observed on the 2DGE could be attributed to an increase in the amount of cytosolic-nucleoplasmic NPM released from the nucleolus with $MPP^+$ treatment. This was further corroborated by time-course analysis of NPM expression, which demonstrated a marked increase in total cytosolic-nucleoplasmic NPM level with just two hours of $MPP^+$ exposure (Figure 2.3). We further demonstrated that NPM transcript level remained relative constant for up to 16 hours of $MPP^+$ treatment (Figure 2.4), indicating that the increase in the cytosolic-nucleoplasmic NPM level was not due to *de novo* protein synthesis. Taken together, these data point to the nucleoli as the most obvious source of both the cytoplasmic- and nucleoplasmic-translocated NPM.

Stress-induced translocation of NPM into the nucleoplasm has been an area well-researched on for the past two decades. Conditions or drugs known to cause NPM dispersal into the nucleoplasm include serum deprivation (Chan *et al.*, 1985), actinomycin D (Yung *et al.*,

1985b), toyocamycin, alpha-amanitin (Yung *et al.*, 1985a) and dororubicin (Chan *et al.*, 1987), among many reported previously. In fact, identification of NPM translocation was originally used to detect drug-resistant cancer cells and to study the efficacy of certain anti-tumour agents (Chan *et al.*, 1987), though the exact role of the nucleoplasmic localised NPM was never investigated until recently. A study of the correlation between NPM-translocation and apoptosis in cells induced by daunomycin was conducted by Chan & Chan in 1999, who found that drug concentration required for induction of DNA fragmentation and chromatin condensation in the HeLa cells coincided with the drug concentration required for NPM-translocation. This observation thus suggested a positive role for NPM in the regulation of apoptotic progression, though the mechanism underlying its possible involvement was not speculated. Korgaonkar *et al.* (2005) further demonstrated that NPM inhibits ARF's p53-dependent activity by targeting it to nucleoli and impairing the ARF-Mdm2 association. It follows that stress-induced NPM translocation into the nucleoplasm allows ARF to interact with Mdm2 in the nucleoplasm, which in turn spares p53 from being degraded by Mdm2. The activated p53 can then proceed to halt cell cycle progression and/or initiate apoptotic response. Nucleoplasmic redistribution of NPM may thus be crucial in regulating the cell's p53 responsiveness during stressful conditions.

The recent discovery of a C-terminal NPM mutant in Acute Myeloid Leukemia (AML) (Falini *et al.*, 2005) has led to our speculation that NPM may possess a cytoplasmic function that may be distinct from its nuclear or nucleolar functions. Here, we demonstrated that in response to diverse stress signals, NPM was translocated into the cytoplasm as well (Figure 2.1 and 2.2). The extent of cytoplasmic NPM translocation was observed to correlate very closely with the drug dosage used. Though we have established cytoplasmic build-up of NPM as a general

phenomenon in response to cell stress, the exact cytoplasmic function of NPM remains hitherto unknown. To date, many of the functions ascribed to NPM are reliant on its nuclear localisation. For example, NPM is a partner of the NF-kappaB nuclear transcription complex in the induction of MnSOD by phorbol 12-myristate 13-acetate and cytokines (Dhar *et al.*, 2004). Also, in response to UV damage, NPM undergoes nucleoplasmic redistribution and regulates p53 level by interacting with HDM2 and preventing it from degrading p53 (Kurki *et al.*, 2004). Notably, one cytoplasmic role recently ascribed to NPM is its involvement in centrosome duplication during mitosis. NPM associates specifically with unduplicated centrosomes, and dissociates from centrosomes by CDK2/cyclin E-mediated phosphorylation (Okuda *et al.*, 2000). The Ran-Crm1 nucleo-cytoplasmic shuttling complex was further shown to promote a local enrichment of NPM on centrosomes, thereby preventing unnecessary centrosome reduplication that can lead to supernumerary centrosomes and multipolar spindles that are associated with most human cancer cells (Wang *et al.*, 2005). While it is plausible that cytoplasmic build-up of NPM is required for suppression of centrosome reduplication during stressful conditions, it is unknown if cellular stress can lead to centrosome reduplication.

A possible clue to a cytoplasmic role of NPM in stress response comes from the caspase inhibition and overexpression studies. It was reported previously in an *in vivo* model of ischemic tolerance that widespread caspase-3 activation occurred without cell death in the preconditioned tissues. Moreover, activation of caspase-3 was found to induce up-regulation of Hsp70, and blocking caspase-3 activation would prevent such an up-regulation, and lead to a loss of neuroprotection in the mouse ischemic model (McLaughlin *et al.*, 2003). Based on these observations, it was proposed that the initial energetic stress during preconditioning leads to

limited activation of caspase-3. Once activated, caspases are held in check by interaction and sequestration with proteins such as Hsc 70, thereby depleting the free pool of Hsc 70. This in turn leads to increased synthesis of Hsp 70, which is capable of binding and sequestering components of the apoptotic machinery such as Apaf-1 and Apoptosis Inducing Factor (AIF), among several of Hsp 70's anti-apoptotic roles described so far (Beere *et al.*, 2000; Saleh *et al.*, 2000; Jäättelä *et al.*, 1998). In our current investigation, we similarly demonstrated marked cytoplasmic accumulation of NPM in HeLa cells with overexpression of caspase-8 (but not caspase-3 or -6) (Figure 2.8). Assuming that NPM plays a protective role just like Hsp70 in the mouse ischemic model, the 'deployment' of NPM into the cytoplasm may serve to delay full-fledge apoptotic response until necessaary and thus prevent the cell from dying with slight provocation of the death signalling network. This hypothesis is further supported by our time-course analysis of cytosolic-nucoleoplasmic NPM level in MN9D cells exposed to $MPP^+$ (Section 2.3.2). We showed that elevation in NPM level occurred alongside with the appearrance of cleaved caspase-8. However, upon reaching the peak by the $4^{th}$ hour, total cytosolic-nucleoplasmic NPM level began to decrease and this coincided with the cleaving of caspase-7 and PARP, which indicated the onset of apoptosis (Figure 2.3.3). It thus appeared that the brief initial elevation in NPM level resulted in a temporary 'stall' in apoptotic signalling downstream of caspasse-8, which was subsequently 'revived' with the fall in NPM level after the fourth hour. The ascription of an anti-apoptotic role to NPM in this case will hardly be surprising, since NPM, like the multifunctional Hsp70 protein which mediates neuroprotection in the ischemic model, also functions as a molecular chaperone promoting the renaturation of denatured proteins (Szebeni & Olson, 1999).

It should be emphasized at this point of our discussion that the anti-apoptotic function of the cytoplasmic-localised NPM assumed here is only speculative. It is still highly possible that cytoplasmic NPM may instead be involved in positive regulation of the apoptotic signalling network, in a way similar to that mediated by another molecular chaperone Hsp60. The latter has been shown to be able to improve the vulnerability of pro-caspase-3 to proteolytic maturation by upstream caspases during apoptosis (Xandoudakis *et al.*, 1999). Hsp60 was further shown to translocate into the cytoplasm from the mitochondria during apoptosis, and this coincided with the mitochondrial-to-cytoplasmic translocation and activation of pro-caspase-3 (Samali *et al.*, 1999). It is hence probable that NPM may play a similar role as Hsp60, and like the latter, its translocation into the cytoplasm may allow it to interact with and positively regulate the components of the apoptotic pathway. At this juncture, based on the results gathered so far, the ascription of either a definitive pro-apoptotic or pro-survival role to cytoplasmic-localised NPM will be too premature.

Apart from attempts to elucidate the exact nature of cytoplasmic NPM's involvement during stressful conditions, we also investigated factors promoting or mediating cytoplasmic translocation of NPM. Among the drugs used to induce cytoplasmic NPM translocation, the transcriptional inhibitor actinomycin D and topoisomerase inhibitor camptothecin are known to be potent nucleolar disrupting agents promoting rapid dispersal of nucleolar-bound NPM into the nucleoplasm. The large pool of nucleoplasmic-dispersed NPM would then be available for Crm1 mediated translocation into the cytoplasm, which would otherwise not be accessible to Crm1 mediated nucleo-cytoplasmic transport during non-stressful conditions due to its sequestration to the nucleolus. It thus follows that stress-induced massive disruption of the nucleolus is a pre-

requisite for cytoplasmic translocation of NPM to commence. As attractive as this proposal might be, we further discovered that non-nucleolar disrupting agents such as $MPP^+$ and heat shock could also lead to cytoplasmic NPM build-up. Unlike actinomycin D and another nucleoli disrupting agent α-amanitin, $MPP^+$ was incapable of direct nucleolar disruption leading to passive 'leaking' of the GFP-tagged NPM out of isolated HeLa nuclei (Figure 2.6). We did however observe that with $MPP^+$ treatment, the outline of the nucleoli seemed to be less 'define' with some nucleoplasmic NPM dispersed in between. This might indicate a limited release of NPM into the nucleoplasm, which could then proceed to actively shuttle into the cytoplasm with the aid of Crm1. As mentioned before, activation of caspase-8 by $MPP^+$ may promote cytoplasmic NPM build-up, and it could well be an essential mediating factor signalling for the restricted release of NPM from the nucleoli without disrupting the latter. As such, massive nucleoli disruption may not exactly be a requirement before cytoplasmic NPM translocation can occur, though it may be a contributing factor leading to rapid availability of a large pool of nucleoplasmic NPM for translocation purpose.

Apart from caspase-8, we went on to further determine if an NPM-interacting partner, p53, mediates the cytoplasmic translocation of NPM as well. It was established previously that nucleolin translocation into the nucleoplasm requires the presence of p53 as a nucleoplasmic anchor, such that in p53-null Sao2 cells, no such translocation could occur following exposure to IR and camptothecin (Daniely *et al.*, 2002). Owing to its central position in DNA damage response and apoptosis activation (Levine, 1997), p53 would seem like an 'ideal' candidate for regulating cytoplasmic NPM translocation. However, cytoplasmic NPM build-up was still observed (with concomitant decrease in nuclear NPM level) even in the p53-null MEF cells

following UV irradiation (Figure 2.9). This observation thus indicates that unlike in the case of nucleolin, p53 is *not* a crucial factor regulating stress-induced cytoplasmic translocation of NPM.

In conclusion, our results point to cytoplasmic NPM accumulation as a common phenomenon in response to diverse stress signals, in addition to the well-established nucleoplasmic accumulation of NPM. Activation of caspase-8, which is usually the first caspase to become activated during stress-induced death signalling, was demonstrated to be sufficient to induce cytoplasmic NPM build-up. Meanwhile, stress-induced massive nucleolar disruption may also contribute to the phenomenon by "supplying" a ready pool of nucleoplasmic NPM for Crm1-mediated translocation into the cytoplasm. While the overall results are indicative of NPM's involvement in apoptotic regulation, its precise cytoplasmic role still remains elusive at this juncture. Perhaps, deciphering NPM's connection with the cytoplasmic apoptotic machinery may hold the key to this mystery, as we shall see in the next chapter.

# Chapter III. NPM retards the apoptotic signalling cascade via inhibition of caspase-6 and -8

## 3.1 Introduction

Cellular response to genotoxic stress includes cell cycle arrest and activation of DNA repair mechanism. However, in the event of irreparable cellular damage, cells respond with induction of apoptosis. Apoptosis is an evolutionarily conserved mode of cell death characterised by a discrete set of biochemical and morphological events resulting in an ordered disassembly of the cell (Kerr *et al.,* 1972; Vaux *et al.,* 1994; Steller, 1995). The biochemical orchestration of the apoptotic death is mediated largely by the activity of a group of conserved cysteinyl-aspartate proteases that are activated in response to a variety of proapoptotic stimuli (Nicholson, 1996; Thornberry *et al.,* 1997; Thornberry & Lazebnik, 1998).

There are at least 14 caspases identified in mammalian cells, which are normally expressed as inactive precursor molecules (procaspases), that in response to an apoptotic stimulus are proteolytically cleaved at specific Asp-X junctions to generate catalytically active heterodimers (Thornberry & Lazebnik, 1998). The mature enzyme consists of two large (~p20) and two small (~p10) subunits, derived from a pair of interdigitated proenzyme molecules (Rotonda *et al.,* 1996). Caspases are divided into two subgroups based on their functions in the apoptotic pathways. The initiator caspases consisting of caspase-1, -2, -4, -5, -8, -9, -10, -11, and -12 which receive the initial death stimulus. The activation of this cascade of caspases usually converges to activate a common set of the downstream effector caspases. Effector caspases (consisting of caspase-3, -6, -7 and -14) are directly responsible for the cleavage of housekeeping proteins, causing death to the cells and also giving rise to the morphological characteristics observed during apoptosis. They can also inactivate proteins that inhibit apoptosis by cleaving

them into fragments. Various initiator and effector caspases are involved in different death signalling pathways.

### *3.1.1 Different roles of caspases in the death pathways*

Cellular survival is an intricate balance between factors that either promote or inhibit apoptosis. Several pathways and protein families together set a threshold for apoptosis to assure that apoptosis only takes place in response to an appropriate death signal, whereas cell death is prevented when cellular survival is required. Apoptotic cell suicide can be initiated by a plethora of stimuli that generally feed into one of two known death signalling pathways as shown in Figure 3.1, with various caspases playing crucial roles in signal transmission and death execution (Budihardjo *et al.,* 1999; Green, 2000). The intrinsic pathway feeds cell death signals through the mitochondria, which appears to act as a generic damage sensor and monitor of metabolic status. The mitochondrion apoptotic pathway initiates with signalling from pro-apoptotic proteins from the Bcl-2 family such as Bax, which trigger the release of cytochrome c. The cytosolic presence of cytochrome *c* will result in the formation of the apoptosome, consisting of Apaf-1, procaspase-9 and cytochrome *c* itself. In the presence of ATP, procaspase-9 is cleaved resulting in the activation of caspase-3, which in turns activates the caspase activation cascade (Figure 3.1 a) (Green & Reed, 1998).

On the other hand, the extrinsic pathway is initiated by binding of extracellular death ligands belonging to the Tumour Necrosis Factor (TNF) superfamily (e.g., TNF-α, Fas ligand and Apo3L) to their respective transmembrane death receptors found on the surface of the cell (Figure 3.1b). This leads to the recruitment of adaptor proteins such as FADD (Fas-associated

death domain) to the receptor (Blagosklonny, 2000). The adaptor proteins in turn recruit procaspases to form the death-inducing signalling complex (DISC), and the procaspases are then activated to form the enzymatically active heterotetramers. Caspase-8 and caspase-10 are the caspases recruited in this pathway, with caspase-8 playing a major role. The activation of caspase 8, similar to caspase 9 in intrinsic pathway, leads to effector caspases activation (Chan *et al.,* 2000; Siegel *et al.,* 2000). In addition, the bcl-2 family member Bid is cleaved by the activation of pro-caspase-8 through the extrinsic pathway, and translocates to the mitochondrion to promote cytochrome *c* release, thereby completing a positive feedback loop of caspase activation and providing a link to the intrinsic death pathway.

### *3.1.2 Keeping death in check – the Inhibitor of Apoptosis (IAP) family*

Given their intimate involvement throughout the entire apoptotic signalling pathway, the caspases represent strategic targets for regulating and setting certain threshold for apoptosis induction. The Inhibitor of Apoptosis (IAP) is a family of proteins regulating the activity of the caspase cascade by blocking both the mitochondrial-dependent and -independent apoptotic pathways (Jia *et al.*, 2003; Carson *et al.*, 2002). IAPs were first identified in baculoviruses, and they belong to a family of homologous proteins characterised by the presence of one or more baculoviral IAP repeat (BIR) domains, together with an ability to suppress apoptosis (Crook *et al.*, 1993; Birnbaum *et al.*, 1994). The IAP proteins identified in humans include X-chromosome linked IAP (XIAP), cellular inhibitor of apoptosis 1 and 2 (cIAP1, cIAP2), neuronal apoptosis inhibitor protein (NAIP), livin and survivin. The IAP may regulate caspase activities by two

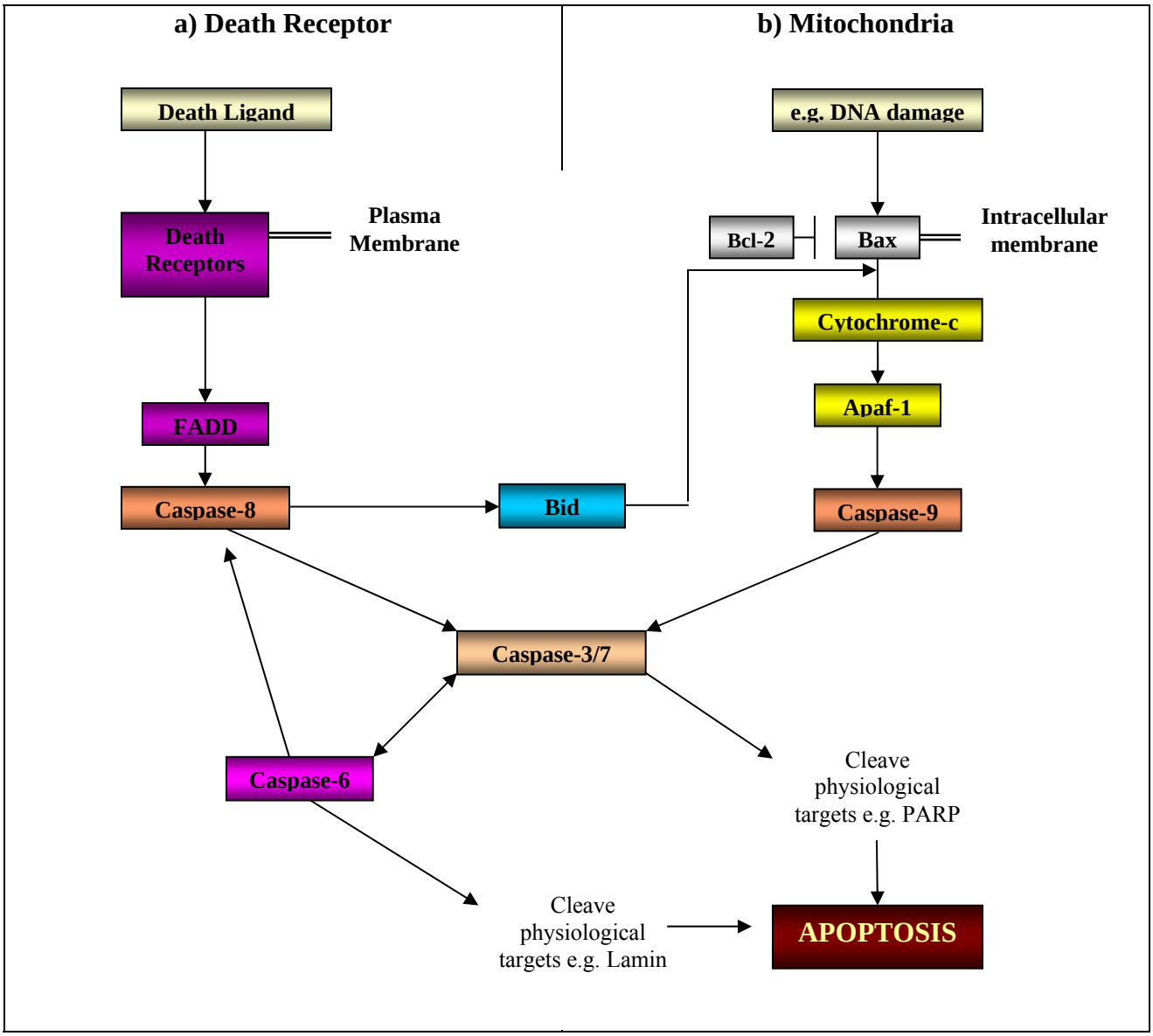


**Figure 3.1 Illustration of the different proteins involved in the two apoptotic pathways.** In the death receptor pathway (a), death ligands such as TRAIL or Fas bind to the death receptors e.g. DR5 or CD-95 respectively. This triggers the recruitment of FADD and procaspase-8 to the death receptor, forming the Death-Inducing Signalling Complex (DISC) which leads to caspase-8 cleaving and activation. In the mitochondrial pathway (b), apoptotic stimuli such as DNA damage triggers the dimerisation and insertion of the pro-apoptotic Bax into the mitochondrial membrane, allowing the efflux of cytochrome *c* into the cytoplasm. The cytosolic presence of cytochrome-c will result in the formation of the apoptosome, consisting of Apaf-1, procaspase-9 and cytochrome-c itself. In the presence of ATP, procaspase-9 is cleaved and activated. Both activated caspase-8 and -9 cleave procaspase-3, which in turn activates caspase-6. The executor caspase-3 and -6 then cleave and inactivate other cellular targets. Activated caspas8-8 also cleaves Bid, which can trigger cytochrome *c* release as well. Legend: FADD, Fas-associated death domain, PARP, Poly-(ADP-ribose) Polymerase.

ways, either by direct caspase inhibition, or by promoting the degradation of the caspases.

Using the BIR domain, the IAPs can bind to and inhibit caspases. For example, the third BIR of XIAP can bind to the initiator caspase-9, preventing the homodimerisation of caspase-9 and keeping caspase-9 in an inactive monomeric state. This in turns prevents the activation of caspase-9, which requires homodimerisation of the enzyme before it can cleave downstream effector caspase such as caspase-3 (Shiozaki *et al.*, 2003; Srinivasula *et al.*, 2001). Meanwhile, XIAP inhibits caspase-3 (and caspase-7) by interaction of its second BIR and the preceding linker region with active caspase-3 dimer. This in turn prevents the interaction of caspase-3 dimers with their cellular substrates, hence inhibiting the proteolytic degradation of the cell that marks the final execution stage of apoptosis (Huang *et al.*, 2001b; Riedl *et al.*, 2001; Suzuki *et al.*, 2001b).

Apart from BIR, several IAPs also contain the RING finger possessing ubiquitin protein ligase activity (Deveraux *et al.*, 1999). Ubiquitin ligases can target specific proteins for ubiquitination and subsequent degradation by the proteasome. cIAP2 and XIAP can trigger the ubiquitination of caspase-3 and -7, suggesting that RING-dependent proteosomic caspase degradation may be another mechanism of the IAPs' anti-apoptotic activity (Huang *et al.*, 2000; Suzuki *et al.*, 2001c).

A number of proteins have been identified which regulate IAP's turnover. SMAC and Omi/HtrA2 are proteins that reside in the mitochondrial intermembrane space and translocate to the cytosol during apoptosis (Hedge *et al.*, 2002; Verhagen *et al.*, 2000; Suzuki *et al.*, 2001a; Marins *et al.*, 2002; van Loo G *et al.*, 2002). Processed SMAC and Omi/HtrA2 can compete with

the caspases for binding to IAPs, hence liberating the caspases from IAP repression. SMAC can interact with several IAPs, including XIAP, c-IAP1, c-IAP2, Survivin and Livin' thereby interfere with inhibition of caspase-3, -7 and -9 (Chai *et al.*, 2000; Srinivasula *et al.*, 2000). Another protein, the XIAP-associated factor (XAF-1) interacts with XIAP and antagonizes XIAP inhibition of the caspases and subsequently apoptosis. It also triggers the translocation of XIAP into the nucleus, thereby preventing their inhibitory interaction with the cytosolic caspases (Liston *et al.*, 2001).

The IAPs and their antagonists thus represent potent death mediators, which determine the extent of death signal penetration within a cell through caspase regulation. They are, however, not the only players residing within the cell's anti-apoptosis squad, as another group of proteins, which forms the most ancient defence system in all living organisms, have also been discovered to play similar functions to the IAPs in regulating apoptotic signalling.

### *3.1.3 Heat shock proteins (Hsps) as death determinants*

Both heat shock responses and apoptosis are mechanisms engaged to cope with stressful conditions, though one is being protective, while other potentially lethal. It is therefore likely that the apoptotic process evolved with an inherent susceptibility to intervention by one or more of the heat shock proteins (Hsps) at different points in the apoptotic cascade. Recent evidences suggest that the coordinated balance between these two opposing pathways governs the ultimate fate of the cell - whether it lives or dies (Beere *et al.*, 2000).

The Hsps are a large family of highly conserved proteins that can be classified into groups based primarily on size which can vary anywhere from 10 – 170 kDa. The six major size classes currently recognised are Hsp100, Hsp90, Hsp70, Hsp60, Hsp40, and the small heat shock proteins, which can range from 10-30 kDa (Gething, 1997). The Hsps are constitutively expressed in the cells and their levels can be rapidly induced in response to cellular stress. Hsps function collectively to protect the cells from adverse environmental, physical or chemical stresses through their ability to bind to and stabilise proteins that are in a non-native conformation. Interactions with these unstable protein conformations prevent the formation of large protein aggregates and facilitate normal protein folding, membrane translocation, and the degradation and removal of damaged proteins (Feder & Hofmann, 1999).

The protective role of the Hsps may be extended to include the anti-apoptotic role for several members of the Hsp family, including Hsp90, Hsp70 and Hsp27. Hsp70 is able to directly inhibit caspase processing by interacting with Apaf-1, hence preventing the recruitment of procaspases-9 to the apoptosome (Beere *et al.*, 2000). Hsp90 and Hsp27 are also shown to be able to inhibit the formation of a functionally competent apoptosome. Hsp90 associates with Apaf-1 directly to prevent its oligomerisation that is required before procaspases-9 recruitment into the apoptosome (Pandey *et al.*, 2000b), while Hsp27 binds to and sequesters cytochrome *c* away from its target Apaf-1 (Bruey *et al.*, 2000).

Like the IAPs, the anti-apoptotic mechanisms of some of the Hsps involve inhibition interaction with the caspases. αB-crystallin, a small heat shock protein that is related to Hsp27, binds to caspase-3 that has been partially processed by caspase-9 or caspase-8 cleavage and inhibits the autoproteolytic removal of its prodomain to produce its large subunit (Kamradt *et al.*,

2001). Meanwhile, Hsp27 associates with caspase-3, but not Apaf-1 or caspase-9, and inhibits activation of caspase-3 by caspase-9-mediated proteolysis (Pandey *et al.*, 2000a). Because this autocatalytic maturation is required for caspase-3 activation by both the mitochondrial and death receptor pathways, the inhibition of caspase-3 maturation by αB-crystallin and Hsp27 is a parsimonious strategy to inhibit both pathways. In the case of Hsp60, however, its direct interaction with procaspases-3 actually accelerates the maturation of procaspase-3 by different upstream activator caspases and this effect was dependent on ATP hydrolysis. It was proposed that the ATP-dependent chaperoning activity of Hsp60 improves the vulnerability of pro-caspase-3 to proteolytic maturation by upstream caspases and that this represents an important regulatory event in apoptotic cell death (Samali *et al.*, 1999; Xanthoudakis *et al.*, 1999).

These recent discoveries reveal an important connection between Hsps and the apoptotic machinery. Given that cellular homeostasis represents an equilibrium between survival and death, it follows that HSPs should play a pivotal role in maintaining this delicate balance via regulation of caspase activation within the death signalling pathways.

### *3.1.4 Other anti-apoptotic regulators involved in death signalling*

Apart from the IAP and Hsps family, there are other molecules which play pivotal roles in suppression of caspase activation at different points in the apoptotic cascade. Cellular FLICE-inhibitory protein (c-FLIP) specifically regulates the extrinsic apoptotic process through inhibition of caspase-8 activation. c-FLIP is expressed in both a long-form (c-$FLIP_L$) and a short-form (c-$FLIP_S$) due to alternative splicing. The Death Effector Domains (DEDs) of c-$FLIP_L$ and c-$FLIP_S$ interact with the DEDs of FADD and procaspasse-8. Through the binding of c-FLIP to

FADD and procaspase-8 at the death receptor complexes, c-FLIP presumably prevents the processing of procaspase-8 and thus inhibits downstream apoptotic events (Irmler *et al.*, 1997; Tschopp *et al.*, 1998).

Though members of the Bcl-2 family do not directly inhibit caspase activation like c-FLIP, they do exert profound influence on the caspase activation status within the intrinsic pathway through regulation of cytochrome *c* release from the mitochondria. Proteins belonging to the Bcl-2 family are key regulators of cell death and survival, and individual family members can serve to inhibit or promote apoptosis (Cory & Adams, 2002). In general, Bcl-2 proteins regulate the apoptotic cascade mainly at the level of the mitochondria. Members of the Bcl-2 family possess either anti-apoptotic or pro-apoptotic function. They are characterised by the presence of conserved sequence motifs, known as Bcl-2 homology (BH) domains. Anti-apoptotic members share all four BH domains, designated as BH1-4; the multidomain pro-apoptotic members contain BH1-3 domains, whereas another subgroup of pro-apoptotic members only possess a BH3 domain (Cory & Adams, 2002). The BH3-only proteins act as sensors for distinct apoptosis pathways, whereas multidomain pro-apoptotic Bax and Bak are executioners of death orders relayed by the BH3-only proteins. Upon activation by an apoptotic signal, the BH3-only protein such as Bid and Bim, activate the pro-apoptotic Bcl-2 proteins Bax and Bak to permeabilize the mitochondrial outer membrane leading to the release of cytochrome c and other proteins from the intermembrane space (Shimizu *et al.*, 2000; Korsmeyer *et al.*, 2000). The impact of pro-apoptotic Bcl-2 proteins on mitochondria can be inhibited by anti-apoptotic members such as Bcl-2 and/or Bcl-$X_L$. Anti-apoptotic Bcl-2 family members appear to function, at least in part, by interacting with and antagonizing pro-apoptotic family members (Sedlak *et al.*,

1995; Kelekar *et al.*, 1997). Although the mechanism underlying the regulation of mitochondrial membrane permeability is not completely understood, current hypotheses suggest that Bcl-2 family members regulate the outer mitochondrial membrane by interaction with the voltage-dependent anion channel (VDAC) (Shimizu *et al.*, 1999).

### *3.1.5 Involvement of NPM in the regulation of apoptosis*

Insights into the anti-apoptotic mechanisms of many cell death mediators were gained on the foundation of numerous previous studies demonstrating the oncogenic potential and/or protective effect of these molecules against cell death. For example, Hsp27 delivered with a herpes simplex virus-based vector protects dorsal root ganglion neurons from apoptosis induced by nerve growth factor withdrawal (Wagstaff *et al.*, 1999). Over-expression of Hsp27 or Hsp70 protects cardiac cells against three different apoptosis-inducing stimuli, as well as against thermal or hypoxic stress (Heads *et al.*, 1994; Jayakumar *et al.*, 2001). On the flip side, partial deletion of neuronal apoptosis inhibitor protein (NAIP) gene resulted in uncontrolled cell death in certain neurodegenerative disorders, such as type I spinal muscular atrophy (SMA) (Roy *et al.*, 1995). Meanwhile, the prototypical anti-apoptotic member, Bcl-2, was first discovered because of its involvement in 95% of follicular B-cell lymphomas as a result of a chromosomal translocation t(14;18) (Tsujimoto *et al.*, 1985). High levels of bcl-2 did not act to increase proliferation but rather increased cell survival (Henderson *et al.*, 1991), thus defining a new class of oncogenes with anti-apoptotic functions.

Several lines of studies indicate that NPM may also play a role in the regulation of apoptosis. Overexpression of NPM results in a decrease in susceptibility of human leukaemia

HL-60 cells to sodium butyrate and retinoic acid-induced apoptosis, while down-regulation of NPM through anti-sense NPM transfection increases this susceptibility (Liu *et al.,* 1999; Hsu & Yung, 2000). Increased stability of NPM is also shown to be involved in ant-apoptotic effect of the oncogene ras during serum deprivation. NPM in serum-deprived NIH-3T3 cells was found to be highly unstable with a short half-life, while NPM in serum-deprived ras-transformed (RAS-3T3) cells was as stable as that in serum-supplemented NIH-3T3 or RAS-3T3 cells. Treatment of RAS-3T3 cells with NPM antisense oligomer significantly potentiated the apoptosis induced by serum deprivation (Chou & Yung, 2001). Also, suppression of NPM expression by small interfering RNA targeting NPM increases hypoxia-induced apoptosis, whereas overexpression of NPM protects against hypoxic cell death (Li *et al.,* 2004). Finally, development of the forebrain and haematopoiesis was shown to be profoundly disrupted in *Npm1(-/-)* mutants as a result of excessive apoptosis, indicating a pivotal role for NPM in apoptosis regulation in these developmental processes (Grisendi *et al.,* 2005).

In the previous chapter, NPM was shown to translocate into the cytoplasm in response to stress signals such as a sub-lethal heat shock. In the event of acute toxic exposure, such translocation preceded the onset of the apoptotic events such as cleaving of PARP and executioner caspase-7. This led to the speculation that early translocation of NPM may represent a transient cytoprotective mechanism suppressing cell death in the event of mild stress. In acute myelogenous leukaemia (AML) with a normal karyotype, a C-terminal frame-shift mutation of the *NPM* gene results in cytoplasmic dislocation of NPM (Falini *et al.,* 2005), which may possibly function in cancer pathogenesis through cell death inhibition. Given that over-expression of NPM can inhibit apoptosis, and that both the intrinsic and extrinsic signalling

pathways are initiated in the cytoplasm, the current investigation was undertaken to determine the role that cytoplasm-localised NPM may play in regulating death signal transmission, particularly with regard to suppression of caspase signalling.

## 3.2 Materials and Methods

### *3.2.1 Cloning of Human and Mouse NPM*

Total RNA was prepared using TRIZOL (Invitrogen, USA) from the mouse MN9D cells according to the protocol by TRIZOL's manufacturer. Amplification of the human and mouse NPM cDNA was performed using the Access RT-PCR kit (Promega, USA) from the extracted RNA, using the following primers:

For mouse NPM: Forward primer 5' – CTC ATG GAA GAC TCG ATG GAT ATG G –3'

Reverse Primer 5' – TCT TAA ACA GAC TTC CTC CAC TGC C –3'

For human NPM: Forward primer 5' – CCG ATG GAA GAT TCG ATG GAC ATG –3'

Reverse Primer 5' – TTA AAG AGA CTT CCT CCA CTG –3'

The PCR cycles were (i) 95°C for 5 min; (ii) 95°C for 1 min, 50°C for 2 min, 72°C for 1 min (30 cycles); and (iii) 72°C for 10 min. The full-length PCR product was purified by low melting-agarose gel electrophoresis and cloned into pGem-T Easy vector (Promega, USA).

### *3.2.2 Expression of Recombinant NPM*

Full-length NPM cDNA in pGEM T-Easy (Promega, USA) was used for constructing recombinant NPM protein. The restriction enzyme EcoRI was used to cleave out the NPM cDNA, which was then ligated into pET32a using non-direction cloning.

Polyhistidine-tagged NPM was expressed in *Escherichia coli* BL21(DE3)pLysS bacteria (Novagen, USA). After 3 h of growth at 37 °C the culture was transferred to room temperature and 0.5 mM isopropyl thiogalactopyranoside (Biorad, USA) was added to induce expression of recombinant proteins for 3 h. Bacteria were harvested by centrifugation, resuspended, and lysed by sonification as described previously (Holstein *et al.*, 1996). 1% Triton X-100 (Sigma, USA) and Complete protease inhibitor mixture (Roche Molecular Biochemicals, USA) were included in the lysis buffer. Recombinant proteins were purified by affinity chromatography on Ni-NTA agarose (Qiagen, USA) according to the manufacturer's recommendations.

### *3.2.3 Cell culture and induction of apoptosis*

MN9D (obtained with courtesy of Dr Jun Chen, University of Pittsburgh and with agreement from Dr Alfred Heller (University of Chicago), HeLa (a gift from Dr Ge Rou Wen, NUS), SHSY5Y (a gift from Dr Lim Kah Leong, National Neuroscience Institute, Singapore), 293T and NIH 3T3 (both gifts from Dr Low Boon Chuan, NUS) cell lines were cultured in DMEM medium (RPMI 1640 medium for 293T cells) supplemented with 10% fetal bovine serum and 1% penicillin/streptomycin in a humidified atmosphere of 5% $CO_2$ at 37°C. To induce apoptosis, MN9D cells were treated with 500μM of $MPP^+$, NIH 3T3 with 50μM of cyclohexamide, SHSY5Y and 293T cells with 1μM rotenone and HeLa cells with UV radiation 50 $Jm^{-2}$, 4 ug/ml of camptothecin or 0.5 μM of actinomycin D for varying length of time.

### *3.2.4 Plasmids and Transfection*

pcDNA3.1-GFP-NPM codes for the mouse NPM gene fused to a GFP tag and is used in transient transfection investigation in this chapter. The mouse NPM cDNA was then subcloned into pcDNA3.1 plasmid using the EcoRI restriction site for non-directional cloning. For plasmid transfection, HeLa cells were seeded at a density of 1.5 x $10^5$ per well in six-well plates in DMEM supplemented with 10% fetal bovine serum. 24 h later, the cells were transfected with varying amount of plasmid DNA using Lipofectamine (Invitrogen, USA) according to the manufacturer's instructions. After 24-48 hours, the cells were harvested and protein extracted for further analysis. As the transfection effeciancy of the HeLa cells with pcDNA3.1-GFP-NPMis quite high (>50% when judged visually using fluorescence microscopy), cell-sorting was not utlised to enrich for the transfected cells before protein extraction.

### *3.2.5 RNA Interference*

The siRNA sequence-targeting NPM gene corresponded to nucleotides 103−125 of the coding region relative to the first nucleotide of the start codon (sense, 5'-UGAUGAAAAUGAGCACCAGTT-3'; antisense, 5'-CUGGUGCUCAUUUUCAUCATT-3'). As a control, the inverted sequence was used (sense, 5'-GACCACGAGUAAAAGUAGUTT-3'; antisense, 5'-ACUACUUUUACUCGUGGUCTT-3'). MN9D cells were plated in a six-well plate at a density of 2.35 x $10^5$ cells per well 24 hours before performing the transfection protocol. Just prior to transfection, the medium was removed and 500 µl of fresh DMEM supplemented with 10% FBS was added to each well. During transfection, 10 µl of transit-TKO transfection reagent was added, dropwise, into 100 µl of serum-free DMEM, vortexed and incubated for 20 min. The

RNA duplex was then added to the mixture to a final concentration of 10 nM and incubated for another 20 min for complex formation. The complex was then added, dropwise, to each well and the cells incubated at 37°C for 24 hours before being exposed to 500 µl $MPP^+$ for another 12 hours. The cells were subsequently harvested and subjected to subcellular fractionation to obtain the cytoplasmic fraction for western blot analysis.

### *3.2.6 Preparation of subcellular fractions*

Nuclear and cytosolic fractions were prepared using the Nuclear/Cytosol fractionation kit (BioVision, USA), according to the manufacturer's protocol. Briefly, cells were washed with PBS two times to remove the medium. A volume of 200µl of Cytoplasm Extraction Buffer A (CEB-A) was added and the cells scraped down using a rubber policeman. The cell suspension was then vortexed for 15 sec and incubated on ice for 10 min. 11µl of the Cytoplasm Extraction Buffer B (CEB-B) was next added to the suspension and vortexed for 5 sec. The suspension was then incubated on ice for 1 min, vortexed for another 5 sec, before being centrifuged at 16, 000 g for 5 min at 4°C. The supernantant, which is the cytoplasmic fraction, was then collected. Next, 100µl of the Nuclear Extraction Buffer (NEB) added to the pellet and vortexed vigorously for 15 sec and incubated on ice for 10 min before being subjected to another round of vortexing. This was repeated over a duration of 40 min, after which the suspension was centrifuged at 16, 000 g for 10 min at 4°C. The supernatant, which is the nuclear fraction, was then collected. The fractions were immunoblotted against the nuclear marker oct-1 to ensure clean separation of the two fractions.

### *3.2.7 Electrophoresis and Western Blot analysis*

Equal amount of proteins were resuspended in SDS-PAGE buffer (62.5 mM Tris-HCl, pH 6.8, 2% SDS, 10% glycerol, 5% dithiothreitol) and boiled in a water bath for 5 min. Lysates were stored at -20°C until further analysis. Proteins were separated under reducing conditions for 2 h at 120 V in 12 or 15% SDS-polyacrylamide gels. Gels were transblotted onto the nitrocellulose membranes at 100V for 1.5 h. Membranes were blocked for 1h in TBS Tween with 5% milk powder, and then incubated overnight with anti-NPM (Zymed, USA, 1:10000), -caspase-3 (Santa Cruz, USA, 1:1000), -caspase-6 (Cell Signalling Technology, USA, 1:2000), -caspase-7 (Neomarkers, USA, 1:600), -caspase-8 (Cell Signalling Technology, USA, 1:1000), -cleaved PARP (Cell Signalling Technology, USA, 1:2000), -oct-1 (Chemicon, USA, 1:1000), -cytochrome *c* (Becton Dickinson, USA, 1:1000), -cleaved Bid (Chemicon, USA, 1:1000), Lamin A/C (Cell Signalling Technology, USA, 1:1000) and actin (Santa Cruz, USA, 1:1000), followed by incubation with HRP-conjugated secondary antibodies (Santa Cruz, USA), goat-anti-mouse or anti-rabbit (1:1000). Protein bands were visualised by applying chemiluminescent substrate (Pierce, USA).

### *3.2.8 Preparation of S100 cytosolic Cell-free Extracts*

To make S100 cell-free extracts, the cell pellet was resuspended at $10^8$ cells/0.5 ml of ice-cold buffer A (20mM Hepes-KOH, pH7.5, 10mM KCl, 1.5 mM $MgCl_2$, 1 mM EDTA, 1 mM EGTA, 3 mM dithiothreitol, and protease inhibitor cocktail (Calbiochem, USA). After

incubation on ice for 15 min, the cells were disrupted by Dounce homogenizing for 15 times in a Wheaton Dounce homogenizer with a tight pestle. The lysates were directly centrifuged at 100,000 x g for 1 hour in a Beckman Optima TLX-100 ultracentrifuge. The resulting supernatants (S100 cell-free extracts) were collected.

### *3.2.9 Immunodepletion*

4 μg of anti-NPM (Zymed, USA) or anti-HA $IgG_{2a}$ (Santa Cruz, USA) was incubated with 100 μl of S100 extract for 1 h on ice. The immune complexes were then cleared by incubation with protein A/G bead pellet (from 10 μl of 25% v/v, Santa Cruz, USA) for 4 hour in a rotator at 4°C. The beads were subsequently pelleted by centrifugation for 2 min in a microcentrifuge at 4°C, and the resulting supernatant were collected and incubated for various length of time at 37°C for caspase activation, before being analysed by immunoblotting.

### *3.2.10 In vitro caspase activation*

Untreated 293T cells were harvested, collected by centrifugation, and washed twice with ice-cold PBS. The cell pellet was resuspended at $10^8$ cells/0.5 ml of ice-cold buffer A. After incubation on ice for 10 min, the cells were disrupted by Dounce homogenizing for 20 times and centrifuged at 15,000 x g for 20 min, 4°C before collecting the supernatant. 100 μl of the supernatant was incubated with cytochrome *c* (300 nM) and ATP (900 nM) at 37°C for 3 hour to activate the caspase cascade. To determine the effect of recombinant NPM on caspase activation, 5 μM of these proteins were included in the incubation mixture.

### *3.2.11 Immunofluorescence microscopy*

HeLa cells were cultured as described in Section 2.2.1. After exposure of the cells to 0.5 μg/mL of actinomycin D for four hours, the cells were then handled separately depending on which active caspase was to be visualised. For observation of active caspase-8, the cells were incubated for 1 h at 37°C in fresh DMEM medium with 1x IETD-FLICA (amount used according to the manufacturer's instructions) for *in situ* detection of active caspase-8. The cells were then rinsed once with PBS and fixed in 3% paraformaldehyde for 30 min at room temperature. Cells were then incubated in blocking buffer (10% horse serum/0.4% Triton X-100 in PBS) for 10 min, followed by a wash with 0.4% Triton X-100 in PBS. The cells were then incubated with primary antibody (anti-NPM, 1:200, Zymed USA) overnight at 4°C in a humidified chamber. Excess antibody was removed by washing with PBS (five times, 5 min), followed by incubation with anti-mouse FITC-conjugated secondary antibody (Santa Cruz, USA) for 45 min at room temperature, with protection against light. Hoechst 33342 was added to a final concentration of 4 μM and incubated for an additional 5 min at room temperature, before washing with 0.4% Triton X-100 in PBS (5 times, 5 min each).

For visualisation of active caspase-6, the cells were fixed directly after exposure to actinomycin D. The cells were next incubated with blocking buffer and washed as above. However, instead of anti-NPM, the cells were incubated first with anti-cleaved caspase-6 (Cell signalling Technology, USA, 1:50) overnight at 4°C in a humidified chamber. Excess antibody was removed by washing with PBS (five times, 5 min), followed by incubation with anti-rabbit

FITC-conjugated secondary antibody (Santa Cruz, USA) for 45 min at room temperature, with protection against light. After another five washes of PBS, the cells were finally incubated with anti-NPM (Zymed, USA, 1:200) overnight at 4°C in a humidified chamber. Excess antibody was again removed by washing with PBS (five times, 5 min), followed by incubation with anti-mouse FITC-conjugated secondary antibody (Santa Cruz, USA) for 45 min at room temperature. Hoechst 33342 was added to a final concentration of 4 μM and incubated for an additional 5 min at room temperature, before washing with 0.4% Triton X-100 in PBS (5 times, 5 min each). In both cases, images were collected using an inverted fluorescence microscope (Axiovert 25; Carl Zeiss Meditech, Germany).

## 3.3 Results

### *3.3.1 Depletion of endogenous NPM using small interfering RNA (siRNA) transfection increased caspase activation and apoptosis*

To investigate how the translocated NPM mediates its anti-apoptotic effect, we first examined the effect of depletion of endogenous NPM on the caspase-activation cascade in intact cells. Using siRNA to knock down NPM protein levels in MN9D cells, we showed that cytoplasmic NPM protein levels were efficiently and specifically reduced in the presence of a NPM-specific double-stranded RNA (dsRNA) oligomer (Figure 3.2). As a control, we used an siRNA containing the inverted sequence. Using western blot analysis, an increase in the amount of cleaved fragments was observed for caspase-6, -7, -8 and -9, as well as cleaved Bid, with depletion of endogenous NPM. Caspase-3 is not activated in intact MN9D cells treated with $MPP^+$ as demonstrated previously in our laboratory (Chee *et al.,* 2005), so western blot analysis for caspase-3 was not performed in this case. Depletion of the endogenous NPM also resulted in more cytochrome *c* release, as well as an increase in the amount of cleaved PARP, which indicate elevated cell death with NPM siRNA treatment. This is consistent with previous observations that depletion of NPM with small interfering RNA increases apoptosis induced by different agents in various other cell types, though none looks into the status of caspase activation with NPM depletion (Li *et al.,* 2004; Maiguel *et al.,* 2004; Li *et al.,* 2005). Our results here thus indicate that depletion of NPM increases the activation of various caspases involved in both the intrinsic and extrinsic death pathways.

### *3.3.2 Over-expression of GFP-tagged NPM decreased caspase activation and apoptosis*

Since depletion of endogenous NPM could enhance caspase activation and apoptosis, we went on to test the reverse, i.e. if over-expression of NPM could instead suppress the activation of the same caspases and inhibit apoptosis in HeLa cells exposed to UV-irradiation. As shown in Figure 3.3, transfection of the pcDNA3.1-GFP-NPM plasmid resulted in appearance of a band of approximately 55-60 kDa that corresponded to the molecular weight of GFP-tagged NPM, while transfection of the empty vector pcDNA3.1-GFP resulted in no such band in the control experiment. Over-expression of GFP-tagged NPM coincided with an increase in the amount of pro-caspase and partially cleaved caspase for caspase-3, -6, -7, -8 and -9. For caspase-7, -8 and -9, we were able to further demonstrate a concomitant decrease in the amount of cleaved caspases as well with GFP-NPM over-expression. Decreases in the amount of cleaved Bid, cleaved PARP, and cytoplasmic cytochrome *c* were also observed. Our results here thus indicate the silencing of the caspase signalling pathway with NPM over-expression, which in turn led to the attenuation of the death response. These observations are in agreement with the findings in Section 3.3.1 - that NPM appears to negatively regulate caspase activation and the apoptotic response.

### *3.3.3 Recombinant NPM retarded cytochrome c-induced caspase activation in S100 cytosolic fraction*

Studies using cell-free systems have shown that cytochrome c, in association with dATP, is capable of initiating apoptosis-like changes in cytosols derived from a variety of cell types (Liu *et al.*, 1996; Kluck *et al.*, 1997a,b; Deveraux *et al.*, 1998; Pan *et al.*, 1998a). The apoptosis-promoting activity of cytochrome c is due to its ability to interact with Apaf-1 (Zou *et al.*, 1997)

and binding of cytochrome *c* to Apaf-1 enables this protein to recruit caspase-9 and to stimulate processing of the inactive caspase-9 zymogen to its active form (Li *et al.*, 1997; Srinivasula *et al.*, 1998). Once active, caspase-9 then presumably triggers a cascade of caspase activation events leading to apoptosis. The sequence of the protease cascade in a cytochrome *c* induced cell-free system was reported to be in the order: caspase-9, -3/-7, -6 and –8 (Slee *et al.,* 1999). Caspase-8 "back-cleaves" caspase-3 and -7 as well (Hirata *et al.,* 1998), forming a positive feedback loop downstream of caspase-9. Here, the HEK 293–derived cell free system was used to investigate the effect of recombinant NPM on cytochrome *c* induced caspase activation cascade in an *in vitro* system. Addition of cytochrome *c* and dATP to a final concentration of 300 nM and 900nM respectively resulted in cleaving of caspase-3, -6, -7, -8, and -9 as demonstrated by a marked decrease in the amount of procaspase (compare Lane 1 and Lane 3 in Figure 3.4). Meanwhile, the addition of recombinant polyhistidine-tagged NPM (5 μM) to the cytochrome *c* induced HEK293 cytosolic extract inhibited the activation of caspase-3, -6, -7 and -8, but not that of caspase-9 (Compare Lane 4 and 5 to Lane 3 of Figure 3.4). The inhibitory effect of NPM appeared not to have an energy requirement, as addition of exogenous dATP led to instead a slight decrease in the procaspase amount for caspase-6, -7 and -8. The latter can be explained by the fact that formation of the apoptosome requires dATP, and thus presence of more dATP will result in more caspase activation, which may counteract the inhibitory effect of the recombinant NPM. In the absence of cytochrome *c*, neither NPM nor dATP had no effect on caspase activation (Lane 6, Figure 3.4). The results described herein suggest a role for NPM in inhibiting the caspase amplification loop downstream of caspase-9.

### *3.3.4. Immunodepletion of NPM increased caspase activation in apoptotic-stimulated S100 cytosolic fraction*

To further ascertain that NPM is indeed inhibiting the caspase activation cascade, another *in vitro* system was set up using an apoptotic-induced cell free system derived from three different cell lines. The cells were first subjected to various apoptotic stimulation for only two hours in order to initiate low level of caspase activation. Mouse-derived neuronal MN9D cells were exposed to the neurotoxin $MPP^+$, human-derived neuronal SHSY5Y cells with the neurotoxin rotenone and human kidney-derived HEK 293 cells with the topoisomerase-II inhibitor etoposide, before extracting the S100 cytosolic fraction from the treated cells. Depletion of NPM was then performed using anti-NPM monoclonal antibody, and mock depletions using control monoclonal antibody. The immunodepleted fractions were then incubated at 37°C for six hours to allow full-fledge caspase activation in the presence or absence of the endogenous NPM. NPM depletion results in greater activation of caspase-3, -6, -7 and -8, as demonstrated by a marked increase in the amount of cleaved fragments for these caspases (Figure 3.5). On the other hand, caspase-9 showed similar extent of activation with or without NPM depletion. The results obtained here further confirm the involvement of NPM in inhibiting the caspase activation loop downstream of caspase-9 activation and this may represent a general mechanism used in retarding caspase-mediated death signalling in various cell types and across different species.

### *3.3.5 NPM inhibited the activities of recombinant caspase-6 and -8*

To determine the specific caspase(s) within the activation loop inhibited by NPM, we investigated the effect of NPM on the activities of the various recombinant active caspases added to HEK 293 cells-derived S100 cytosolic extracts. Here, cleavage of their respective colorimetric substrates was monitored at OD 400 nm in the absence or presence of recombinant NPM (5μM). Meansurements made in the presence of recombinant NPM were then divided by that made in the absence of recombinant NPM. This figures obtained were next converted to percentage, and subtracted from 100% to obtain the final figures, which were indicative of the extent of inhibition of the caspases' activities with addition of exogenous NPM. Among the five caspases examined, caspase-6 and -8 were the most significantly inhibited (56.1% and 58.6% respectively) in the presence of recombinant NPM. The activities of the other caspases were either not inhibited (caspase-9) or inhibited only modestly (<10.0% inhibition, caspase-3 and -7) (Figure 3.6 A).

To further ascertain that NPM inhibits the activities of caspase-6 and –8 specifically, we evaluated the influence of NPM on the cleavage of the various physiological targets by the five caspases examined above. Addition of exogenous NPM reduced the cleaving of lamin and Bid by recombinant caspase-6 and -8 respectively added to HEK 293-derived cell free extracts. As observed in Figure 3.6 (B), addition of recombinant NPM resulted in less cleaving of full length Bid by caspase-8, as well as presence of less cleaved lamin A fragment. On the other hand, no reduced cleaving of PARP (substrate for active caspase-3 and -7) and caspase-3 (substrate for active caspase-9) was observed with addition of recombinant NPM.

Cleaving and activation of the procaspases by upstream active caspases is crucial in ensuring rapid and massive death signal amplification. It thus follows that inhibition of any step within the caspase activation loop can retard death signal relay significantly, leading to a halt in cell death. As both caspase-6 and -8 are important components of the caspase amplification loop, experiments were designed to evaluate the influence of NPM on the activation of various proenzymes by active caspase-6 and -8. Reaction mixtures were reconstituted using HEK293-derived cell free extract, and the activation of the procaspases was measured by monitoring cleavage of their respective colorimetric substrates. As shown in Figure 3.7 (A), activation of caspase-3 by caspase-8 was markedly inhibited by 63.8% in the presence of recombinant NPM. Inhibition of procaspases-3 processing by caspase-8 was further confirmed by immunoblot against both large and small subunit of caspase-3 (Figure 3.7 B). While addition of recombinant caspase-8 resulted in cleavage of procaspases-3 and appearance of the 17 kDa cleaved fragment, presence of the exogenous NPM resulted in the 'disappearance' of that cleaved fragment. In a similar manner, it was shown that activation of procaspases-8 by caspase-6 was inhibited by 47.1% in the presence of recombinant NPM, and immunoblot against caspase-8 demonstrated the 'disappearance' of the p44/47 intermediate cleaved band with addition of the exogenous NPM. Surprisingly, cleaving of procaspases-3 by caspase-6 was not affected by the addition of recombinant NPM, as shown by both the colorimetric assay and immunoblotting.

Taken together, the data indicated that NPM acts to retard the caspase amplification loop by inhibiting procaspases-3 and -8 processing by active caspase-8 and -6 respectively. NPM also inhibits the cleaving of various cellular targets by both caspases, which may further contribute to blockage of cell death. Hence, among the five caspases examined and known to be involved in

the two death signalling pathways, caspase-6 and -8 were identified to be the inhibitory target of NPM.

### *3.3.6 Activation of caspase-6 and -8 coincided with stress-induced cytoplasmic translocation of NPM*

In Chapter two, we demonstrated cytoplasmic translocation of NPM as a general phenomenon in response to stress. We further showed in this chapter that NPM inhibits the activities of caspase-6 and -8. It will thus be interesting to determine if cytoplasmic NPM translocation coincides with caspase-6 and -8 activation. Here, HeLa cells were exposed to the transcriptional inhibitor actinomycin D for four hours, and the cells were subsequently fixed and decorated with antibodies against NPM and active caspase-6. For visualisation of active caspase-8, we used VEID-FLICA, which is a fluorochrome-labelled inhibitor of caspase that allows for *in situ* detection of caspase activities in the cell. The four hours time point was chosen since the cytoplasmic NPM level was shown to peak by the fourth hour after $MPP^+$ exposure in the MN9D cells (See Section 2.3.2). As expected, nucleoplasmic dispersal of NPM was observed for all treated HeLa cells, indicating the occurrence of nucleoli disruption. A subset of cells also showed green fluorescence, indicating the presence of activated caspases. As shown in Figure 3.8, active caspase-6 is localised mainly and uniformly in the nucleus while active caspase-8 is localised in both the cytoplasm and nucleus. However, we observed that in general, cells with prominent cytoplasmic NPM localisation showed little or no green fluorescence, indicating the absence of caspase-6 and -8 activation in these cells. This observation lends support to the

hypothesis that cytoplasmic NPM plays a protective role during stress by suppressing or delaying caspase activation until necessary.

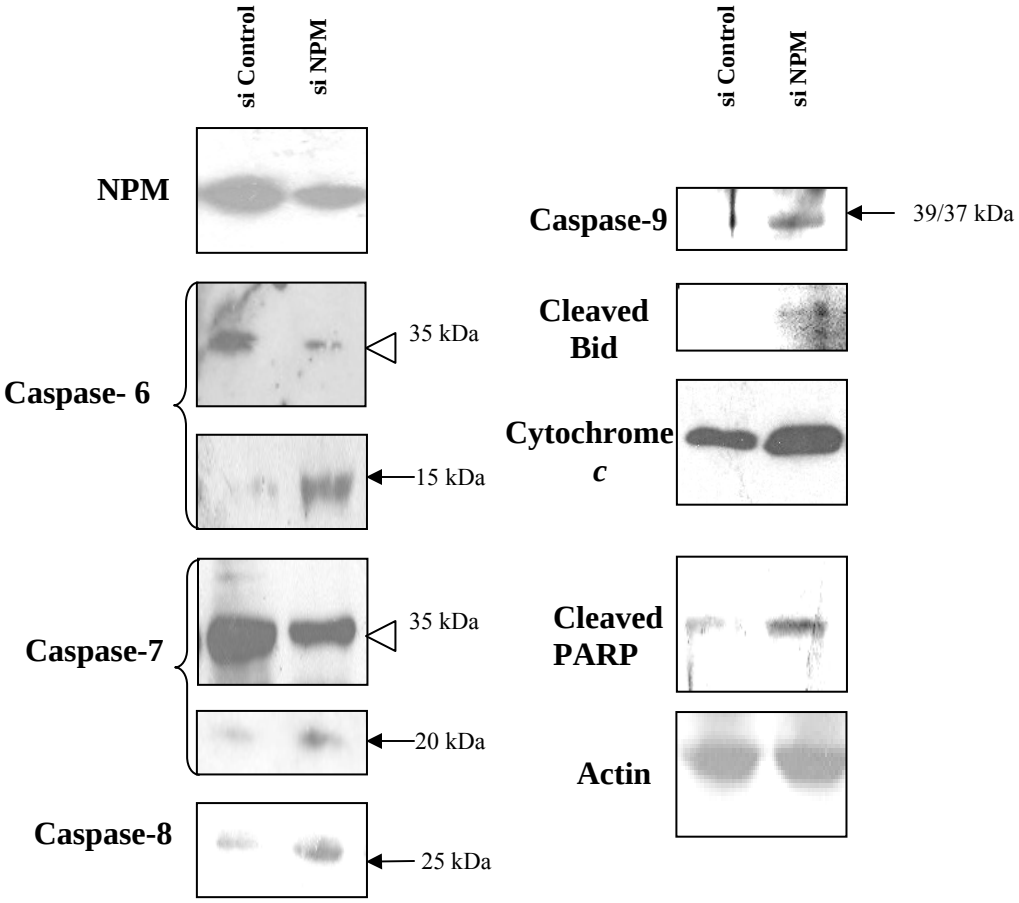


**Figure 3.2. Depletion of endogenous NPM leads to enhanced activation of the various caspases and intensified apoptotic signal progression in $MPP^+$-treated MN9D cells.** MN9D cells were treated with NPM-specific or non-specific siRNA as described in Materials and Methods, Section 3.2.5. 48 hours after siRNA treatment, the cells were exposed to 500 μM of MPP+ for 12 hours. Harvested cells were subjected to subcellular fraction as described in Materials and Methods, Section 2.2.5. Collected cytoplasmic fractions were next subjected to SDS-PAGE and immunoblot analysis using anti-NPM, anti-caspase-6, anti-caspase-7, anti-caspase-8, anti-caspase-9, anti-Bid, anti-cytochrome *c*, anti-cleaved PARP or anti-actin antibody, as indicated to the left of each panel. 20 μg of the cytoplasmic extract (80 μg for caspase-8 immunoblotting) was electrophoresed for immunoblotting. White triangle indicates procaspase, and black arrow indicates cleaved caspase fragment.

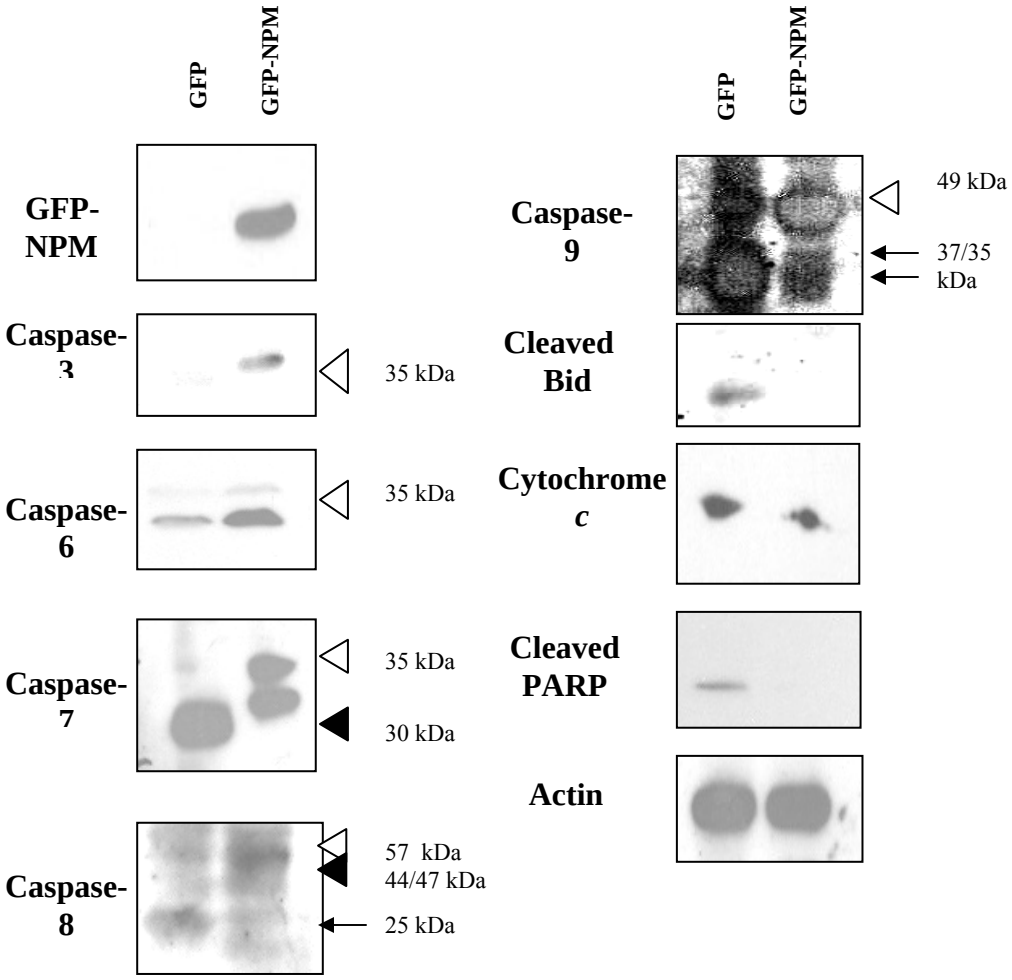


**Figure 3.3. Overexpression of NPM leads to reduced activation of the various caspases, as well as attenuated apoptotic signal progression in UV-irradiated HeLa cells.** HeLa cells were transfected with 30 μg (in a 10-cm diameter tissue culture plate) of GFP or GFP-NPM overexpressing plasmid as described in Materials and Methods, Section 3.2.4. 24 hours after transfection, the cells were irradiated with UV-C (40 W) for four hours. Harvested cells were subjected to subcellular fraction as described in Materials and Methods, Section 2.2.5. Collected cytoplasmic fractions were next subjected to SDS-PAGE and immunoblot analysis using anti-NPM, anti-caspase-6, anti-caspase-7, anti-caspase-8, anti-caspase-9, anti-Bid, anti-cytochrome *c*, anti-cleaved PARP or anti-actin antibody, as indicated to the left of each panel. 20 μg of the cytoplasmic extract (80 μg for caspase-8 immunoblotting) was electrophoresed for immunoblotting. White triangle indicates procaspase, black triangle indicates intermediate cleaved fragment, and black arrow indicates cleaved caspase fragment.

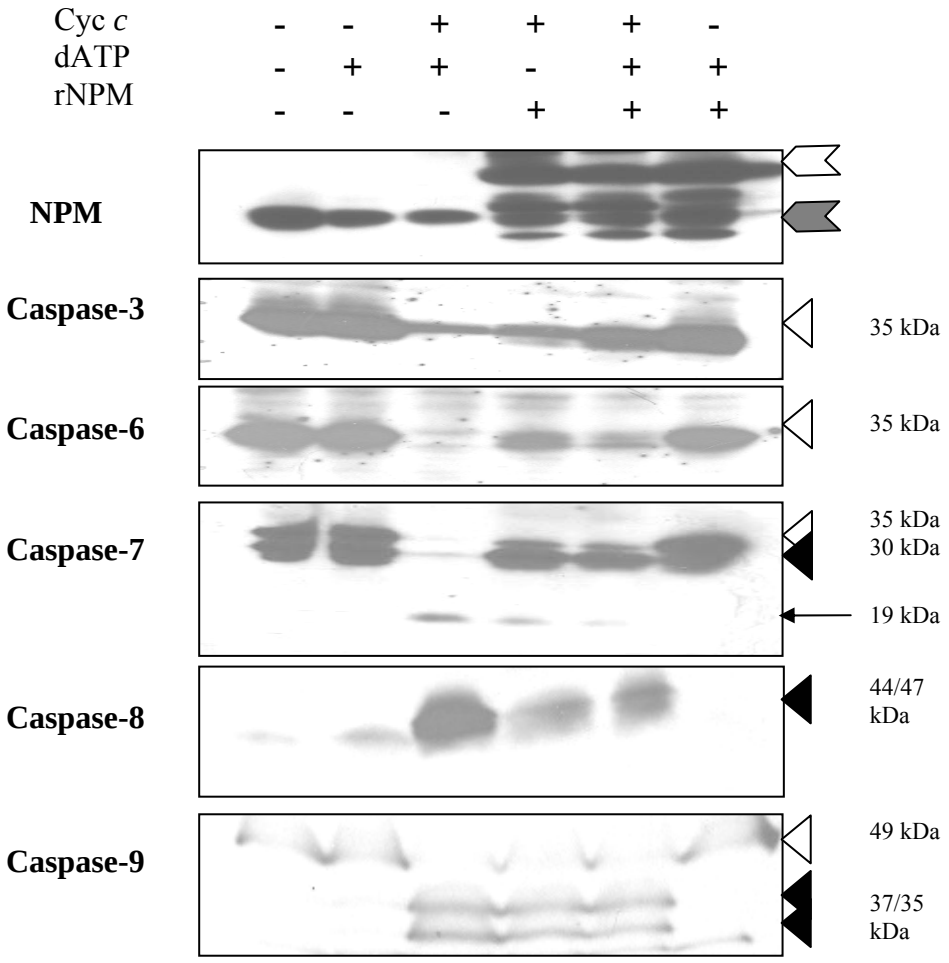


**Figure 3.4. Inhibition of cytochrome *c*-induced caspase activation by recombinant NPM *in vitro*.** S100 cytosolic fractions extracted from HEK 293 cells were incubated with cytochrome c (300 nM), in the presence or absence of dATP (900 nM) and recombinant His-tagged NPM (5 μM), for three hours at 37˚C. The various extracts were next subjected to SDS-PAGE and immunoblot analysis using anti-NPM, anti-caspase-6, anti-caspase-7, anti-caspase-8 or anti-caspase-9 antibody, as indicated to the left of each panel. White broad arrow indicates higher molecular weight His-tagged recombinant NPM, grey broad arrow indicates endogenous NPM, white triangle indicates procaspase, black triangle indicates intermediate cleaved fragment, and black arrow indicates cleaved caspase fragment. Cyc *c*: Cytochrome *c*, rNPM: recombinant NPM.

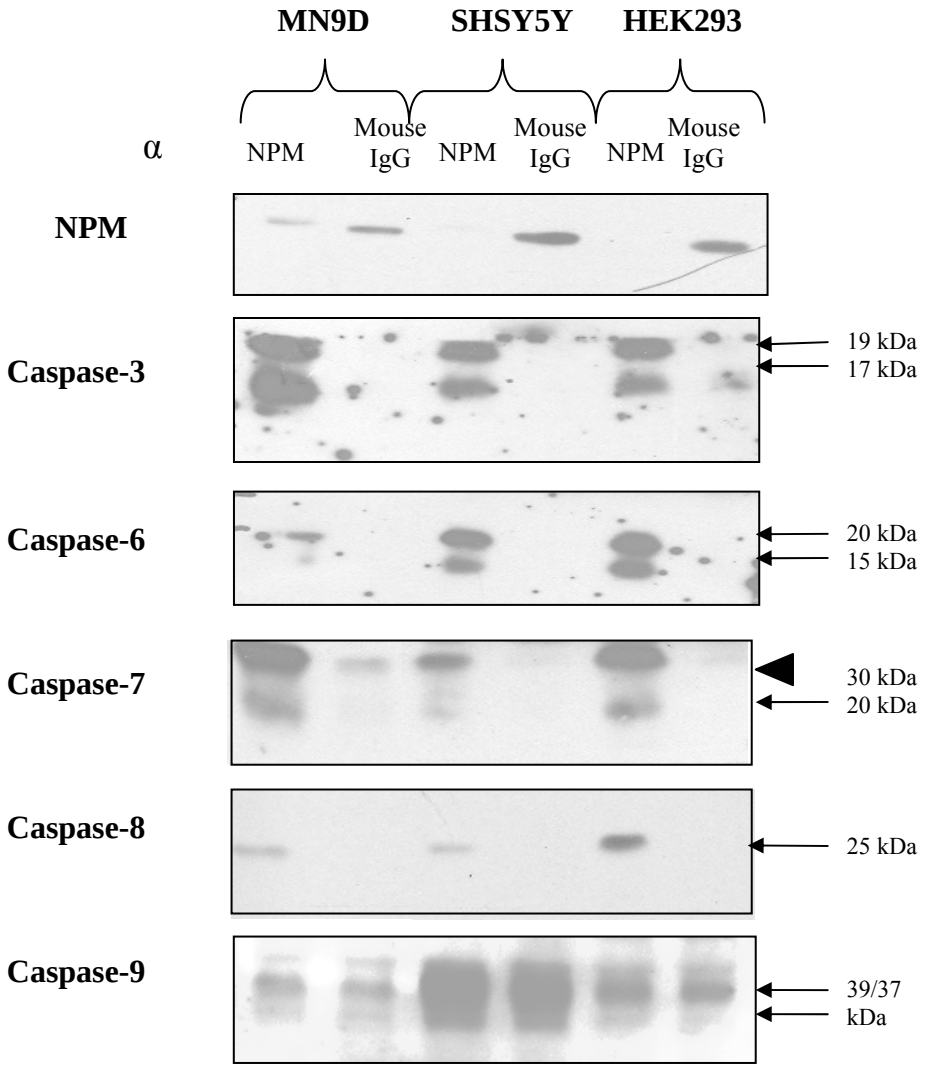


**Figure 3.5. Acceleration of caspase activation with immunodepletion of endogenous NPM *in vitro*.** HEK 293 cells were subjected to slight apoptotic induction by treatment with 5 μM of the potent neurotoxin rotenone for one hour before extraction of S100 cytosolic fractions. The extracts were then subjected to immunodepletion as described in Material and Methods, Section 3.2.9, using 4μg of anti-NPM or anti-HA antibodies Immunodepleted extracts were then incubated for five hours at 37˚C. The various extracts were next subjected to SDS-PAGE and immunoblot analysis using anti-NPM, anti-caspase-6, anti-caspase-7, anti-caspase-8 or anti-caspase-9 antibody, as indicated to the left of each panel. Black triangle indicates intermediate cleaved fragment, and black arrow indicates cleaved caspase fragment.

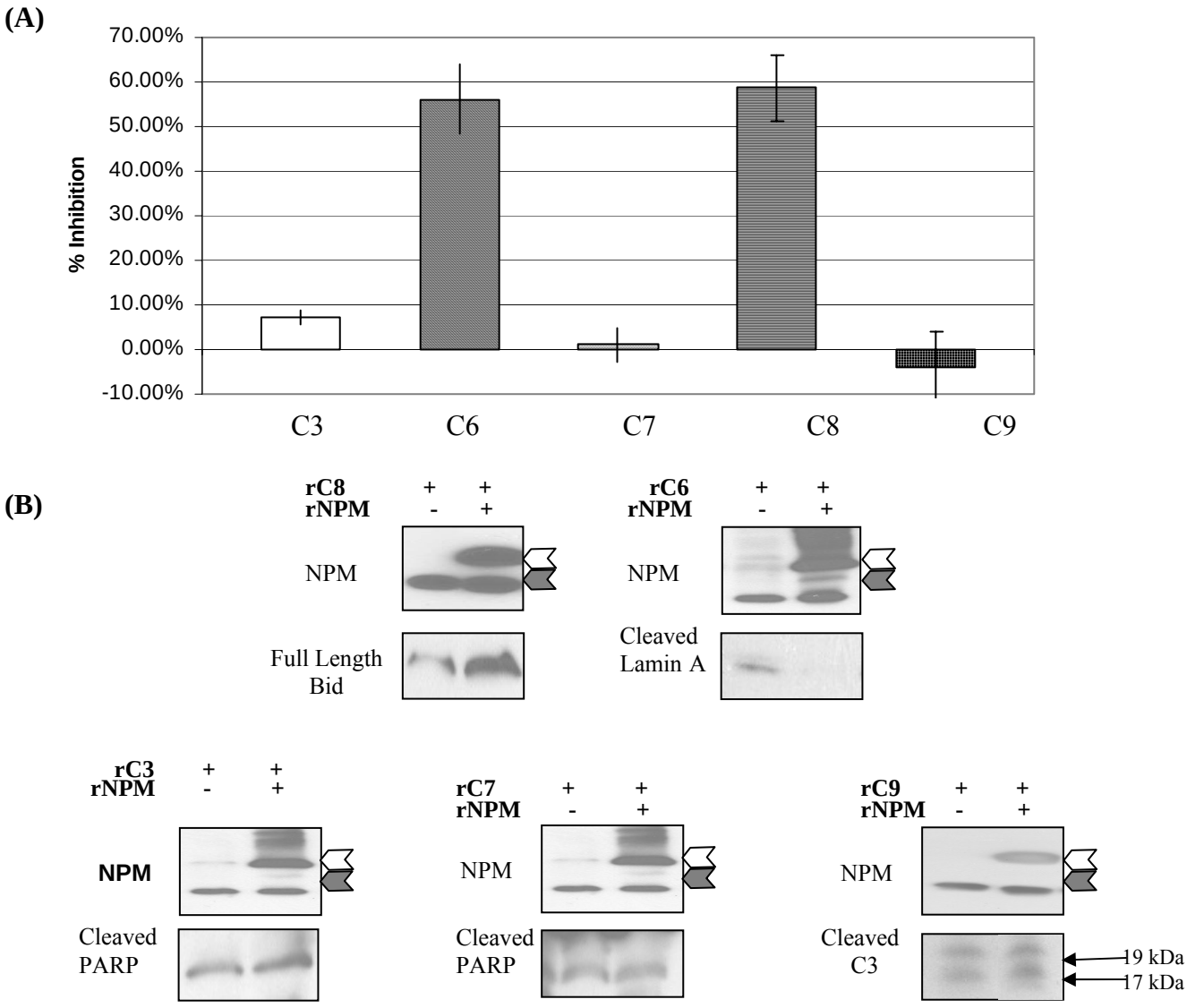


**Figure 3.6. NPM inhibits the activities of caspase-6 and -8, but not caspase-3, -7 or -9.** S100 cytosolic fractions extracted from HEK 293 cells were incubated with one unit of the various indicated recombinant active caspases (32 units for recombinant active caspase-8) in the absence or presence of 5 μM of recombinant His-tagged NPM for one hour at 30˚C. (A) Caspase activities were measured colorimetrically using DEVD-pNA (for caspase-3 and -7), VEID-pNA (for caspase-6), (IETD-pNA (for caspase-8) or LEHD-pNA (for caspase-9). Endogenous caspase activities were also measured using control extracts without addition of recombinant caspase, and the measurements subtracted from readings obtained for extracts with recombinant caspase addition, before further tabulations. Data are expressed as per cent inhibition, based on the average ratio of velocities ($v_i/v_0$) of three independent experiments (mean $\pm$ s.e.) performed in the presence ($v_i$) or absence ($v_0$) of recombinant NPM. (B) Alternatively, after incubation, the various extracts were next subjected to SDS-PAGE and immunoblot analysis using anti-NPM, anti-Bid (for recombinant caspase-8 addition), anti-lamin A (for recombinant caspase-6 addition), anti-PARP (for recombinant caspase-3 or -7 addition) or anti-caspase-3 (for recombinant caspase-9 addition) antibody, as indicated to the left of each panel. White broad arrow indicates higher molecular weight His-tagged recombinant NPM, grey broad arrow indicates endogenous NPM, and black arrows indicate cleaved caspase.

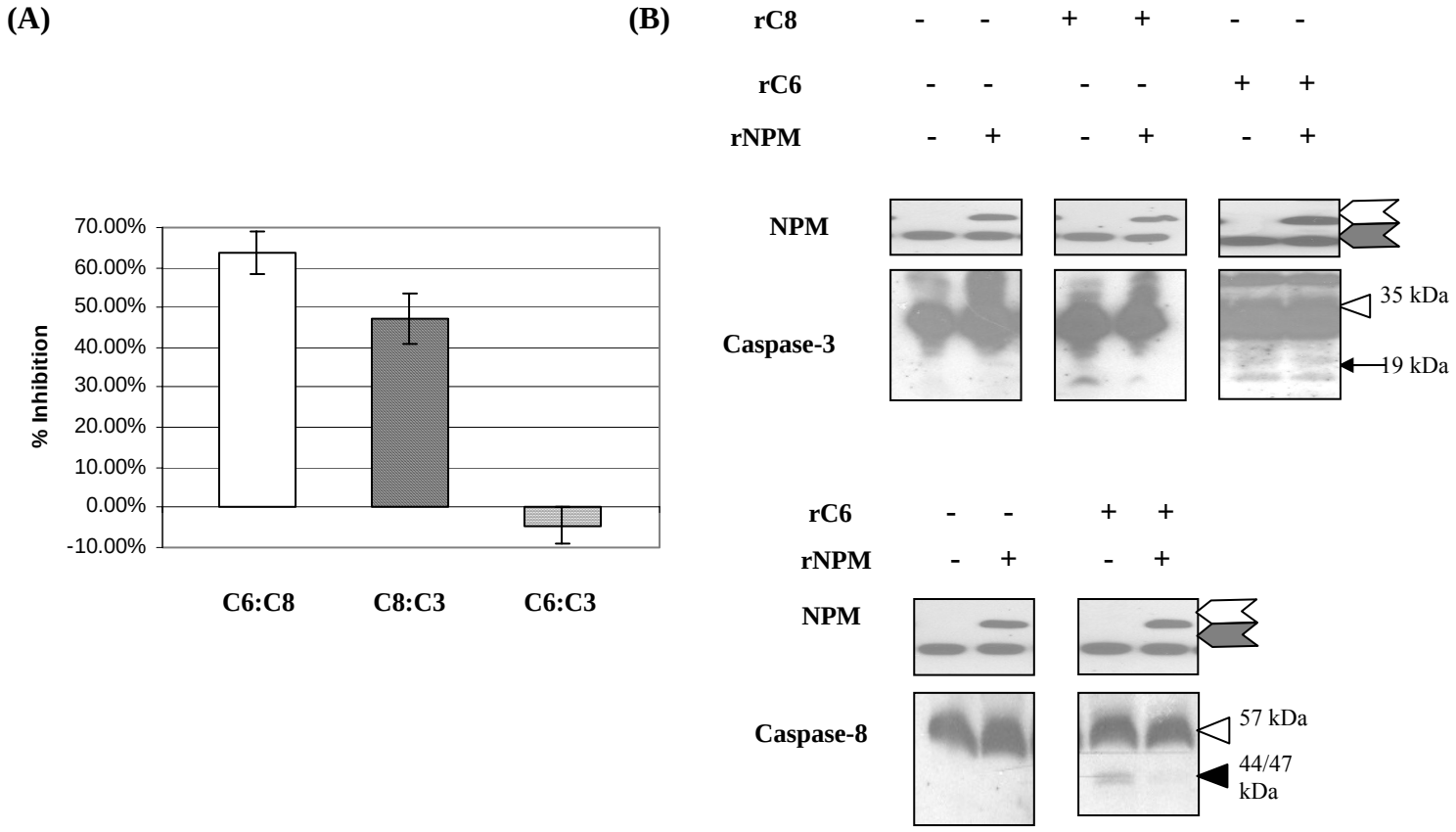


**Figure 3.7. NPM inhibits the cleaving of procaspases by recombinant active caspase-6 and -8.** S100 cytosolic fractions extracted from HEK 293 cells were incubated with one unit of recombinant active caspase-6 or 32 units of recombinant active caspase-8 in the absence or presence of 5 μM of recombinant His-tagged NPM for one hour at 30˚C. (A) Caspase activities were measured colorimetrically using IETD-pNA (with addition of recombinant caspase-6) or DEVD-pNA (with addition of recombinant caspase-6 or -8). Endogenous caspase activities were also measured using control extracts without addition of recombinant caspase, and the measurements subtracted from readings obtained for extracts with recombinant caspase addition, before further tabulations. Data are expressed as per cent inhibition, based on the average ratio of velocities ($v_i/v_0$) of three independent experiments (mean $\pm$ s.e.) performed in the presence ($v_i$) or absence ($v_0$) of recombinant NPM. (B) Alternatively, after incubation, the various extracts were next subjected to SDS-PAGE and immunoblot analysis using anti-NPM, anti-caspase-3 (for recombinant caspase-6 or -8 addition), or anti-caspase-8 (for recombinant caspase-6 addition) antibody, as indicated to the left of each panel. White broad arrow indicates higher molecular weight His-tagged recombinant NPM, grey broad arrow indicates endogenous NPM, white triangle indicates procaspase, black triangle indicates intermediate cleaved fragment, and black arrow indicates cleaved caspase fragment.

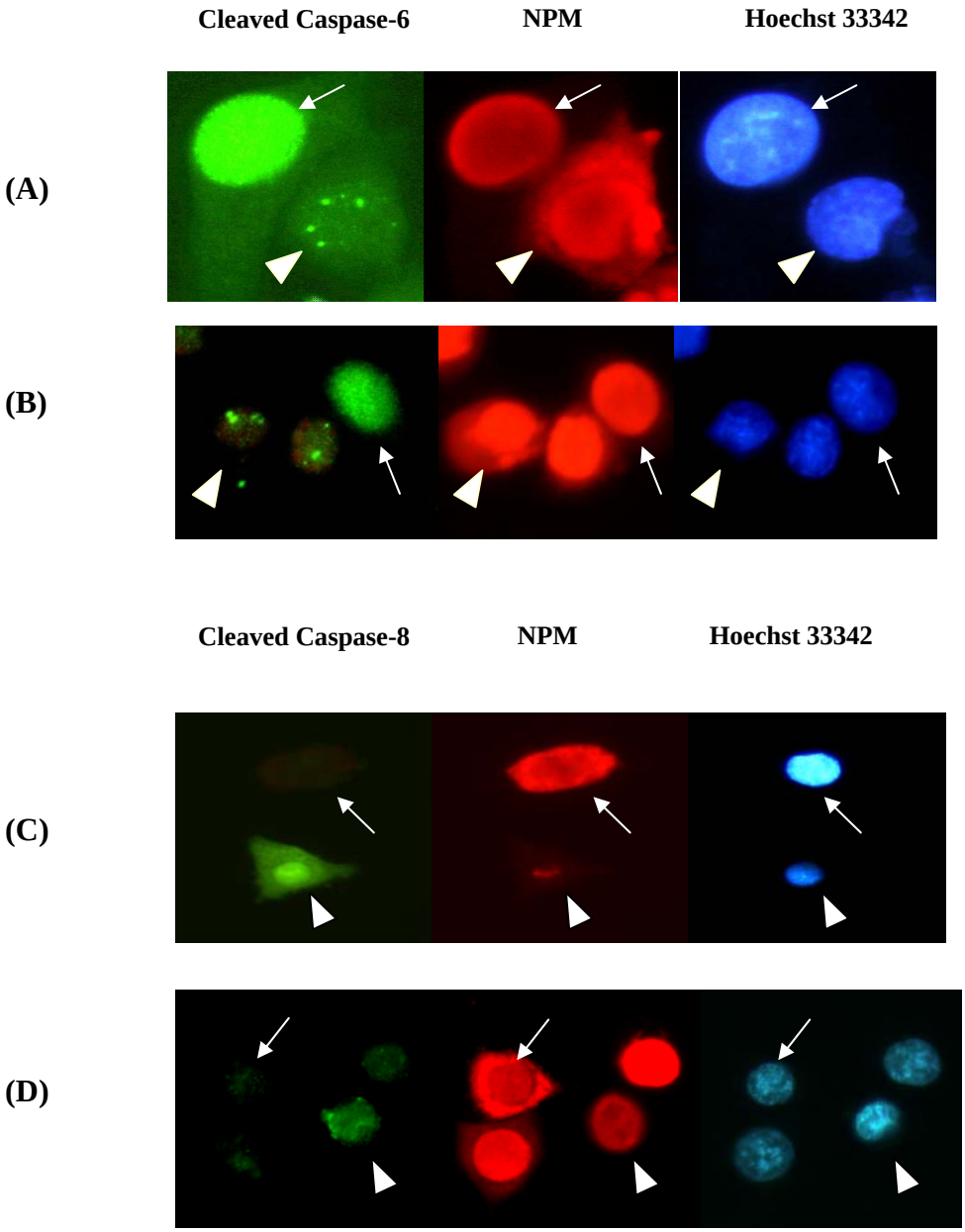


**Figure 3.8. Activation of caspase-6 and -8 coincided with stress-induced cytoplasmic translocation of NPM.** HeLa cells were exposed to with 0.40 μM of actinomycin D for four hours, after which the cells were fixed by treatment with 3% (wt/vol) paraformaldehyde for 30 min at RT and stained for NPM, active caspase-6 (A-B) or active caspase-8 (C-D) as described in Materials and Methods, Section 3.2.11. Localisation of NPM, active caspase-6 and -8 were observed by fluorescence microscopy using a Zeiss Axiophot (Germany) White arrow indicates a cell with prominent nucleoplasmic and cytoplasmic NPM localisation with $MPP^+$ treatment; white triangle indicates with only nuclear NPM localisation and caspase activation.

## 3.4 Discussion

Multicellular organisms have evolved a number of molecular mechanisms for responding to cellular damage and environmental stress. Included among these is the induction of a subfamily of heat shock proteins designated as chaperonins (Beissinger & Buchner, 1998; Bukau & Horwich, 1998), which are capable of inhibiting the caspase signalling pathway at multiple points. Among the various hsps, Hsp27 and αB-crystallin are known to inhibit caspase-3 maturation through direct physical interaction with caspase-3, with the mechanism underlying such inhibition being similar to that effected by the IAPs. In this study, we have identified another molecular chaperone, NPM, as a caspase inhibitor. However, unlike the IAPs and Hsps that are collectively known to specifically inhibit caspase-3, -7 and -9, NPM inhibits caspase-6 and -8 instead. While caspase-3, -7 and –9 are key players in the mitochondrial (intrinsic) pathway, caspase-6 and -8 are instead known to be part of the death receptor (extrinsic) pathway relaying signals from DISC to downstream effectors. It thus follows that simultaneous induction of both the Hsps/IAPs and cytoplasmic NPM during stress conditions can lead to blockage of the two death pathways altogether, hence ensuring a complete halt in apoptotic signalling regardless of the source of the death stimuli. In this context, we noted in Chapter two that a one-hour 42°C heat shock resulted in increase amount of cytoplasmic Hsp70 and NPM (Figure 2.2 D). Hsp70 is known to interact with Apaf-1 and prevent the recruitment of pro-caspase-9 into the apoptosome through Apaf-1 (Saleh *et al.*, 2000). Its cytoplasmic up-regulation with heat shock may thus help suppress unwanted caspase activation via the mitochondria pathway. This in turn complements the protective action of cytoplasmic NPM, which shuts down the death receptor pathway through inhibition of heat-stress induced caspases-8 activation.

Caspase-8 is a key mediator of apoptotic signals triggered by death receptors such as Fas /CD95, TNF-R1, and TRAIL-R1/TRAIL-R2. In the case of the TRAIL receptors and Fas/CD95, caspase-8 is directly recruited into the DISC by the adapter protein FADD (Schulze-Osthoff *et al.*, 1998; Peter & Krammer, 2003). Once formed, the DISC promotes the proximity-induced activation of caspase-8, which then proceeds to be further processed via an auto-proteolysis mechanism.(Salvesen & Dixit, 1999; Yang *et al.*, 1998). Active caspase-8 then activates effector caspases, such as caspase-3, leading to cell execution via degradation of the nucleus and other intracellular structures (Scaffidi *et al.*, 1998). This direct activation of caspase-dependent cell execution, which does not require mitochondria, is believed to occur in select cell types, including thymoctyes, that are classified as Type I cells (Scaffidi *et al.*, 1998; Ozoren & El-deiry, 2002). This death pathway of Type I cells plays an important role in the immune response that is involved in the deletion of transformed cells (Hickman *et al.*, 2002). As such, regulation of caspase-8 mediated death receptor pathway through NPM may be of utmost importance in maintenance of an optimal immune response and for homeostatic regulation of the Type I cells. In acute myelogenous leukaemia (AML) with a normal karyotype, a C-terminal frame-shift mutation of the *NPM* gene results in cytoplasmic dislocation of NPM (Falini *et al.,* 2005), which may possibly function in cancer pathogenesis through caspase-8 inhibition at the death receptor. It was shown previously that Fas has a novel role in the regulation of myelopoiesis and that Fas may act as a tumor suppressor to control leukaemogenic transformation in myeloid progenitor cells (Traver *et al.*, 1998). Over-inhibition of caspase-8, which functions downstream of Fas, by the cytoplasmic-dislocated NPM ,may hence lead to neoplastic transformation of myeloid progenitor cells in the case of AML, as we shall further examine in Chapter V.

Various studies have proposed that caspase-8 is not only activated in the death receptor pathway, but can also be activated independently of death receptors, for instance during genotoxic stress-induced apoptosis (Ferarri *et al.*, 1998; Wesselborg *et al.*, 1999; Engels, *et al.*, 2000; Cowling & Downward, 2002; Milner *et al.*, 2002) or by direct cleavage through other proteases including the CTL protease granzyme B and human immunodeficiency virus type 1 protease (Fernandes-Alnemri *et al.*, 1996; Nie *et al.*, 2002). During stress-induced apoptosis triggered by anti-cancer drugs or ionizing irradiation, it was proposed that caspase-8 activation is mediated in a post-mitochondrial event by the prior cleavage through caspase-6 (Cowling & Downward, 2002). In all these studies, the activated caspase-8 was proposed to trigger a feedback amplification loop through the cleavage of Bid (Engels *et al.*, 2000; Tang *et al.*, 2000) to produce tBid, which then translocates into the mitochondria to facilitate the release of cytochrome *c*. The direct target of caspase-8, caspase-3, has also been shown to be able to cleave Bid as well after activation (Slee *et al.*, 2000). Inhibition of caspase-8 by NPM should therefore enable silencing of apoptotic signalling not involving death receptors. Two lines of evidence presented in this chapter supported this notion. Firstly, depletion of endogenous NPM using siRNA in the $MPP^+$-treated MN9D cells resulted in increase activation of multiple caspases. Increases in the amount of cytochrome *c* release and Bid cleaving were observed at the same time (Figure 3.2). Secondly, over-expression of GFP-tagged NPM in UV-exposed HeLA cells led to the reverse situation, i.e. markedly reduced activation of caspase-3, -6, -7, -8 and -9. Significant decreases in the amount of cleaved Bid and cytochrome *c* observed herein indicated silencing of the caspase-8-activated mitochondrial-signalling branch (Figure 3.3). Cleavage of Bid during UV radiation-induced apoptosis was already shown to occur downstream of the point of Bcl-2 action (Slee *et al.*, 2000). Likewise, MPTP ($MPP^+$ precursor)-mediated caspase-8 activation and Bid cleavage were

demonstrated to occur downstream of caspase-9 activation via cytochrome *c* release (Viswanath *et al.*, 2001). In both cases, NPM was shown to be effective here in inhibition of caspase-8-mediated feedback loop for the amplification of mitochondrial cytochrome *c* release.

Further characterisation of NPM's caspase inhibition function in the context of an *in vitro* system revealed NPM's possible involvement in regulating the progression of the downstream caspase amplification loop. Addition of recombinant NPM was shown to readily halt the cytochrome *c* induced caspase activation cascade involving caspase-3, -6, -7 and -8 (Figure 3.4), while removal of endogenous NPM with immnodepletion enhanced the activation of the same caspases markedly (Figure 3.5). Following initial caspase activation at the death receptors or mitochondria, the small amount of activated caspases is usually shunted into the caspase amplification loop for rapid signal amplification. It was previously demonstrated that caspase-8 cleaves pro-caspase-3 (Stennicke *et al.*, 1998), caspase-3 activates procaspase-6 (Hirata *et al.*, 1998) and that caspase-6 cleaves procaspase-8 (Cowling & Downward, 2002). The caspase amplification loop is made up of these caspases cleaving one another in that sequential order, thereby leading to an escalation of caspase activities enabling a swift death response. In this context, we noted that recombinant NPM inhibited the cleaving of procaspases-8 and -3 by active caspase-6 or -8 respectively (Figure 3.7). Thus, by strategically inhibiting the activities of caspase-6 and -8 within the amplification cascade, NPM can effectively quench the activation of all caspases involved in the activation loop, regardless of the source of the death stimulus.

An obvious consequence of caspase activation is the cleaving of a plethora of proteins known as the 'death substrates'. Many caspase substrates are just cleaved as bystanders, because they happen to contain a caspase cleavage site in their sequence. Several targets, however, have a

discrete function in propagation of the cell death process. Many regulatory proteins are inactivated by caspases, while other substrates can be activated. Caspase substrates can also regulate the key morphological changes in apoptosis (Fischer *et al.*, 2003). For example, caspase-6 activity is shown to be essential for lamin A cleavage and that when lamin A is present it must be cleaved in order for the chromosomal DNA to undergo complete condensation during apoptotic execution (Ruchaud *et al.*, 2002). Also, as mentioned before, cleaving of Bid by caspase-8 is required before it can translocate to the mitochondria to promote insertion of BAX into mitochondria for cytochrome *c* release to occur (Luo *et al.*, 1998). Preventing the cleavage of these 'death substrates' can thus halt or delay apoptotic progression. Our data here showed that recombinant NPM can specifically inhibit the cleaving of lamin A and Bid by recombinant active caspase-6 and -8 respectively (Figure 3.6 B), which is consistent with current and previous observations that NPM over-expression can inhibit apoptosis. Apart from inhibiting caspase-8 maturation at the death receptors and halting progression of the caspase activation loop, inhibition of 'death substrate' cleavage by caspase-6 and -8 affords an additional layer of protection against cell death during stressful conditions.

All in all, despite significant cross-talk and 'biofeedback' between the 'extrinsic' and 'intrinsic' death signalling pathways, caspase-8 remains an integral component in various apoptotic signalling settings. NPM's inhibition of caspase-8 during stress conditions thus represents a parsimonious strategy in attaining effective silencing of the intricate death-signalling network, as illustrated in Figure 3.9.

To date, no known natural inhibitor of caspase-6 is ever reported. Meanwhile, the only caspase-8 inhibitor known is the cellular FLICE-inhibitory protein (c-FLIP). Both NPM and c-

FLIP have been separately reported to be over-expressed in various tumour types (Dolcet *et al.*, 2005; Zhou *et al.*, 2004; Jonsson *et al.*, 2003). c-FLIP has high sequence homology to caspase-8, and is structurally similar to the latter as well, since it contains two death effector domains and a caspase-like domain. However, this domain lacks residues that are important for its catalytic activity, most notably the cysteine within the active site (Irmler *et al.*, 1997). It is hence hypothesised that c-FLIP inhibits caspase-8 processing at the death receptor complex by direct binding to both caspase-8 and the adaptor FADD. Meanwhile, NPM shows no significant protein sequence homology to caspase-8. The mechanism of inhibition of caspase-8 by NPM may thus be different from that effected by c-FLIP, and possibly novel. A discernible difference between NPM and c-FLIP in terms of their mode of inhibition is that the former inhibits the activities of caspase-8, while the latter merely prevents the recruitment of caspase-8 and FADD for proximity-induced cleavage of caspase-8. As such, the inhibitory effect of NPM on the caspase signalling network is much more widespread as compared to c-FLIP, whose action is hitherto only reported to be limited to the death receptor complex.

We have seen in Chapter two the phenomenon of stress-induced NPM cytoplasmic translocation mediated by Crm-1, and speculated on a protective function for the translocated NPM. Here, based on both *in vivo* and *in vitro* results gathered so far, we are finally able to ascribe a definitive anti-apoptotic function to NPM based on its inhibitory effect on caspase-6 and -8. Taken together, it will not be unreasonable to assume that the major consequence of NPM' translocation into the cytoplasm during stress is the inhibition of caspase-8 activation by DISC and/or the mitochondria pathway, both of which are not known to be localised in the nucleus. Nevertheless, the notion that NPM may further inhibit caspase-6 and -8 activation in the

nuclear milieu cannot be discounted based on a few observations. Firstly, as observed in Figure 3.8, significant amount of activated caspase-6 and -8 was observed to be localised in the nucleus. In fact, activated caspase-6 seemed almost exclusively nuclear-bound, which is consistent with the fact that it cleaves lamin A that is critical to maintaining the integrity of the nuclear envelope (Takahashi *et al.*, 1996). Some of caspase-8's substrates are also known to be localised in the nucleus, such as PARP-2 (Benchoua *et al.*, 2002). Secondly, many lines of evidence point to the possibility that caspase-6 and -8 activation can occur in the nucleus as well. For example, FADD, which predominantly associates with death receptors and was long believed to be a cytoplasmic protein, was recently shown to also reside in the nucleus (Gomez-Angelats & Cidlowski, 2003; Screaton *et al.*, 2003; Sheikh & Huang, 2003). This suggests that FADD-mediated caspase-8 activation also occurs in the nucleus. Meanwhile, nuclear localisation of the DEDD protein, which shares sequence homology in its death effector domain (DED) to FADD and caspase-8, was shown to lead to caspase-6 activation in the nucleus (Schickling *et al.*, 2001). Given these observations, we may be able to extrapolate NPM's caspase inhibitory role into the nucleus, especially since it is more highly abundant there relative to the cytoplasm during stressful conditions.

Based on the results gathered so far, we hypothesise that the release of NPM from the nucleoli may constitute a stress-induced protective mechanism inhibiting aberrant activation of caspase-6 and -8 in the cytoplasm and/or nucleus, which may otherwise result in dire consequences especially if the activated caspases enter the amplification loop. While we are able to prove that NPM can inhibit the activities of caspase-6 and -8 using *in vitro* and *in vivo* assays, we have yet to prove any physical association between them. The demonstration of actual

physical interactions between NPM and the caspases will go further in lending stronger support to the caspases inhibitory function proposed herein, as we shall see in the next chapter.

**Figure 3.9. Illustrations of the inhibitory effect of NPM on the two death pathways.** (A) In death-receptor-mediated death signalling, binding of the death ligands to the death receptors on the plasma membrane triggers activation of caspase-8, which in turns cleaves downstream targets such as procaspase-3 and Bid. During the early stages of stress response, NPM translocates into the cytoplasm and inhibits the activities of caspase-8 and -6, which are required for apoptotic signal relay from the death receptors all the way to death substrates cleaving. Cytoplasmic NPM not only prevents proximity-induced activation of caspase-8 at the death receptors by DISC, but also inhibited the cleaving of Bid by activated caspase-8. Without the truncated Bid to trigger cytochrome *c* release from the mitochondria, the mitochondrial pathway is effectively blocked. Cytoplasmic NPM also prevents already activated caspase-6 and -8 from cleaving procaspase-8 and procaspase-3 respectively, and through this averts full-fledged activation of the caspase amplification loop involving all these caspases. Lastly, cytoplasmic NPM also inhibits the cleavage of the death substrate lamin A by active caspase-6, hence maintaining the integrity of the nuclear envelop and prevents nuclear condensation from setting in.(B) Meanwhile, in mitochondria

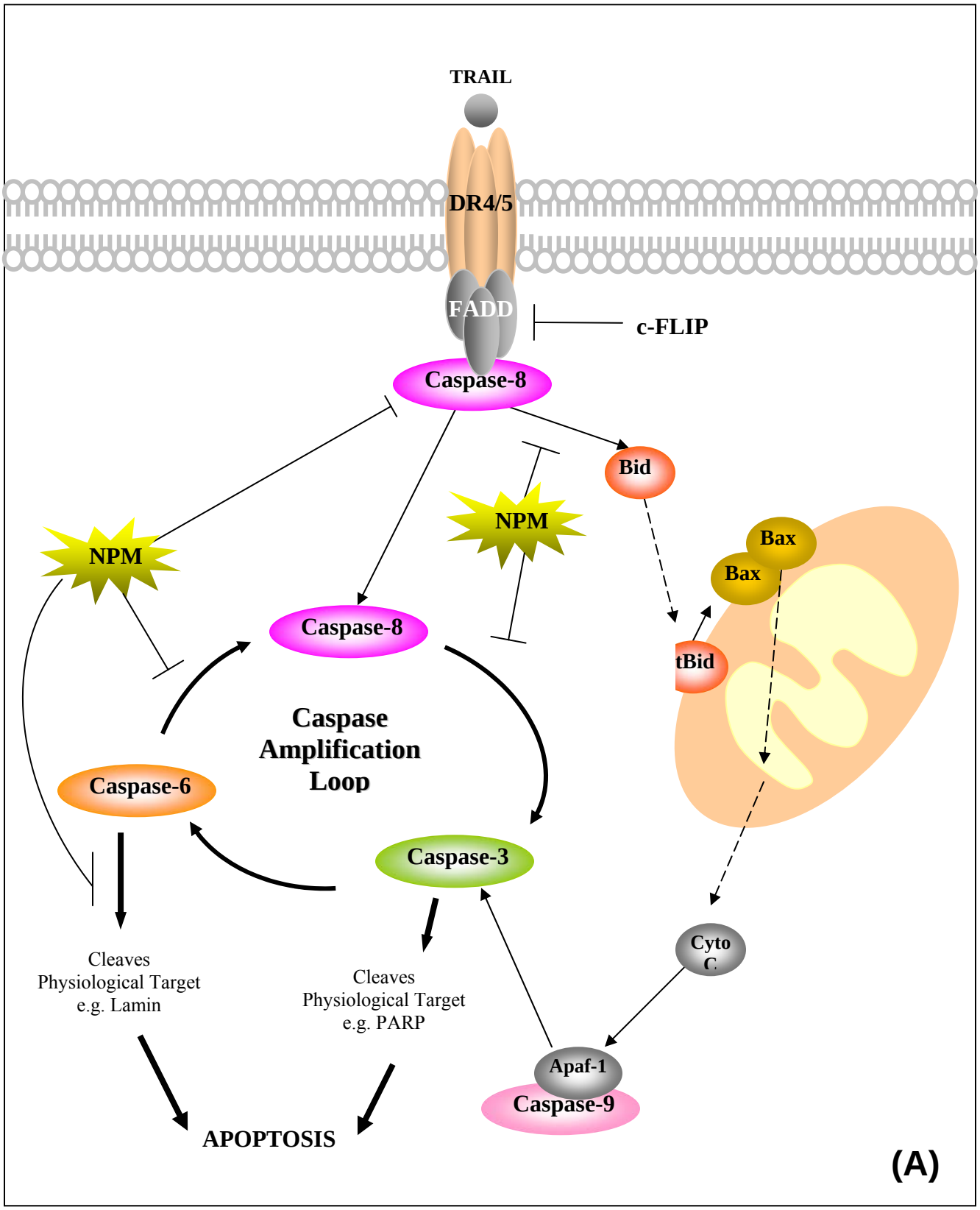
TRAIL
DR4/5
FADD
c-FLIP
Caspase-8
Bid
NPM
NPM
Bax
Bax
Caspase-8
tBid
Caspase
Amplification
Loop
Caspase-6
Caspase-3
Cyto
C
Cleaves
Physiological Target
e.g. Lamin
Cleaves
Physiological Target
e.g. PARP
Apaf-1
Caspase-9
APOPTOSIS
(A)

***(Continued from previous page)*** -mediated death signalling pathway, cellular and/or DNA damage triggers the release of cytochrome *c* from the mitochondria. The cytosolic presence of cytochrome *c* will result in the formation of the apoptosome, consisting of Apaf-1, procaspase-9 and cytochrome *c* itself. In the presence of ATP, the apoptosome activates caspase-9, which in turn cleaves procaspase-3. Activated cvaspase-3 then participates in the caspase amplification loop, leading to the subsequent activation of caspase-6 and -8 as well. In this case, cytoplasmic NPM prevents activated caspase-6 and -8 from cleaving other procaspase, hence halting the progression of the caspase amplification loop. It also inhibits activated caspase-8 from cleaving Bid, hence preventing caspase-8 from triggering a feedback amplification loop leading to more cytochrome *c* release. As in the case of the death receptor pathway, cytoplasmic NPM also inhibits cleaving of lamin A by activated caspase-6. In both cases (A & B), cytoplasmic NPM not only inhibits proximal events occurring just downstream of apoptotic stimulation, but also halts distal events as well.

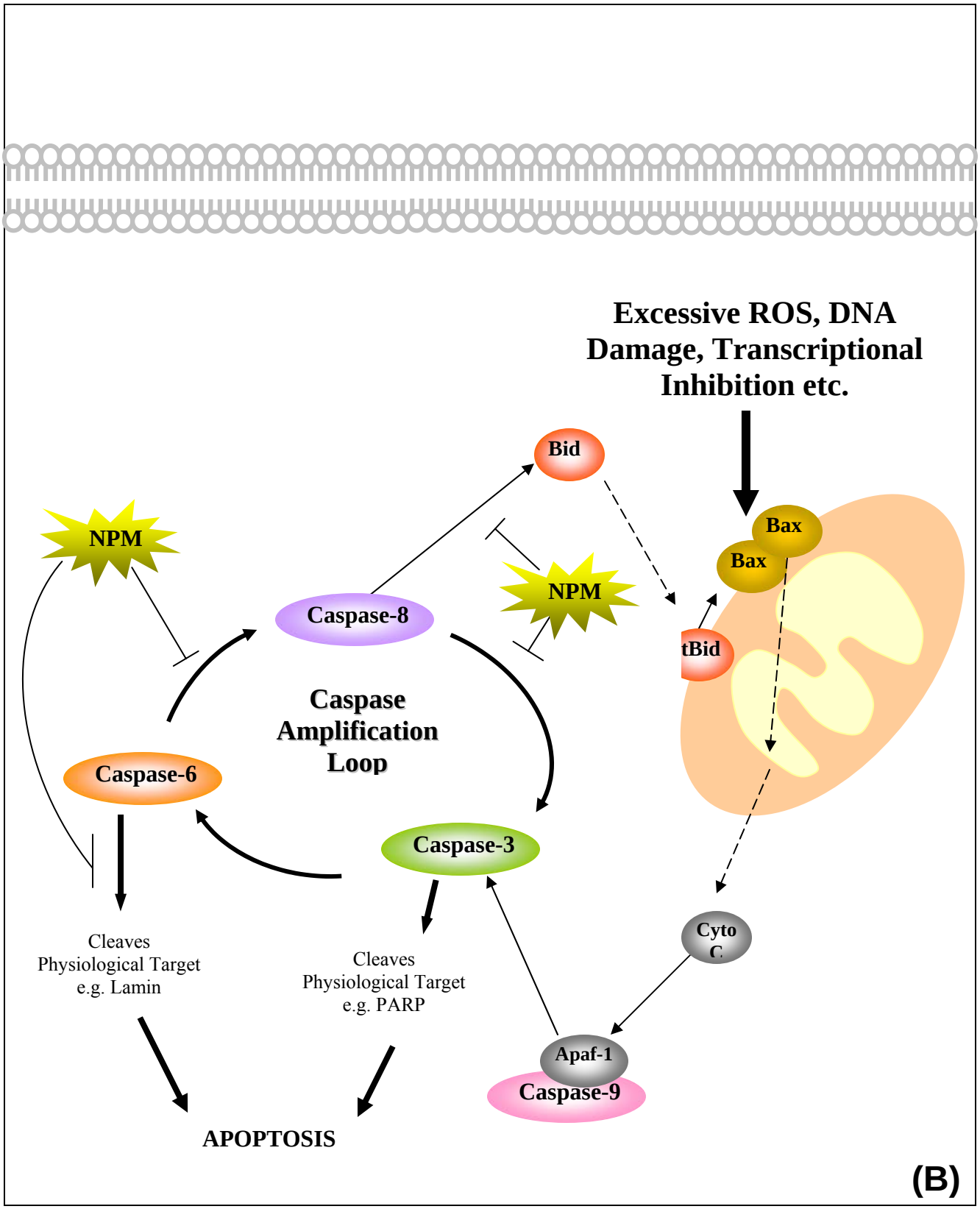
Excessive ROS, DNA Damage, Transcriptional Inhibition etc.
Bid
NPM
NPM
Bax
Bax
Caspase-8
tBid
Caspase Amplification Loop
Caspase-6
Caspase-3
Cleaves Physiological Target e.g. Lamin
Cleaves Physiological Target e.g. PARP
Cyto C
Apaf-1
Caspase-9
APOPTOSIS
(B)

# Chapter IV. NPM interacts with caspase-6 and caspase-8

## 4.1 Introduction

Protein-protein interactions are essential for the cellular function of virtually every protein. Protein interactions are crucial for the formation of structural complexes, intracellular signalling, cell-cell communication and practically every other aspect of cellular function. The 'guilt-by-association' concept has been used for elucidating functional roles from pairs of interacting proteins (Lo *et al.*, 2005). Here, identification of its partner of known function will be instrumental in uncovering the possible function of a protein of hitherto unknown function. Knowledge of protein-protein interactions is also useful for probing biological pathways and regulation of signalling, metabolic, gene expression and replication processes. Meanwhile, alteration of protein-protein interactions is known to contribute to many diseases. Hence, the manipulation of protein-protein interactions that contribute to disease is a potential therapeutic strategy.

Protein interactions are central to the functioning of the caspase-signalling cascade. A striking example is the formation of the Death-Inducing Signalling Complex (DISC) at the Fas receptor. Only a few seconds after receptor triggering, a highly complex mixture of signal transducing molecules consisting of the death receptors, adaptor proteins, caspase-8 and caspase-10 are recruited to the intracellular part of the receptor via interactions between homologous death domains (DD) or death effector domains (DED) (reviewed by Curtin & Cotter, 2003). This newly formed complex is capable of transmitting multiple specific signals, provoking a highly regulated cellular response. Another example is the formation of the large signalling complex, the apoptosome, in response to apoptotic signalling from the mitochondria. Cytochrome-*c* released from the mitochondria interacts and activates Apaf-1, which subsequently oligomerises

to form an approximately 700-1400-kDa caspase-activating complex known as the Apaf-1 apoptosome. The initiator caspase-9 is next recruited to the complex by binding to Apaf-1 through CARD-CARD (caspase recruitment domain) interactions to form a holoenzyme complex (Li *et al.*, 1997; Srinivasula *et al.*, 1998). The holoenzyme complex then recruits the effector caspase-3 through an interaction between the active site cysteine in caspase-9 and the critical aspartate, which is the cleavage site for generating the large and small subunits of caspase-3 (Li *et al.*, 1997). The formation of the mega-apoptotic complex through multiple protein-interactions thus initiates the caspase cascade responsible for the execution phase of apoptosis, and marks the cell's irrevocable commitment to its own demise.

Apart from the evident structural requirements provided by a plethora of protein-protein interactions, there are a large number of transient protein-protein interactions providing tight regulations of the apoptosis progression. Some IAPs use specific BIRs (baculovirus IAP repeats) domains to inhibit particular caspases. XIAP, for example, binds the downstream effector proteases caspase-3 and caspase-7 through its BIR2 domain (requiring both BIR2 and portions of a flanking segment of the protein located between BIR1 and BIR2) (Takahashi *et al.*, 1998), whereas it binds the upstream initiator protease, caspase-9 through its BIR3 domain (Shiozaki *et al.*, 2003). The RINGs domain of cIAPs are implicated in interactions with the cellular components of the ubiquitination machinery (Yang & Li,., 2000), thus controlling turnover of these RING-containing proteins and of other proteins with which they associate. Meanwhile, the cell death–inducing activity of most BH3 domain proteins depends on their ability to dimerise with antiapoptotic Bcl-2 family members and thus to function as trans-dominant inhibitors of proteins such as Bcl-2 and Bcl-$X_L$ (reviewed in Kelekar & Thompson, 1998). Alternatively, certain BH3-only proteins, in particular Bid and Bim, can either bind proapoptotic multidomain

proteins (such as Bax or Bak) and function as apoptosis agonists, or dimerise with antiapoptotic family members (such as Bcl-2 or Bcl-$X_L$) and function as apoptosis antagonists (Wang *et al.*, 1996; Desagher *et al.*, 1999).

In Chapter III, it was shown that NPM inhibits the caspase amplification cascade, both *in vivo* and *in vitro*, via direct inhibition of both caspase-6 and caspase-8. Here, we attempt to elucidate the mechanism underlying such specific inhibitions by determining whether NPM interacts with caspase-6 and -8 physically. Presence of an interaction will strongly implicate NPM in the direct regulation of the caspase-signalling cascade using the "guilt-by-association" principle.

## 4.2 Materials and methods

### *4.2.1 Immunoprecipitation*

MN9D and HeLa cells were treated with 500μM $MPP^+$ for 12 hours or exposed to UV for 8 hours. The cells were then lysed using a mild lysis buffer (150mM NaCl, 50mM Tris, 1% TritonX-100). Co-immunoprecipitation was performed using the Seize™ Primary Immunoprecipitation Kit (Pierce, USA) according to the manufacturer's instructions. Briefly, the cell lysates were incubated with AminoLink® Plus Coupling gel previously coupled to the primary antibodies (anti-NPM Zymed, USA; anti-caspase-6, Santa Cruz, USA; anti-caspase-8 , Santa Cruz, USA and anti-HA, Santa Cruz, USA) overnight at 4˚C. The mixture in the columns were then washed using the IP Buffer three times and the columns were centrifuged at 12,000 x g for 1 minute to remove the spent buffer between each wash. The bound antigens were eluted using the Elution Buffer and the eluted fractions were concentrated using Ultrafree-MC centrifugal filter unit Biomax-5 (Millipore, USA) before being analysed by immunoblotting.

### *4.2.2 Electrophoresis and Western Blot analysis*

Please refer to section 3.2.5 for details. The following antibodies were used in this chapter: with anti-NPM (Zymed, USA, 1:10000), -caspase-3 (Cell Signalling Technology, USA, 1:1000), -caspase-6 (Cell Signalling Technology, USA, 1:2000), -caspase-7 (Neomarkers, USA, 1:600), -caspase-8 (Cell Signalling Technology, USA, 1:1000) and -caspase-9 (Becton Dickinson, USA, 1:1000), followed by incubation with HRP-conjugated secondary antibodies (Santa Cruz, USA), goat-anti-mouse or anti-rabbit (1:1000).

### ***4.2.3*** *Preparation of S100 cytosolic Cell-free Extracts*

Please see Section 3.2.6 for details. 1 μl of recombinant caspase-6 of concentration 1 unit/μl or 36 unit of concentration 36 unit/μl (both from Biovision, USA) was added to the cell-free extract for IP or *in vitro* assay of the inhibitory effect of NPM. Production of recombinant NPM, added to a final concentration of 5 μM, was described in Section 3.2.2.

## 4.3 Results

### *4.3.1 NPM co-precipitates cleaved caspase-6 and -8 in $MPP^+$ treated MN9D cell*

To investigate the possibility of an interaction between NPM and caspase-6 /-8, co-immunoprecipitation (IP) studies were performed. Using extracts from $MPP^+$ treated MN9D cell, we showed that antibody against NPM co-precipitated only cleaved caspase-6 and -8 (Figure 4.1). Meanwhile, antibodies against caspase-6 and -8 precipitated both proform and cleaved forms of their target antigens. These are used as positive controls demonstrating that the antibodies used for immunoblotting are capable of detecting both the cleaved and proform of the caspases. Co-precipitation experiments in the reverse direction were also performed and both anti-caspase-6 and anti-caspase-8 antibodies used for IP (which recognize both the pro- and cleaved caspases) pulled down NPM.

The experiments revealed that that caspase-8 co-precipiated with both proform and cleaved form of caspase-6, which is in agreement with previous observations that caspase-6 is a direct activator of caspase-8 (Cowling & Downward, 2002). This is in stark contrast to the observation that NPM co-precipitated only cleaved caspases, and serves to demonstrate that the exclusive interactions of NPM with cleaved caspase-6 and -8 as observed here are *bona fide.*

### *4.3.2 NPM co-precipitates both proform and cleaved caspase-6 and -8 in UV-irradiated HeLa cells*

We have previously shown that over-expression of GFP-tagged NPM in UV-irradiated HeLa cells halted the progression of the caspases signalling network (Figure 3.1). Here, using the

lysates from UV-exposed HeLa, NPM was shown to form a complex with all forms of caspase-6 and -8 (procaspase, intermediate-cleaved and fully cleaved forms) (Figure 4.2). This is in contrast to the results obtained for the MN9D cells, where NPM was demonstrated to interact with only the cleaved form of both caspases-6 and -8. We further demonstrated a lack of physical interaction between NPM and caspases-3, -7 or -9. Taken together, the results were in agreement with our previous findings in Chapter III, which demonstrated that recombinant NPM specifically inhibited the activities of caspases-6 and -8, but not that of caspases-3, -7 and -9, using the *in vitro* colorimetric assay (Figure 3.5).

### *4.3.3 Increased caspases concentration reversed the inhibitory effect of NPM*

If NPM suppresses general caspase activation by targeting caspases-6 and -8, then increasing the concentration of caspases-6 or -8 in extracts should overwhelm the inhibitory effect of recombinant NPM. To test this argument, we added increasing units of active caspase-8 into the S100 cytosolic extracts derived from untreated HEK293 cells, in the presence of 5 μM recombinant polyhistidine-tagged NPM. While the presence of the recombinant NPM reduced the presence of cleaved caspase-3 markedly, doubling the amount of active caspase-8 (Biovision, USA) from 36 to 72 units added to the extracts restored the amount of cleaved caspase-3 to a level comparable to that in the absence of recombinant NPM (Figure 4.3). Finally, the addition of 120 units of active caspase-8, slightly more than three times the minimal amount used, resulted in even greater amount of cleavage of caspase-3. We thus conclude here that the inhibitory effect of NPM on caspase-8 is reversible with increasing concentration of active caspase-8.

### *4.3.4 NPM forms an inhibitory complex with the active caspases and their substrates*

Since NPM interacts with cleaved caspase-6 and -8, we tested if such interactions sequester the active caspases from their physiological substrates. Using the HEK293-derived cell free extract, we previously demonstrated that in the presence of recombinant NPM, recombinant active caspase-8 and -6 showed reduced cleaving of their substrate procaspase-3 and –8 respectively (Figure 3.7). We next used co-immunoprecipitation to determine if recombinant NPM addition will result in less active caspase-6 and -8 being co-precipitated with their respective substrates. Surprisingly, procaspase-8 was observed to co-precipitate even more active caspase-6 in the presence of recombinant NPM. The recombinant NPM was also precipitated with procaspase-8 (Fig. 4.4 A). Similar phenomenon was also observed for procaspases-3, which co-precipitated more active caspase-8 and recombinant NPM (Fig. 4.4 B). These findings indicate that NPM may serve as an inhibitor delaying dissociation between the active caspases and their substrates, hence reducing the pool of available active caspases for further substrate binding and cleaving.

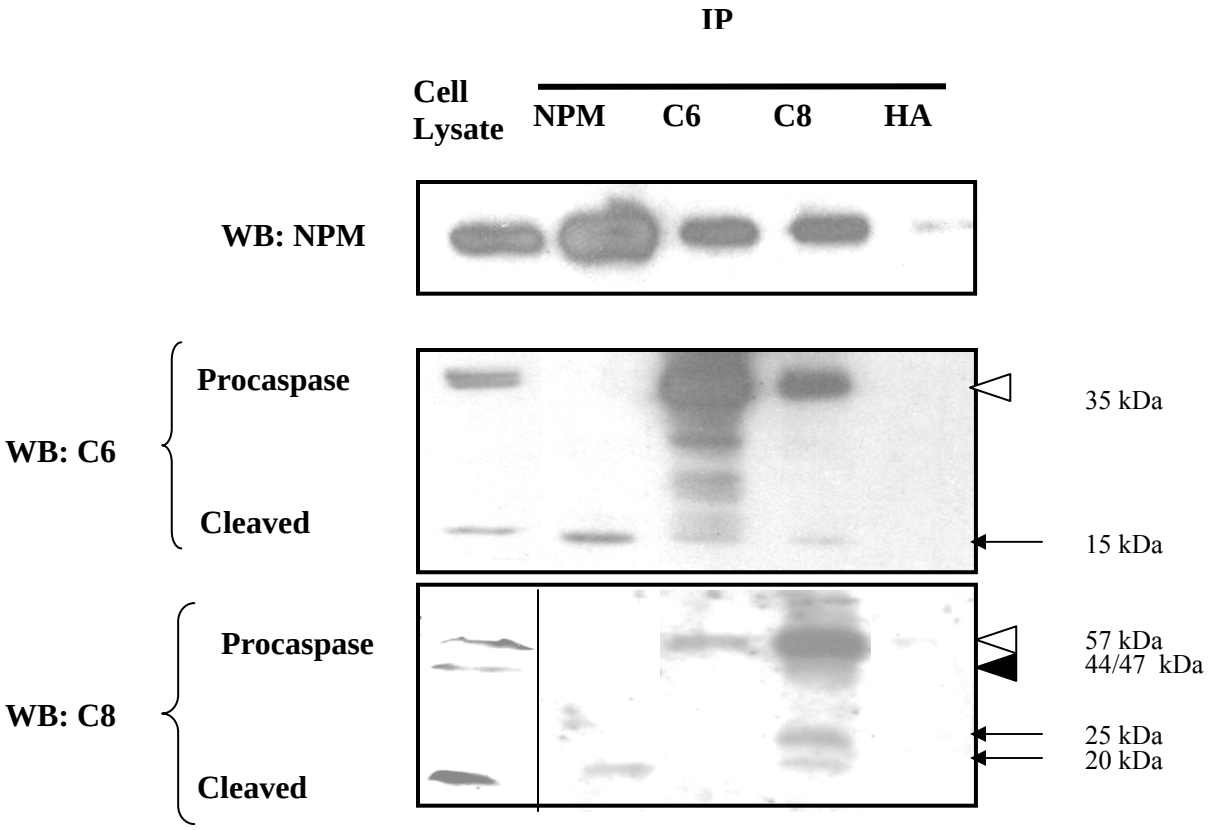


**Figure 4.1. NPM interacts with active caspase-6 and -8 in $MPP^+$-treated MN9D cells.** MN9D cells were treated with 500 μM $MPP^+$ for 12 hours, after which the cells were harvested and the total cell lysates extracted. Immunoprecipitation was carried out as described in Materials and Methods, Section 4.2.1 using antibodies against NPM, caspase-6 and caspase-8, followed by Western blotting using antibodies to NPM, caspase-6 or caspase-8, as indicated to the left of the panel. 20 μg of the total cell lysates extract (80 μg for caspase-8 immunoblotting) were loaded as positive control. White triangle indicates procaspase, black triangle indicates intermediate cleaved fragment, and black arrow indicates cleaved caspase fragment.

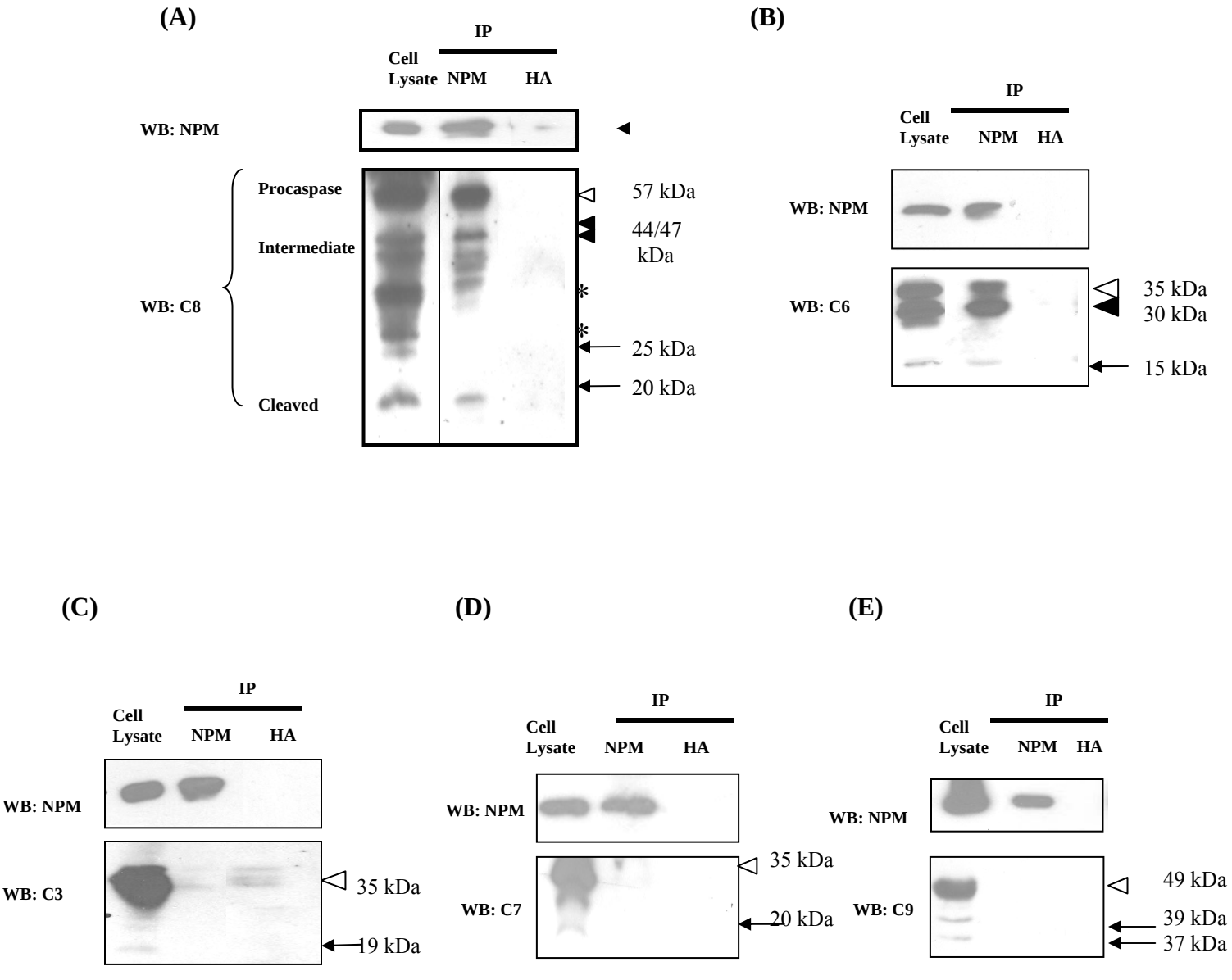


**Figure 4.2. NPM interacts with proform and cleaved caspase-6 and -8 in UV-irradiated HeLa cells.** HeLa cells were irradiated with UV (40 W) for four hours, after which the cells were harvested and the total cell lysates extracted. Immunoprecipitation was carried out as described in Materials and Methods, Section 4.2.1 using antibodies against NPM or Hemaglutinnin (HA, negative control), followed by Western blotting using antibodies to NPM (A-E), caspase-8 (A), caspase-6 (B), caspase-3 (C), caspase-7 (D) and caspase-9 (E), as indicated to the left of the panel. 20 μg of the total cell lysates extract (80 μg for caspase-8 immunoblotting) were loaded as positive control. White triangle indicates procaspase, black triangle indicates intermediate cleaved fragment, black arrow indicates cleaved caspase fragment and asterisk indicates unidentifiable band. The positive control for caspase-8 blot is spliced and juxtapose next to the IP blot.

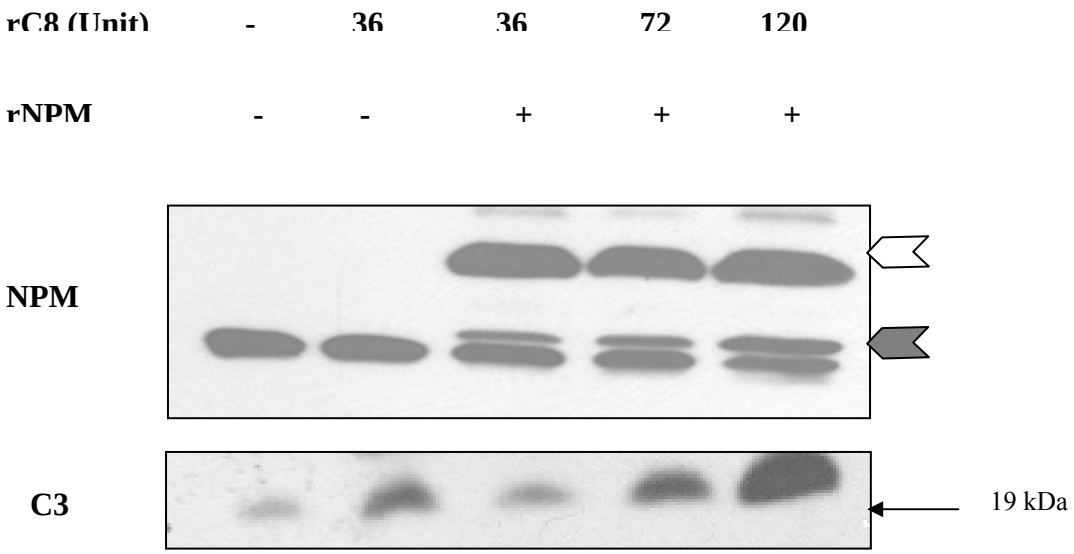


**Figure 4.3. Increased active caspase-8 amount reversed the caspase inhibitory effect of NPM.** S100 cytosolic cell-free extracts were prepared from non-treated HEK 293 cells. Varying amount of recombinant active caspase-8 was added to the extract in the absence or presence of 5 μM of His-tagged recombinant NPM. The various extracts were then incubated at 37˚C for four hours, before being subjected to SDS-PAGE and immunoblot analysis using anti-NPM and anti-caspase-3 antibody, as indicated to the right of each panel. White broad arrow indicates th higher molecular weight His-tagged recombinant NPM, grey broad arrow indicates endogenous NPM, and black arrow indicates cleaved caspase-3. rC8: recombinant active caspase 8, rNPM: recombinant nucleophosmin.

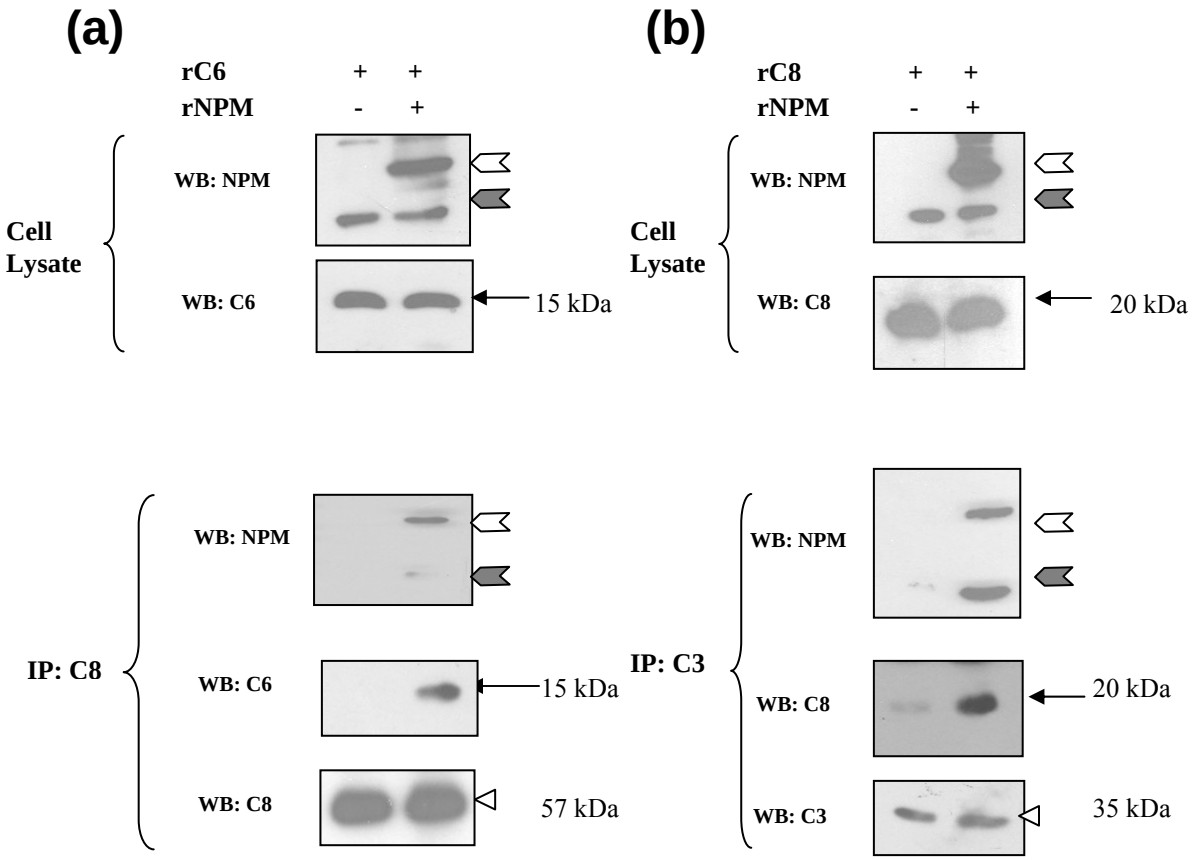


**Figure 4.4. NPM and active caspase-6/-8 form a complex *in vivo* with the caspase substrates.** S100 cytosolic cell-free extracts were prepared from non-treated HEK 293 cells. 1 untit of recombinant active caspase-6 (A) or 32 units of recombinant active caspase-8 (B) was added in the absence or presence of 5 μM of His-tagged recombinant NPM. The extracts were then incubated at 37˚C for 15 min. Immunoprecipitation was carried out using the various extracts as described in Materials and Methods, Section 4.2.1 using antibodies against procaspase-8 (A) or procaspase-3 (B), followed by Western blotting using antibodies to NPM (A, B), caspase-6 (A), caspase-8 (A, B) or caspase-3 (B), as indicated to the left of the panel. 20 μg of the total cell lysates were loaded to indicate the presence of comparable amount of added recombinant caspase-6 (A) or -8 (B) with or without added recombinant NPM. White broad arrow indicates higher molecular weight His-tagged recombinant NPM, grey broad arrow indicates endogenous NPM, white triangle indicates procaspase, black triangle indicates intermediate cleaved fragment, and black arrow indicates cleaved caspase fragment.

## 4.4 Discussion

While physical interactions with the caspases have been taken to constitute a direct evidence implicating several molecules in an anti-apoptotic function, the form(s) of caspase found in these associations differ(s) from inhibitor to inhibitor, thus suggesting differences between the underlying inhibition mechanisms. c-IAP1, c-IAP2, XIAP, and survivin have been reported to bind to and inhibit the active forms of the terminal caspases-3 and -7, but do not interact with caspase-8, which is the most proximal caspase from the TNF-α/Fas receptor (Deveraux *et al.*, 1997; Roy *et al.*, 1997; Conway *et al.*, 2000). c-IAP1, c-IAP2, and XIAP also bind to the zymogen form of caspase-9 thereby preventing its proteolytic processing as well as the processing of downstream proteases, such as caspase-3, -6, and -7 (Deveraux *et al.*, 1998). Livin, which is a member of the IAP family, was observed to co-immunoprecipitate with pro-caspase-9 and a partially activated form of caspase-9 containing the $NH_2$-terminal prodomain. No interaction of Livin was seen with the fully active 12- and 20-kDa subunits of caspase-9 using the Biacore, suggesting that the prodomain is required for the interaction (Kasof & Gomes, 2001). Meanwhile, the small heat shock protein αB-crystallin was shown to bind to the p24 partially processed caspase-3 and inhibits its autoproteolytic maturation, which is consistent with *in vitro* studies demonstrating that αB-crystallin inhibited the autoproteolytic maturation of the p24 partially processed caspase-3 intermediate (Kamradt *et al.*, 2001).

Generally speaking, the inhibition of initiator caspase (e.g. caspase-9) appears to involved interaction of the inhibitor molecule with the zymogen, thereby preventing its processing. In contrast, inhibition of the executor caspases (3 and 7) seems to involve a different mechanism – one that calls for direct interaction of the inhibitor molecule with the cleaved or partially cleaved

caspase instead, thereby inhibiting its proteolytic activity. The differences in the two mechanisms may reflect the difference in the role and hierarchy of these two groups of caspases (initiator versus effector) within the death-signalling network, as well as their sequence variations. NPM's physical interaction with caspase-6 and -8, as discovered in this chapter, seems to present a unique case. Both 1) exclusive interaction with only the cleaved caspases, and 2) interactions with all forms (proform, partially cleaved and fully cleaved) of the caspases, were detected, albeit in different cell lines. While inhibiting the active caspases' activities is perceivably sufficient in halting death signal relay, preventing further processing of the proform and intermediate cleaved fragments may provide additional protection against the death stimulus. The difference in the interaction modes observed here may also stem from the differences in the host species and tissue from which the cell lines were derived from – MN9D cells are mouse midbrain in origin, while HeLa cells are human cervical adenocarcinoma-derived. It can also be argued that the existence of two interaction modes for caspase-8 with its inhibitor may reflect the uniqueness in the former's hierarchical role within the death-signalling pathway. Caspase-8 functions both as an initiator and executor caspase. It not only triggers and amplifies the apoptotic process at cytoplasmic sites, but can also act as an executioner in the nucleus, where it cleaves PARP-2, a member of the poly(ADP-ribose) polymerase family involved in DNA repair (Benchoua, *et al.*, 2002). Thus, while inhibiting procaspase cleavage can help prevent caspase-8 from relaying death signals and fulfilling its 'initiator' role, inhibiting the activities of already-cleaved fragments can prevent cleavage of caspase-8's 'death substrates' further downstream. So far, such dual inhibition mode is not observed for other caspases, which are only known to belong to one of the two caspase classification groups. In any case, both modes of interaction

involve the cleaved caspase fragments, and this seems to form the basis of NPM's inhibition of caspase-6 and -8.

We have hypothesized, based on the results gathered so far, that stress-induced elevation in cytoplasmic NPM level may lead to inhibition of the activities of caspase-6 and –8 (See Chapter II and III). This in turn begs the question of how the cell may overcome the inhibitory hurdle set by the elevated amount of NPM when it is eventually committed to death. It was previously reported that while Hsp70 was able to inhibit processing of procaspases-9 by preventing the recruitment of the latter to Apaf-1, over-expression of Apaf-1 was demonstrated to be able to abrogate the inhibitory effect of Hsp70 on procaspases-9 processing (Beere *et al.*, 2000). We similarly observed in Figure 4.3 that doubling the amount of active caspase-8 was able to overcome the inhibitory effect of the exogenously added recombinant NPM and restore the amount of cleaved caspase-3 to a level comparable to that without addition of the recombinant NPM. Coupled to the fact that NPM interacts with cleaved caspse-6 and -8, this observation raised the possibility that inhibition of procaspase-3 activation is mediated by simple competition for active caspase-8. Using the pull-down assay, we therefore examined if the binding of active caspase-6 and -8 to their respective substrates, procaspases-8 and -3, is disrupted by the presence of the exogenously added recombinant NPM. Surprisingly, we noted instead an increase in the amount of active caspase-6 and -8 being precipitated along with procaspases-8 and –6 in the presence of exogenous NPM (Figure 4.4). Both endogenous and added NPM were also co-precipitated with the procaspases as well. In both cases, the amount of procaspases pulled down in the presence and absence of recombinant NPM is not markedly different from each other. Taken together, the observations indicate the formation of an inhibition complex comprising of NPM, active caspase-6/-8 and their substrates. The addition of

recombinant NPM appears to 'freeze' the interaction of the active caspase-6 and -8 with their substrates, though the order of interaction within the complex remains unknown unless elucidated with structural biology means. Given our previous observations that recombinant NPM could inhibit the cleaving of procaspases-3 and -8 by active caspase-8 and -6 respectively, we hypothesize that the formation of the inhibition complex may prevent the dissociation of active caspase-6 and -8 from their current targets, thereby making them unavailable for cleaving other procaspases. The validation of this hypothesis is, however, complicated by the fact that procaspases-8, the substrate to active caspase-6, was shown to interact with NPM in at least the HeLa cells, though the procaspases-3 showed no interaction with NPM (Figure 4.2). In any case, the inhibition of procaspases cleaving by active caspe-6 and -8 is unlikely to be due to simple competition. This is reminiscent to situation of Hsp70's inhibition of procaspases-9 recruitment to Apaf-1 apoptosome, where Hsp70's addition was demonstrated to be unable to disrupt the interaction between procaspases-9 and the CARD domain of Apaf-1 (Beere *et al.*, 2000).

All in all, physical associations between NPM and caspase-6 and -8 are demonstrated here, and it is likely that NPM promotes the formation of an inhibitory complex involving the active caspases and their current substrates, thereby effectively sequestering them away from many other available substrate molecules. The use of biophysical methods such as nuclear magnetic resonance (NMR) to investigate the crystal structure of NPM in complex with active caspase-6 and -8 is likely to shed light on the structural basis for such inhibitions, as well as reveal the order of contact of components within the NPM-caspase-substrate inhibition complex.

# Chapter V. Role of cytoplasmic NPM in the pathogenesis of Acute Myeloid Leukaemia (AML)

## 5.1 Introduction

Normal development of haematopoietic cells and maintenance of tissue homeostasis requires tight regulation of proliferation, differentiation and death processes. Deregulation of any of those processes can result in leukaemia (Thompson, 1995). Many genetic changes occur in many different types of leukaemia. For many, the most important changes are chromosomal translocations. A number of acute and chronic leukaemias and non-Hodgkin's lymphomas subtypes are associated with *specific* translocations. The genes located at breakpoints are often involved in lymphocytic or myeloid cell proliferation and/or differentiation. When these genes are translocated into a new genetic "environment", they are upregulated and overexpressed or mutated. These changes often result in loss of growth control and malignancy. For instance, chronic myelogenous leukaemia results from a cytogenetic aberration consisting of a reciprocal translocation between the long arms of chromosomes 22 and 9; t(9;22). This translocation relocates an oncogene called *abl* from the long arm of chromosome 9 to the long arm of chromosome 22 in the *bcr* region. The resulting *bcr-abl* fusion gene encodes a chimeric protein with strong tyrosine kinase activity (Lugo *et al.*, 1990), which is necessary and sufficient for leukaemogenesis (Daley *et al.*, 1990; Heisterkamp *et al.*, 1990).

NPM has also been found to be involved in several chromosomal translocations, resulting in the formation of oncogenic fusion proteins. The NPM-ALK fusion gene, formed by the t(2;5)(p23;q35) translocation in non-Hodgkin's lymphoma, encodes a 75-kDa hybrid protein that contains the amino-terminal 117 amino acid residues of the nucleolar phosphoprotein nucleophosmin (NPM) joined to the entire cytoplasmic portion of the receptor tyrosine kinase ALK (anaplastic lymphoma kinase) (Morris *et al.*, 1994). ALK is a cell membrane-spanning

receptor tyrosine kinase and a member of the insulin receptor superfamily. Although the precise physiological function and regulation of ALK have not been well defined, oligomerisation of the fusion proteins mediated by the NPM portion, which contains the homodimerisation domain, is thought to result in dysregulated expression and constitutive activity of the ALK kinase (Bischof *et al.*, 1997). This in turn leads to aberrant phosphorylation of multiple intracellular substrates downstream of NPM-ALK, which plays a key role in lymphomagenesis (Pulford *et al.*, 2004; Duyster *et al.*, 2001). Meanwhile, in acute promyelocytic leukaemia (APL), a t(5;17)(q32;q12) chromosomal translocation fuses the gene for nucleophosmin (NPM) to the retinoic acid receptor alpha (RARA) (Redner *et al.*, 1996). Signalling through RAR and activation of RAR target genes induce proliferation arrest, differentiation, and apoptosis in a wide variety of cell types. Retinoids have tumor-suppressive activity, and consequently, defects in RAR signalling are implicated in cancers (Altucci & Gronemeyer, 2001; Freemantle *et al*., 2003). The chromosomal translocation results in functionally altered receptors that act as constitutive repressors of transcription, thereby preventing cell differentiation and resulting leukaemogenesis (Redner *et al.*, 2000).

The NPM sequence contained in the NPM-RAR cDNA is identical to the NPM sequences contained in the NPM-ALK fusion gene mentioned above. In both cases, the NPM homodimerisation domain is retained in the fusion proteins. While homodimerisation of the fusion proteins mediated through the NPM portion can lead to constitutive activation of their fusion partner, interaction of wild type NPM with the fusion proteins has been speculated to further contribute to oncogenesis by inhibiting the normal cellular functions of NPM. This is reminiscent of PML−RAR, the fusion protein resulting from a translocation involving the promyelocytic leukaemia gene (PML) and the retinoic acid receptor alpha gene, which is another

oncogenic fusion protein found in acute promyelocytic leukaemias (APLs) (He *et al.*, 1999). PML−RAR is a bifunctional protein that blocks differentiation (through its RAR moiety) and inhibits stress-induced apoptosis (Grignani *et al.*, 1993) through the effect of its PML component on p53. PML can interact directly with p53, and regulate the latter's acetylation, as well as premature senescence induced by oncogenic Ras (Pearson *et al.*, 2000). The region of PML involved in p53 binding is lost in the PML−RAR fusion protein, and PML−RAR strongly inhibits p53 activity through interaction with wild-type PML in a dominant negative manner (Fogal *et al.*, 2000). Similar to PML, NPM has been shown to interact with p53, and positively regulate its stability and transcriptional activity. NPM-RAR and NPM-ALK has been speculated to be able to sequester wild type NPM away from p53, hence leading to p53's degradation. As the tumour suppressor p53 induces cellular senescence and/or apoptosis in response to oncogenic signals, the decline in p53 level in this case inadvertently promotes leukaemogenesis (Colombo *et al.*, 2002).

Though chromosomal translocations have been prominently implicated in the pathogenesis of many leukaemic types, conventional chromosome banding analysis of approximately 50% of the acute myeloid leukaemia (AML) patients lack clonal chromosome aberrations (Byrd *et al.*, 2002; Grimwade *et al.*, 1998). AML is a heterogeneous group of malignant leukaemia with diverse genetic abnormalities. It is characterised by an accumulation in the bone marrow and peripheral blood of large numbers of abnormal, immature myeloid cells. These cells are capable of dividing and proliferating, but cannot differentiate into mature haematopoietic cells (i.e., neutrophils). Falini *et al* (2005) investigated the subcellular localisation of NPM1 in bone marrow biopsy specimens from 591 adult patients with primary AML, 135 patients with secondary AML, and 980 haematopoietic or extrahaematopoietic malignancies

other than AML using immunohistochemical methods. Cytoplasmic NPM1 ($NPM1c^+$) was exclusively detected in primary AML with an incidence of 35.2%. It was associated with a broad spectrum of morphologic AML subtypes with the highest frequency in monocytic leukaemias. Notably, in none of the $NPMc^+$ AML specimens was NPM-ALK, NPM-RAR or any other NPM-containing fusion protein found. Sequencing of the *NPM1* coding region identified an exon 12 mutations leading to a frameshift in the C-terminal region of the NPM1 protein that is necessary for nucleolar localisation of NPM1 (Nishimura *et al.*, 2002). Meanwhile, transfection of mutated *NPM1* into NIH-3T3 cells confirmed that exon 12 mutations result in delocalisation of NPM1. Thus, based on these findings, mutations in *NPM1* exon 12 and the resulting shift of NPM1 into the cytoplasm are the most frequent events that have been identified in adult AML lacking chromosomal translocation to date.

Given that NPM's usual localisation and functioning is in the nucleus, the cytoplasmic NPM mutant (NPMc) was thought to represent a 'loss-of-function' mutant. In other words, disruption of wild type NPM's regular nuclear duties was conjectured to underlie the pathogenesis of AML with a normal karyotype. A vital function of nuclear NPM is in the regulation of the stability and localisation of the tumour suppressor Arf, which inhibits cell proliferation through both p53-dependent and -independent mechanisms (Sherr, 2001). By binding and inhibiting the p53-antagonist Mdm2 in the nucleoplasm, Arf is able to induce cell cycle arrest through p53 activation (Llanos *et al.*, 2001). NPM in turn binds the Arf protein and protects it from degradation by the ubiquitin-proteasome pathway (Kuo *et al.*, 2004). Indeed, the stability of Arf protein is markedly decreased in cells that lack NPM expression. The amino-terminal region of Arf is dynamically disordered in aqueous solution and becomes highly structured upon binding to Mdm2 (Bothner *et al.*, 2001). NPM was thought to bind newly

synthesised Arf and serve as a molecular chaperone to favour acquisition of a tertiary and stable structure, thus preventing its degradation or aggregation (Colombo *et al.*, 2005). While the leukaemia-associated NPMc mutant was shown to be capable of binding Arf as well, it was unable to prevent degradation of the latter, unlike its wild type counterpart. In addition, NPMc was found to provoke dislocation of remaining Arf from the nucleus into the cytoplasm, which potentially disrupts the Arf-Mdm2 inhibitory interaction and leads to suppression of p53 activation. All in all, the inability of NPMc to protect Arf from degradation and to target it to the nucleus for p53 regulation, as outlined in Figure 5.1, was proposed to be the main cause underlying the pathogenesis of AML with a normal karyotype (Colombo *et al.*, 2005).

Though the hypothesis put forth by Colombo *et al.* (2005) appears plausible, its strength was undermined considerably with further investigations by den Besten *et al.* (2005). The latter likewise demonstrated that NPMc-dependent export of p19-Arf from the nucleus inhibited p19-Arf's functional interaction with the p53 negative regulator, Mdm2, and blunted Arf-induced activation of the p53 transcriptional program. Surprisingly, despite the ability of NPMc to interfere with the activities of Arf, NPMc was shown to lack a proliferation-promoting function exhibited by its wild type counterpart. Overexpression of wild type NPM, but not NPMc, overcame premature senescence of Atm-null Nih-3T3 cells, a phenotype that can be rescued by inactivation of Arf or p53. Overcoming senescence has been proposed to play a critical role in human cancer pathogenesis (Yeager *et al.*, 1998). Thus, the inability of NPMc to do so implies that perturbation of Arf function might be insufficient to explain the oncogenic effects of the NPMc mutation, and that perturbation of *other* function of wild type NPM by NPMc may contribute more substantially toward AML's pathogenesis.

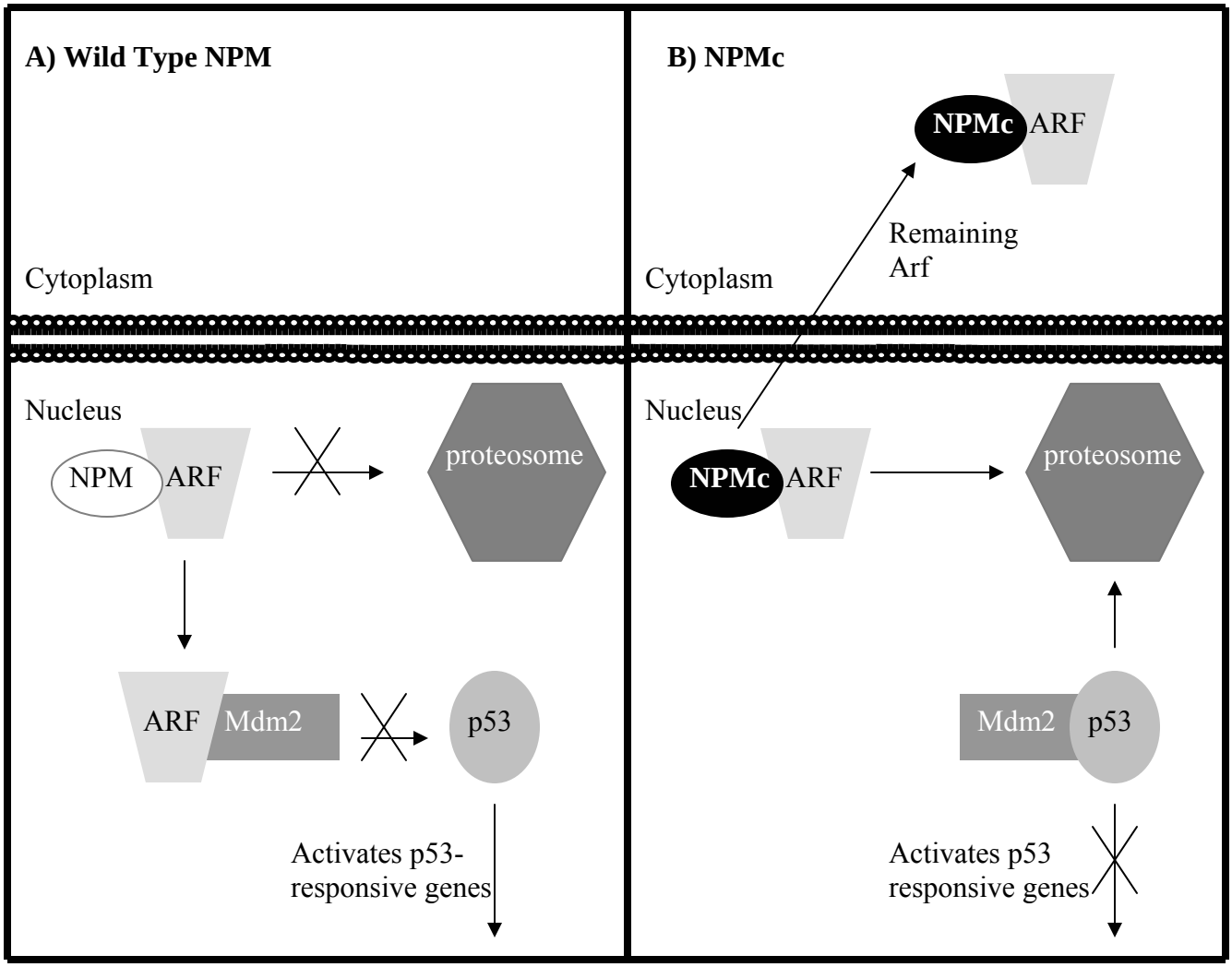


**Figure 5.1 The "ARF disruption" model as proposed by den Beston *et al.* (2005).** In a normal myelogenous cell (A), wild type NPM binds ARF and prevents it from being targeted for proteosomal degradation in response to cellular or DNA damage. ARF in turn associates with Mdm2 and prevents it from degrading p53. Heightened p53 then triggers cell cycle arrest or apoptosis. Meanwhile, in a myelogenous cell harbouring the *NPM1* mutation, the mutant NPMc is unable to protect ARF from proteosomal degradation. In addition, the cytoplasmic dislocated NPMc sequesters the remaining ARF away from the nucleus, and prevents it from interacting with Mdm2. Without binding to ARF, Mdm2 is free to associate with and target p53 for degradation. This in turn leads to attenuation of the cell's p53 response and is proposed to underlie the pathogenesis of $NPMc^+$ AML.

Based on results gathered in the previous chapter, we have ascribed to NPM a definitive anti-apoptotic role involving the direct inhibition of caspase-6 and -8. We have also shown that

in response to diverse stress stimuli, NPM is transiently translocated into the cytoplasm, which is the site of death signal initiation and amplification by the mitochondrial and death receptor pathways, to possibly delay full-fledge caspase activation until the cell becomes irrevocably committed to cell death. These observations in turn open up the possibility that localisation of NPMc in the cytoplasm may permanently elevate the threshold for caspase-8 activation, and aberrantly prevent cell death even in the face of considerable death provocations. This in turn suggests NPMc as an oncogene with an anti-apoptotic, rather than anti-proliferative, function, as in the case of bcl-2 in follicular B-cell lymphomas (Hockenbery *et al.*, 1990). In this Chapter, we explore this possibility, by investigating the caspase inhibitory capacity of NPMc in relation to its wild type counterpart, in both the HeLa cells and the AML patients-derived myelogenic cell models.

## 5.2 Materials and methods

### *5.2.1 Cell culture and induction of apoptosis*

HeLa (a gift from Dr Ge Rou Wen, NUS) was cultured as described in Section 2.2.1. OCI-AML2 and OCI-AML3 cell lines were purchased from DSMZ (German National Resource Centre for Biological Material) and cultured in Alpha MEM medium (Invitrogen, USA) supplemented with 20% fetal bovine serum and 1% penicillin/streptomycin in a humidified atmosphere of 5% $CO_2$ at 37°C. Both AML cell lines were treated with recombinant TRAIL (Chemicon, USA) at a final concentration of 50 ng/mL for 12 hours before being harvested for immunoblot analysis. For apoptosis assay, the cells were treated with recombinant TRAIL of the same concentration for 0, 6, 12 or 24 hours before harvesting.

### *5.2.2 Electrophoresis and Western Blot analysis*

As described in Section 3.2.5. The following antibodies were used in this chapter: with anti-NPM (Neomarker, USA, 1:1000), -caspase-3 (Cell Signalling Technology, USA, 1:1000), -caspase-6 (Cell Signalling Technology, USA, 1:2000), -caspase-7 (Neomarkers, USA, 1:600), -caspase-8 (Cell Signalling Technology, USA, 1:1000), -oct-1 (Chemicon, USA, 1:1000) or –actin (Santa Cruz, USA, 1:1000), followed by incubation with HRP-conjugated secondary antibodies (Santa Cruz, USA), either goat-anti-mouse or anti-rabbit (1:1000).

### *5.2.3 Plasmids and Transfection*

The construction of pcDNA3.1-GFP-human-NPM used in this chapter is as described in Section 3.2.4. The NPMc mutant was constructed using multiple steps PCR. Human NPM1 fragment corresponding to human protein sequence 1-287 (out of 294 amino acids) was initiately amplified using the wild type human NPM1 as the template with Turbo Taq polymerase (Strategene, USA) to ensure high sequence fidelity during amplification. The following primers were used for the initiate amplification:

CytoNPM-F Forward primer 5' – CGA TGG AAG ATT CGA TGG ACA –3'

CytoNPM-B1 Reverse primer 5' – TGC CAG ACA GAG ATC TTG AAT AGC CT –3'

The resulting C-terminal truncated wild type NPM1 fragment was purified by low melting-agarose gel electrophoresis and used as template for a second round of PCR amplification for extension of the truncated fragment, using the following primers:

CytoNPM-F Forward primer 5' – CGA TGG AAG ATT CGA TGG ACA –3'

CytoNPM-B2 Reverse primer 5' – AAA GAG ACT TCC TCC ACT GCC AGA CAG AGA TC –3'

The extended portion contains the mutated NPMc sequence not found in wild type NPM1. The PCR product obtained from this second round of amplification was again subjected to gel

extraction clean up. Complete extension of the mutated NPMc portion was finally performed with this second round amplification products as the template using the following primers:

CytoNPM-F Forward primer 5' – CGA TGG AAG ATT CGA TGG ACA –3'

CytoNPM-B3 Reverse primer 5' – CTA TTT TCT TAA AGA GAC TTC CTC CAC –3'

The same exact protocol was used for the construction of the NPMc mutant, except that the reverse primers used were different. In this mutant, the lysine and valines originally present in the NPMc C-terminal mutant portion were replaced, thereby abolishing the nuclear export signal (NES). Wild type human NPM1 cDNA was again used as the initiate template for first round PCR amplification with the following primers:

CytoNPM-F Forward primer 5' – CGA TGG AAG ATT CGA TGG ACA –3'

Mutant-CytoNPM-B1 Reverse primer 5' – TGC CTC ACA GAG ATC TTG AAT AGC CT – 3'

The primers used for the second round PCR amplification were as follow:

CytoNPM-F Forward primer 5' – CGA TGG AAG ATT CGA TGG ACA –3'

Mutant-CytoNPM-B2 Reverse primer 5' – AAA GAG GCT TCC TCC GCT GCC TCA CAG AGA TC –3'

The primers used for the third round PCR amplification were as follow:

CytoNPM-F Forward primer 5' – CGA TGG AAG ATT CGA TGG ACA –3'

Mutant-CytoNPM-B3 Reverse primer 5' –GCT TTT CTA AAA GAG GCT TCC TCC AC–3'

For all three rounds of amplifications for the construction of NPMc or mutant NPMc, the PCR cycling conditions were (i) 95°C for 5 min; (ii) 95°C for 1 min, 55 °C for 1 min, 68°C for 2 min (30 cycles); and (iii) 68°C for 10 min. The full-length PCR products were purified by low melting-agarose gel electrophoresis and separately cloned into pGEM-T Easy vector (Promega, USA) for sequencing. The NPMc and mutant NPMc cDNAs were then subcloned into pcDNA3.1-GFP using the EcoRI restriction site for non-directional cloning. Transfection of HeLa cells with pcDNA3.1-GFP empty vector, pcDNA3.1-GFP-human-NPM, pcDNA3.1-GFP-NPMc or pcDNA3.1-GFP-mutant-NPM using Lipofectamine 2000 (Invitrogen, USA) were as described in Section 2.2.2.

### *5.2.4 Preparation of S100 cytosolic Cell-free Extracts*

As described in Section 3.2.6. 10 units of concentration 36 unit/μl (Biovision, USA) was added to the HeLa cell-free extract for *in vitro* assay of the inhibitory effect of NPM and the various NPM mutants on caspase activation initiated by the addition of rat-heart derived cytochrome c (300 nM, Sigma, USA) and ATP (900 nM, Sigma, USA)

### *5.2.5 Preparation of subcellular fractions*

Nuclear and cytosolic fractions were prepared as described in Section 2.2.5.

### *5.2.6 Immunodepletion*

As described in Section 3.2.9. The N-terminal targeting NPM antibody (Cell signalling, USA) was used for immunodepletion of NPM and NPMc from the cytosolic extracts of OCI-AML2 or OCI-AML-3 cell lines.

### *5.2.7 Apoptosis assay*

Apoptosis was assessed by examination of nuclear morphology. Cells were loaded with 4 μM of Hoechst 33342 (cell-permeable, blue fluorescent chromatin stain, Sigma, USA) for 10 min. Apoptosis was characterised by scoring condensed and fragmented highly fluorescent nuclei of GFP-, GFP-NPM-, GFP-NPMc- or GFP-Mutant-NPMc-transfected HeLa cells. Each set of experiments was repeated at least three times, with at least 300 cells counted in each instance.

### *5.2.8 Immunofluorescence microscopy*

HeLa cells tranfected with GFP, GFP-NPM, GFP-NPMc or GFP-Mutant-NPMc were exposed to Hoechst 33342 at a final concentration of 4 μM and incubated for an additional 5 min at room temperature, before being observed. Images were collected using an inverted fluorescence microscope (model Axiovert 25; Carl Zeiss Meditech, Germany).

## 5.3 Results

### *5.3.1 Creation of the NPMc and NPMc mutant*

The NPMc mutant was reported to result from mutations affecting exon 12 of the human *NPM1* gene. Six sequence variants (designated NPMc mutant A-F) were observed, all leading to a frame shift in the region encoding the C-terminal of the NPM protein. The most frequent mutation (mutant A) was a duplication of a TCTG tetranucleotide at positions 956 through 959 of the wild type sequence. The resulting shift in the reading frame alters the C-terminal portion of the NPM protein by replacing the last seven amino acids (WQWRKSL, where the amino acids are designated by their single-letter codes) with 11 different residues (CLAVEEVSLRK) (Falini *et al.*, 2005). A motif containing leucine-valine residues, constituting the nuclear-export-signal (NES) motif was further discovered in the C-terminal of NPMc mutants. The typical nuclear-export signal consists of a short stretch of hydrophobic amino acids (predominantly leucines) and fits the consensus sequence Lx(1-3)Lx(2-3)LxL (with x indicating any residues) (Henderson & Eleftheriou, 2000). NES can be recognised by the nuclear export receptor NES for cytoplasmic export of the protein harbouring it. It was hence speculated that Crm1-mediated export of NPMc mutant may underlie tumorigenesis in acute myelogenous leukaemia (Nakagawa *et al.*, 2005).

Since NPMc mutant A is the most frequent frame shift mutant (77%) reported among the six NPMc variants (Falini NEJM 2005), it was chosen for further investigations here. The NPMc cDNA was constructed using a three-step PCR with wild type human NPM1 as the initiate template, and subsequently cloned into pcDNA3.1-GFP for over-expression in the HeLa cells. Expectedly, GFP-tagged NPMc was localised almost exclusively in the cytoplasm in slightly more than 90% of the transfected HeLa cells (Figure 5.2 B). This is in stark contrast to the

exclusively nuclear localisation of the GFP-tagged wild type NPM in majority of the transfected HeLa cells (93.1%).

To investigate if the presence of the 'unintended' NES at the C-terminal of NPMc is solely responsible for the overwhelming cytoplasmic localisation of the mutant protein, an NPMc mutant was created. In this mutant, the two lysines and valines present in the C-terminal portion of NPMc were mutated to other amino acids, as shown in Figure 5.2a, so as to abolish the putative NES completely. The NPMc mutant was likewise constructed using a three-step PCR, and over-expression of the GFP-tagged protein showed almost exclusive nuclear localisation in 95.8% of the transfected HeLa cells (Figure 5.2 B), thereby indicating that the C-terminal NPMc NES is indeed a significant factor underlying cytoplasmic NPM export and the pathogenesis of AML. This is corroborated by our observation that treatment of the NPMc transfected HeLa cells with the nuclear export receptor Crm1 inhibitor, Leptomycin B, likewise resulted in a reversion in the localisation of NPMc from the cytoplasm back into the nucleus for 96.3% of the transfected cells (Figure 5.2 B). Notably, both mutation of the NPMc C-terminal NES or treatment with Leptomycin B did not resume the nucleolar localisation of the protein, which was prominently observed in the wild type NPM trasfected cells. Tryptophans 288 and 290 in the C-terminal region of wild type human NPM were previously demonstrated to be important for its nucleolar localisation (Nishimura *et al.*, 2002). The frame-shift mutation in AML, which occurred just before amino acid 288, removed the two C-terminal tryptophan and replaced it with the leukaemic associated NES. As such, the absence of the two tryptophans in the NPMc mutant is most likely the underlying cause behind the failure to resume NPM's nucleolar localisation with inactivation of the mutant-associated NES.

### *5.3.2 NPMc has anti-apoptotic activities as observed for wild type NPM and NPMc mutant*

Unlike wild type NPM, NPMc was previously shown to lack a proliferating promoting function due to its inability to rescue proliferation in the Atm-null mouse embryonic fibroblasts (den Besten *et al.*, 2005). While promotion of proliferation remains a major tumorigenic factor, cell death resistance has increasingly been implicated in several cancer types like the human follicular B-cell lymphoma, in which the t(14; 18) chromosomal translocation of human follicular B-cell lymphoma juxtaposes the bcl-2 gene with the immunoglobulin heavy chain locus (Hockenbery *et al.*, 1990). The bcl-2 immunoglobulin fusion gene is markedly deregulated resulting in inappropriately elevated levels of bcl-2 RNA and protein, which in turn leads to blockage of cell death and causes tumorigenesis. With this example in mind, we proceeded to check if NPMc manifest any significant anti-apoptotic activity that may underlie leukaemogenesis.

We have shown in Chapter III and IV that NPM specifically inhibited the activities of caspase-6 and -8, and interacts with them physically. Auto-proteolysis usually occurs when the procaspases is overexpressed in the cells, presumably as a result of proximity-induced proteolysis. Marked increases in cell death, tabulated as percentage of transfected cells with condensed nuclei when stained with Hoechst 33342, were noted here when HeLa cells were co-transfected with GFP and either human caspase-6 or -8 (23.1% and 24.7% respectively, as compared to 7.45% for GFP alone transfection, Figure 5.3). Expectedly, co-transfection of either caspases with GFP-tagged wild type NPM rescued the cells from caspase-induced death almost completely (9.4% for caspase-6 transfection and 7.4% for caspase-8 transfection, as compared to 7.8% for wild type NPM alone transfection). The same phenomenon was observed with GFP-

tagged NPMc mutant co-transfection, with full cell death rescue observed for caspase-6 and -8 transfection (6.6% for caspase-6 transfection and 6.3% for caspase-8 transfection, as compared to 6.8% for wild type NPM transfection alone). Co-transfection with GFP-tagged NPMc significantly rescued caspase-induced cell death as well, though the decrease in cell death for caspase-6 co-transfection was not as marked as that for caspase-8 co-transfection (12.7% for caspase-6 transfection and 10.6% for caspase-8 transfection, as compared to 8.4% for wild type NPM transfection alone). All in all, the data here indicate that NPMc possesses anti-apoptotic activities just like its wild type counterpart and its NES mutant, despite differences in the subcellular localisation of their respective NPM proteins.

### *5.3.3 Cytoplasmic abundance of NPMc led to marked inhibition of the progression of cytochrome c-induced caspase activation cascade*

It was demonstrated in Section 3.3.3 in Chapter III that addition of recombinant NPM could inhibit cytochrome *c* induced activation of caspase-3, -6, -7, and -8. Since NPMc is prominently localised and concentrated in the cytoplasm (as observed in Figure 5.2 B), we speculate that the dramatic elevation in cytoplasmic NPM level may lead to inhibition of caspase activation cascade. To test this hypothesis, HeLa cells were transfected with same amount (20 μg plasmid per 10cm diameter culture dish) of the various plasmids for overexpression of GFP alone, GFP-NPM, GFP-wild type NPMc and GFP-NPMc mutant. An extra plate of HeLa cells was transfected with GFP-NPMc-overexpressing plasmid and treated with 40 nM Leptomycin B two hours prior to harvesting of the cells. 24 hours after transfection, the cells were first observed for GFP overexpression under the microscope before harvesting, and the S100 cytoplasmic fractions obtained as described in Section 5.2.4. Caspase activation was next induced in each

fraction with the addition of cytochrome *c*. Subsequent immunoblot analysis demonstrated an expected greater abundance of GFP-tagged NPMc in the cytoplasmic fraction when compared to the other samples (Figure 5.4). Reduced cleaving of procaspase-3, -6 and -7 was observed to coincide with cytoplasmic accumulation of NPMc, indicating that cytoplasmic dislocated NPMc mutant might halt cell death in the myelogenous cells through inhibition of the caspase activation cascade, thus leading to leukaemogenesis.

### *5.3.4 OCI/AML3 cell line manifested exclusive cytoplasmic NPM localisation*

Human cell lines derived from AML patients bearing recurrent chromosomal abnormalities and/or gene mutation represent remarkable tools for biological and molecular studies of these diseases (MacLeod & Drexler, 2005). Quentmeier *et al.* (2005) reported that the OCI/AML3 cell line bears the characteristic molecular and biological features of the NPMc positive AML. The OCI/AML3 cell line was the only human myeloid cell line, among 79 tested by the group, to harbour mutation at exon-12 of the *NPM1* gene. The cell line was established from the peripheral blood taken from a 57-year-old male patient with AML subtype M4 (Wang *et al.*, 1989). In contrast, the OCI/AML2 cell line, also established from an aged patient with AML subtype M4 (Wang *et al.*, 1989), revealed no cytoplasmic NPM dislocation and mutation at exon 12 of the gene. These two cell lines were thus acquired and used as contrasting cell models to study the effect of differential subcellular localisation of NPM on TRAIL-induced cell death and caspase-8's activity.

Immunoblot analysis of the nuclear and cytoplasmic fractions was first performed to confirm the predominant subcellular localisation of their respective NPM variants before

conducting further investigations. As shown in Figure 5.5, OCI/AML2 manifested a typical nuclear localisation of the NPM, while OCI/AML3 displayed an expected cytoplasmic localisation of NPMc as reported by Quentmeier *et al.* (2005). Cytoplasmic fractions were shown to be free from nuclear contamination, as no nuclear protein oct-1 was detected. Notably, the commassie blue-stained protein gel not only showed equal protein loading, but also revealed very similar protein banding patterns for the cytoplasmic and nuclear fractions of both cell lines. Despite being isolated from different patients, the two cell lines are probably physiologically very similar to each other, and would thus serve as a good pair of contrasting cell models for our investigations here.

### *5.3.5 Caspase-8 and -3 activation was significantly halted in TRAIL-treated OCI/AML3*

TNF-related apoptosis-inducing ligand (TRAIL), a member of the TNF family, is being developed as an antitumor agent as it induces apoptosis in a wide range of tumor cell lines but not in most normal cells (Walczak *et al.*, 1999). TRAIL induces apoptosis by binding to two membrane-bound receptors, TRAIL-R1 (DR4) and TRAIL-R2 (DR5), resulting in the recruitment of the adaptor molecule FADD, followed by the recruitment and activation of caspase-8, into DISC (Bodmer *et al.*, 2000; Kischkel *et al.*, 2000; Sprick *et al.*, 2000). Active caspase-8, the apical caspase in death receptor-induced apoptosis, can then activate other caspases, such as caspase-3, which in turn cleave many cellular substrates resulting in the biochemical and morphological features characteristic of apoptosis (Bratton *et al.*, 2000).

In our investigation, total cell lysates were harvested from TRAIL-treated OCI/AML2 and OCI/AML3 cell lines and the activation status of both caspase-3 and -8 investigated using

immunoblotting. As shown in Figure 5.6, marked decrease in the procaspases amount for caspase-3 and -8 was observed for OCI/AML2, but not OCI/AML3, with TRAIL treatment, indicating that the TRAIL death receptor response might be significantly attenuated in OCI/AML3 cells. Meanwhile, by determining the proportion of TRAIL-exposed cells with condensed nuclei, we expectedly observed considerably lower amount of cell death in OCI/AML3 than in OCI/AML2 cell line for all three time points sampled (Figure 5.7). Taken together, the data suggest that attenuation in cell death in TRAIL-exposed OCI/AML3 may be attributed to impairment in caspase activation. To further determine if the cytoplasmic NPMc is involved in this phenomenon, the cytoplasmic fractions were isolated from the two cell lines and the same amount of recombinant caspase-8 (10 units) was added to each fraction to determine their respective efficiencies in procaspase-3 processing. As shown in Figure 5.8, caspase-3 activation by caspase-8 was markedly halted in OCI/AML3 extract (lane 2, when compared to OCI/AML2 in lane 1), and this coincided with a higher amount of cytoplasmic NPM. On the other hand, immunodepletion of the cytoplasmic NPM from the OCI/AML3 extract enabled resumption of procaspases-3 processing by recombinant caspase-8. This is observed in Figure 5.8 (lane 3 and 4) as a decrease in procaspases-3 amount and increase in cleaved caspase-3 fragment with increasing depletion of cytoplasmic NPM. All in all, the results suggest that the rather subdued TRAIL-induced death receptor signalling in OCI/AML3 is likely to be attributed to inhibition of caspase-8's cleaving activities by the greater amount of cytoplasmic NPMc.

**(A)**

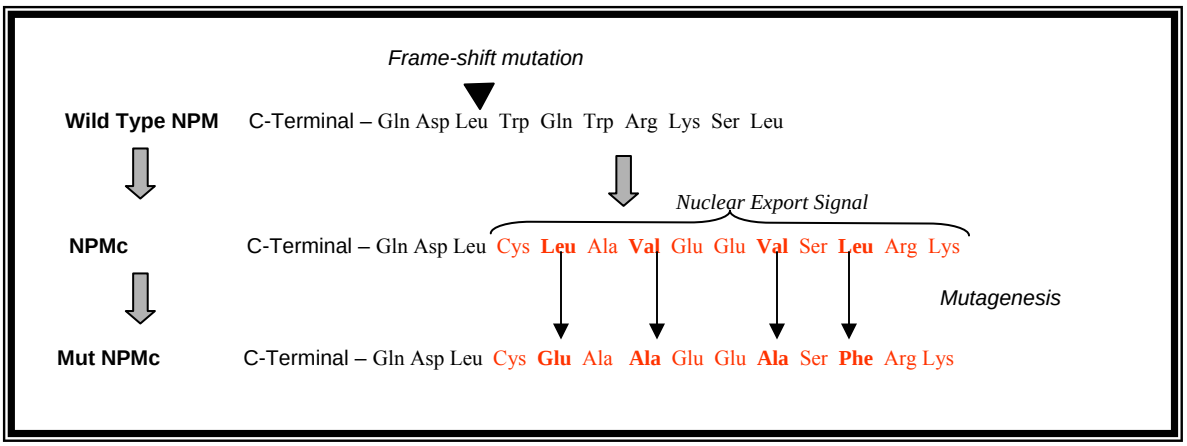


**(B)**

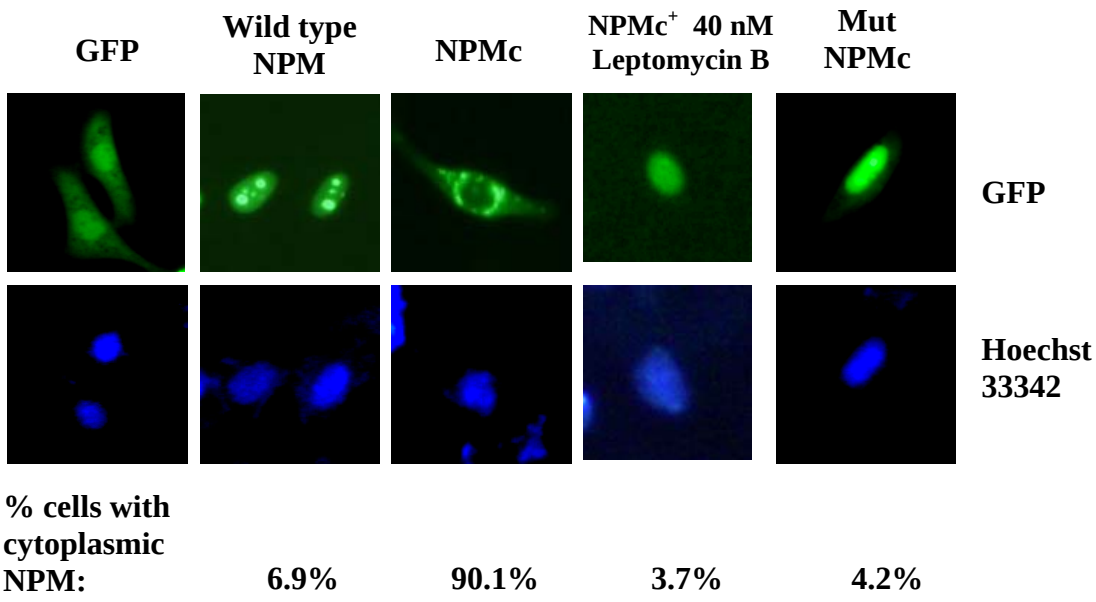


**Figure 5.2. Frame-shift mutation in the C-terminal end of NPM creates a Nuclear Export Signal (NES) that is responsible for cytoplasmic dislocation of the NPMc mutant.** (A) Schematic showing the extreme C-terminal amino acid sequences for wild type NPM and its two mutants. A frame-shift mutation results in replacement of the last seven amino acids by an entirely different 10 residues containing a leucine-valine NES motif in the NPMc mutant. The NES was abolished in a "Mut NPMc" mutant, in which the leucine and valines were replaced with other amino acids using mutagenesis. (B) HeLa cells were transfected with plasmid overexpressing GFP alone, GFP-tagged wild-type NPM, GFP-tagged NPMc or GFP-tagged Mut NPMc for 24 hours. Cells transfected with GFP-tagged NPMc were either treated with 2.5 ng/mL of Leptomycin B for two hours, or left untreated before harvesting. The cells were then stained with Hoechst-33342 for 15 min at room temperature and observed by fluorescence microscopy using a Zeiss Axiophot.

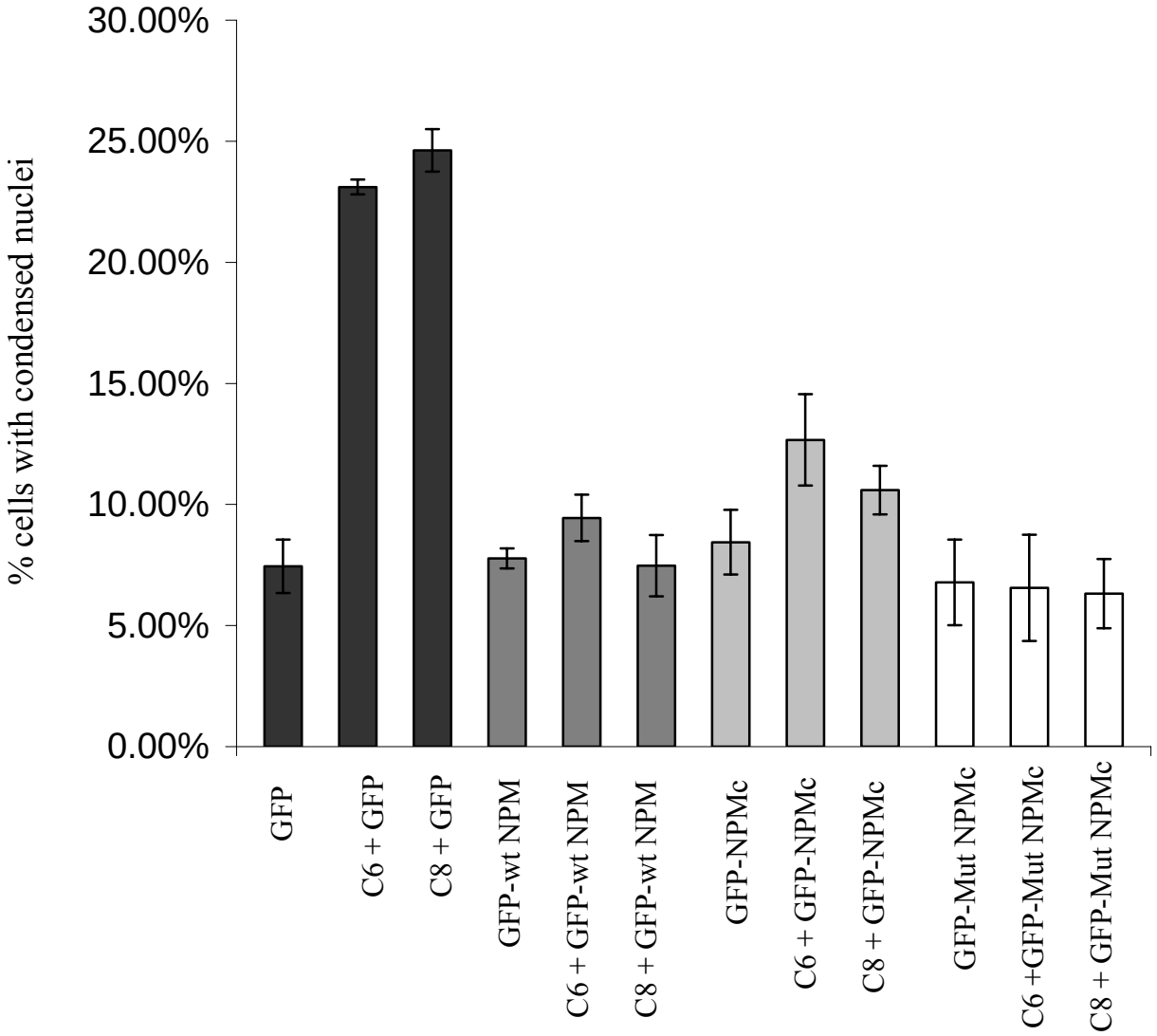


**Figure 5.3. NPMc mutant rescues HeLa cells from caspase-6 or caspase-8 mediated cell death.** HeLa cells were transfected with plasmid overexpressing GFP alone, GFP-tagged wild-type NPM, GFP-tagged NPMc or GFP-tagged Mut NPMc. In each case, the cells were co-transfected with another plasmid overexpressing human caspase-6 or -8, or an empty vector. 24 hours after transfection, the cells were stained with Hoechst-33342 for 15 min at room temperature and observed by fluorescence microscopy using a Zeiss Axiophot (Germany). Apoptosis was characterised by scoring condensed and fragmented highly fluorescent nuclei. Each set of experiments was repeated at least three times, with at least 300 cells counted in each instance.

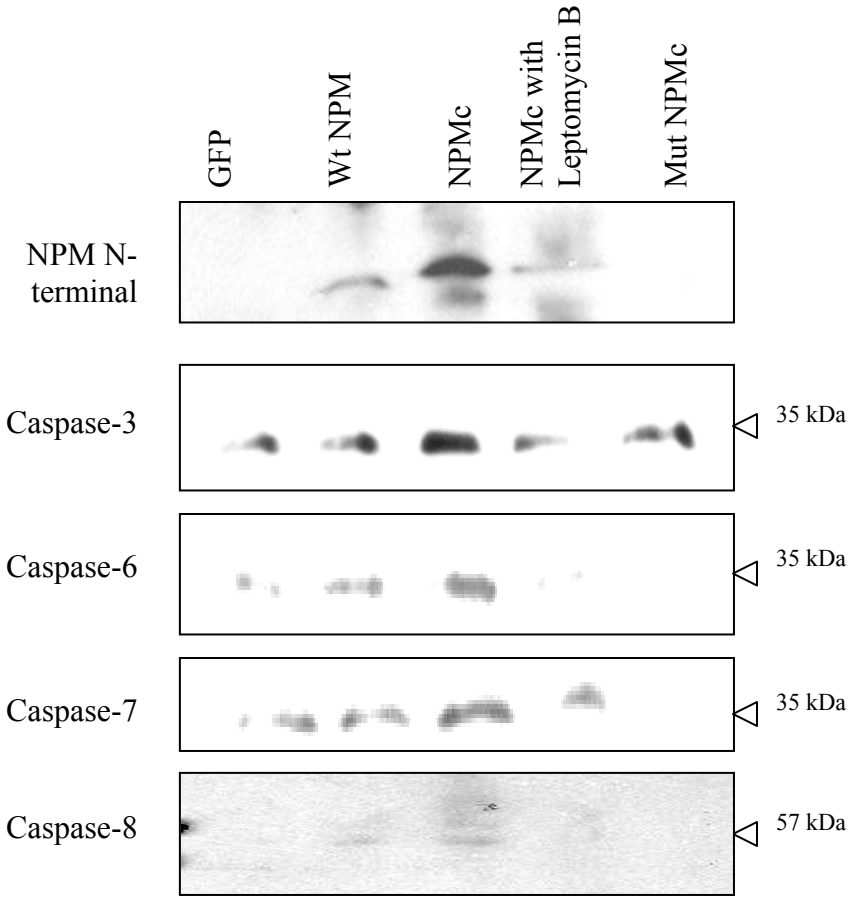


**Figure 5.4. Cytoplasmic abundance of NPMc led to marked inhibition of the progression of cytochrome c-induced caspase activation cascade.** HeLa cells were transfected with plasmid overexpressing GFP alone, GFP-tagged wild-type NPM, GFP-tagged NPMc or GFP-tagged Mut NPMc for 24 hours. Cells transfected with GFP-tagged NPMc were either treated with 2.5 ng/mL of Leptomycin B for two hours, or left untreated before harvesting. The harvested cells were subjected to subcellular fractionation, as described in Materials and Methods, Section 2.2.5, to obtain the cytoplasmic fraction. The cytoplasmic extracts were next subjected to SDS-PAGE and immunoblot analysis using anti-NPM (N-terminal), anti-caspase-3, anti-caspase-6, anti-caspase-7, or anti-caspase-8 antibody, as indicated to the left of each panel. 20 μg of the total cellular extract and cytoplasmic extract extract (40 μg for caspase-8 immunoblotting) were electrophoresed. White triangle indicates procaspases.

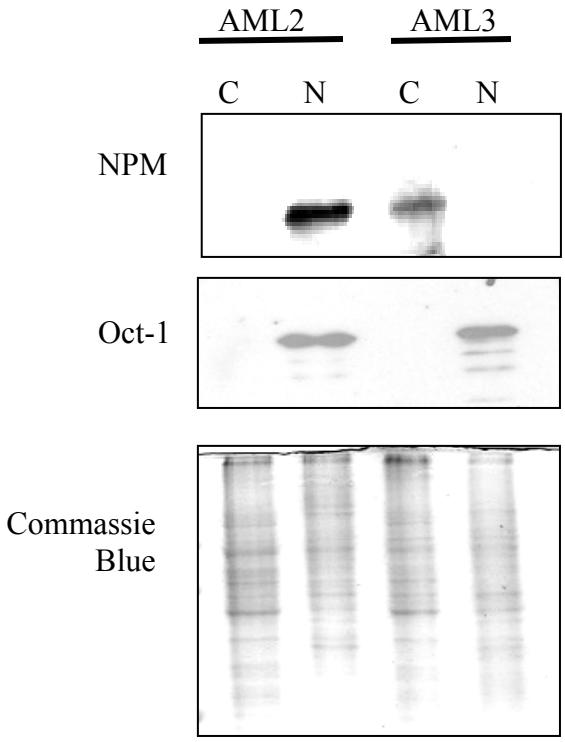


**Figure 5.5. OCI/AML3 cell line manifests exclusive cytoplasmic NPM localisation, while OCI/AML2 shows predominantly nuclear NPM localisation.** Untreated OCI/AML2 or OCI/AML3 cells were subjected to subcellular fractionation, as described in Materials and Methods, Section 2.2.. The cytoplasmic and nuclear extracts were next subjected to SDS-PAGE and immunoblot analysis using anti-NPM (N-terminal) or anti-oct-1 antibody, as indicated to the left of each panel. 20 μg of the cytoplasmic extracts and 10 μg of the nuclear extracts were electrophoresed to monitor subcellular localisation of NPM in the two cell lines. Alternatively, after SDS-PAGE, the gel was stained with Commassie blue protein stain to visualize the one-dimensional protein gel profile, which is used as an equal loading control. C: cytoplasmic fraction, N: nuclear fraction.

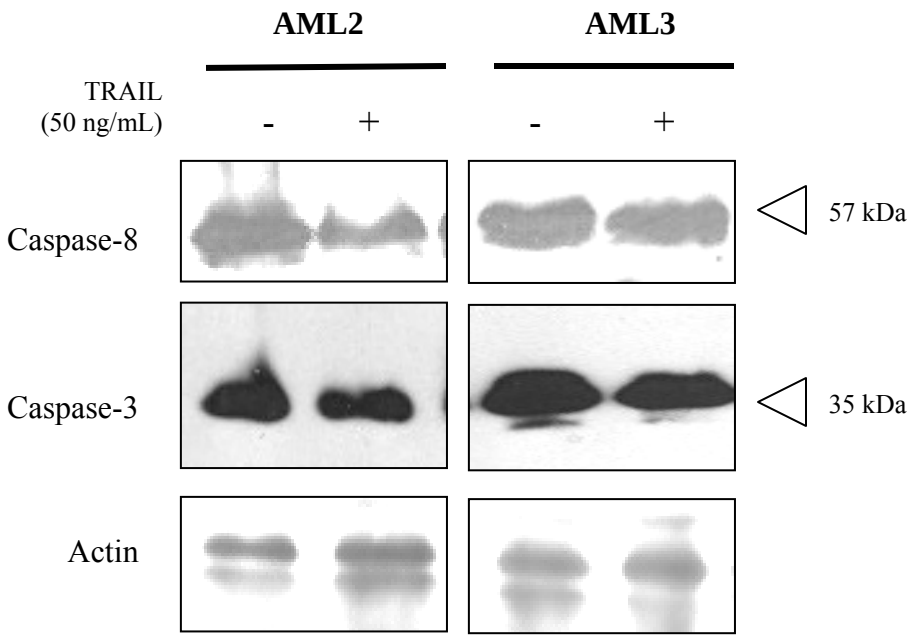


**Figure 5.6. Activation of caspase-8 and -3 are attenuated in TRAIL-treated OCI/AML3 cells, but not OCI/AML2 cells.** OCI/AML2 or OCI/AML3 cells were either treated with 50 ng/mL of TRAIL or left untreated for 12 hours at 37°C. The cells were then harvgested and the total cell lysates extracted as described in Materials and Methods, Section 2.2.4. The protein extracts were next subjected to SDS-PAGE and immunoblot analysis using anti-caspase-8, anti-caspase-3 or anti-actin antibody, as indicated to the left of each panel. 20 μg of the extracts (40 μg for caspase-8 immunoblotting) were electrophoresed to monitor activation status of the two caspases in the two cell lines with TRAIL stimulation. White triangle indicates procaspases.

**(A)**

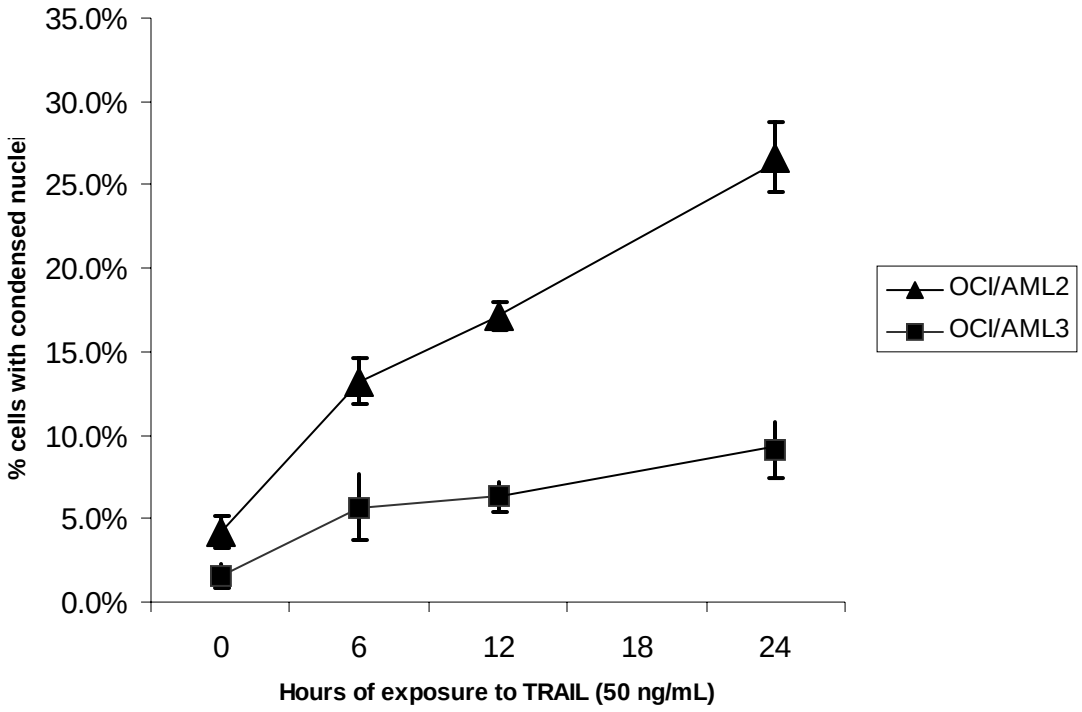


**(B)**

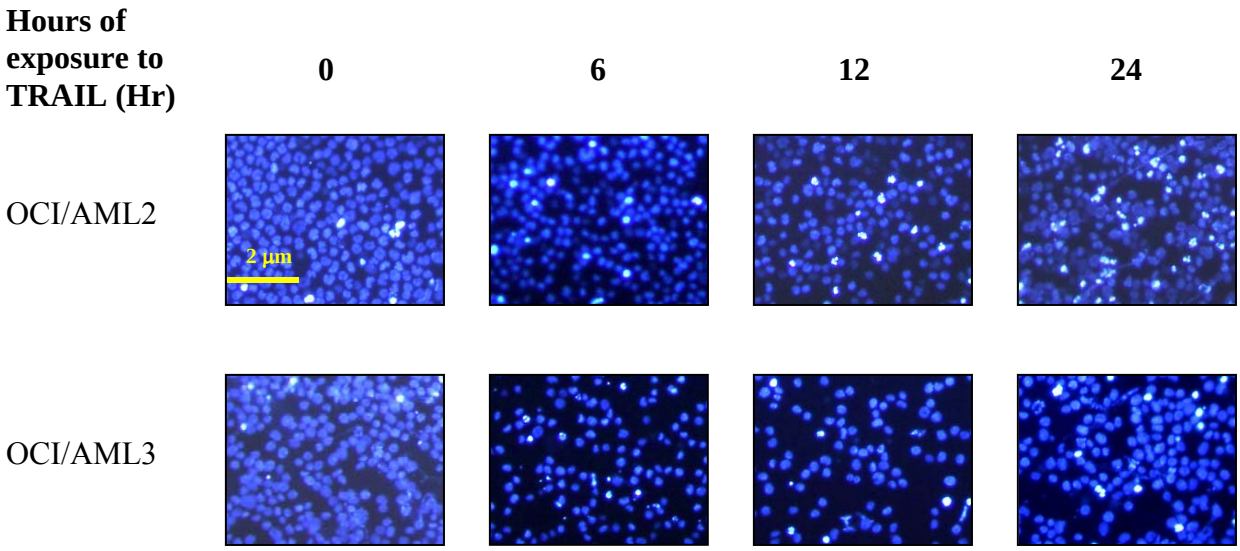


**Figure 5.7. Cell death is attenuated in OCI/AML3, but not OCI/AML2 cells with TRAIL treatment.** OCI/AML2 or OCI/AML3 cells were treated with 50 ng/mL of TRAIL for up to 12 hours at 37°C. The cells were harvested at indicated times and stained with Hoechst-33342 for 15 min at room temperature and observed by fluorescence microscopy using a Zeiss Axiophot (Germany). Apoptosis was characterised by scoring condensed and fragmented highly fluorescent nuclei (B). Each set of experiments was repeated at least three times, with at least 300 cells counted in each instance. The average readings obtained for the two cell lines were then plotted against time as shown in (A).

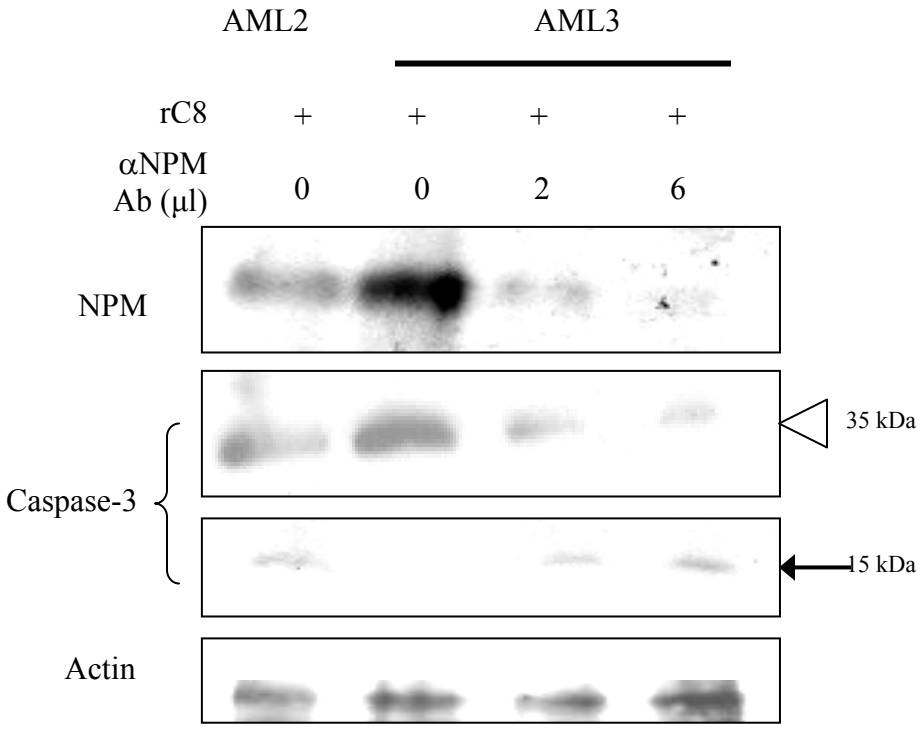


**Figure 5.8. Cytoplasmic abundance of NPMc in OCI/AML3 cell line inhibits cleaving of endogenous procaspase-3 by recombinant active caspase-8.** Cytoplasmic fractions were prepared from OCI/AML2 or OCI/AML3 cells as described in 2.2.5, and normalised to the same protein concentration before use. Portions of the extract from OCI/AML3 cells were further subjected to immunodepletion as described in Materials and Methods, Section 3.2.9, using the indicated amount of anti-NPM (N-terminal) antibody. The immunodepleted extracts were then incubated with 32 units of recombinant active caspase-8 for three hours at 37°C, after which they were subjected to SDS-PAGE and immunoblot analysis using anti-NPM (N-terminal), anti-caspase-3 or anti-actin antibody, as indicated to the left of each panel. 20 μg of the extracts were electrophoresed to monitor activation status of caspase-3 with addition of recombinant caspase-8 in the two extracts. White triangle indicates procaspases, and black arrow indicates cleaved caspase.

## 5.4 Discussion

Arf inhibits cell proliferation through both p53-dependent and -independent mechanisms (Sherr, 2001). Since NPM physically interacts with Arf and protects it from degradation (Korgaonkar *et al.*, 2005), the inhibitory effect of NPM on cellular proliferation is thought to be mediated by Arf itself. With the discovery of the cytoplasmic dislocated NPMc mutant in AML patients, Arf became an immediate 'prime suspect' in the pathogenesis of AML, especially given its role as a tumour suppressor and its physical association with NPM. Dysregulation of Arf expression has previously been implicated in the pathogenesis of another AML subtype. Transcriptional repression of p14(ARF) by the t(8;21) chromosomal translocated fusion protein AML1 ETO is shown to predispose haematopoietic stem cells or progenitor cells to oncogenic transformation (Linggi *et al.*, 2002). The cessation of Arf-associated role in cell cycle arrest is thus shown to underlie oncogenesis in this case, and this easily led to the notion that the disruption of Arf-mediated function may drive leukaemogenesis in $NPMc^+$ AML as well. However, studies undertaken by den Beston *et al.* (2005) demonstrated a loss of proliferation-promoting effect with cytoplasmic dislocation of the mutant NPM, leading to the authors to conclude that destabilisation of Arf with NPM mutation may not be the *de facto* cause behind the pathogenesis of $NPMc^+$ AML.

We have seen in Chapter II that NPM undergoes immediate translocation into the cytoplasm under stressful conditions, and hypothesized, based on results gathered so far, that elevated cytoplasmic NPM level may serve to inhibit caspase-8 and -6's activation. Stress-induced cytoplasmic NPM translocation appears transient, as its level decreased subsequently with prolonged stress (see Section 2.3.2), presumably to lower the death signal threshold again

for apoptosis to commence. Cytoplasmic NPM hence serves as a removable 'road block' to temporarily prevent apoptotic signalling flow, until the cell is committed to death. It thus follows that when the 'road block' becomes permanently lodged in the cytoplasm, as in the case of $NPMc^+$ AML, initiation and progression of apoptotic signalling involving caspase-8 and -6 becomes indefinitely halted as well. Cell death resistance via inhibition of caspase-8 and -6 by excessive cytoplasmic NPM mutant hence represent a plausible explanation behind leukaemogenesis in $NPMc^+$ AML. Apart from data gathered from the previous chapters, two lines of evidences, as presented in this chapter, further support our claim. Firstly, using protein extracts from HeLa cells overexpressing the different NPM variants, we demonstrated that cytochrome *c* induce caspase-3, -6, -7 and -8 activations were halted to a greater extent in the NPMc containing extract, and this coincided with its greater cytoplasmic abundance of this protein as compared to the other NPM variants (Figure 5.4). This is in agreement with our observations in Figure 5.3 that NPMc retained its anti-apoptotic function despite the change in its predominant subcellular localisation, and suggests caspase inhibition as the mechanism underlying its ability to counteract caspase-6 and -8 induced cell death. Secondly, using a pair of AML-relevant cell models, we observed difference in their TRAIL-induced death responses, and correlated it to the difference in their NPM subcellular localisation. OCI/AML3 cell line, which manifested predominantly cytoplasmic NPM localisation, was markedly more resistant to TRAIL induced cell death as compared to OCI/AML2 cell line with mainly nuclear-bound NPM (Figure 5.5 and 5.7). Dissection of the caspase activation pathway in the two cell lines revealed that caspase-8 and its substrate caspase-3 were more readily cleaved in OCI/AML2 than OCI/AML3 with TRAIL treatment (Figure 5.6). As the immediate effect of TRAIL stimulation is the recruitment and activation of procaspase-8 by DISC at the DR4/5 death receptors, our

results here indicate that inhibition of caspase-8 by the abundant cytoplasmic NPMc may underlie the attenuation of TRAIL-induced cell death in OCI/AML3 cell line. A direct relationship between NPM and caspase in AML was further demonstrated by our *in vitro* experiment, in which depletion of the cytoplasmic NPM from the OCI/AML3-derived protein extract led to an instant resumption of caspase-3 cleavage by added recombinant caspase-8 (Figure 5.8). Overall, our results indicate that excessive caspase inhibition by the unusually high amount of cytoplasmic NPM may trigger tenacious cell death resistance, which in turn leads to life span extension of primary myeloid progenitor cells and/or stem cells, and ultimately, AML.

Caspase-8 is an integral component of the death receptor pathway, and is often described as the most apical caspase being activated in the apoptotic signalling cascade (Kruidering & Evan, 2000). Apart from being involved in the TRAIL receptor pathway, caspase-8 also relays apoptotic signal in the Fas/Fas ligand system of apoptosis, which plays a central role in the regulation of homeostasis by elimination of self-reactive lymphocytes during ontogeny, and activated lymphocytes following an immune response (Nagata, 1997). Caspase-8 mutation in human not only results in defective lymphocyte apoptosis and homeostasis , but also defective activation of T lymphocytes, B lymphocytes and natural killer cells, which leads to immunodeficiency (Chun *et al.*, 2002). In this case, caspase-8 deficiency has shown that caspase-8 has a broad role in the activation of T, B and NK cells, in addition to its function in conveying signals from death receptors to apoptosis effector mechanisms (Alam *et al.*, 1999; Kennedy *et al.*, 1999). This thus implicates caspase-8 in non-apoptotic roles as well, and that mutation or inhibition of their activation should result in pleiotropic physiological effects, rather than just cell death inhibition alone. It was also previously noted that activation of the caspase-8 not only mediates TRAIL cytotoxicity, but also promotes monocytic maturation of HL-60 cells. Sechierro

*et al.* (2002) demonstrated that z-IETD-fmk, a selective caspase 8 inhibitor, significantly reduced the cytotoxic activity of TRAIL and was as efficient as z-VAD-fmk in blocking the TRAIL-induced maturation along the monocytic pathway. On the other hand, z-LEHD-fmk, a selective caspase -9 inhibitor, was unable to significantly prevent TRAIL-mediated cytotoxicity and maturative effect. Extrapolating this observation to our own findings here, we can further hypothesize that excessive inhibition of caspase-8 by cytoplasmic NPMc not only inhibited death receptor signalling, but also halted caspase-8-mediated myeloid differentiation. Differentiation blocks are thought to contribute to tumorigenesis, along with mutations that affect cellular proliferation, inactivate cell-cycle checkpoints, and block apoptosis (Hiebert, 2001). In this context, it was previously reported that mutation of the transcription factor C/EBP alpha, which is required for neutrophil differentiation (Zhang *et al.*, 1997), is found in patients with M2 AML, a myeloblastic leukaemia characterised by an early block in neutrophil differentiation (Pabst *et al.*, 2001). As such, inhibition of myeloid differentiation and cell death, both resulting from caspase-8's inhibition by cytoplasmic NPMc, may have synergistic leukaemogenic effect on the immature myeloid blast cells, resulting in their specific immortalisation in AML. While the effect of NPMc expression on myeloid differentiation is not examined in this dissertation, we noted from the supplier's website that the NPMc$^-$ OCI/AML2 cell line appears to express the myeloid differentiation marker CD14 on their cell surface, in contrast to the NPMc$^+$ OCI/AML3 cell line which does not (www.dsmz.de). It thus seems that caspase-8 inhibition by the abundant cytoplasmic NPMc in OCI/AML3 cell line may underlie its inability to undergo differentiation to the same extent as, or further than, the OCI/AML2 cells.

The death receptor systems, which constitute major components of the finely tuned haematopoietic network, serve to eliminate superfluous cells once they have fulfilled their

respective functions. As such, mutation affecting the functioning of Fas, TRAIL or components of DISC may contribute to the development of autoimmunity and/or neoplastic diseases (Greil *et al.*, 2003). Heterozygous mutations in Fas, Fas ligand or caspase-10 were shown to underlie most cases of autoimmune lymphoproliferative syndrome (ALPS), a human disorder that is characterised by defective lymphocyte apoptosis, lymphadenopathy, splenomegaly and autoimmunity (Fisher *et al.*, 1995; Rieux-Laucat *et al.*, 1995; Drappa *et al.*, 1996; Bettinardi *et al.*, 1997; Alam *et al.*, 1999; Kennedy *et al.*, 1999). Meanwhile, mutations in the Fas antigen was shown to contribute to the pathogenesis of multiple myeloma (Landowski *et al.*, 1997) and non-Hodgkin's lymphomas (Grønbæk *et al.*, 1998). Loss of function of the Fas antigen due to mutation is thought to contribute to the pathogenesis and progression of neoplasias by allowing susceptible cells to evade immune surveillance. The prolonged survival would then allow the cell to accumulate mutations leading to malignancy (Nagata, 1997). As caspase-8 is involved in the proximal events downstream of death receptor signalling, disruption of caspase-8's function can potentially lead to oncogenesis as well. For instance, in hepatocellular carcinomas, caspase-8 gene is frequently inactivated by the frameshift somatic mutation with two base-pair deletion (1225_1226delTG), resulting in a premature termination of amino-acid synthesis in the p10 protease subunit (Soung *et al.*, 2005). Also, silencing of caspase-8 expression through methylation and inactivation of its promoter is implicated in the pathogenesis of aggressive childhood neuroblastoma (Teitz *et al.*, 2001) and small cell lung carcinoma (Shivapurkar *et al.*, 2002). Based on results obtained so far, we likewise implicate functional disruption of caspase-8 in the oncogenesis of AML. While tumorigenesis involving caspase-8 inactivation is not without precedence, the mode of caspase-8 inactivation in $NPMc^+$ AML appears to be unique, involving

excessive inhibition of caspase-8's activity by a mutant regulator rather than *caspase-8* mutation or transcriptional defects.

One question that looms large at this juncture concerns the specificity of the tissue/cell type involved in neoplastic transformation with NPM's mutation. Since cytoplasmic NPMc has the potential to inhibit apoptotic signalling involving caspase-8 and -6 in any tissues and cell types throughout the body, why then is the haematopoietic myeloid cells so particularly vulnerable to the oncogenic effect of the mutation? Clues to answering this question may be gleaned from several transgenic animal studies. In the *Npm1*$^{-/-}$ mutants mice, developmental abnormalities were specifically observed in the anterior brain and haematopoietic system. For the latter in particular, the number of haematopoietic precursors in the blood islands of the *Npm1*$^{-/-}$ yolk sacs was greatly reduced, and their ability to differentiate into various lineages was profoundly impaired. *Npm1*$^{-/-}$ embryos showed a noticeable degree of apoptosis, as revealed by staining for activated caspase-3 (Grisendi *et al.*, 2005). These indicate that NPM may have a specific role in the regulation of apoptosis in both the forebrain and haematopoietic system, among many other tissues in the body. It thus follows that disruption of NPM's apoptosis-regulatory function should affect these two tissues the most. Meanwhile, observations from other transgenic mice models further demonstrated specific vulnerability of myeloid precursors cells, among the various haematopoietic lineages, to impairment in death receptor signalling. For example, Fas-inactivating mutation in mice resulted in accumulation of myeloid colony-forming cells in the bone marrow, while the number of granulocytes and macrophages remained constant when compared to the *Fas*$^{+/+}$ mice (Traver *et al.*, 1998). Also, low-level expression of the caspase-8 inhibitor CrmA in mice provided some protection against Fas ligand–induced apoptosis and promoted accumulation of myeloid cells in the bone marrow (Pellegrini *et al.*,

2005). Taken together, these observations indicate the importance of NPM-mediated apoptotic regulation in the homeostasis of the haematopoietic system and in particular, the myeloid cells. This, coupled to the above-mentioned observation that caspase-8 mediates myeloid differentiation, may explain the specific susceptibility of the myeloid precursors to neoplastic transformation in $NPMc^+$ AML patients.

In conclusion, our data strongly implicate impairment in caspase-8 mediated-death receptor signalling, caused by cytoplasmic mutant NPM, in the pathogenesis of $NPMc^+$ AML. This in turn indicates the importance of the death receptor pathway in homeostatic maintenance of the myeloid haematopoietic lineage. More importantly, it highlights the stringent need by the cells to maintain the right amount of apoptotic regulators at the right place and right time, violation of which can lead to dire consequences such as AML.

# Chapter VI. Conclusion and future works

## 6.1 "The accidental tourist": from PD to leukaemic therapeutics

The current investigation started off as a search for potential biomarkers and therapeutic candidates for PD using the proteomics approach. Several proteins were identified through this exercise and their possible involvements in the aetiology of PD were speculated. Among them, NPM stood out as the candidate for further studies due to its recently discovered interaction with the tumour suppressor p53, as well as its ability to inhibit apoptosis when overexpressed. As PD is characterised by the sudden and massive demise of the dopaminergic brain cells leading to impairment of voluntary motor control, NPM's anti-apoptotic potential lends credence to its candidacy for gene therapy or small-peptide drug delivery aiming at rescuing dopaminergic cells from premature death. However, before this aim can be fulfilled, an in-depth look into the mechanisms underlying cell death inhibition by NPM must be undertaken, in order to determine the specific inhibitory target(s) of NPM within the intricate death signalling network. This will in turn facilitate rationale small-peptide drug designing for PD therapeutics.

Though up-regulation in NPM protein level was observed on the 2DGE, we subsequently established that the apparent increase in NPM amount was due to stress-induced release of the nucleoli-bound NPM into the nucleoplasm and cytoplasm. Cytoplasmic translocation of NPM, presumably from the nucleoli and nucleoplasm, appeared to be an early stress response observed in several cell lines examined, and could be invoked merely with caspase-8 activation. *In vitro* and *in vivo* experiments strongly suggest an involvement of NPM in the negative regulation of the caspase-mediated death signalling progression. In particular, NPM was shown to specifically interact with and inhibit the activities of caspase-6 and –8, which are integral components of both the death receptor and mitochondrial death pathways.

Caspase-8 is often the apical caspase activated in the death receptor systems, which serves to eliminate excess unwanted haematopoietic cells through apoptosis (Greil Crit Rev Immunol 2003). It may also regulate the lymphocytic and myeloid differentiation process (Hyung Nature 2002; Siechierro *et al.* Blood 2002). Excessive inhibition of caspase-8 may thus hold oncogenic potential by preventing cell death and differentiation from taking place. This appears to be the case for the NPMc+ AML, characterised by a mutation in the C-terminal end of *NPM1* gene that leads to massive cytoplasmic dislocation of the protein. Excessive cytoplasmic NPM mutant sets an unusually high threshold for caspase-8's self-activation at the death receptors, and this may represent the primary cause underlying AML pathogenesis.

The discovery made herein opens up therapeutic opportunities to develop biology adapted treatment strategies for $NPMc^+$ AML, which accounts for about 35% of adult AML (Quentmeier Leukaemia 2005). Though PD and AML are two very different diseases affecting different organs, they appear to share a common underlying theme, one that revolves around deregulated cell death. In this case, the pathogenetic factor inhibiting apoptosis in AML (i.e. NPMc) may well be the therapeutic element required to stop unnecessary death of the post-mitotic dopaminergic neurons in PD. However, before such translation can be made, more effort is needed in characterizing NPM's pro-survival mechanisms, as well as in understanding how NPM can halt cell death without triggering oncogenesis in PD models.

## 6.2 Proposed hypothesis: cytoplasmic NPM translocation as a novel cytoprotective mechanism

The nucleolus has been proposed to be a major cellular stress sensor and transmits signals to the system for regulating cellular stress response (Rubbi & Miller EMBO 2003). Stress-induced release of the nucleolar components into the nucleoplasm is one such mechanism the organelle employs in regulating cellular p53 response. Nucleoli-bound ribosomal protein L11 and the tumour suppressor ARF both 'leaks' into the nucleoplasm in the event of stress-induced nucleolar disruption, and stabilizes p53 through binding of its antagonist MDM2 (Zhang *et al*, 2003; Llanos *et al.,* 2001). Heightened cellular p53 level in turn allows the cell to cope with stress by initiating cell cycle arrest, so as to allow repair to commence to remove any cellular or DNA lesions posing oncogenic threats. In addition to rapid p53 induction, the cell's intricate death signaling network may also become activated under mild provocation in response to stress. It is therefore essential that the death signaling be halted to allow cellular repair works to commence, and only be reactivated when cellular damages are beyond salvation. Here, our data substantiate one such cytoprotective mechanism that involves translocation of nucleolar components NPM into the cytoplasm for stress-associated anti-apoptotic functions.

NPM is a predominantly nucleolar-bound protein which is known to shuttle between the nucleus and cytoplasm (Borer Cell 1989). As depicted in Figure 6.1(a), low level of cytoplasmic NPM can bind aberrantly activated caspase-6 and -8 and prevent escalation of death signalling in the absence of stress or death stimulation. On the other hand, stress-associated slight activation of caspase-8 can induce Crm1-mediated translocation of NPM from the nucleolus into the cytoplasm to curb further self-activation of caspase-8. The cytoplasmic NPM also binds newly-

cleaved caspase-6 to prevent it from cleaving more procaspase-8 (Figure 6.1 b). Both NPM-bound active caspase-6 and -8 are also less capable of cleaving downstream substrates such as other procaspases, Bid (for caspase-8) and lamin A (for caspase-6). Heightened cytoplasmic NPM level thus set a higher-than-usual threshold for activation of caspase-6 and -8, and prevents the latter two from cleaving downstream targets for death signal relay. As such, active caspase-8–induced cytoplasmic NPM build-up provides negative feedback regulation of apoptotic signalling involving caspase-6 and -8. Meanwhile, nucleolar-disrupting agents such as heat shock can also lead to massive release into the nucleoplasm (Figure 6.1b). This may, in turn, provide a large pool of NPM readily available for Crm1-mediated translocation into the cytoplasm as well for caspase inhibition.

Increasing the cytoplasmic pool of NPM thus help to quench caspase-6 and -8 mediated death signalling under stressful conditions, and presumably allow the cell to cope with insults without launching apoptosis. However, how does the cell overcome such death inhibition when there is the need to die? It appears that a reduction in the initially heightened cytoplasmic NPM level may be necessary in allowing reactivation of caspase-8- and -6-mediated death signalling. Cleavage of NPM by the downstream executor caspase may be one such mechanism responsible for depressing the cytoplasmic NPM amount with prolonged stress. In this context, we noted that caspase-3, a direct downstream target of caspase-8, cleaves NPM directly (Chou Mol Pharmacology 2001). We likewise demonstrated that active caspase-6 cleaves recombinant NPM as well (data not shown). An escalation in the level of active caspase-3 and -6 due to, say irreparable cell-wide oxidative damage, may thus participate in a negative feedback loop that serves to undermine the caspase-inhibitory ability of cytoplasmic NPM for apoptotic signalling to commence.

Maintaining the right amount of cytoplasmic NPM at the right time during the stress response is hence crucial in holding apoptotic signalling in check until necessary. Meanwhile, when NPM becomes aberrantly lodged in the cytoplasm, as in the case of the $NPMc^+$ AML, the threshold for caspase-8's activation by DISC becomes permanently raised (Figure 6.1 c). As activated caspase-8 in myeloid cells not only mediate death signalling but also regulates the myeloid differentiation process, curbing of caspase-8 activation by the unusually high cytoplasmic NPM level may constitute the primary cause underlying immortalisation of the myelogenous blast cells in AML. The discovery of the association between cytoplasmic NPM mutant and leukaemia reiterates the importance of nucleoli-released, cytoplasmic-accumulated NPM in the regulation of the caspase-8-mediated death signalling network, and clearly supports our hypothesis proposing such translocation as a cytoprotective strategy to cope with cellular stress.

**(a)**

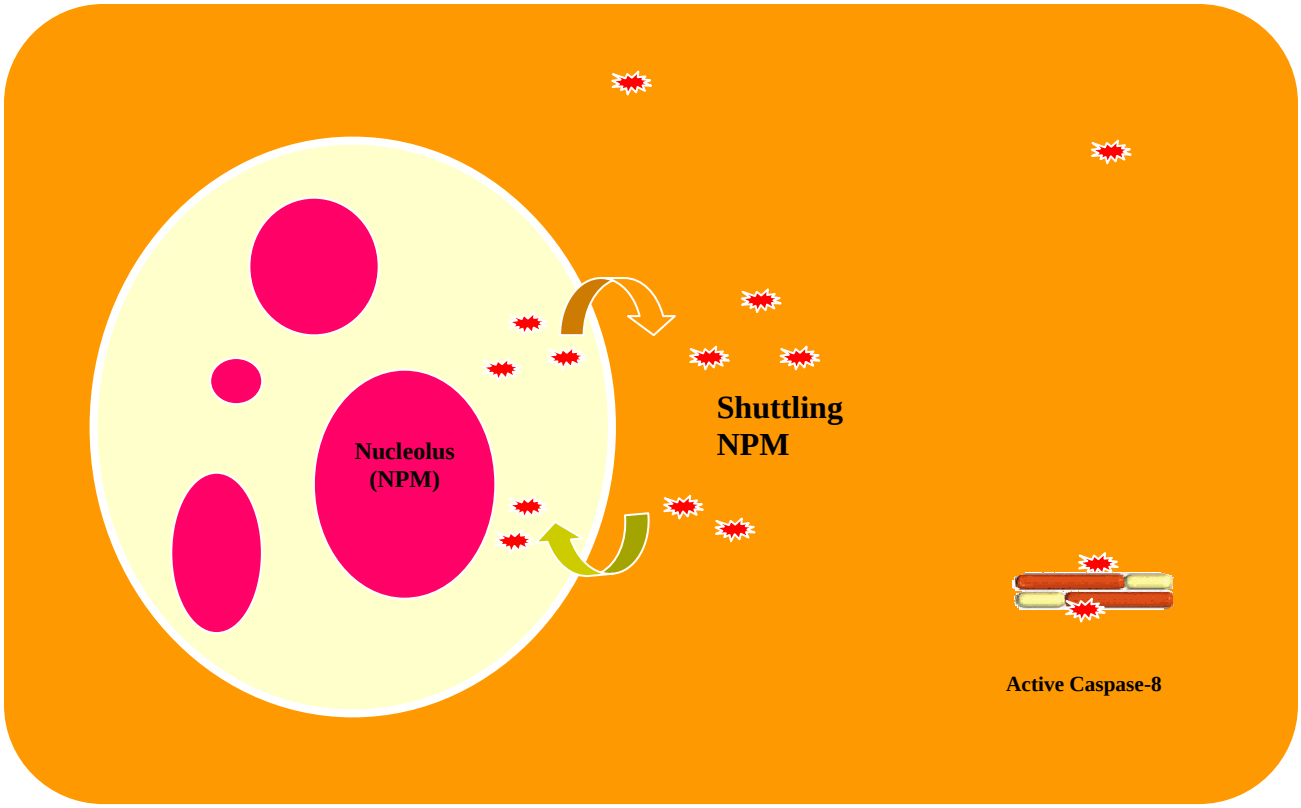


**Figure 6.1. Cytoplasmic NPM inhibits caspase-6 and -8 mediated death signalling**. (a) In an unstressed cell, basal level of cytoplasmic NPM is maintained by constant nucleo-cytoplasmic shuttling of NPM without disruption of the nucleoli. Low level of NPM in the cytoplasm helps to curb aberrant caspase-6 and -8 activation.

**(b)**

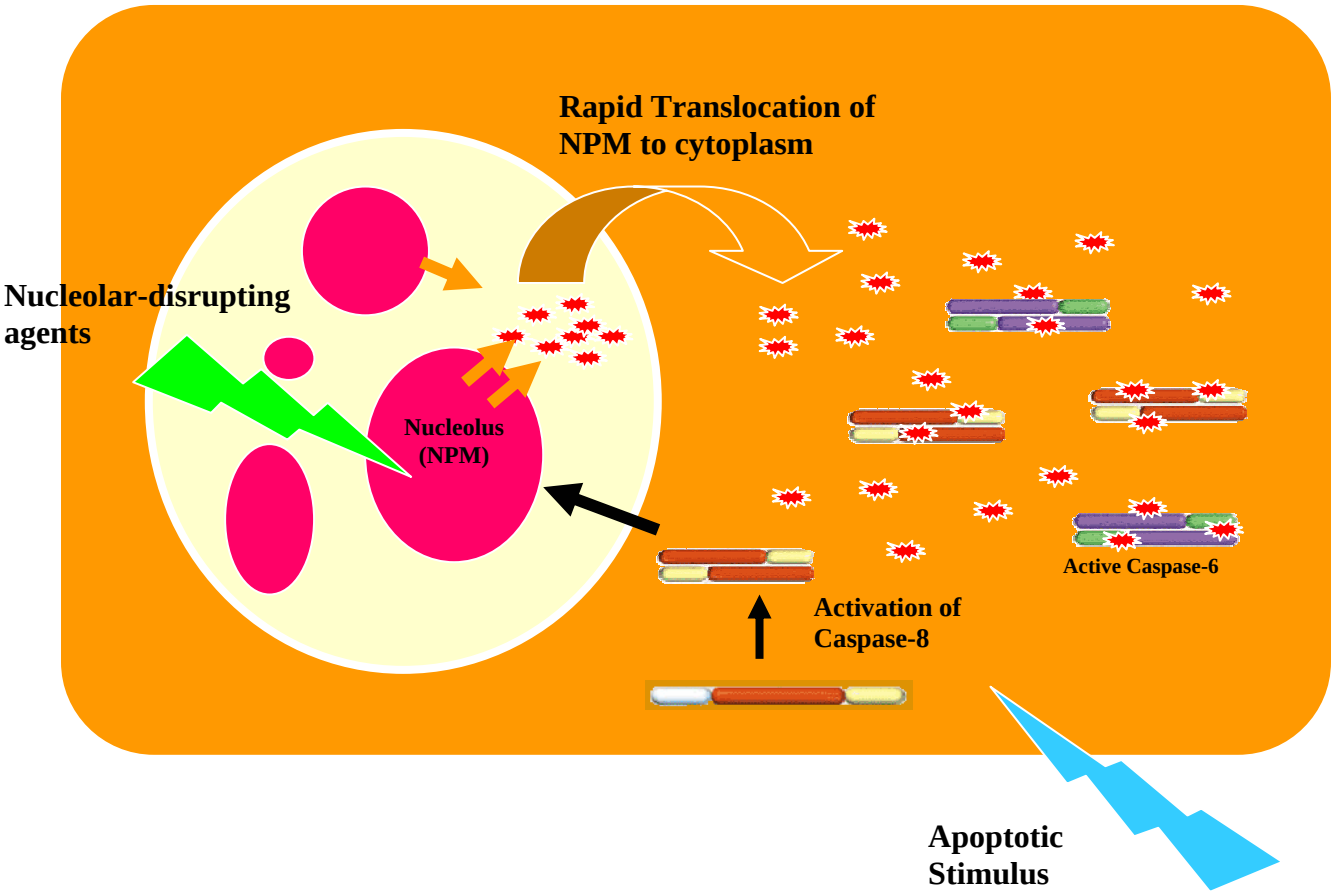


*(Continued from previous page)* (b) Meanwhile, activation of caspase-8 due to apoptotic stimulation results in rapid translocation of nucleolar NPM into the cytoplasm. Nucleolar disrupting agents such as heat shock or exposure to the transcriptional inhibitor actinomycin D also results in massive pool of nucleoplasmic NPM for cytoplasmic translocation. Large amount of cytoplasmic NPM then binds active caspase-6 and -8, inhibits their activities and prevents their further activation, thus effectively bringing death signalling to a halt.

**(c)**

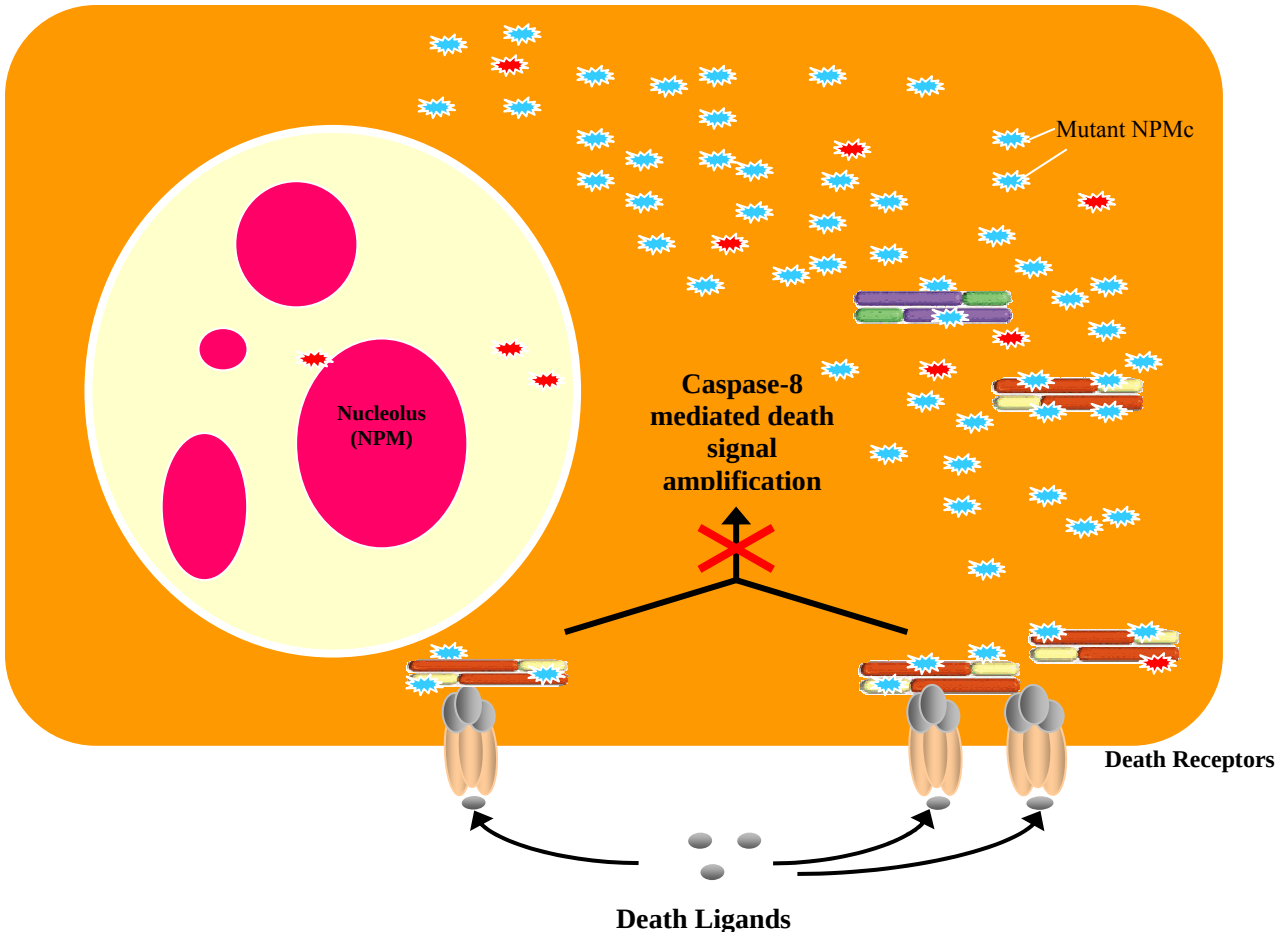


*(Continued from previous page)* (c) In the haematopoietic system, the death receptor pathways operate to eliminate superfluous cells that can cause leukaemogenesis and/or autoimmunity. However, in a patient carrying the frame-shift *NPM1* mutation leading to cytoplasmic dislocation of the protein, the threshold for caspase-8 activation is raised sharply due to cytoplasmic abundance of the mutant protein. As a result, immaturely myelogenous blast cells in the bone marrow become resistant to death ligand-induced cell death. Since caspase-8 activation is required for myeloid differentiation, the undying cells remain undifferentiated as well. Consequently, the immortalised cells acquire other gene mutations that results in rapid cell proliferation, and oncogenesis ensues.

## 6.3 Future works

Current NPM research efforts centre on NPM's association with the tumour suppressors such as p53 and ARF, as well as NPM's involvement in leukaemogenic fusion proteins resulting from chromosomal translocation. The present investigation, which delves into NPM's previously unknown caspase regulatory function, is, to our knowledge, without precedence. The unravelling of a novel caspase-6/-8 inhibitory function for NPM here opens up therapeutic vistas for both PD and $NPMc^+$ AML alike. Further works are, however, required to gain greater biological insights into the mechanism of caspase inhibition by NPM, so as to facilitate rationale drug designing for these diseases. Scope for future works includes the following:

*a) Investigating the possibility of an interaction between caspase-10 and NPM.* - Like caspase-8, caspase-10 is similarly activated at the death receptor. It has been suggested that the two caspases play redundant function in human. This is supported by the observation caspase-8 deficiency in humans is compatible with normal development (Chun et al Nature 2002). Inherited human Caspase 10 mutations has been shown to underlie defective lymphocyte and dendritic cell apoptosis in autoimmune lymphoproliferative syndrome type II (Wang Cell 1999). Given the high sequence similarity between the two caspases, we intend to investigate the possiblity that caspase10 may interact with and be inhibited by NPM as well.

*b) Structural studies of the inhibition mechanism of active caspase-6 and -8 by NPM* - Apart from demonstrating physical interactions between NPM and active caspase-6/-8, we have also shown that NPM promotes the formation of an inhibitory complex involving the active caspases and their current substrates, thereby effectively sequestering them away from many other available substrate molecules (See Chapter 4, Section 4.3.4). The use of biophysical methods such as nuclear magnetic resonance (NMR) to investigate the crystal structure of NPM in complex with active caspase-6 and -8 is expected to shed light on the structural basis for such inhibitions, as well as reveal the order of contact of components within the NPM-caspase-substrate inhibition complex.

*c) Development of therapeutics for AML* - Since inhibition of caspase-8 and -6 by cytoplasmic NPM underlie defective myelogenous cell apoptosis in AML, disruption of the interaction may increase the susceptibility of the leukimic cells to apoptosis in response to chemotherapeutic treatments. Using an ELISA based screening method, we intend to identify small molecular compounds capable of disrupting the interaction between NPM and the active caspases. This compound can be developed as a potential pharmacological agent other cancers with overexpression of NPM.

*d) Development of therapeutics for Parkinson's disease* - Given NPM's ability to inhibit the activities of caspase-6 and -8, NPM can be explored as a therapeutic agent for inhibiting excessive cell death in neurodegenerative disease such as PD. We have mapped NPM's domain of interaction with caspase-6 and -8 to the C-terminal heterodimerisation domain using GST

pull-down assay (Figure 6.2), and is in the midst of determining the portions within NPM's C terminal that is sufficient to effect substantial caspase-6/-8 inhibition *in vitro*. This will facilitate the development of small peptide drugs capable of passing through the blood brain barrier to the target neurons. We may further look into the development of an effective vector system for small NPM peptide deliverance into the dopaminergic neurons to curb excessive cell death, possibly using MPP+ treated mouse/rats as animal models to explore the effectiveness of the NPM peptide inhibitor

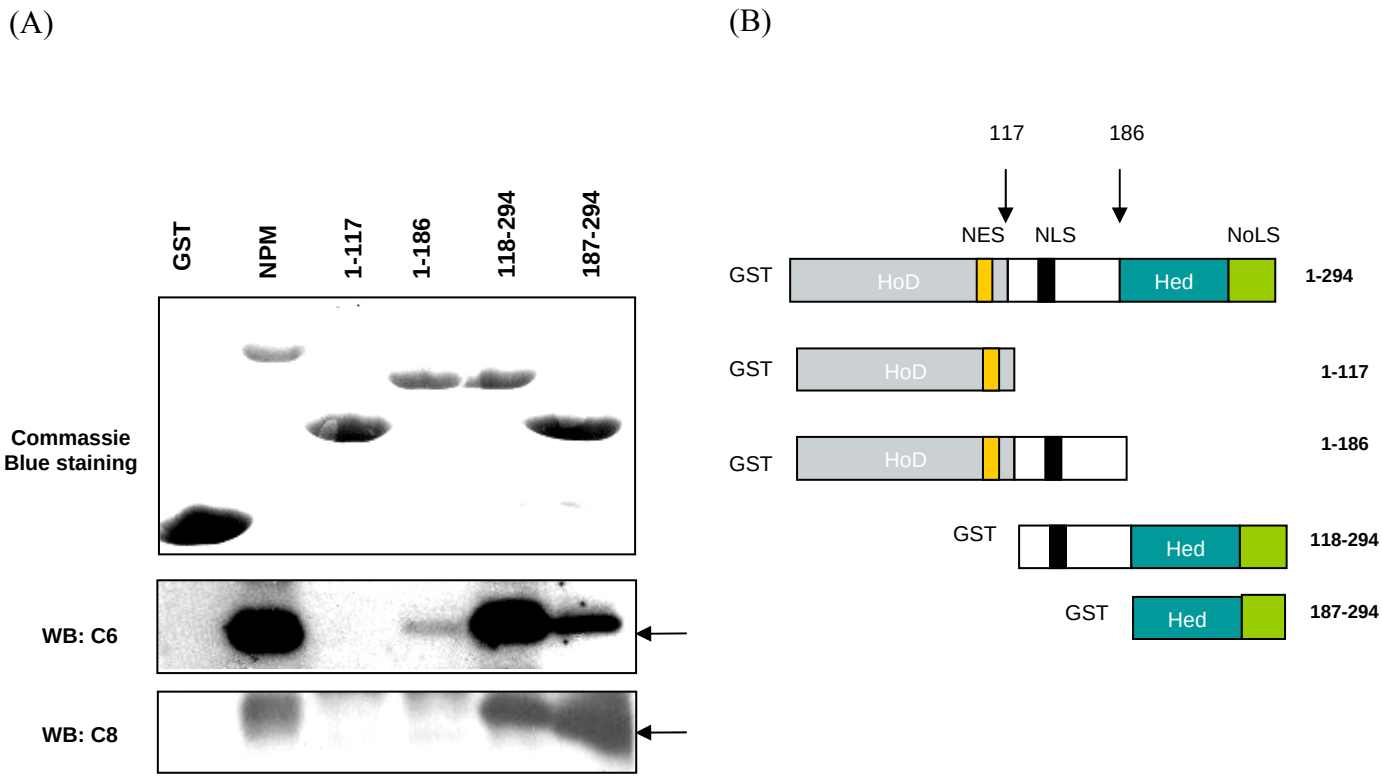


**Figure 6.2 GST pull-down assay showing interaction between C-terminal NPM and active caspase-6/-8**. (a) Whole-cell lysate from apoptotically-induced MN9D cells was used in GST pull-down assay using either empty GST beads, GST-tagged full length NPM or its various deletion mutants. Immunoprecipitates were resolved by SDS−PAGE and subjected to immunoblotting using anti-NPM, anti-caspase-6 or anti-caspase-8 antibody, (b), domain structure of the full-length GST−NPM protein and the various deletion mutants. HeD, heterodimerization domain; HoD, homodimerization domain; NBD, nucleic acid binding domain; NLS, nuclear localization signal. Arrows indicate the exact boundary of deletion in the various mutants. Reproduced with permission from Miss Ang Swee Tin.

## REFERENCES


Adachi, Y., Copeland, T. D., Hatanaka, M. and Oroszlan, S. (1993). Nucleolar targeting signal of Rex protein of human T-cell leukemia virus type I specifically binds to nucleolar shuttle protein B-23. J Biol Chem **268**(19): 13930-13934.

Aebersold, R. and Mann, M. (2003). Mass spectrometry-based proteomics. Nature **422**(6928): 198-207.

Ahn, J. Y., Liu, X., Cheng, D., Peng, J., Chan, P. K., Wade, P. A. and Ye, K. (2005). Nucleophosmin/B23, a nuclear PI(3,4,5)P(3) receptor, mediates the antiapoptotic actions of NGF by inhibiting CAD. Mol Cell **18**(4): 435-445.

Alam, A., Cohen, L. Y., Aouad, S. and Sekaly, R. P. (1999). Early activation of caspases during T lymphocyte stimulation results in selective substrate cleavage in nonapoptotic cells. J Exp Med **190**(12): 1879-1890.

Altucci, L. and Gronemeyer, H. (2001). The promise of retinoids to fight against cancer. Nat Rev Cancer **1**(3): 181-193.

Ashkenazi, A. and Dixit, V. M. (1998). Death receptors: signaling and modulation. Science **281**(5381): 1305-1308.

Bajo, M., Fruehauf, J., Kim, S. H., Fountoulakis, M. and Lubec, G. (2002). Proteomic evaluation of intermediary metabolism enzyme proteins in fetal Down's syndrome cerebral cortex. Proteomics **2**(11): 1539-1546.

Basso, M., Giraudo, S., Corpillo, D., Bergamasco, B., Lopiano, L. and Fasano, M. (2004). Proteome analysis of human substantia nigra in Parkinson's disease. Proteomics **4**(12): 3943-3952.

Baumann, H., Symes, A. J., Comeau, M. R., Morella, K. K., Wang, Y., Friend, D., Ziegler, S. F., Fink, J. S. and Gearing, D. P. (1994). Multiple regions within the cytoplasmic domains of the leukemia inhibitory factor receptor and gp130 cooperate in signal transduction in hepatic and neuronal cells. Mol Cell Biol **14**(1): 138-146.

Beckman, J. S. (1994). Peroxynitrite versus hydroxyl radical: the role of nitric oxide in superoxide-dependent cerebral injury. Ann N Y Acad Sci **738**: 69-75.

Beere, H. M., Wolf, B. B., Cain, K., Mosser, D. D., Mahboubi, A., Kuwana, T., Tailor, P., Morimoto, R. I., Cohen, G. M., *et al.* (2000). Heat-shock protein 70 inhibits apoptosis by preventing recruitment of procaspase-9 to the Apaf-1 apoptosome. Nat Cell Biol **2**(8): 469-475.

Beissinger, M. and Buchner, J. (1998). How chaperones fold proteins. Biol Chem **379**(3): 245-259.

Benchoua, A., Couriaud, C., Guegan, C., Tartier, L., Couvert, P., Friocourt, G., Chelly, J., Menissier-de Murcia, J. and Onteniente, B. (2002). Active caspase-8 translocates into the nucleus of apoptotic cells to inactivate poly(ADP-ribose) polymerase-2. J Biol Chem **277**(37): 34217-34222.

Bender, L. M., Morgan, M. J., Thomas, L. R., Liu, Z. G. and Thorburn, A. (2005). The adaptor protein TRADD activates distinct mechanisms of apoptosis from the nucleus and the cytoplasm. Cell Death Differ **12**(5): 473-481.

Berding, G., Odin, P., Brooks, D. J., Nikkhah, G., Matthies, C., Peschel, T., Shing, M., Kolbe, H., van Den Hoff, J., *et al.* (2001). Resting regional cerebral glucose metabolism in advanced Parkinson's disease studied in the off and on conditions with [(18)F]FDG-PET. Mov Disord **16**(6): 1014-1022.

Bertwistle, D., Sugimoto, M. and Sherr, C. J. (2004). Physical and functional interactions of the Arf tumor suppressor protein with nucleophosmin/B23. Mol Cell Biol **24**(3): 985-996.

Besnault-Mascard, L., Leprince, C., Auffredou, M. T., Meunier, B., Bourgeade, M. F., Camonis, J., Lorenzo, H. K. and Vazquez, A. (2005). Caspase-8 sumoylation is associated with nuclear localization. Oncogene **24**(20): 3268-3273.

Bettinardi, A., Brugnoni, D., Quiros-Roldan, E., Malagoli, A., La Grutta, S., Correra, A. and Notarangelo, L. D. (1997). Missense mutations in the Fas gene resulting in autoimmune lymphoproliferative syndrome: a molecular and immunological analysis. Blood **89**(3): 902-909.

Bhat, K. P., Itahana, K., Jin, A. and Zhang, Y. (2004). Essential role of ribosomal protein L11 in mediating growth inhibition-induced p53 activation. Embo J **23**(12): 2402-2412.

Birnbaum, M. J., Clem, R. J. and Miller, L. K. (1994). An apoptosis-inhibiting gene from a nuclear polyhedrosis virus encoding a polypeptide with Cys/His sequence motifs. J Virol **68**(4): 2521-2528.

Bischof, D., Pulford, K., Mason, D. Y. and Morris, S. W. (1997). Role of the nucleophosmin (NPM) portion of the non-Hodgkin's lymphoma-associated NPM-anaplastic lymphoma kinase fusion protein in oncogenesis. Mol Cell Biol **17**(4): 2312-2325.

Blagosklonny, M. V. (2000). The dilemma of apoptosis in myelodysplasia and leukemia: a new promise of therapeutic intervention? Leukemia **14**(12): 2017-2018.

Borer, R. A., Lehner, C. F., Eppenberger, H. M. and Nigg, E. A. (1989). Major nucleolar proteins shuttle between nucleus and cytoplasm. Cell **56**(3): 379-390.

Bossy-Wetzel, E., Schwarzenbacher, R. and Lipton, S. A. (2004). Molecular pathways to neurodegeneration. Nat Med **10 Suppl**: S2-9.

Bothner, B., Lewis, W. S., DiGiammarino, E. L., Weber, J. D., Bothner, S. J. and Kriwacki, R. W. (2001). Defining the molecular basis of Arf and Hdm2 interactions. J Mol Biol **314**(2): 263-277.

Boyd-Kimball, D., Castegna, A., Sultana, R., Poon, H. F., Petroze, R., Lynn, B. C., Klein, J. B. and Butterfield, D. A. (2005). Proteomic identification of proteins oxidized by Abeta(1-42) in synaptosomes: implications for Alzheimer's disease. Brain Res **1044**(2): 206-215.

Bratton, S. B., MacFarlane, M., Cain, K. and Cohen, G. M. (2000). Protein complexes activate distinct caspase cascades in death receptor and stress-induced apoptosis. Exp Cell Res **256**(1): 27-33.

Brodsky, G., Barnes, T., Bleskan, J., Becker, L., Cox, M. and Patterson, D. (1997). The human GARS-AIRS-GART gene encodes two proteins which are differentially expressed during human brain development and temporally overexpressed in cerebellum of individuals with Down syndrome. Hum Mol Genet **6**(12): 2043-2050.

Bruey, J. M., Ducasse, C., Bonniaud, P., Ravagnan, L., Susin, S. A., Diaz-Latoud, C., Gurbuxani, S., Arrigo, A. P., Kroemer, G., *et al.* (2000). Hsp27 negatively regulates cell death by interacting with cytochrome c. Nat Cell Biol **2**(9): 645-652.

Bukau, B. and Horwich, A. L. (1998). The Hsp70 and Hsp60 chaperone machines. Cell **92**(3): 351-366.

Butterfield, D. A. (2004). Proteomics: a new approach to investigate oxidative stress in Alzheimer's disease brain. Brain Res **1000**(1-2): 1-7.

Butterfield, D. A. and Boyd-Kimball, D. (2004). Proteomics analysis in Alzheimer's disease: new insights into mechanisms of neurodegeneration. Int Rev Neurobiol **61**: 159-188.

Byrd, J. C., Mrozek, K., Dodge, R. K., Carroll, A. J., Edwards, C. G., Arthur, D. C., Pettenati, M. J., Patil, S. R., Rao, K. W., *et al.* (2002). Pretreatment cytogenetic abnormalities are predictive of induction success, cumulative incidence of relapse, and overall survival in adult patients with de novo acute myeloid leukemia: results from Cancer and Leukemia Group B (CALGB 8461). Blood **100**(13): 4325-4336.

Cadwell, C., Yoon, H. J., Zebarjadian, Y. and Carbon, J. (1997). The yeast nucleolar protein Cbf5p is involved in rRNA biosynthesis and interacts genetically with the RNA polymerase I transcription factor RRN3. Mol Cell Biol **17**(10): 6175-6183.

Campos, S. P., Wang, Y., Koj, A. and Baumann, H. (1994). Insulin cooperates with IL-1 in regulating expression of alpha 1-acid glycoprotein gene in rat hepatoma cells. Cytokine **6**(5): 485-492.

Cande, C., Vahsen, N., Kouranti, I., Schmitt, E., Daugas, E., Spahr, C., Luban, J., Kroemer, R. T., Giordanetto, F., *et al.* (2004). AIF and cyclophilin A cooperate in apoptosis-associated chromatinolysis. Oncogene **23**(8): 1514-1521.

Carson, J. P., Behnam, M., Sutton, J. N., Du, C., Wang, X., Hunt, D. F., Weber, M. J. and Kulik, G. (2002). Smac is required for cytochrome c-induced apoptosis in prostate cancer LNCaP cells. Cancer Res **62**(1): 18-23.

Chai, J., Du, C., Wu, J. W., Kyin, S., Wang, X. and Shi, Y. (2000). Structural and biochemical basis of apoptotic activation by Smac/DIABLO. Nature **406**(6798): 855-862.

Chan, P. K., Aldrich, M. and Busch, H. (1985). Alterations in immunolocalization of the phosphoprotein B23 in HeLa cells during serum starvation. Exp Cell Res **161**(1): 101-110.

Chan, P. K., Aldrich, M. B. and Yung, B. Y. (1987). Nucleolar protein B23 translocation after doxorubicin treatment in murine tumor cells. Cancer Res **47**(14): 3798-3801.

Chan, P. K. and Chan, F. Y. (1999). A study of correlation between NPM-translocation and apoptosis in cells induced by daunomycin. Biochem Pharmacol **57**(11): 1265-1273.

Chan, S. W., Hegyi, L., Scott, S., Cary, N. R., Weissberg, P. L. and Bennett, M. R. (2000). Sensitivity to Fas-mediated apoptosis is determined below receptor level in human vascular smooth muscle cells. Circ Res **86**(10): 1038-1046.

Chan, W. Y., Liu, Q. R., Borjigin, J., Busch, H., Rennert, O. M., Tease, L. A. and Chan, P. K. (1989). Characterization of the cDNA encoding human nucleophosmin and studies of its role in normal and abnormal growth. Biochemistry **28**(3): 1033-1039.

Chee, J. L., Guan, X. L., Lee, J. Y., Dong, B., Leong, S. M., Ong, E. H., Liou, A. K. and Lim, T. M. (2005). Compensatory caspase activation in MPP+-induced cell death in dopaminergic neurons. Cell Mol Life Sci **62**(2): 227-238.

Chen, W., Ji, J. and Ru, B. (2005). Proteomic analysis of corticobasal degeneration: a case study of corticobasal degeneration at the proteome level. J Neuropsychiatry Clin Neurosci **17**(3): 364-371.

Cheon, M. S., Kim, S. H., Fountoulakis, M. and Lubec, G. (2003). Heart type fatty acid binding protein (H-FABP) is decreased in brains of patients with Down syndrome and Alzheimer's disease. J Neural Transm Suppl(67): 225-234.

Chinnaiyan, A. M., Hanna, W. L., Orth, K., Duan, H., Poirier, G. G., Froelich, C. J. and Dixit, V. M. (1996). Cytotoxic T-cell-derived granzyme B activates the apoptotic protease ICE-LAP3. Curr Biol **6**(7): 897-899.

Choi, H. K., Won, L. A., Kontur, P. J., Hammond, D. N., Fox, A. P., Wainer, B. H., Hoffmann, P. C. and Heller, A. (1991). Immortalization of embryonic mesencephalic dopaminergic neurons by somatic cell fusion. Brain Res **552**(1): 67-76.

Choi, J., Forster, M. J., McDonald, S. R., Weintraub, S. T., Carroll, C. A. and Gracy, R. W. (2004). Proteomic identification of specific oxidized proteins in ApoE-knockout mice: relevance to Alzheimer's disease. Free Radic Biol Med **36**(9): 1155-1162.

Chondrogianni, N., Stratford, F. L., Trougakos, I. P., Friguet, B., Rivett, A. J. and Gonos, E. S. (2003). Central role of the proteasome in senescence and survival of human fibroblasts: induction of a senescence-like phenotype upon its inhibition and resistance to stress upon its activation. J Biol Chem **278**(30): 28026-28037.

Chondrogianni, N., Tzavelas, C., Pemberton, A. J., Nezis, I. P., Rivett, A. J. and Gonos, E. S. (2005). Overexpression of proteasome beta5 assembled subunit increases the amount of proteasome and confers ameliorated response to oxidative stress and higher survival rates. J Biol Chem **280**(12): 11840-11850.

Chou, C. C. and Yung, B. Y. (2001). Increased stability of nucleophosmin/B23 in anti-apoptotic effect of ras during serum deprivation. Mol Pharmacol **59**(1): 38-45.

Choudhary, J. and Grant, S. G. (2004). Proteomics in postgenomic neuroscience: the end of the beginning. Nat Neurosci **7**(5): 440-445.

Chun, H. J., Zheng, L., Ahmad, M., Wang, J., Speirs, C. K., Siegel, R. M., Dale, J. K., Puck, J., Davis, J., *et al.* (2002). Pleiotropic defects in lymphocyte activation caused by caspase-8 mutations lead to human immunodeficiency. Nature **419**(6905): 395-399.

Claudepierre, T., Dalloz, C., Mornet, D., Matsumura, K., Sahel, J. and Rendon, A. (2000). Characterization of the intermolecular associations of the dystrophin-associated glycoprotein complex in retinal Muller glial cells. J Cell Sci **113 Pt 19**: 3409-3417.

Cohen, G. M. (1997). Caspases: the executioners of apoptosis. Biochem J **326 (Pt 1)**: 1-16.

Colombo, E., Marine, J. C., Danovi, D., Falini, B. and Pelicci, P. G. (2002). Nucleophosmin regulates the stability and transcriptional activity of p53. Nat Cell Biol **4**(7): 529-533.

Conway, E. M., Pollefeyt, S., Cornelissen, J., DeBaere, I., Steiner-Mosonyi, M., Ong, K., Baens, M., Collen, D. and Schuh, A. C. (2000). Three differentially expressed survivin cDNA variants encode proteins with distinct antiapoptotic functions. Blood **95**(4): 1435-1442.

Cory, S. and Adams, J. M. (2002). The Bcl2 family: regulators of the cellular life-or-death switch. Nat Rev Cancer **2**(9): 647-656.

Cowling, V. and Downward, J. (2002). Caspase-6 is the direct activator of caspase-8 in the cytochrome c-induced apoptosis pathway: absolute requirement for removal of caspase-6 prodomain. Cell Death Differ **9**(10): 1046-1056.

Crook, N. E., Clem, R. J. and Miller, L. K. (1993). An apoptosis-inhibiting baculovirus gene with a zinc finger-like motif. J Virol **67**(4): 2168-2174.

Curtin, J. F. and Cotter, T. G. (2003). Live and let die: regulatory mechanisms in Fas-mediated apoptosis. Cell Signal **15**(11): 983-992.

Daley, G. Q., Van Etten, R. A. and Baltimore, D. (1990). Induction of chronic myelogenous leukemia in mice by the P210bcr/abl gene of the Philadelphia chromosome. Science **247**(4944): 824-830.

Daniely, Y. and Borowiec, J. A. (2000). Formation of a complex between nucleolin and replication protein A after cell stress prevents initiation of DNA replication. J Cell Biol **149**(4): 799-810.

Daniely, Y., Dimitrova, D. D. and Borowiec, J. A. (2002). Stress-dependent nucleolin mobilization mediated by p53-nucleolin complex formation. Mol Cell Biol **22**(16): 6014-6022.

David, D. C., Hauptmann, S., Scherping, I., Schuessel, K., Keil, U., Rizzu, P., Ravid, R., Drose, S., Brandt, U., *et al.* (2005). Proteomic and functional analyses reveal a mitochondrial dysfunction in P301L tau transgenic mice. J Biol Chem **280**(25): 23802-23814.

Davis, G. C., Williams, A. C., Markey, S. P., Ebert, M. H., Caine, E. D., Reichert, C. M. and Kopin, I. J. (1979). Chronic Parkinsonism secondary to intravenous injection of meperidine analogues. Psychiatry Res **1**(3): 249-254.

de la Monte, S. M. and Hedley-Whyte, E. T. (1990). Small cerebral hemispheres in adults with Down's syndrome: contributions of developmental arrest and lesions of Alzheimer's disease. J Neuropathol Exp Neurol **49**(5): 509-520.

den Besten, W., Kuo, M. L., Williams, R. T. and Sherr, C. J. (2005). Myeloid leukemia-associated nucleophosmin mutants perturb p53-dependent and independent activities of the Arf tumor suppressor protein. Cell Cycle **4**(11): 1593-1598.

Desagher, S., Osen-Sand, A., Nichols, A., Eskes, R., Montessuit, S., Lauper, S., Maundrell, K., Antonsson, B. and Martinou, J. C. (1999). Bid-induced conformational change of Bax is responsible for mitochondrial cytochrome c release during apoptosis. J Cell Biol **144**(5): 891-901.

Deveraux, Q. L. and Reed, J. C. (1999). IAP family proteins--suppressors of apoptosis. Genes Dev **13**(3): 239-252.

Deveraux, Q. L., Roy, N., Stennicke, H. R., Van Arsdale, T., Zhou, Q., Srinivasula, S. M., Alnemri, E. S., Salvesen, G. S. and Reed, J. C. (1998). IAPs block apoptotic events induced by caspase-8 and cytochrome c by direct inhibition of distinct caspases. Embo J **17**(8): 2215-2223.

Deveraux, Q. L., Takahashi, R., Salvesen, G. S. and Reed, J. C. (1997). X-linked IAP is a direct inhibitor of cell-death proteases. Nature **388**(6639): 300-304.

Dhar, S. K., Lynn, B. C., Daosukho, C. and St Clair, D. K. (2004). Identification of nucleophosmin as an NF-kappaB co-activator for the induction of the human SOD2 gene. J Biol Chem **279**(27): 28209-28219.

Diaz, G. D., Li, Q. and Dashwood, R. H. (2003). Caspase-8 and apoptosis-inducing factor mediate a cytochrome c-independent pathway of apoptosis in human colon cancer cells induced by the dietary phytochemical chlorophyllin. Cancer Res **63**(6): 1254-1261.

Ding, H. F., Lin, Y. L., McGill, G., Juo, P., Zhu, H., Blenis, J., Yuan, J. and Fisher, D. E. (2000). Essential role for caspase-8 in transcription-independent apoptosis triggered by p53. J Biol Chem **275**(49): 38905-38911.

Dolcet, X., Llobet, D., Pallares, J., Rue, M., Comella, J. X. and Matias-Guiu, X. (2005). FLIP is frequently expressed in endometrial carcinoma and has a role in resistance to TRAIL-induced apoptosis. Lab Invest **85**(7): 885-894.

Doyle, V., Virji, S. and Crompton, M. (1999). Evidence that cyclophilin-A protects cells against oxidative stress. Biochem J **341 (Pt 1)**: 127-132.

Drappa, J., Vaishnaw, A. K., Sullivan, K. E., Chu, J. L. and Elkon, K. B. (1996). Fas gene mutations in the Canale-Smith syndrome, an inherited lymphoproliferative disorder associated with autoimmunity. N Engl J Med **335**(22): 1643-1649.

Drewes, G. and Bouwmeester, T. (2003). Global approaches to protein-protein interactions. Curr Opin Cell Biol **15**(2): 199-205.

Dumaz, N. and Meek, D. W. (1999). Serine15 phosphorylation stimulates p53 transactivation but does not directly influence interaction with HDM2. Embo J **18**(24): 7002-7010.

Duyster, J., Bai, R. Y. and Morris, S. W. (2001). Translocations involving anaplastic lymphoma kinase (ALK). Oncogene **20**(40): 5623-5637.

Engels, I. H., Stepczynska, A., Stroh, C., Lauber, K., Berg, C., Schwenzer, R., Wajant, H., Janicke, R. U., Porter, A. G., *et al.* (2000). Caspase-8/FLICE functions as an executioner caspase in anticancer drug-induced apoptosis. Oncogene **19**(40): 4563-4573.

Falini, B., Mecucci, C., Tiacci, E., Alcalay, M., Rosati, R., Pasqualucci, L., La Starza, R., Diverio, D., Colombo, E., *et al.* (2005). Cytoplasmic nucleophosmin in acute myelogenous leukemia with a normal karyotype. N Engl J Med **352**(3): 254-266.

Fankhauser, C., Izaurralde, E., Adachi, Y., Wingfield, P. and Laemmli, U. K. (1991). Specific complex of human immunodeficiency virus type 1 rev and nucleolar B23 proteins: dissociation by the Rev response element. Mol Cell Biol **11**(5): 2567-2575.

Feder, M. E. and Hofmann, G. E. (1999). Heat-shock proteins, molecular chaperones, and the stress response: evolutionary and ecological physiology. Annu Rev Physiol **61**: 243-282.

Fernandes-Alnemri, T., Armstrong, R. C., Krebs, J., Srinivasula, S. M., Wang, L., Bullrich, F., Fritz, L. C., Trapani, J. A., Tomaselli, K. J., *et al.* (1996). In vitro activation of CPP32 and Mch3 by Mch4, a novel human apoptotic cysteine protease containing two FADD-like domains. Proc Natl Acad Sci U S A **93**(15): 7464-7469.

Ferrari, D., Stepczynska, A., Los, M., Wesselborg, S. and Schulze-Osthoff, K. (1998). Differential regulation and ATP requirement for caspase-8 and caspase-3 activation during CD95- and anticancer drug-induced apoptosis. J Exp Med **188**(5): 979-984.

Feuerstein, N., Spiegel, S. and Mond, J. J. (1988). The nuclear matrix protein, numatrin (B23), is associated with growth factor-induced mitogenesis in Swiss 3T3 fibroblasts and with T lymphocyte proliferation stimulated by lectins and anti-T cell antigen receptor antibody. J Cell Biol **107**(5): 1629-1642.

Fischer, U., Janicke, R. U. and Schulze-Osthoff, K. (2003). Many cuts to ruin: a comprehensive update of caspase substrates. Cell Death Differ **10**(1): 76-100.

Fisher, G. H., Rosenberg, F. J., Straus, S. E., Dale, J. K., Middleton, L. A., Lin, A. Y., Strober, W., Lenardo, M. J. and Puck, J. M. (1995). Dominant interfering Fas gene mutations impair apoptosis in a human autoimmune lymphoproliferative syndrome. Cell **81**(6): 935-946.

Fogal, V., Gostissa, M., Sandy, P., Zacchi, P., Sternsdorf, T., Jensen, K., Pandolfi, P. P., Will, H., Schneider, C., *et al.* (2000). Regulation of p53 activity in nuclear bodies by a specific PML isoform. Embo J **19**(22): 6185-6195.

Fornerod, M., Ohno, M., Yoshida, M. and Mattaj, I. W. (1997). CRM1 is an export receptor for leucine-rich nuclear export signals. Cell **90**(6): 1051-1060.

Fountoulakis, M., Juranville, J. F., Dierssen, M. and Lubec, G. (2002). Proteomic analysis of the fetal brain. Proteomics **2**(11): 1547-1576.

Freemantle, S. J., Spinella, M. J. and Dmitrovsky, E. (2003). Retinoids in cancer therapy and chemoprevention: promise meets resistance. Oncogene **22**(47): 7305-7315.

Friedlander, R. M. (2003). Apoptosis and caspases in neurodegenerative diseases. N Engl J Med **348**(14): 1365-1375.

Futcher, B., Latter, G. I., Monardo, P., McLaughlin, C. S. and Garrels, J. I. (1999). A sampling of the yeast proteome. Mol Cell Biol **19**(11): 7357-7368.

Garrels, J. I. (1979). Two dimensional gel electrophoresis and computer analysis of proteins synthesized by clonal cell lines. J Biol Chem **254**(16): 7961-7977.

Gething, M. J. (1997). Protein folding. The difference with prokaryotes. Nature **388**(6640): 329, 331.

Ginisty, H., Sicard, H., Roger, B. and Bouvet, P. (1999). Structure and functions of nucleolin. J Cell Sci **112 (Pt 6)**: 761-772.

Gomez-Angelats, M. and Cidlowski, J. A. (2003). Molecular evidence for the nuclear localization of FADD. Cell Death Differ **10**(7): 791-797.

Gorg, A., Obermaier, C., Boguth, G. and Weiss, W. (1999). Recent developments in two-dimensional gel electrophoresis with immobilized pH gradients: wide pH gradients up to pH 12, longer separation distances and simplified procedures. Electrophoresis **20**(4-5): 712-717.

Greil, R., Anether, G., Johrer, K. and Tinhofer, I. (2003). Tuning the rheostat of the myelopoietic system via Fas and TRAIL. Crit Rev Immunol **23**(4): 301-322.

Grignani, F., Ferrucci, P. F., Testa, U., Talamo, G., Fagioli, M., Alcalay, M., Mencarelli, A., Grignani, F., Peschle, C., *et al.* (1993). The acute promyelocytic leukemia-specific PML-RAR alpha fusion protein inhibits differentiation and promotes survival of myeloid precursor cells. Cell **74**(3): 423-431.

Grimwade, D., Walker, H., Oliver, F., Wheatley, K., Harrison, C., Harrison, G., Rees, J., Hann, I., Stevens, R., *et al.* (1998). The importance of diagnostic cytogenetics on outcome in AML: analysis of 1,612 patients entered into the MRC AML 10 trial. The Medical Research Council Adult and Children's Leukaemia Working Parties. Blood **92**(7): 2322-2333.

Grisendi, S., Bernardi, R., Rossi, M., Cheng, K., Khandker, L., Manova, K. and Pandolfi, P. P. (2005). Role of nucleophosmin in embryonic development and tumorigenesis. Nature **437**(7055): 147-153.

Gronbaek, K., Straten, P. T., Ralfkiaer, E., Ahrenkiel, V., Andersen, M. K., Hansen, N. E., Zeuthen, J., Hou-Jensen, K. and Guldberg, P. (1998). Somatic Fas mutations in non-Hodgkin's lymphoma: association with extranodal disease and autoimmunity. Blood **92**(9): 3018-3024.

Gygi, S. P., Rochon, Y., Franza, B. R. and Aebersold, R. (1999). Correlation between protein and mRNA abundance in yeast. Mol Cell Biol **19**(3): 1720-1730.

Hanash, S. (2003). The emerging field of protein microarrays. Proteomics **3**(11): 2075.

Hanash, S. M. (2000). Biomedical applications of two-dimensional electrophoresis using immobilized pH gradients: current status. Electrophoresis **21**(6): 1202-1209.

Hartmann, A., Hunot, S., Michel, P. P., Muriel, M. P., Vyas, S., Faucheux, B. A., Mouatt-Prigent, A., Turmel, H., Srinivasan, A., *et al.* (2000). Caspase-3: A vulnerability factor and final effector in apoptotic death of dopaminergic neurons in Parkinson's disease. Proc Natl Acad Sci U S A **97**(6): 2875-2880.

Hartmann, A., Michel, P. P., Troadec, J. D., Mouatt-Prigent, A., Faucheux, B. A., Ruberg, M., Agid, Y. and Hirsch, E. C. (2001). Is Bax a mitochondrial mediator in apoptotic death of dopaminergic neurons in Parkinson's disease? J Neurochem **76**(6): 1785-1793.

Hasegawa, E., Takeshige, K., Oishi, T., Murai, Y. and Minakami, S. (1990). 1-Methyl-4-phenylpyridinium (MPP+) induces NADH-dependent superoxide formation and enhances NADH-dependent lipid peroxidation in bovine heart submitochondrial particles. Biochem Biophys Res Commun **170**(3): 1049-1055.

Haupt, S., Berger, M., Goldberg, Z. and Haupt, Y. (2003). Apoptosis - the p53 network. J Cell Sci **116**(Pt 20): 4077-4085.

He, L. Z., Merghoub, T. and Pandolfi, P. P. (1999). In vivo analysis of the molecular pathogenesis of acute promyelocytic leukemia in the mouse and its therapeutic implications. Oncogene **18**(38): 5278-5292.

Heads, R. J., Yellon, D. M. and Latchman, D. S. (1995). Differential cytoprotection against heat stress or hypoxia following expression of specific stress protein genes in myogenic cells. J Mol Cell Cardiol **27**(8): 1669-1678.

Hegde, R., Srinivasula, S. M., Zhang, Z., Wassell, R., Mukattash, R., Cilenti, L., DuBois, G., Lazebnik, Y., Zervos, A. S., *et al.* (2002). Identification of Omi/HtrA2 as a mitochondrial apoptotic serine protease that disrupts inhibitor of apoptosis protein-caspase interaction. J Biol Chem **277**(1): 432-438.

Heisterkamp, N., Jenster, G., ten Hoeve, J., Zovich, D., Pattengale, P. K. and Groffen, J. (1990). Acute leukaemia in bcr/abl transgenic mice. Nature **344**(6263): 251-253.

Henderson, B. R. and Eleftheriou, A. (2000). A comparison of the activity, sequence specificity, and CRM1-dependence of different nuclear export signals. Exp Cell Res **256**(1): 213-224.

Henderson, S., Rowe, M., Gregory, C., Croom-Carter, D., Wang, F., Longnecker, R., Kieff, E. and Rickinson, A. (1991). Induction of bcl-2 expression by Epstein-Barr virus latent membrane protein 1 protects infected B cells from programmed cell death. Cell **65**(7): 1107-1115.

Herrera, J. E., Savkur, R. and Olson, M. O. (1995). The ribonuclease activity of nucleolar protein B23. Nucleic Acids Res **23**(19): 3974-3979.

Heukeshoven, J. and Dernick, R. (1988). Improved silver staining procedure for fast staining in PhastSystem Development Unit. I. Staining of sodium dodecyl sulfate gels. Electrophoresis **9**(1): 28-32.

Hickman, J. A. (2002). Apoptosis and tumourigenesis. Curr Opin Genet Dev **12**(1): 67-72.

Hiebert, S. (2001). Differentiation or leukemia: is C/EBPalpha the answer? Nat Med **7**(4): 407-408.

Hirata, H., Takahashi, A., Kobayashi, S., Yonehara, S., Sawai, H., Okazaki, T., Yamamoto, K. and Sasada, M. (1998). Caspases are activated in a branched protease cascade and control distinct downstream processes in Fas-induced apoptosis. J Exp Med **187**(4): 587-600.

Hsu, C. Y. and Yung, B. Y. (2000). Over-expression of nucleophosmin/B23 decreases the susceptibility of human leukemia HL-60 cells to retinoic acid-induced differentiation and apoptosis. Int J Cancer **88**(3): 392-400.

Huang, D. C. and Strasser, A. (2000). BH3-Only proteins-essential initiators of apoptotic cell death. Cell **103**(6): 839-842.

Huang, W. H., Yung, B. Y., Syu, W. J. and Lee, Y. H. (2001a). The nucleolar phosphoprotein B23 interacts with hepatitis delta antigens and modulates the hepatitis delta virus RNA replication. J Biol Chem **276**(27): 25166-25175.

Huang, Y., Park, Y. C., Rich, R. L., Segal, D., Myszka, D. G. and Wu, H. (2001b). Structural basis of caspase inhibition by XIAP: differential roles of the linker versus the BIR domain. Cell **104**(5): 781-790.

Huber, L. A., Pfaller, K. and Vietor, I. (2003). Organelle proteomics: implications for subcellular fractionation in proteomics. Circ Res **92**(9): 962-968.

Hughes, A. J., Daniel, S. E., Blankson, S. and Lees, A. J. (1993). A clinicopathologic study of 100 cases of Parkinson's disease. Arch Neurol **50**(2): 140-148.

Imamoto, N., Shimamoto, T., Takao, T., Tachibana, T., Kose, S., Matsubae, M., Sekimoto, T., Shimonishi, Y. and Yoneda, Y. (1995). In vivo evidence for involvement of a 58 kDa component of nuclear pore-targeting complex in nuclear protein import. Embo J **14**(15): 3617-3626.

Irmler, M., Thome, M., Hahne, M., Schneider, P., Hofmann, K., Steiner, V., Bodmer, J. L., Schroter, M., Burns, K., *et al.* (1997). Inhibition of death receptor signals by cellular FLIP. Nature **388**(6638): 190-195.

Isakov, N., Witte, S. and Altman, A. (2000). PICOT-HD: a highly conserved protein domain that is often associated with thioredoxin and glutaredoxin modules. Trends Biochem Sci **25**(11): 537-539.

Itahana, K., Bhat, K. P., Jin, A., Itahana, Y., Hawke, D., Kobayashi, R. and Zhang, Y. (2003). Tumor suppressor ARF degrades B23, a nucleolar protein involved in ribosome biogenesis and cell proliferation. Mol Cell **12**(5): 1151-1164.

Jaattela, M., Wissing, D., Kokholm, K., Kallunki, T. and Egeblad, M. (1998). Hsp70 exerts its anti-apoptotic function downstream of caspase-3-like proteases. Embo J **17**(21): 6124-6134.

Jaeken, J. and Van den Berghe, G. (1984). An infantile autistic syndrome characterised by the presence of succinylpurines in body fluids. Lancet **2**(8411): 1058-1061.

Jaschke, A., Mi, H. and Tropschug, M. (1998). Human T cell cyclophilin18 binds to thiol-specific antioxidant protein Aop1 and stimulates its activity. J Mol Biol **277**(4): 763-769.

Jayakumar, J., Suzuki, K., Sammut, I. A., Smolenski, R. T., Khan, M., Latif, N., Abunasra, H., Murtuza, B., Amrani, M., *et al.* (2001). Heat shock protein 70 gene transfection protects mitochondrial and ventricular function against ischemia-reperfusion injury. Circulation **104**(12 Suppl 1): I303-307.

Jenner, P. (2003). Oxidative stress in Parkinson's disease. Ann Neurol **53 Suppl 3**: S26-36; discussion S36-28.

Jia, L., Patwari, Y., Kelsey, S. M., Srinivasula, S. M., Agrawal, S. G., Alnemri, E. S. and Newland, A. C. (2003). Role of Smac in human leukaemic cell apoptosis and proliferation. Oncogene **22**(11): 1589-1599.

Jin, S. and Levine, A. J. (2001). The p53 functional circuit. J Cell Sci **114**(Pt 23): 4139-4140.

Jonsson, G., Paulie, S. and Grandien, A. (2003). High level of cFLIP correlates with resistance to death receptor-induced apoptosis in bladder carcinoma cells. Anticancer Res **23**(2B): 1213-1218.

Kamada, S., Kikkawa, U., Tsujimoto, Y. and Hunter, T. (2005). Nuclear translocation of caspase-3 is dependent on its proteolytic activation and recognition of a substrate-like protein(s). J Biol Chem **280**(2): 857-860.

Kamradt, M. C., Chen, F. and Cryns, V. L. (2001). The small heat shock protein alpha B-crystallin negatively regulates cytochrome c- and caspase-8-dependent activation of

caspase-3 by inhibiting its autoproteolytic maturation. J Biol Chem **276**(19): 16059-16063.

Kasof, G. M. and Gomes, B. C. (2001). Livin, a novel inhibitor of apoptosis protein family member. J Biol Chem **276**(5): 3238-3246.

Kehlenbach, R. H., Dickmanns, A., Kehlenbach, A., Guan, T. and Gerace, L. (1999). A role for RanBP1 in the release of CRM1 from the nuclear pore complex in a terminal step of nuclear export. J Cell Biol **145**(4): 645-657.

Kelekar, A., Chang, B. S., Harlan, J. E., Fesik, S. W. and Thompson, C. B. (1997). Bad is a BH3 domain-containing protein that forms an inactivating dimer with Bcl-XL. Mol Cell Biol **17**(12): 7040-7046.

Kelekar, A. and Thompson, C. B. (1998). Bcl-2-family proteins: the role of the BH3 domain in apoptosis. Trends Cell Biol **8**(8): 324-330.

Kennedy, N. J., Kataoka, T., Tschopp, J. and Budd, R. C. (1999). Caspase activation is required for T cell proliferation. J Exp Med **190**(12): 1891-1896.

Kim, S. H., Fountoulakis, M., Cairns, N. and Lubec, G. (2001). Protein levels of human peroxiredoxin subtypes in brains of patients with Alzheimer's disease and Down syndrome. J Neural Transm Suppl(61): 223-235.

Kingsbury, A. E., Mardsen, C. D. and Foster, O. J. (1998). DNA fragmentation in human substantia nigra: apoptosis or perimortem effect? Mov Disord **13**(6): 877-884.

Kischkel, F. C., Lawrence, D. A., Chuntharapai, A., Schow, P., Kim, K. J. and Ashkenazi, A. (2000). Apo2L/TRAIL-dependent recruitment of endogenous FADD and caspase-8 to death receptors 4 and 5. Immunity **12**(6): 611-620.

Kitada, T., Asakawa, S., Hattori, N., Matsumine, H., Yamamura, Y., Minoshima, S., Yokochi, M., Mizuno, Y. and Shimizu, N. (1998). Mutations in the parkin gene cause autosomal recessive juvenile parkinsonism. Nature **392**(6676): 605-608.

Klose, J., Nock, C., Herrmann, M., Stuhler, K., Marcus, K., Bluggel, M., Krause, E., Schalkwyk, L. C., Rastan, S., *et al.* (2002). Genetic analysis of the mouse brain proteome. Nat Genet **30**(4): 385-393.

Kluck, R. M., Martin, S. J., Hoffman, B. M., Zhou, J. S., Green, D. R. and Newmeyer, D. D. (1997). Cytochrome c activation of CPP32-like proteolysis plays a critical role in a Xenopus cell-free apoptosis system. Embo J **16**(15): 4639-4649.

Kolch, W., Mischak, H. and Pitt, A. R. (2005). The molecular make-up of a tumour: proteomics in cancer research. Clin Sci (Lond) **108**(5): 369-383.

Kolchinsky, A. and Mirzabekov, A. (2002). Analysis of SNPs and other genomic variations using gel-based chips. Hum Mutat **19**(4): 343-360.

Kondo, T., Minamino, N., Nagamura-Inoue, T., Matsumoto, M., Taniguchi, T. and Tanaka, N. (1997). Identification and characterization of nucleophosmin/B23/numatrin which binds the anti-oncogenic transcription factor IRF-1 and manifests oncogenic activity. Oncogene **15**(11): 1275-1281.

Korgaonkar, C., Hagen, J., Tompkins, V., Frazier, A. A., Allamargot, C., Quelle, F. W. and Quelle, D. E. (2005). Nucleophosmin (B23) targets ARF to nucleoli and inhibits its function. Mol Cell Biol **25**(4): 1258-1271.

Korsmeyer, S. J., Wei, M. C., Saito, M., Weiler, S., Oh, K. J. and Schlesinger, P. H. (2000). Pro-apoptotic cascade activates BID, which oligomerizes BAK or BAX into pores that result in the release of cytochrome c. Cell Death Differ **7**(12): 1166-1173.

Kruidering, M. and Evan, G. I. (2000). Caspase-8 in apoptosis: the beginning of "the end"? IUBMB Life **50**(2): 85-90.

Kuo, M. L., den Besten, W., Bertwistle, D., Roussel, M. F. and Sherr, C. J. (2004). N-terminal polyubiquitination and degradation of the Arf tumor suppressor. Genes Dev **18**(15): 1862-1874.

Kurki, S., Peltonen, K., Latonen, L., Kiviharju, T. M., Ojala, P. M., Meek, D. and Laiho, M. (2004). Nucleolar protein NPM interacts with HDM2 and protects tumor suppressor protein p53 from HDM2-mediated degradation. Cancer Cell **5**(5): 465-475.

Landowski, T. H., Qu, N., Buyuksal, I., Painter, J. S. and Dalton, W. S. (1997). Mutations in the Fas antigen in patients with multiple myeloma. Blood **90**(11): 4266-4270.

Lee, D. J., Keramidas, A., Moorhouse, A. J., Schofield, P. R. and Barry, P. H. (2003). The contribution of proline 250 (P-2') to pore diameter and ion selectivity in the human glycine receptor channel. Neurosci Lett **351**(3): 196-200.

Lee, H. Z., Wu, C. H. and Chang, S. P. (2005). Release of nucleophosmin from the nucleus: Involvement in aloe-emodin-induced human lung non small carcinoma cell apoptosis. Int J Cancer **113**(6): 971-976.

Lee, J. P., Palfrey, H. C., Bindokas, V. P., Ghadge, G. D., Ma, L., Miller, R. J. and Roos, R. P. (1999). The role of immunophilins in mutant superoxide dismutase-1linked familial amyotrophic lateral sclerosis. Proc Natl Acad Sci U S A **96**(6): 3251-3256.

Lesch, M. and Nyhan, W. L. (1964). A Familial Disorder of Uric Acid Metabolism and Central Nervous System Function. Am J Med **36**: 561-570.

Levine, A. J. (1997). p53, the cellular gatekeeper for growth and division. Cell **88**(3): 323-331.

Li, J., Zhang, X., Sejas, D. P., Bagby, G. C. and Pang, Q. (2004). Hypoxia-induced nucleophosmin protects cell death through inhibition of p53. J Biol Chem **279**(40): 41275-41279.

Li, J., Zhang, X., Sejas, D. P. and Pang, Q. (2005). Negative regulation of p53 by nucleophosmin antagonizes stress-induced apoptosis in human normal and malignant hematopoietic cells. Leuk Res.

Li, P., Nijhawan, D., Budihardjo, I., Srinivasula, S. M., Ahmad, M., Alnemri, E. S. and Wang, X. (1997). Cytochrome c and dATP-dependent formation of Apaf-1/caspase-9 complex initiates an apoptotic protease cascade. Cell **91**(4): 479-489.

Li, Y. P., Busch, R. K., Valdez, B. C. and Busch, H. (1996). C23 interacts with B23, a putative nucleolar-localization-signal-binding protein. Eur J Biochem **237**(1): 153-158.

Linggi, B., Muller-Tidow, C., van de Locht, L., Hu, M., Nip, J., Serve, H., Berdel, W. E., van der Reijden, B., Quelle, D. E., *et al.* (2002). The t(8;21) fusion protein, AML1 ETO, specifically represses the transcription of the p14(ARF) tumor suppressor in acute myeloid leukemia. Nat Med **8**(7): 743-750.

Liston, P., Fong, W. G., Kelly, N. L., Toji, S., Miyazaki, T., Conte, D., Tamai, K., Craig, C. G., McBurney, M. W., *et al.* (2001). Identification of XAF1 as an antagonist of XIAP anti-Caspase activity. Nat Cell Biol **3**(2): 128-133.

Liu, W. H., Hsu, C. Y. and Yung, B. Y. (1999). Nucleophosmin/B23 regulates the susceptibility of human leukemia HL-60 cells to sodium butyrate-induced apoptosis and inhibition of telomerase activity. Int J Cancer **83**(6): 765-771.

Liu, X., Kim, C. N., Yang, J., Jemmerson, R. and Wang, X. (1996). Induction of apoptotic program in cell-free extracts: requirement for dATP and cytochrome c. Cell **86**(1): 147-157.

Llanos, S., Clark, P. A., Rowe, J. and Peters, G. (2001). Stabilization of p53 by p14ARF without relocation of MDM2 to the nucleolus. Nat Cell Biol **3**(5): 445-452.

Lo, S. L., Cai, C. Z., Chen, Y. Z. and Chung, M. C. (2005). Effect of training datasets on support vector machine prediction of protein-protein interactions. Proteomics **5**(4): 876-884.

Lubec, G., Krapfenbauer, K. and Fountoulakis, M. (2003). Proteomics in brain research: potentials and limitations. Prog Neurobiol **69**(3): 193-211.

Lugo, T. G., Pendergast, A. M., Muller, A. J. and Witte, O. N. (1990). Tyrosine kinase activity and transformation potency of bcr-abl oncogene products. Science **247**(4946): 1079-1082.

Luo, X., Budihardjo, I., Zou, H., Slaughter, C. and Wang, X. (1998). Bid, a Bcl2 interacting protein, mediates cytochrome c release from mitochondria in response to activation of cell surface death receptors. Cell **94**(4): 481-490.

MacBeath, G. (2002). Protein microarrays and proteomics. Nat Genet **32 Suppl**: 526-532.

MacLeod, R. A. and Drexler, H. G. (2005). Cytogenetic analysis of cell lines. Methods Mol Biol **290**: 51-70.

Maiguel, D. A., Jones, L., Chakravarty, D., Yang, C. and Carrier, F. (2004). Nucleophosmin sets a threshold for p53 response to UV radiation. Mol Cell Biol **24**(9): 3703-3711.

Mandel, S., Grunblatt, E., Riederer, P., Amariglio, N., Jacob-Hirsch, J., Rechavi, G. and Youdim, M. B. (2005). Gene Expression Profiling of Sporadic Parkinson's Disease Substantia Nigra Pars Compacta Reveals Impairment of Ubiquitin-Proteasome Subunits, SKP1A, Aldehyde Dehydrogenase, and Chaperone HSC-70. Ann N Y Acad Sci **1053**: 356-375.

Mao, Y., Mehl, I. R. and Muller, M. T. (2002). Subnuclear distribution of topoisomerase I is linked to ongoing transcription and p53 status. Proc Natl Acad Sci U S A **99**(3): 1235-1240.

Marissen, W. E., Gradi, A., Sonenberg, N. and Lloyd, R. E. (2000). Cleavage of eukaryotic translation initiation factor 4GII correlates with translation inhibition during apoptosis. Cell Death Differ **7**(12): 1234-1243.

Maxwell, E. S. and Fournier, M. J. (1995). The small nucleolar RNAs. Annu Rev Biochem **64**: 897-934.

McLaughlin, B., Hartnett, K. A., Erhardt, J. A., Legos, J. J., White, R. F., Barone, F. C. and Aizenman, E. (2003). Caspase 3 activation is essential for neuroprotection in preconditioning. Proc Natl Acad Sci U S A **100**(2): 715-720.

Melese, T. and Xue, Z. (1995). The nucleolus: an organelle formed by the act of building a ribosome. Curr Opin Cell Biol **7**(3): 319-324.

Mihara, M. and Moll, U. M. (2003). Detection of Mitochondrial Localization of p53. Methods Mol Biol **234**: 203-210.

Milner, A. E., Palmer, D. H., Hodgkin, E. A., Eliopoulos, A. G., Knox, P. G., Poole, C. J., Kerr, D. J. and Young, L. S. (2002). Induction of apoptosis by chemotherapeutic drugs: the role of FADD in activation of caspase-8 and synergy with death receptor ligands in ovarian carcinoma cells. Cell Death Differ **9**(3): 287-300.

Mitsui, K., Nakagawa, T. and Tsurugi, K. (1988). On the size and the role of a free cytosolic pool of acidic ribosomal proteins in yeast Saccharomyces cerevisiae. J Biochem (Tokyo) **104**(6): 908-911.

Mochizuki, H., Goto, K., Mori, H. and Mizuno, Y. (1996). Histochemical detection of apoptosis in Parkinson's disease. J Neurol Sci **137**(2): 120-123.

Morris, S. W., Kirstein, M. N., Valentine, M. B., Dittmer, K. G., Shapiro, D. N., Saltman, D. L. and Look, A. T. (1994). Fusion of a kinase gene, ALK, to a nucleolar protein gene, NPM, in non-Hodgkin's lymphoma. Science **263**(5151): 1281-1284.

Muscari, C., Guarnieri, C., Stefanelli, C., Giaccari, A. and Caldarera, C. M. (1995). Protective effect of spermine on DNA exposed to oxidative stress. Mol Cell Biochem **144**(2): 125-129.

Nadeau, K., Das, A. and Walsh, C. T. (1993). Hsp90 chaperonins possess ATPase activity and bind heat shock transcription factors and peptidyl prolyl isomerases. J Biol Chem **268**(2): 1479-1487.

Nagata, S. (1997). Apoptosis by death factor. Cell **88**(3): 355-365.

Nicholson, D. W. (1996). ICE/CED3-like proteases as therapeutic targets for the control of inappropriate apoptosis. Nat Biotechnol **14**(3): 297-301.

Nicholson, D. W. and Thornberry, N. A. (2003). Apoptosis. Life and death decisions. Science **299**(5604): 214-215.

Nicklas, W. J., Vyas, I. and Heikkila, R. E. (1985). Inhibition of NADH-linked oxidation in brain mitochondria by 1-methyl-4-phenyl-pyridine, a metabolite of the neurotoxin, 1-methyl-4-phenyl-1,2,5,6-tetrahydropyridine. Life Sci **36**(26): 2503-2508.

Nie, Z., Phenix, B. N., Lum, J. J., Alam, A., Lynch, D. H., Beckett, B., Krammer, P. H., Sekaly, R. P. and Badley, A. D. (2002). HIV-1 protease processes procaspase 8 to cause mitochondrial release of cytochrome c, caspase cleavage and nuclear fragmentation. Cell Death Differ **9**(11): 1172-1184.

Nishimura, Y., Ohkubo, T., Furuichi, Y. and Umekawa, H. (2002). Tryptophans 286 and 288 in the C-terminal region of protein B23.1 are important for its nucleolar localization. Biosci Biotechnol Biochem **66**(10): 2239-2242.

Nitta, T., Igarashi, K. and Yamamoto, N. (2002). Polyamine depletion induces apoptosis through mitochondria-mediated pathway. Exp Cell Res **276**(1): 120-128.

Nozawa, Y., Van Belzen, N., Van der Made, A. C., Dinjens, W. N. and Bosman, F. T. (1996). Expression of nucleophosmin/B23 in normal and neoplastic colorectal mucosa. J Pathol **178**(1): 48-52.

Nusspaumer, G., Remacha, M. and Ballesta, J. P. (2000). Phosphorylation and N-terminal region of yeast ribosomal protein P1 mediate its degradation, which is prevented by protein P2. Embo J **19**(22): 6075-6084.

O'Farrell, P. Z. and Goodman, H. M. (1976). Resolution of simian virus 40 proteins in whole cell extracts by two-dimensional electrophoresis: heterogeneity of the major capsid protein. Cell **9**(2): 289-298.

Okuda, M. (2002). The role of nucleophosmin in centrosome duplication. Oncogene **21**(40): 6170-6174.

Okuda, M., Horn, H. F., Tarapore, P., Tokuyama, Y., Smulian, A. G., Chan, P. K., Knudsen, E. S., Hofmann, I. A., Snyder, J. D., *et al.* (2000). Nucleophosmin/B23 is a target of CDK2/cyclin E in centrosome duplication. Cell **103**(1): 127-140.

Olanow, C. W. and Tatton, W. G. (1999). Etiology and pathogenesis of Parkinson's disease. Annu Rev Neurosci **22**: 123-144.

Olson, M. O. (2004). Sensing cellular stress: another new function for the nucleolus? Sci STKE **2004**(224): pe10.

Olson, M. O., Dundr, M. and Szebeni, A. (2000). The nucleolus: an old factory with unexpected capabilities. Trends Cell Biol **10**(5): 189-196.

Olson, M. O., Hingorani, K. and Szebeni, A. (2002). Conventional and nonconventional roles of the nucleolus. Int Rev Cytol **219**: 199-266.

Ossareh-Nazari, B., Bachelerie, F. and Dargemont, C. (1997). Evidence for a role of CRM1 in signal-mediated nuclear protein export. Science **278**(5335): 141-144.

Ozoren, N. and El-Deiry, W. S. (2002). Defining characteristics of Types I and II apoptotic cells in response to TRAIL. Neoplasia **4**(6): 551-557.

Pabst, T., Mueller, B. U., Zhang, P., Radomska, H. S., Narravula, S., Schnittger, S., Behre, G., Hiddemann, W. and Tenen, D. G. (2001). Dominant-negative mutations of CEBPA, encoding CCAAT/enhancer binding protein-alpha (C/EBPalpha), in acute myeloid leukemia. Nat Genet **27**(3): 263-270.

Palacino, J. J., Sagi, D., Goldberg, M. S., Krauss, S., Motz, C., Wacker, M., Klose, J. and Shen, J. (2004). Mitochondrial dysfunction and oxidative damage in parkin-deficient mice. J Biol Chem **279**(18): 18614-18622.

Pan, G., Humke, E. W. and Dixit, V. M. (1998). Activation of caspases triggered by cytochrome c in vitro. FEBS Lett **426**(1): 151-154.

Pandey, A. and Mann, M. (2000). Proteomics to study genes and genomes. Nature **405**(6788): 837-846.

Pandey, P., Farber, R., Nakazawa, A., Kumar, S., Bharti, A., Nalin, C., Weichselbaum, R., Kufe, D. and Kharbanda, S. (2000a). Hsp27 functions as a negative regulator of cytochrome c-dependent activation of procaspase-3. Oncogene **19**(16): 1975-1981.

Pandey, P., Saleh, A., Nakazawa, A., Kumar, S., Srinivasula, S. M., Kumar, V., Weichselbaum, R., Nalin, C., Alnemri, E. S., *et al.* (2000b). Negative regulation of cytochrome c-mediated oligomerization of Apaf-1 and activation of procaspase-9 by heat shock protein 90. Embo J **19**(16): 4310-4322.

Pang, Q., Christianson, T. A., Koretsky, T., Carlson, H., David, L., Keeble, W., Faulkner, G. R., Speckhart, A. and Bagby, G. C. (2003). Nucleophosmin interacts with and inhibits the catalytic function of eukaryotic initiation factor 2 kinase PKR. J Biol Chem **278**(43): 41709-41717.

Pasinetti, G. M. and Ho, L. (2001). From cDNA microarrays to high-throughput proteomics. Implications in the search for preventive initiatives to slow the clinical progression of Alzheimer's disease dementia. Restor Neurol Neurosci **18**(2-3): 137-142.

Pearson, M., Carbone, R., Sebastiani, C., Cioce, M., Fagioli, M., Saito, S., Higashimoto, Y., Appella, E., Minucci, S., *et al.* (2000). PML regulates p53 acetylation and premature senescence induced by oncogenic Ras. Nature **406**(6792): 207-210.

Pederson, T. (1998). The plurifunctional nucleolus. Nucleic Acids Res **26**(17): 3871-3876.

Pellegrini, M., Bath, S., Marsden, V. S., Huang, D. C., Metcalf, D., Harris, A. W. and Strasser, A. (2005). FADD and caspase-8 are required for cytokine-induced proliferation of hemopoietic progenitor cells. Blood **106**(5): 1581-1589.

Pluk, H., Soffner, J., Luhrmann, R. and van Venrooij, W. J. (1998). cDNA cloning and characterization of the human U3 small nucleolar ribonucleoprotein complex-associated 55-kilodalton protein. Mol Cell Biol **18**(1): 488-498.

Polymeropoulos, M. H., Lavedan, C., Leroy, E., Ide, S. E., Dehejia, A., Dutra, A., Pike, B., Root, H., Rubenstein, J., *et al.* (1997). Mutation in the alpha-synuclein gene identified in families with Parkinson's disease. Science **276**(5321): 2045-2047.

Prestayko, A. W., Klomp, G. R., Schmoll, D. J. and Busch, H. (1974). Comparison of proteins of ribosomal subunits and nucleolar preribosomal particles from Novikoff hepatoma ascites cells by two-dimensional polyacrylamide gel electrophoresis. Biochemistry **13**(9): 1945-1951.

Pulford, K., Morris, S. W. and Turturro, F. (2004). Anaplastic lymphoma kinase proteins in growth control and cancer. J Cell Physiol **199**(3): 330-358.

Quentmeier, H., Martelli, M. P., Dirks, W. G., Bolli, N., Liso, A., Macleod, R. A., Nicoletti, I., Mannucci, R., Pucciarini, A., *et al.* (2005). Cell line OCI/AML3 bears exon-12 NPM gene mutation-A and cytoplasmic expression of nucleophosmin. Leukemia **19**(10): 1760-1767.

Ramsamooj, P., Notario, V. and Dritschilo, A. (1995). Modification of nucleolar protein B23 after exposure to ionizing radiation. Radiat Res **143**(2): 158-164.

Redner, R. L., Chen, J. D., Rush, E. A., Li, H. and Pollock, S. L. (2000). The t(5;17) acute promyelocytic leukemia fusion protein NPM-RAR interacts with co-repressor and co-activator proteins and exhibits both positive and negative transcriptional properties. Blood **95**(8): 2683-2690.

Redner, R. L., Rush, E. A., Faas, S., Rudert, W. A. and Corey, S. J. (1996). The t(5;17) variant of acute promyelocytic leukemia expresses a nucleophosmin-retinoic acid receptor fusion. Blood **87**(3): 882-886.

Ren, Y., Busch, R., Durban, E., Taylor, C., Gustafson, W. C., Valdez, B., Li, Y. P., Smetana, K. and Busch, H. (1996). Overexpression of human nucleolar proteins in insect cells: characterization of nucleolar protein p120. Protein Expr Purif **7**(2): 212-219.

Riedl, S. J., Renatus, M., Schwarzenbacher, R., Zhou, Q., Sun, C., Fesik, S. W., Liddington, R. C. and Salvesen, G. S. (2001). Structural basis for the inhibition of caspase-3 by XIAP. Cell **104**(5): 791-800.

Rieux-Laucat, F., Le Deist, F., Hivroz, C., Roberts, I. A., Debatin, K. M., Fischer, A. and de Villartay, J. P. (1995). Mutations in Fas associated with human lymphoproliferative syndrome and autoimmunity. Science **268**(5215): 1347-1349.

Rothman, R. B., Cadet, J. L., Akunne, H. C., Silverthorn, M. L., Baumann, M. H., Carroll, F. I., Rice, K. C., de Costa, B. R., Partilla, J. S., *et al.* (1994). Studies of the biogenic amine transporters. IV. Demonstration of a multiplicity of binding sites in rat caudate membranes for the cocaine analog [125I]RTI-55. J Pharmacol Exp Ther **270**(1): 296-309.

Roy, N., Deveraux, Q. L., Takahashi, R., Salvesen, G. S. and Reed, J. C. (1997). The c-IAP-1 and c-IAP-2 proteins are direct inhibitors of specific caspases. Embo J **16**(23): 6914-6925.

Roy, N., Mahadevan, M. S., McLean, M., Shutler, G., Yaraghi, Z., Farahani, R., Baird, S., Besner-Johnston, A., Lefebvre, C., *et al.* (1995). The gene for neuronal apoptosis inhibitory protein is partially deleted in individuals with spinal muscular atrophy. Cell **80**(1): 167-178.

Rubbi, C. P. and Milner, J. (2003). Disruption of the nucleolus mediates stabilization of p53 in response to DNA damage and other stresses. Embo J **22**(22): 6068-6077.

Ruchaud, S., Korfali, N., Villa, P., Kottke, T. J., Dingwall, C., Kaufmann, S. H. and Earnshaw, W. C. (2002). Caspase-6 gene disruption reveals a requirement for lamin A cleavage in apoptotic chromatin condensation. Embo J **21**(8): 1967-1977.

Saleh, A., Srinivasula, S. M., Balkir, L., Robbins, P. D. and Alnemri, E. S. (2000). Negative regulation of the Apaf-1 apoptosome by Hsp70. Nat Cell Biol **2**(8): 476-483.

Salvesen, G. S. and Dixit, V. M. (1999). Caspase activation: the induced-proximity model. Proc Natl Acad Sci U S A **96**(20): 10964-10967.

Samali, A., Cai, J., Zhivotovsky, B., Jones, D. P. and Orrenius, S. (1999). Presence of a pre-apoptotic complex of pro-caspase-3, Hsp60 and Hsp10 in the mitochondrial fraction of jurkat cells. Embo J **18**(8): 2040-2048.

Savkur, R. S. and Olson, M. O. (1998). Preferential cleavage in pre-ribosomal RNA byprotein B23 endoribonuclease. Nucleic Acids Res **26**(19): 4508-4515.

Scaffidi, C., Fulda, S., Srinivasan, A., Friesen, C., Li, F., Tomaselli, K. J., Debatin, K. M., Krammer, P. H. and Peter, M. E. (1998). Two CD95 (APO-1/Fas) signaling pathways. Embo J **17**(6): 1675-1687.

Schickling, O., Stegh, A. H., Byrd, J. and Peter, M. E. (2001). Nuclear localization of DEDD leads to caspase-6 activation through its death effector domain and inhibition of RNA polymerase I dependent transcription. Cell Death Differ **8**(12): 1157-1168.

Schmidt-Zachmann, M. S., Hugle-Dorr, B. and Franke, W. W. (1987). A constitutive nucleolar protein identified as a member of the nucleoplasmin family. Embo J **6**(7): 1881-1890.

Schulze-Osthoff, K., Ferrari, D., Los, M., Wesselborg, S. and Peter, M. E. (1998). Apoptosis signaling by death receptors. Eur J Biochem **254**(3): 439-459.

Screaton, R. A., Kiessling, S., Sansom, O. J., Millar, C. B., Maddison, K., Bird, A., Clarke, A. R. and Frisch, S. M. (2003). Fas-associated death domain protein interacts with methyl-CpG binding domain protein 4: a potential link between genome surveillance and apoptosis. Proc Natl Acad Sci U S A **100**(9): 5211-5216.

Secchiero, P., Gonelli, A., Mirandola, P., Melloni, E., Zamai, L., Celeghini, C., Milani, D. and Zauli, G. (2002). Tumor necrosis factor-related apoptosis-inducing ligand induces monocytic maturation of leukemic and normal myeloid precursors through a caspase-dependent pathway. Blood **100**(7): 2421-2429.

Sedlak, T. W., Oltvai, Z. N., Yang, E., Wang, K., Boise, L. H., Thompson, C. B. and Korsmeyer, S. J. (1995). Multiple Bcl-2 family members demonstrate selective dimerizations with Bax. Proc Natl Acad Sci U S A **92**(17): 7834-7838.

Sheikh, M. S. and Huang, Y. (2003). Death receptor activation complexes: it takes two to activate TNF receptor 1. Cell Cycle **2**(6): 550-552.

Shi, Y., Zhai, H., Wang, X., Han, Z., Liu, C., Lan, M., Du, J., Guo, C., Zhang, Y., *et al.* (2004). Ribosomal proteins S13 and L23 promote multidrug resistance in gastric cancer cells by suppressing drug-induced apoptosis. Exp Cell Res **296**(2): 337-346.

Shikama, Y., U, M., Miyashita, T. and Yamada, M. (2001). Comprehensive studies on subcellular localizations and cell death-inducing activities of eight GFP-tagged apoptosis-related caspases. Exp Cell Res **264**(2): 315-325.

Shimizu, S., Konishi, A., Kodama, T. and Tsujimoto, Y. (2000). BH4 domain of antiapoptotic Bcl-2 family members closes voltage-dependent anion channel and inhibits apoptotic mitochondrial changes and cell death. Proc Natl Acad Sci U S A **97**(7): 3100-3105.

Shimizu, S., Narita, M. and Tsujimoto, Y. (1999). Bcl-2 family proteins regulate the release of apoptogenic cytochrome c by the mitochondrial channel VDAC. Nature **399**(6735): 483-487.

Shiozaki, E. N., Chai, J., Rigotti, D. J., Riedl, S. J., Li, P., Srinivasula, S. M., Alnemri, E. S., Fairman, R. and Shi, Y. (2003). Mechanism of XIAP-mediated inhibition of caspase-9. Mol Cell **11**(2): 519-527.

Shivapurkar, N., Toyooka, S., Eby, M. T., Huang, C. X., Sathyanarayana, U. G., Cunningham, H. T., Reddy, J. L., Brambilla, E., Takahashi, T., *et al.* (2002). Differential inactivation of caspase-8 in lung cancers. Cancer Biol Ther **1**(1): 65-69.

Siegel, R. M., Chan, F. K., Chun, H. J. and Lenardo, M. J. (2000). The multifaceted role of Fas signaling in immune cell homeostasis and autoimmunity. Nat Immunol **1**(6): 469-474.

Singh, A. B., Kaushal, V., Megyesi, J. K., Shah, S. V. and Kaushal, G. P. (2002). Cloning and expression of rat caspase-6 and its localization in renal ischemia/reperfusion injury. Kidney Int **62**(1): 106-115.

Slee, E. A., Harte, M. T., Kluck, R. M., Wolf, B. B., Casiano, C. A., Newmeyer, D. D., Wang, H. G., Reed, J. C., Nicholson, D. W., *et al.* (1999). Ordering the cytochrome c-initiated caspase cascade: hierarchical activation of caspases-2, -3, -6, -7, -8, and -10 in a caspase-9-dependent manner. J Cell Biol **144**(2): 281-292.

Slee, E. A., Keogh, S. A. and Martin, S. J. (2000). Cleavage of BID during cytotoxic drug and UV radiation-induced apoptosis occurs downstream of the point of Bcl-2 action and is catalysed by caspase-3: a potential feedback loop for amplification of apoptosis-associated mitochondrial cytochrome c release. Cell Death Differ **7**(6): 556-565.

Soung, Y. H., Lee, J. W., Kim, S. Y., Sung, Y. J., Park, W. S., Nam, S. W., Kim, S. H., Lee, J. Y., Yoo, N. J., *et al.* (2005). Caspase-8 gene is frequently inactivated by the frameshift

somatic mutation 1225_1226delTG in hepatocellular carcinomas. Oncogene **24**(1): 141-147.

Spector, D. L., Ochs, R. L. and Busch, H. (1984). Silver staining, immunofluorescence, and immunoelectron microscopic localization of nucleolar phosphoproteins B23 and C23. Chromosoma **90**(2): 139-148.

Sprick, M. R., Weigand, M. A., Rieser, E., Rauch, C. T., Juo, P., Blenis, J., Krammer, P. H. and Walczak, H. (2000). FADD/MORT1 and caspase-8 are recruited to TRAIL receptors 1 and 2 and are essential for apoptosis mediated by TRAIL receptor 2. Immunity **12**(6): 599-609.

Srinivasula, S. M., Ahmad, M., Fernandes-Alnemri, T. and Alnemri, E. S. (1998). Autoactivation of procaspase-9 by Apaf-1-mediated oligomerization. Mol Cell **1**(7): 949-957.

Srinivasula, S. M., Datta, P., Fan, X. J., Fernandes-Alnemri, T., Huang, Z. and Alnemri, E. S. (2000). Molecular determinants of the caspase-promoting activity of Smac/DIABLO and its role in the death receptor pathway. J Biol Chem **275**(46): 36152-36157.

Srinivasula, S. M., Hegde, R., Saleh, A., Datta, P., Shiozaki, E., Chai, J., Lee, R. A., Robbins, P. D., Fernandes-Alnemri, T., *et al.* (2001). A conserved XIAP-interaction motif in caspase-9 and Smac/DIABLO regulates caspase activity and apoptosis. Nature **410**(6824): 112-116.

Stennicke, H. R., Jurgensmeier, J. M., Shin, H., Deveraux, Q., Wolf, B. B., Yang, X., Zhou, Q., Ellerby, H. M., Ellerby, L. M., *et al.* (1998). Pro-caspase-3 is a major physiologic target of caspase-8. J Biol Chem **273**(42): 27084-27090.

Sun, X. M., Butterworth, M., MacFarlane, M., Dubiel, W., Ciechanover, A. and Cohen, G. M. (2004). Caspase activation inhibits proteasome function during apoptosis. Mol Cell **14**(1): 81-93.

Suzuki, Y., Imai, Y., Nakayama, H., Takahashi, K., Takio, K. and Takahashi, R. (2001a). A serine protease, HtrA2, is released from the mitochondria and interacts with XIAP, inducing cell death. Mol Cell **8**(3): 613-621.

Suzuki, Y., Nakabayashi, Y., Nakata, K., Reed, J. C. and Takahashi, R. (2001b). X-linked inhibitor of apoptosis protein (XIAP) inhibits caspase-3 and -7 in distinct modes. J Biol Chem **276**(29): 27058-27063.

Suzuki, Y., Nakabayashi, Y. and Takahashi, R. (2001c). Ubiquitin-protein ligase activity of X-linked inhibitor of apoptosis protein promotes proteasomal degradation of caspase-3 and enhances its anti-apoptotic effect in Fas-induced cell death. Proc Natl Acad Sci U S A **98**(15): 8662-8667.

Szebeni, A., Hingorani, K., Negi, S. and Olson, M. O. (2003). Role of protein kinase CK2 phosphorylation in the molecular chaperone activity of nucleolar protein b23. J Biol Chem **278**(11): 9107-9115.

Szebeni, A. and Olson, M. O. (1999). Nucleolar protein B23 has molecular chaperone activities. Protein Sci **8**(4): 905-912.

Takahashi, A., Alnemri, E. S., Lazebnik, Y. A., Fernandes-Alnemri, T., Litwack, G., Moir, R. D., Goldman, R. D., Poirier, G. G., Kaufmann, S. H., *et al.* (1996). Cleavage of lamin A by Mch2 alpha but not CPP32: multiple interleukin 1 beta-converting enzyme-related proteases with distinct substrate recognition properties are active in apoptosis. Proc Natl Acad Sci U S A **93**(16): 8395-8400.

Takahashi, A. and Earnshaw, W. C. (1996). ICE-related proteases in apoptosis. Curr Opin Genet Dev **6**(1): 50-55.

Takahashi, R., Deveraux, Q., Tamm, I., Welsh, K., Assa-Munt, N., Salvesen, G. S. and Reed, J. C. (1998). A single BIR domain of XIAP sufficient for inhibiting caspases. J Biol Chem **273**(14): 7787-7790.

Tan, A., Bitterman, P., Sonenberg, N., Peterson, M. and Polunovsky, V. (2000). Inhibition of Myc-dependent apoptosis by eukaryotic translation initiation factor 4E requires cyclin D1. Oncogene **19**(11): 1437-1447.

Tanaka, M., Sasaki, H., Kino, I., Sugimura, T. and Terada, M. (1992). Genes preferentially expressed in embryo stomach are predominantly expressed in gastric cancer. Cancer Res **52**(12): 3372-3377.

Tang, D., Lahti, J. M. and Kidd, V. J. (2000). Caspase-8 activation and bid cleavage contribute to MCF7 cellular execution in a caspase-3-dependent manner during staurosporine-mediated apoptosis. J Biol Chem **275**(13): 9303-9307.

Teitz, T., Lahti, J. M. and Kidd, V. J. (2001). Aggressive childhood neuroblastomas do not express caspase-8: an important component of programmed cell death. J Mol Med **79**(8): 428-436.

Thompson, C. B. (1995). Apoptosis in the pathogenesis and treatment of disease. Science **267**(5203): 1456-1462.

Thornberry, N. A. and Lazebnik, Y. (1998). Caspases: enemies within. Science **281**(5381): 1312-1316.

Thornberry, N. A., Rano, T. A., Peterson, E. P., Rasper, D. M., Timkey, T., Garcia-Calvo, M., Houtzager, V. M., Nordstrom, P. A., Roy, S., *et al.* (1997). A combinatorial approach defines specificities of members of the caspase family and granzyme B. Functional

relationships established for key mediators of apoptosis. J Biol Chem **272**(29): 17907-17911.

Traver, D., Akashi, K., Weissman, I. L. and Lagasse, E. (1998). Mice defective in two apoptosis pathways in the myeloid lineage develop acute myeloblastic leukemia. Immunity **9**(1): 47-57.

Tschopp, J., Irmler, M. and Thome, M. (1998). Inhibition of fas death signals by FLIPs. Curr Opin Immunol **10**(5): 552-558.

Tsujimoto, Y., Cossman, J., Jaffe, E. and Croce, C. M. (1985). Involvement of the bcl-2 gene in human follicular lymphoma. Science **228**(4706): 1440-1443.

Valdez, B. C., Perlaky, L., Henning, D., Saijo, Y., Chan, P. K. and Busch, H. (1994). Identification of the nuclear and nucleolar localization signals of the protein p120. Interaction with translocation protein B23. J Biol Chem **269**(38): 23776-23783.

van Loo, G., Saelens, X., Matthijssens, F., Schotte, P., Beyaert, R., Declercq, W. and Vandenabeele, P. (2002). Caspases are not localized in mitochondria during life or death. Cell Death Differ **9**(11): 1207-1211.

Venkatasubbarao, S. (2004). Microarrays--status and prospects. Trends Biotechnol **22**(12): 630-637.

Verhagen, A. M., Ekert, P. G., Pakusch, M., Silke, J., Connolly, L. M., Reid, G. E., Moritz, R. L., Simpson, R. J. and Vaux, D. L. (2000). Identification of DIABLO, a mammalian protein that promotes apoptosis by binding to and antagonizing IAP proteins. Cell **102**(1): 43-53.

Virmani, A., Gaetani, F., Imam, S., Binienda, Z. and Ali, S. (2002). The protective role of L-carnitine against neurotoxicity evoked by drug of abuse, methamphetamine, could be related to mitochondrial dysfunction. Ann N Y Acad Sci **965**: 225-232.

Viswanath, V., Wu, Y., Boonplueang, R., Chen, S., Stevenson, F. F., Yantiri, F., Yang, L., Beal, M. F. and Andersen, J. K. (2001). Caspase-9 activation results in downstream caspase-8 activation and bid cleavage in 1-methyl-4-phenyl-1,2,3,6-tetrahydropyridine-induced Parkinson's disease. J Neurosci **21**(24): 9519-9528.

Vogelstein, B., Lane, D. and Levine, A. J. (2000). Surfing the p53 network. Nature **408**(6810): 307-310.

Wagstaff, M. J., Collaco-Moraes, Y., Smith, J., de Belleroche, J. S., Coffin, R. S. and Latchman, D. S. (1999). Protection of neuronal cells from apoptosis by Hsp27 delivered with a herpes simplex virus-based vector. J Biol Chem **274**(8): 5061-5069.

Walczak, H., Miller, R. E., Ariail, K., Gliniak, B., Griffith, T. S., Kubin, M., Chin, W., Jones, J., Woodward, A., *et al.* (1999). Tumoricidal activity of tumor necrosis factor-related apoptosis-inducing ligand in vivo. Nat Med **5**(2): 157-163.

Wang, C., Curtis, J. E., Geissler, E. N., McCulloch, E. A. and Minden, M. D. (1989). The expression of the proto-oncogene C-kit in the blast cells of acute myeloblastic leukemia. Leukemia **3**(10): 699-702.

Wang, D., Baumann, A., Szebeni, A. and Olson, M. O. (1994). The nucleic acid binding activity of nucleolar protein B23.1 resides in its carboxyl-terminal end. J Biol Chem **269**(49): 30994-30998.

Wang, J., Zheng, L., Lobito, A., Chan, F. K., Dale, J., Sneller, M., Yao, X., Puck, J. M., Straus, S. E., *et al.* (1999). Inherited human Caspase 10 mutations underlie defective lymphocyte and dendritic cell apoptosis in autoimmune lymphoproliferative syndrome type II. Cell **98**(1): 47-58.

Wang, K., Yin, X. M., Chao, D. T., Milliman, C. L. and Korsmeyer, S. J. (1996). BID: a novel BH3 domain-only death agonist. Genes Dev **10**(22): 2859-2869.

Wang, W., Budhu, A., Forgues, M. and Wang, X. W. (2005). Temporal and spatial control of nucleophosmin by the Ran-Crm1 complex in centrosome duplication. Nat Cell Biol **7**(8): 823-830.

Weinstein, L. B. and Steitz, J. A. (1999). Guided tours: from precursor snoRNA to functional snoRNP. Curr Opin Cell Biol **11**(3): 378-384.

Wesselborg, S., Engels, I. H., Rossmann, E., Los, M. and Schulze-Osthoff, K. (1999). Anticancer drugs induce caspase-8/FLICE activation and apoptosis in the absence of CD95 receptor/ligand interaction. Blood **93**(9): 3053-3063.

Wilson, K. P., Black, J. A., Thomson, J. A., Kim, E. E., Griffith, J. P., Navia, M. A., Murcko, M. A., Chambers, S. P., Aldape, R. A., *et al.* (1994). Structure and mechanism of interleukin-1 beta converting enzyme. Nature **370**(6487): 270-275.

Wissing, S., Ludovico, P., Herker, E., Buttner, S., Engelhardt, S. M., Decker, T., Link, A., Proksch, A., Rodrigues, F., *et al.* (2004). An AIF orthologue regulates apoptosis in yeast. J Cell Biol **166**(7): 969-974.

Witte, S., Villalba, M., Bi, K., Liu, Y., Isakov, N. and Altman, A. (2000). Inhibition of the c-Jun N-terminal kinase/AP-1 and NF-kappaB pathways by PICOT, a novel protein kinase C-interacting protein with a thioredoxin homology domain. J Biol Chem **275**(3): 1902-1909.

Wolf, B. B. and Green, D. R. (1999). Suicidal tendencies: apoptotic cell death by caspase family proteinases. J Biol Chem **274**(29): 20049-20052.

Wu, M. H., Chang, J. H. and Yung, B. Y. (2002). Resistance to UV-induced cell-killing in nucleophosmin/B23 over-expressed NIH 3T3 fibroblasts: enhancement of DNA repair and up-regulation of PCNA in association with nucleophosmin/B23 over-expression. Carcinogenesis **23**(1): 93-100.

Wu, M. H. and Yung, B. Y. (2002). UV stimulation of nucleophosmin/B23 expression is an immediate-early gene response induced by damaged DNA. J Biol Chem **277**(50): 48234-48240.

Xanthoudakis, S., Roy, S., Rasper, D., Hennessey, T., Aubin, Y., Cassady, R., Tawa, P., Ruel, R., Rosen, A., *et al.* (1999). Hsp60 accelerates the maturation of pro-caspase-3 by upstream activator proteases during apoptosis. Embo J **18**(8): 2049-2056.

Xie, T., Tong, L., Barrett, T., Yuan, J., Hatzidimitriou, G., McCann, U. D., Becker, K. G., Donovan, D. M. and Ricaurte, G. A. (2002). Changes in gene expression linked to methamphetamine-induced dopaminergic neurotoxicity. J Neurosci **22**(1): 274-283.

Yang, X., Chang, H. Y. and Baltimore, D. (1998). Autoproteolytic activation of pro-caspases by oligomerization. Mol Cell **1**(2): 319-325.

Yang, Y. L. and Li, X. M. (2000). The IAP family: endogenous caspase inhibitors with multiple biological activities. Cell Res **10**(3): 169-177.

Yatin, S. M., Yatin, M., Aulick, T., Ain, K. B. and Butterfield, D. A. (1999). Alzheimer's amyloid beta-peptide associated free radicals increase rat embryonic neuronal polyamine uptake and ornithine decarboxylase activity: protective effect of vitamin E. Neurosci Lett **263**(1): 17-20.

Yeager, T. R., DeVries, S., Jarrard, D. F., Kao, C., Nakada, S. Y., Moon, T. D., Bruskewitz, R., Stadler, W. M., Meisner, L. F., *et al.* (1998). Overcoming cellular senescence in human cancer pathogenesis. Genes Dev **12**(2): 163-174.

Yoneda-Kato, N., Look, A. T., Kirstein, M. N., Valentine, M. B., Raimondi, S. C., Cohen, K. J., Carroll, A. J. and Morris, S. W. (1996). The t(3;5)(q25.1;q34) of myelodysplastic syndrome and acute myeloid leukemia produces a novel fusion gene, NPM-MLF1. Oncogene **12**(2): 265-275.

Yung, B. Y., Bor, A. M. and Chan, P. K. (1990). Short exposure to actinomycin D induces "reversible" translocation of protein B23 as well as "reversible" inhibition of cell growth and RNA synthesis in HeLa cells. Cancer Res **50**(18): 5987-5991.

Yung, B. Y., Busch, H. and Chan, P. K. (1985a). Translocation of nucleolar phosphoprotein B23 (37 kDa/pI 5.1) induced by selective inhibitors of ribosome synthesis. Biochim Biophys Acta **826**(4): 167-173.

Yung, B. Y., Busch, R. K., Busch, H., Mauger, A. B. and Chan, P. K. (1985b). Effects of actinomycin D analogs on nucleolar phosphoprotein B23 (37,000 daltons/pI 5.1). Biochem Pharmacol **34**(22): 4059-4063.

Yung, B. Y., Yang, Y. H. and Bor, A. M. (1991). Nucleolar protein B23 translocation after deferoxamine treatment in a human leukemia cell line. Int J Cancer **48**(5): 779-784.

Zatsepina, O. V., Todorov, I. T., Philipova, R. N., Krachmarov, C. P., Trendelenburg, M. F. and Jordan, E. G. (1997). Cell cycle-dependent translocations of a major nucleolar phosphoprotein, B23, and some characteristics of its variants. Eur J Cell Biol **73**(1): 58-70.

Zhang, D. E., Zhang, P., Wang, N. D., Hetherington, C. J., Darlington, G. J. and Tenen, D. G. (1997). Absence of granulocyte colony-stimulating factor signaling and neutrophil development in CCAAT enhancer binding protein alpha-deficient mice. Proc Natl Acad Sci U S A **94**(2): 569-574.

Zhang, H., Shi, X., Paddon, H., Hampong, M., Dai, W. and Pelech, S. (2004). B23/nucleophosmin serine 4 phosphorylation mediates mitotic functions of polo-like kinase 1. J Biol Chem **279**(34): 35726-35734.

Zhang, Y., Wolf, G. W., Bhat, K., Jin, A., Allio, T., Burkhart, W. A. and Xiong, Y. (2003). Ribosomal protein L11 negatively regulates oncoprotein MDM2 and mediates a p53-dependent ribosomal-stress checkpoint pathway. Mol Cell Biol **23**(23): 8902-8912.

Zhou, X. D., Yu, J. P., Liu, J., Luo, H. S., Chen, H. X. and Yu, H. G. (2004). Overexpression of cellular FLICE-inhibitory protein (FLIP) in gastric adenocarcinoma. Clin Sci (Lond) **106**(4): 397-405.

Zou, H., Henzel, W. J., Liu, X., Lutschg, A. and Wang, X. (1997). Apaf-1, a human protein homologous to C. elegans CED-4, participates in cytochrome c-dependent activation of caspase-3. Cell **90**(3): 405-413.

Zou, H., Li, Y., Liu, X. and Wang, X. (1999). An APAF-1.cytochrome c multimeric complex is a functional apoptosome that activates procaspase-9. J Biol Chem **274**(17): 11549-11556.